TESIS DOCTORAL

ANÁLISIS Y SÍNTESIS DE IMPACTOS DEL CAMBIO GLOBAL EN EL ESTADO Y VULNERABILIDAD DE MASAS DE AGUA SUBTERRÁNEAS

UNIVERSIDAD
DE GRANADA

LETICIA BAENA RUIZ

Director: Dr. David Pulido Velázquez

Programa de doctorado de Ingeniería Civil

Universidad de Granada

Granada, abril 2021

TESIS DOCTORAL

Análisis y síntesis de impactos del cambio global en el estado y vulnerabilidad de masas de agua subterráneas

Leticia Baena Ruiz

Director: Dr. David Pulido Velázquez

Programa de doctorado de Ingeniería Civil

Universidad de Granada

UNIVERSIDAD DE GRANADA

GOBIERNO DE ESPAÑA · MINISTERIO DE CIENCIA E INNOVACIÓN · Instituto Geológico y Minero de España

Granada, abril 2021

Editor: Universidad de Granada. Tesis Doctorales
Autor: Leticia Baena Ruiz
ISBN: 978-84-1306-918-0
URI: http://hdl.handle.net/10481/69406

“Nunca reconoceremos el valor del agua

hasta que el pozo esté seco”

Thomas Fuller

Agradecimientos

Quisiera comenzar dando las gracias a mi director de tesis, el Dr. David Pulido Velázquez. Sin él no hubiera sido posible la realización de este trabajo. Gracias la confianza depositada en mí desde el primer momento y por todos los conocimientos transmitidos durante estos años. Su experiencia y calidad científica impecable han sido de gran ayuda para la realización de esta tesis. Ha sido un placer tener la oportunidad de trabajar en el Instituto Geológico y Minero de España (IGME) y poder realizar esta tesis en el marco de proyectos competitivos europeos y nacionales, los cuales me han aportado una gran cantidad de conocimientos en el campo de los recursos hídricos subterráneos, así como la financiación necesaria para la realización de esta tesis.

Gracias a todos los compañeros del IGME, incluido mi director David Pulido, que me han acompañado durante este tiempo, por su gran amabilidad y por el apoyo y ánimo recibido en todo momento por parte de todos. Gracias por compartir el día a día y por hacer más ameno este camino. Espero seguir compartiendo con vosotros muchos más años.

Quisiera agradecer también a todas las personas que han participado en los diferentes trabajos realizados para esta tesis, por su dedicación y aportación científica.

Por supuesto a toda mi familia, por su incondicional apoyo y admiración y por ayudarme a conseguir mis objetivos. A Javier y a mi hijo Javi les agradezco que estén siempre a mi lado, aportándome buenos momentos y enseñándome a valorar las pequeñas cosas.

Índices de calidad

Baena-Ruiz, L., Pulido-Velazquez, D., Collados-Lara, AJ. et al. Global Assessment of Seawater Intrusion Problems (Status and Vulnerability). Water Resour Manage 32, 2681–2700 (2018). https://doi.org/10.1007/s11269-018-1952-2

> Impact factor JCR: 2,987 out of 7,913; Position: 18 out of 91 (Q1) in the Water resources area. / Factor de impacto JCR: 2,987 de 7,913; Posición: 18 de 91 (Q1) en el área de Recursos hídricos.

Baena-Ruiz, L., Pulido-Velazquez, D., Collados-Lara, AJ. et al. Summarizing the impacts of future potential global change scenarios on seawater intrusion at the aquifer scale. Environ Earth Sci 79, 99 (2020). https://doi.org/10.1007/s12665-020-8847-2

> Impact factor JCR: 2,18 out of 7,913; Position: 43 out of 94 (Q2) in the Water resources area. / Factor de impacto JCR: 2,18 de 7,913; Posición: 43 de 94 (Q2) en el área de Recursos hídricos.

Baena-Ruiz, L., Pulido-Velazquez, D. GIS-SWIAS: tool to summarize seawater intrusion status and vulnerability at aquifer scale. Scientific Programming. Scientific Programming (2021). https://doi.org/10.1155/2021/8818634.

> Impact factor JCR: 0,963 out of 7,707; Position: 86 out of 108 (Q4) in the Computer science, software engineering area. / Factor de impacto JCR: 0,963 de 7,707; Posición: 86 de 108 (Q4) en el área de Ciencias de la computación, ingeniería de software

Baena-Ruiz, L.; Pulido-Velazquez, D. A Novel Approach to Harmonize Vulnerability Assessment in Carbonate and Detrital Aquifers at Basin Scale. Water 2020, 12, 2971. https://doi.org/10.3390/w12112971

> Impact factor JCR: 2,544 out of 9,13; Position: 31 out of 94 (Q2) in the Water resources area. / Factor de impacto JCR: 2,544 de 9,13; Posición: 31 de 94 (Q2) en el área de Recursos hídricos.
>
> This paper has been included in “Editor’s choice” section in Water (MDPI). Este paper ha sido incluido en la sección “Editor’s choice” de la revista Water (MDPI).

Baena-Ruiz, L.; Pulido-Velazquez, D.; Collados-Lara, A.-J.; Gómez-Gómez, J.-d.-D. A Preliminary Lumped Assessment of Pollution Risk at Aquifer Scale by Using the Mean Residence Time. Analyses of Potential Climate Change Impacts. Water 2021, 13, 943. https://doi.org/10.3390/w13070943

> Impact factor JCR: 2,544 out of 9,13; Position: 31 out of 94 (Q2) in the Water resources area. / Factor de impacto JCR: 2,544 de 9,13; Posición: 31 de 94 (Q2) en el área de Recursos hídricos.

Financiación

Esta tesis doctoral ha sido posible gracias a la concesión de varios contratos asociados a proyectos competitivos (nacionales y europeos) en el Instituto Geológico y Minero de España. En concreto, un contrato de dos años de duración con el programa de Garantía Juvenil financiado por el Ministerio de Economía y Competitividad de España junto con fondos del Banco Europeo de Inversiones y el Fondo Social Europeo, en el marco del proyecto "Generación, simulación e integración de escenarios hidrológicos futuros en el análisis de impactos y estrategias de adaptación al cambio global en sistemas de recursos hídricos"; un contrato de trece meses de duración adscrito al proyecto GeoE.171.008-TACTIC del Programa de Financiación de Investigación e Innovación de la Unión Europea "Horizonte 2020"; y un contrato de 12 meses de duración adscrito al proyecto SIGLO-AN (RTI2018-101397-B-I00) del Ministerio de Ciencia, Innovación y Universidades de España.

Tabla de contenidos

Listado de figuras

Listado de tablas

Resumen extendido

La contaminación del agua subterránea es un problema a nivel mundial, afectando a numerosos acuíferos y al suministro procedente de los mismos, así como a ecosistemas de alto valor ecológico. La contaminación de las masas de agua subterráneas está relacionada con los usos del suelo, y depende tanto de la vulnerabilidad de los acuíferos a la contaminación, como del funcionamiento del sistema y la capacidad de renovación del mismo (Zwahlen 2003). Además, en zonas costeras, los acuíferos pueden experimentar problemas de contaminación por intrusión marina asociada normalmente con la sobreexplotación de los mismos (Custodio 2010; García-Menéndez et al. 2016). La intrusión marina incrementa la salinidad del agua subterránea disminuyendo la disponibilidad de agua dulce y deteriorando los ecosistemas dependientes.

Los problemas en las aguas subterráneas no sólo proceden de la contaminación, sino también de los impactos sobre la disponibilidad del recurso debido a la sobreexplotación de los acuíferos. Factores como la actividad agraria de regadío en grandes extensiones y el aumento de la población estacional en ciertas zonas producen un incremento de las presiones en los recursos hídricos subterráneos que resultan insostenibles en el tiempo. Esta sobreexplotación de las masas de agua subterránea está condicionada por la escasez de agua superficial, problema que se agrava como consecuencia del cambio climático (CC) (Tramblay et al., 2020).

De acuerdo con la Directiva Marco del Agua (DMA, EU 2000) y la Directiva 2006/118/CE relativa a la protección de las aguas subterráneas contra la contaminación y el deterioro (Directiva Hija de Aguas subterráneas) (EU 2006), es fundamental que las aguas subterráneas alcancen un buen estado químico y cuantitativo, con el fin de proteger la salud humana, los ecosistemas naturales y garantizar el suministro del recurso. A partir de la incorporación de esta normativa ha aumentado la necesidad de desarrollar metodologías que permitan caracterizar de una manera rápida y sencilla las masas de agua subterráneas con el fin de identificar aquellas que se encuentren en riesgo por algún tipo de presión (Ballesteros et al. 2016). Así mismo, se requiere el seguimiento y evaluación del estado y la vulnerabilidad de las masas de agua subterráneas para garantizar el cumplimiento de los objetivos marcados mediante estrategias de gestión sostenibles.

La DMA tiene como objeto no sólo mejorar el estado de los sistemas acuáticos si no también la protección de los mismos a largo plazo contribuyendo a un uso del agua sostenible.

En una situación de globalización y de clima cambiante como en la que nos encontramos, y teniendo en cuenta los retos planteados por la DMA, es necesario diseñar estrategias de adaptación que nos permitan adelantarnos a posibles situaciones futuras mediante una gestión sostenible, identificando los riesgos y proponiendo medidas para paliar sus efectos (Iglesias y Garrote 2015)

Los estudios de CC estiman que se producirá una modificación en la distribución espaciotemporal de las variables climáticas e hidrológicas, efecto que ya se aprecia en los últimos años en la Península. En concreto, para las cuencas mediterráneas, se espera una importante disminución de los recursos debido al aumento de la frecuencia de periodos de sequía con el consecuente impacto ambiental, económico y social (Iglesias et al, 2017). Una disminución de la precipitación junto con un probable aumento de la temperatura producirá grandes impactos futuros en la recarga de los acuíferos (Pulido-Velázquez et al., 2017). Este hecho, unido a un incremento de las extracciones de agua subterránea debido a la escasez de recursos superficiales, supondría un significativo deterioro tanto cuantitativo como cualitativo de las masas de aguas subterráneas.

Para el análisis de los impactos hidrológicos futuros del CC es necesario contar con modelos previamente calibrados para propagar el efecto de las variables climáticas en las variables hidrológicas. Se precisa simular series climáticas futuras generadas a escala local a partir del reescalado de las simulaciones con modelos climáticos (Collados-Lara et al. 2018).

Además de la caracterización del estado global de las masas de agua, para el diseño de estrategias de adaptación sostenibles también es necesario evaluar la vulnerabilidad de las mismas a la contaminación. El grado de protección precisado por las masas de agua subterráneas depende de

la vulnerabilidad intrínseca, que se define como la susceptibilidad de los acuíferos a la contaminación por acción antrópica (Foster 1987). Cuando en la evaluación de la vulnerabilidad se introducen factores relativos a un contaminante determinado se habla de vulnerabilidad específica (Vrba and Zaporozec 1994).

Existen numerosas metodologías para evaluar la vulnerabilidad intrínseca, desde modelos de simulación basados en procesos físicos hasta técnicas basadas en índices. Estos últimos tienen un coste computacional mucho menor que los anteriores y los datos requeridos para su aplicación suelen estar disponibles para cualquier caso de estudio (Kumar et al 2015). Atendiendo a las metodologías basadas en índices, se han desarrollado diferentes aproximaciones. Algunos son aplicables a cualquier tipo de acuífero, como DRASTIC (Aller et al. 1987), mientras que otros son específicos para sistemas acuíferos concretos, como el método COP para acuíferos kársticos (Vias et al. 2006). A pesar de que el método DRASTIC se desarrolló para evaluar la vulnerabilidad en cualquier tipo de acuífero, numerosas investigaciones han puesto de manifiesto que su uso no es siempre adecuado en acuíferos kársticos (Panagopoulos et al. 2006; Jiménez-Madrid et al. 2013). También existen métodos específicos para evaluar la vulnerabilidad a la intrusión como por ejemplo GALDIT (Chachadi y Lobo-Ferreira 2005). Estas metodologías basadas en índices consisten en la combinación de mapas de propiedades intrínsecas y/o de los contaminantes que se evalúan, obteniendo el índice de vulnerabilidad mediante la asignación de una puntuación a cada variable. Los índices suelen dividirse en rangos que determinan el grado de vulnerabilidad de la masa de agua y se representan espacialmente en forma de mapas para identificar las zonas más susceptibles a la contaminación. Bajo este enfoque, los distintos métodos en ocasiones dan lugar a resultados muy diferentes e incluso contradictorios en una misma zona de estudio, siendo difícil la comparación y validación de los resultados (Gogu et al., 2003). Por este motivo surge la necesidad de unificar criterios y proponer metodologías de aplicación general para la evaluación de la vulnerabilidad en diferentes tipologías de acuíferos, que permita comparar resultados con el objetivo de establecer medidas prioritarias en la gestión a escala de cuenca.

Los mapas de vulnerabilidad obtenidos con los métodos expuestos deben ser validados para evaluar la fiabilidad de los resultados. En la literatura se encuentran diferentes técnicas de validación de los mapas de vulnerabilidad como por ejemplo correlación con contaminantes (Huan et al 2012), tiempo de tránsito por la zona no saturada zone (Neukum et al 2007; Zivanovic et al 2016), modelos de transporte de contaminantes (Neukum and Azzam 2009; Yu et al 2015) o mediante la determinación del tiempo de residencia de forma distribuida (Dedewanou et al 2015; Schwartz 2006). Estos métodos, aunque ofrecen una gran precisión, presentan limitaciones, especialmente en referencia a la escala de aplicación, disponibilidad de los datos necesarios para su aplicación y coste computacional. Cuando se trata de un estudio a escala regional resulta imposible aplicar un mismo método en todos los acuíferos y, por tanto, comparar los resultados, debido a los inconvenientes mencionados. Un método agregado, sin embargo, permite realizar una evaluación preliminar y puede ser aplicado en zonas de gran extensión con información limitada, permitiendo comparar el estado global y la vulnerabilidad de diferentes acuíferos.

Una adecuada gestión de las aguas subterráneas debe atender no sólo a cuestiones relacionadas con la calidad del agua, sino también a la protección de la cantidad de recurso/reservas disponibles (DMA, 2000). El conocimiento de variables como la capacidad de renovación del agua subterránea en los acuíferos, servirá de ayuda en el proceso de toma de decisiones en la planificación y gestión de los recursos hídricos subterráneos, así como para identificar problemas relacionados con el estado cualitativo y cuantitativo de los ecosistemas dependientes (Newman et al. 2010). Los acuíferos que tienen un tiempo de renovación pequeño son más vulnerables a la explotación (Pulido-Velázquez et al. 2020; Martos-Rosillo et al. 2013), situación que se verá agravada en el futuro debido al cambio climático. El tiempo de renovación también está relacionado con la resiliencia de los sistemas a periodos de explotación intensiva, aspecto clave para la identificación de acuíferos estratégicos para la gestión de sequías y para la definición de estrategias de adaptación al CC.

Esta investigación pretende contribuir al avance del conocimiento en algunas lagunas identificadas en la literatura en relación con la caracterización del estado global, vulnerabilidad y riesgo a la contaminación de las masas de agua subterráneas. Se analizan tanto periodos históricos, como potenciales impactos de escenarios futuros de CC, con el objetivo de generar información para identificar/valorar medidas de gestión sostenibles (medidas de adaptación). Se plantean metodologías simples basadas en índices, que permiten una evaluación rápida y sencilla a partir de un limitado número de datos disponibles, obteniendo una primera aproximación del estado global y vulnerabilidad de las masas de agua subterráneas. La información generada ayuda a identificar recursos/reservas estratégicas y/o vulnerables, y a la definición de medidas para una gestión sostenible. La metodología propuesta ha sido implementada en ArcGIS mediante el desarrollo de tres modelos en el entorno "Model Builder". Esta herramienta permite realizar los cálculos necesarios para determinar los índices propuestos en un instante de tiempo determinado, su evolución en un periodo histórico o en potenciales escenarios futuros de cambio climático. Existen otras herramientas para evaluar la intrusión en un acuífero, pero ninguno de ellas permite analizar conjuntamente la evolución del estado global y la vulnerabilidad a la intrusión, proporcionando resultados amigables en forma de gráficos, estadísticos y series temporales. Esta tesis también contribuye al avance en la armonización de metodologías de análisis de la vulnerabilidad y riesgo a la contaminación, así como su validación de manera agregada a escala de acuífero. Finalmente, se propone un novedoso análisis agregado del riesgo a la contaminación a partir del tiempo de renovación medio del acuífero, que permite obtener una primera aproximación sobre la sostenibilidad de la explotación del sistema ante escenarios históricos y potenciales escenarios futuros de CC. Esta metodología, que ha sido empleada en un caso de estudio a escala de cuenca, puede ser aplicable a un amplio número de acuíferos ya que utiliza datos frecuentemente disponibles en la mayoría de los casos.

De acuerdo con las motivaciones expuestas, la finalidad de esta tesis doctoral es el desarrollo de metodologías que permitan analizar de forma agregada, el estado global y la vulnerabilidad de las masas de agua subterránea y evaluar el impacto de potenciales escenarios de CC con el fin de poder establecer medidas de gestión sostenibles en el futuro. Para demostrar su utilidad, estas metodologías se aplican a varios casos de estudio, a escala de acuífero y de cuenca. Dentro de este objetivo general se pueden distinguir los siguientes objetivos específicos:

(1) Propuesta de metodología basada en índices para sintetizar el estado global y la vulnerabilidad a la intrusión en acuíferos costeros.
(2) Análisis del impacto de potenciales escenarios futuros de cambio global (CG) en el estado y vulnerabilidad de acuíferos costeros.
(3) Desarrollo de una herramienta automática en entorno ArcGIS para facilitar la aplicación de la metodología propuesta de análisis y síntesis del estado global y la vulnerabilidad a la intrusión a escala de acuífero.
(4) Estudio de la vulnerabilidad a la contaminación de masas de agua subterráneas en sistemas a escala de cuenca. Armonización de la evaluación mediante una metodología aplicable a acuíferos detríticos y kársticos.
(5) Análisis agregado del riesgo a la contaminación a partir del tiempo de renovación medio del acuífero. Estudio de impactos del CC en la sostenibilidad de la explotación de los sistemas analizados.

Los objetivos de esta tesis incluyen aspectos metodológicos y su aplicación a casos de estudio concretos, que permiten evaluar la utilidad de las metodologías propuestas. Como casos de estudio para el análisis del estado global y la vulnerabilidad a la intrusión, se han seleccionado dos acuíferos mediterráneos costeros con problemas de salinización debido a la sobreexplotación (Plana de Oropesa y Torreblanca y Plana de Vinaroz). La metodología propuesta para armonizar la evaluación de la vulnerabilidad en diferentes tipologías de acuíferos y el análisis agregado del riesgo a la contaminación se ha aplicado en la Cuenca del Alto Guadiana. Esta cuenca integra ocho masas de agua subterráneas incluyendo acuíferos de diferente tipología, con graves problemas de contaminación por nitratos. Además, algunos de ellos sometidos a una explotación intensiva, lo que ha llevado al deterioro de ecosistemas dependientes de alto valor ecológico

(humedales RAMSAR). En la cuenca del Alto Guadiana se analizan también potenciales impactos del CC en el riesgo a la contaminación. Estos casos de estudio se describen en los distintos capítulos de la tesis.

Las principales contribuciones de esta tesis doctoral son:

- Propuesta de metodología basada en índices para sintetizar el estado global y la vulnerabilidad a la intrusión en acuíferos costeros.

Se ha propuesto un nuevo método para el análisis, a escala de acuífero, del estado global y vulnerabilidad a la intrusión en acuíferos costeros a partir de un análisis mixto agregado-distribuido. El método está basado en un enfoque conceptual de la intrusión que permite sintetizar los resultados de una manera visual a escala de acuífero. Se proponen índices que se obtienen a partir de información sobre la geometría del acuífero y datos históricos de monitoreo (concentración de cloruros y nivel piezométrico). El método no requiere la implementación de modelos complejos y se puede aplicar incluso en casos de estudio con un reducido número de datos disponibles. Esta aproximación requiere estimar previamente mapas con la distribución de la concentración media del ion cloruro en el acuífero en el periodo histórico a considerar. Estos mapas se pueden obtener mediante interpolación espacial de datos procedentes de las redes de observación o, de forma más precisa, mediante un modelo de densidad variable. Para identificar la zona afectada por intrusión es necesario fijar un umbral de concentración de cloruros, que, dependiendo del objetivo perseguido, puede ser el fondo geoquímico natural, o cualquier umbral definido como aceptable para usos específicos del agua (el valor considerado para consumo humano, o incluso cualquier otro valor de referencia establecido por las autoridades competentes). Combinando el mapa de concentración de cloruros con el espesor saturado en el acuífero, y teniendo en cuenta el umbral establecido, se puede calcular el volumen de recurso afectado y no afectado por intrusión. Estos volúmenes se representan en forma de sección conceptual mediante rectángulos definidos por el Espesor afectado (T_{ha}) y la Penetración (P) de la intrusión en sentido perpendicular a la costa. La intensidad de la intrusión en esa zona queda definida por el Incremento de concentración (IC) por encima del umbral establecido, calculado como la diferencia entre la concentración de cloruros en el volumen afectado y dicho valor de referencia. El producto de espesor afectado, penetración de la intrusión e incremento de concentración da como resultado la Masa de la zona afectada (Ma), que se define como la masa total adicional de cloruros que tiene una concentración por encima del umbral establecido. Este índice agregado (Ma) permite analizar la evolución del estado global de intrusión en un acuífero, así como comparar el estado de diferentes acuíferos con el fin de establecer medidas prioritarias en la gestión. Los resultados de esta metodología se presentan mediante mapas y secciones transversales representativas de valores instantáneos o medios en un periodo determinado, así como series temporales de índices agregados para todo el acuífero. Las series temporales permiten además analizar la evolución del problema de manera agregada, así como la resiliencia y tendencia de la intrusión en el acuífero. La Resiliencia se ha definido como el máximo cambio relativo del índice Ma en un periodo de seis años, de acuerdo con los horizontes de los planes de gestión. La Tendencia se calcula como la diferencia relativa entre los valores de Ma al principio y final del periodo de seis años. Así, la Resiliencia muestra el cambio potencial a corto plazo, mientras que la Tendencia indica la evolución de la masa afectada en el periodo temporal considerado. El análisis de la vulnerabilidad a la intrusión se realiza de manera análoga, pero en lugar de emplear la concentración de cloruros como indicador, se utiliza el valor de la vulnerabilidad previamente calculado mediante el método GALDIT. En este caso se propone usar como umbral el valor de vulnerabilidad a partir del cual la vulnerabilidad es alta (esto es, GALDIT≥7,5). El índice de vulnerabilidad agregado L_GALDIT se define como el valor de vulnerabilidad (índice GALDIT) ponderado por el volumen en cada celda o zona del acuífero. Este método puede ser útil para identificar acuíferos en riesgo de no alcanzar los objetivos de la DMA y permite comparar el problema de intrusión en varios acuíferos y en diferentes periodos temporales. Se ha aplicado en los acuíferos Plana de Oropesa-Torreblanca y Plana de Vinaroz, en la provincia de Castellón, dos acuíferos costeros con graves problemas de intrusión. Los resultados muestran que, aunque la Plana de Oropesa-Torreblanca se encuentra más afectada que

la Plana de Vinaroz en términos de concentración de cloruros, tiene una capacidad de recuperación mayor, aunque ello requeriría cambios importantes en la explotación. Además, la Plana de Oropesa-Torreblanca presenta una mayor vulnerabilidad a la intrusión, tanto en términos de magnitud como en extensión de la misma. La Plana de Vinaroz también es vulnerable en toda su extensión, aunque con vulnerabilidad moderada, y sólo una parte del acuífero se encuentra afectada con altas concentraciones de cloruros.

- Análisis del impacto de potenciales escenarios futuros de cambio global (CG) en el estado y vulnerabilidad de acuíferos costeros.

En el acuífero costero Plana de Oropesa-Torreblanca, que presenta graves problemas de contaminación por intrusión marina, se analizan los impactos de varios escenarios de CG (incluyendo CC y medidas de adaptación) en el estado global y vulnerabilidad a la intrusión. Las medidas de adaptación incorporan recursos complementarios en el sistema de acuerdo con el desarrollo urbanístico. Para la evaluación de los impactos de los escenarios de CG se utiliza un modelo de densidad variable, que es alimentado con los resultados de una cadena de modelos que simulan recarga, necesidades hídricas de los cultivos y retorno de regadíos, previamente calibrados en este acuífero. Esto permite extraer concentración de cloruros y niveles piezométricos para los potenciales escenarios futuros. Los escenarios de CC fueron generados mediante el ensamblado de diferentes proyecciones locales. Se definió un escenario futuro de usos del suelo teniendo en cuenta el planeamiento urbanístico de la zona. Mediante la combinación de los escenarios de CC con el escenario de usos de suelo se generaron cuatro escenarios de CG. La metodología basada en índices desarrollada para sintetizar la dinámica de la intrusión en un acuífero (primer objetivo descrito) se combina con los resultados del modelo para evaluar el impacto de los potenciales escenarios de CG en términos de intrusión y vulnerabilidad a escala de acuífero, teniendo en cuenta que, en lugar de una única serie histórica, tenemos múltiples potenciales series equiprobables. Esta metodología permite comparar el impacto medio sobre la intrusión de los diferentes escenarios futuros para un determinado horizonte temporal. Se analiza además la influencia del CC en los escenarios de CG mediante un análisis de sensibilidad comparando los escenarios de CG con un escenario que sólo incluye las medidas de adaptación suponiendo que no hay CC. Para analizar la dinámica temporal del índice agregado que sintetiza el estado global (Ma) en el futuro se propone un nuevo índice, Recovery rate, definido como la reducción media del índice Ma en un periodo determinado, que representa la velocidad de recuperación media del sistema en el horizonte temporal fijado. Los resultados muestran que los escenarios de CG producirán una mayor variabilidad en el estado global y vulnerabilidad a la intrusión. El análisis de impactos de escenarios de CG muestra el efecto de las medidas de adaptación para hacer frente al aumento de las necesidades hídricas en el futuro, aunque otras medidas de adaptación complementarias serán necesarias para afrontar el CC.

- Desarrollo de una herramienta automática en entorno ArcGIS para facilitar la aplicación de la metodología propuesta de análisis y síntesis del estado global y la vulnerabilidad a la intrusión a escala de acuífero.

Se ha desarrollado una nueva herramienta de ArcGIS, GIS-SWIAS (GIS tool to analyse SeaWater Intrusion status and vulnerability at Aquifer Scale), que implementa la metodología anterior para el análisis del estado global y vulnerabilidad a la intrusión a escala de acuífero. Se trata de una herramienta amigable que puede ser utilizada en cualquier caso de estudio, completamente integrada en el entorno ArcGIS. Es la primera herramienta en la literatura para realizar un análisis de este tipo en ArcGIS. Es de fácil manejo y es capaz de realizar gran cantidad de operaciones con alto coste computacional de manera eficiente. La herramienta proporciona resultados en forma de mapas y secciones transversales, series temporales y estadísticos para mostrar la intensidad, magnitud y evolución temporal de la intrusión en un acuífero en instantes de tiempo determinados o en un periodo temporal. La herramienta se compone de tres modelos desarrollados en Model Builder de ArcGIS: el primer modelo realiza los cálculos para obtener el mapa distribuido de concentración de cloruros en el acuífero; el segundo modelo realiza los cálculos para obtener un mapa distribuido de nivel piezométrico; el tercer modelo genera la sección

representativa del acuífero identificando la zona afectada y una tabla en formato .xlsx con los estadísticos de las variables que resumen el estado global del acuífero ante el problema de intrusión (T_{ha}, P, Ma, entre otros). Además, si se analizan diferentes instantes de tiempo, este último modelo también proporciona un gráfico mostrando la evolución de las variables P, T_{ha}, porcentaje de volumen afectado, concentración de cloruros en el acuífero y el índice Ma. Esta herramienta se puede utilizar para analizar la intrusión en casos en los que no hay disponible un modelo de flujo, mediante la interpolación de datos de monitoreo, aunque si se dispone de información de concentración de cloruros y nivel piezométrico de un modelo previamente calibrado, la herramienta permite también analizar la sostenibilidad de escenarios de gestión futuros. Dada su versatilidad, GIS-SWIAS es una herramienta útil tanto para investigadores como técnicos para analizar la intrusión a escala de acuífero bajo diferentes escenarios, lo que puede ser de ayuda en el proceso de toma de decisiones para la selección de estrategias de gestión sostenibles. Esta herramienta ha sido probada para el análisis histórico y de escenarios futuros en los acuíferos Plana de Oropesa-Torreblanca y Plana de Vinaroz.

- Estudio de la vulnerabilidad a la contaminación de masas de agua subterráneas en sistemas a escala de cuenca. Armonización de la evaluación mediante una metodología aplicable a acuíferos detríticos y kársticos.

Se ha realizado un análisis de la vulnerabilidad a la contaminación en las masas carbonatadas de la Cuenca Alta del río Guadiana aplicando dos métodos conocidos, DRASTIC y COP. El método DRASTIC ha sido aplicado en estudios previos a cualquier tipo de acuífero, mientras que el método COP fue diseñado específicamente para acuíferos carbonatados. Estos métodos muestran resultados muy diferentes en algunos de los acuíferos analizados. Debido a que la validación de los mapas de vulnerabilidad obtenidos muestra una mayor fiabilidad del método COP en la zona de estudio, se propone realizar una optimización del método DRASTIC con el fin de poder extender el análisis de vulnerabilidad a todas las masas de la Cuenca del Alto Guadiana, incluyendo las detríticas, y obtener resultados que sean comparables entre los distintos acuíferos. Este enfoque es análogo a la hipótesis del medio poroso equivalente que se utiliza para aplicar en acuíferos kársticos soluciones numéricas desarrolladas para acuíferos detríticos. Este intento de armonización del método DRASTIC se resuelve mediante un problema de optimización que combina análisis estadístico espacial y minería de datos para encontrar una solución óptima del problema. Las funciones objetivo de este problema son maximizar la coincidencia en la clasificación de la vulnerabilidad con el método COP y minimizar la distancia entre las clases de vulnerabilidad de DRASTIC y COP. Las variables de decisión en el problema de optimización son (1) los rangos del índice DRASTIC y de sus parámetros numéricos y (2) los pesos de los parámetros de DRASTIC. El dominio de búsqueda de la solución óptima se compone de un número finito de combinaciones de la clasificación de DRASTIC y de cada uno de sus parámetros numéricos. Las distintas clasificaciones se establecen en función de criterios estadísticos según la distribución de los datos en el área de estudio. El valor de los pesos para cada parámetro varía entre 1 y 5, siguiendo la propuesta original del método DRASTIC. El problema se divide en dos pasos para su resolución. Primero se realiza una optimización de los rangos de DRASTIC y de sus parámetros mediante la combinación de todas las clasificaciones posibles definidas anteriormente. Debido a la gran cantidad de combinaciones posibles que se generan al variar uno a uno los parámetros del índice DRASTIC, se aplica un algoritmo sencillo de árboles de decisión para delimitar el dominio del problema en el segundo paso. En este segundo paso se realiza una optimización del peso de cada parámetro de DRASTIC para aquellas combinaciones seleccionadas en el paso anterior. La solución óptima (O-DRASTIC) encontrada para los acuíferos carbonatados, que tiene un porcentaje de coincidencia del 75% con los resultados de COP para estos acuíferos, fue probada en también en los acuíferos detríticos de la cuenca, mostrando una mejora significativa en los resultados de validación de los mapas de vulnerabilidad con respecto al método original. Un análisis de sensibilidad realizado sobre los cambios en los parámetros de la solución óptima frente al método original revela la influencia de algunas características intrínsecas de los acuíferos en la magnitud de la vulnerabilidad.

- Análisis agregado del riesgo a la contaminación a partir del tiempo de renovación medio del acuífero. Estudio de impactos del CC en la sostenibilidad de la explotación de los sistemas analizados.

Se propone un nuevo método que permite realizar una primera estimación y/o validación agregada del riesgo a la contaminación de un acuífero a partir del tiempo medio de residencia del agua subterránea en el mismo, estimado preliminarmente con un índice agregado sencillo (T=Almacenamiento/recarga media). El riesgo a la contaminación se calcula combinando el mapa de vulnerabilidad (obtenido aplicando el método DRASTIC optimizado anteriormente, O-DRASTIC) y los usos del suelo que determinan la potencial amenaza de contaminación. El mapa de riesgo distribuido en el acuífero se pondera por la superficie del mismo para obtener el índice agregado L-RISK, que evalúa el riesgo a la contaminación a escala de acuífero. Estos dos índices agregados se emplearon para calibrar un modelo de regresión lineal basado en la hipótesis de que un tiempo de residencia corto está relacionado con un mayor riesgo a la contaminación. Se probaron diferentes transformaciones de las variables L-RISK y T para determinar el modelo que ofrece una mejor correlación en los ocho acuíferos de estudio en la Cuenca del Alto Guadiana. Este modelo permite analizar un gran número de acuíferos utilizando datos frecuentemente disponibles. El método es útil para identificar potenciales acuíferos estratégicos para establecer medidas de gestión sostenibles de los recursos hídricos subterráneos, especialmente durante periodos de sequía. Además, también permite realizar un análisis preliminar del impacto del CC en el índice L-RISK. Los resultados muestran una amplia variabilidad del índice T en los distintos acuíferos (8-76 años). Aquellos que tienen un índice T mayor pueden considerarse como recursos subterráneos estratégicos. El análisis futuro muestra un incremento en el valor medio de T (entre un 8 y 44%) y un descenso del índice L-RISK en todos los acuíferos (1-18%).

Como en todo trabajo de investigación, para el desarrollo de esta tesis ha sido necesario establecer ciertas hipótesis que conllevan algunas limitaciones. A continuación, se exponen las principales limitaciones, las cuales ayudan a identificar futuras líneas de investigación.

- La metodología propuesta para el análisis del estado global y vulnerabilidad a la intrusión no es aplicable en acuíferos en pequeñas islas, en las que la intrusión presenta una distribución particular. Como línea futura se plantea la adaptación de la misma para el estudio de estos casos.

- La identificación de la zona afectada por intrusión, se ha llevado a cabo a partir del umbral de concentración de cloruros establecido para las aguas de consumo humano y los valores de referencia determinados por la Confederación para la evaluación del estado químico de las masas de agua subterráneas. Como futura línea de investigación, teniendo en cuenta las significativas diferencias resultantes de la aplicación de diferentes métodos descritos en la literatura, se propone avanzar en la identificación de una aproximación que permita homogeneizar criterios para la definición del fondo hidrogeoquímico y los valores umbrales, y que sea aplicable de forma general.

- La optimización del método DRASTIC desarrollada con el objetivo de armonizar resultados para cualquier tipo de acuífero ha sido aplicada en los ocho acuíferos de la cuenca del Alto Guadiana. Como trabajo futuro se plantea verificar la aplicabilidad de la solución óptima obtenida en otros casos de estudio.

- La validez del modelo de regresión propuesto para el análisis del riesgo a la contaminación a partir del tiempo de residencia medio también podría ser estudiada en otros casos de estudio.

- En el análisis del riesgo a la contaminación en la cuenca del Alto Guadiana no se han tenido en cuenta variables como el grado de fertilización aplicada a cada cultivo, tipo de regadío ni los procesos de lixiviación del nitrógeno. En el futuro se plantea considerarlos en algunos acuíferos piloto de la cuenca, analizando y modelando los procesos físico-químicos que afectan al transporte de contaminantes tanto en la zona saturada como no saturada.

- En relación con la estimación del tiempo medio de residencia del agua subterránea, además de testear otros índices agregados sencillos, se propone realizar en algunos casos piloto una

evaluación distribuida más precisa mediante la calibración de modelos de flujo y transporte en los que se integre información sobre edades del agua deducida de ensayos previos con trazadores.

- Para propagar los impactos del CC se utilizan modelos previamente calibrados (recarga, requerimiento de cultivos, modelos de flujo), en los que se asume que los parámetros permanecen invariantes en los horizontes futuros, manteniendo la relación entre los inputs y outputs identificada en el periodo histórico.

- Los escenarios futuros de CC simulados corresponden al escenario de emisiones más pesimista (RCP 8.5) publicado en el último informe del IPCC (AR5). Sería interesante evaluar otros escenarios más probables.

Palabras clave: hidrología, recursos hídricos, contaminación de aguas subterráneas, vulnerabilidad a la contaminación, intrusión, métodos basados en índices, cambio climático

Referencias

Aller, L.; Bennett, T.; Lehr, J.H.; Petty, R.J.; Hackett, G. DRASTIC: A Standardized Method for Evaluating Ground Water Pollution Potential Using Hydrogeologic Settings; NWWA/Epa-600/2-87-035; Kerr Environmental Research Laboratory, Office of Research and Development, US Environmental Protection Agency: Washington, DC, USA, 1987.

Ballesteros BJ, Morell I, García-Menéndez O, Renau-Pruñonosa A (2016) A standardized index for assessing seawater intrusion in coastal aquifers: the SITE index. Water Resour Manag 30(13):4513–4527. https://doi. org/10.1007/s11269-016-1433-4

Chachadi AG, Lobo-Ferreira JP (2005) Assessing aquifer vulnerability to sea-water intrusion using GALDIT method: part 2 – GALDIT indicator descriptions. IAHS and LNEC, Proceedings of the 4th The Fourth Inter Celtic Colloquium on Hydrology and Management of Water Resources, eld at Universidade do Minho, Guimarães, Portugal, July 11–13, 2005.

Collados-Lara, A. J., Pulido-Velazquez, D., & Pardo-Igúzquiza, E. (2018). An integrated statistical method to generate potential future climate scenarios to analyse droughts. Water, 10(9), 1224.

Custodio E (2010) Coastal aquifers of Europe: an overview. Hydrogeol J 18:269–280

Dedewanou, M.; Binet, S.; Rouet, J.L.; Coquet, Y.; Bruand, A.; Noel, H. Groundwater Vulnerability and Risk Mapping Based on Residence Time Distributions: Spatial Analysis for the Estimation of Lumped Parameters. Water Resour. Manag. 2015, 29, 5489–5504, doi:10.1007/s11269-015-1130-8.

EU, 2000. Water framework directive, 2000, Directive 2000/60/EC of the European parliament and the council of 23 October 2000. Establishing a framework for community action in the field of water policy. In: E. Commission (Ed.), Official Journal of the European Communities, pp. L 327/1.

EU, 2006. Groundwater directive, 2006, directive 2006/118/EC of the European parliament and the council of 12 December 2006. On the protection of groundwater against pollution and deterioration. In: E. Commission (Ed.), Official Journal of the European Union, pp. L 372/19.

Foster, S.S.D. Fundamental concepts in aquifer vulnerability, pollution risk and protection strategy. Hydrol. Resour. Proc. Inf. 1987, 38, 69–86.

García-Menéndez O, Morell I, Ballesteros BJ, Renau-Pruñonosa A, Esteller MV (2016) Spatial characterization of the seawater upconing process in a coastal Mediterranean aquifer (Plana de Castellón, Spain): evolution and controls. Environ Earth Sci 75:728. https://doi.org/10.1007/s12665-016-5531-7

Gogu, R.C.; Hallet, V.; Dassargues, A. Comparison of aquifer vulnerability assessment techniques. Application to the Nylon river basin (Belgium). Environ. Earth Sci. 2003, 44, 881–892, doi:10.1007/s00254-003-0842-x.

Huan, H.;Wang, J.; Teng, Y. Assessment and validation of groundwater vulnerability to nitrate based on a 638 modified DRASTIC model: A case study in Jilin City of northeast China. Sci. Total Environ. 2012, 440, 14–639 23.

Iglesias, A., & Garrote, L. (2015). Adaptation strategies for agricultural water management under climate change in Europe. Agricultural water management, 155, 113-124.

Iglesias, A., Garrote, L., Flores, F. et al. Challenges to Manage the Risk of Water Scarcity and Climate Change in the Mediterranean. Water Resour Manage 21, 775–788 (2007). https://doi.org/10.1007/s11269-006-9111-6

Jiménez-Madrid, A.; Carrasco, F.; Martínez, C.; Gogu, R.C. DRISTPI, a new groundwater vulnerability mapping method for use in karstic and non-karstic aquifers. Q. J. Eng. Geol. Hydrogeol. 2013, 46, 245–255, doi:10.1144/qjegh2012-038.

Kumar, P.; Bansod, B.K.; Debnath, S.K.; Thakur, P.K.; Ghanshyam, C. Index-based groundwater vulnerability mapping models using hydrogeological settings: A critical evaluation. Environ. Impact Assess. Rev. 2015, 51, 38–49, doi:10.1016/j.eiar.2015.02.001.

Martos-Rosillo, S.; Marín-Lechado, C.; Pedrera, A.; Vadillo, I.; Motyka, J.; Molina, J.L.; Ortiz, P.; Ramírez, J.M.M. Methodology to evaluate the renewal period of carbonate aquifers: A key tool for their management in arid and semiarid regions, with the example of Becerrero aquifer, Spain. Hydrogeol. J. 2013, 22, 679–689, doi:10.1007/s10040-013-1086-9.

Newman, B.D.; Osenbrück, K.; Aeschbach-Hertig, W.; Solomon, D.K.; Cook, P.; Rozanski, K.; Kipfer, R.; Aeschbach, W. Dating of 'young' groundwaters using environmental tracers: Advantages, applications, and research needs. Isot. Environ. Health Stud. 2010, 46, 259–278, doi:10.1080/10256016.2010.514339.

Neukum, C.; Azzam, R. Quantitative assessment of intrinsic groundwater vulnerability to contamination using numerical simulations. Sci. Total Environ. 2009, 408, 245–254, doi:10.1016/j.scitotenv.2009.09.046.

Neukum, C.; Hötzl, H.; Himmelsbach, T. Validation of vulnerability mapping methods by field investigations and numerical modelling. Hydrogeol. J. 2007, 16, 641–658, doi:10.1007/s10040-007-0249-y.

Panagopoulos, G.P.; Antonakos, A.K.; Lambrakis, N.J. Optimization of the DRASTIC method for groundwater vulnerability assessment via the use of simple statistical methods and GIS. Hydrogeol. J. 2006, 14, 894–911, doi:10.1007/s10040-005-0008-x.

Pulido-Velazquez, D., Collados-Lara, Antonio-Juan, Alcalá, Francisco J., 2017, Assessing impacts of future potential climate change scenarios on aquifer recharge in continental Spain. Journal of Hydrology. Published on line. https://doi.org/10.1016/j.jhydrol.2017.10.0770022-1694/

Pulido-Velazquez, D.; Romero, J.; Collados-Lara, A.-J.; Alcalá, F.J.; Fernández-Chacón, F.; Baena-Ruiz, L. Using the Turnover Time Index to Identify Potential Strategic Groundwater Resources to Manage Droughts within Continental Spain. Water 2020, 12, 3281, doi:10.3390/w12113281.

Schwartz, M.O. Numerical modelling of groundwater vulnerability: The example Namibia. Environ. Earth Sci. 2006, 50, 237–249, doi:10.1007/s00254-006-0204-6.

Tramblay, Yves & Koutroulis, Aristeidis & Samaniego, Luis & Vicente-Serrano, Sergio & Volaire, F. & Boone, Aaron & Le Page, Michel & Llasat, Maria & Albergel, Clement & Burak,

Selmin & Cailleret, Maxime & Cindric, Ksenija & Davi, Hendrik & Dupuy, Jean-luc & Greve, Peter & Grillakis, Manolis & Hanich, Lahoucine & Jarlan, Lionel & Martin-Stpaul, Nicolas & Polcher, Jan. Jordi Martinez-Vilaltaq, Florent Mouillote, David Pulido-Velazquez et al. (2020). Challenges for drought assessment in the Mediterranean region under future climate scenarios. Earth-Science Reviews. 210. 10.1016/j.earscirev.2020.103348.

Vías, J.M.; Andreo, B.; Perles, M.J.; Carrasco, F.; Vadillo, I.; Jiménez, P. Proposed method for groundwater vulnerability mapping in carbonate (karstic) aquifers: The COP method. Hydrogeol. J. 2006, 14, 912–925, doi:10.1007/s10040-006-0023-6.

Vrba J, Zaporozec A (1994) Guidebook on mapping groundwater vulnerability. IAH Int Contrib to Hydrogeol 16, Heise, Hannover, Germany, 131 pp

Yu, C.; Yao, Y.; Cao, G.; Zheng, C. A field demonstration of groundwater vulnerability assessment using transport modeling and groundwater age modeling, Beijing Plain, China. Environ. Earth Sci. 2014, 73, 5245–5253, doi:10.1007/s12665-014-3769-5.

Živanović, V.; Jemcov, I.; Dragišić, V.; Atanacković, N.; Magazinović, S. Karst groundwater source protection based on the time-dependent vulnerability assessment model: Crnica springs case study, Eastern Serbia. Environ. Earth Sci. 2016, 75, 1224, doi:10.1007/s12665-016-6018-2.

Zwahlen, F. COST Action 620 Vulnerability and Risk Mapping for the Protection of Carbonate (Karst) Aquifers Final Report; Office of the Official Publications of the European Communities: Brussels, Belgium, 2003; ISBN 928946416X.

Summary

Groundwater plays a significant role in the supply of water demands in many regions across the world, especially in arid and semiarid areas. The distribution of these groundwater resources and their quantity and quality characteristics depends on the interactions between anthropogenic activity, the hydrosphere, and climate conditions. They might produce negative impacts, not only in the availability of resources for different uses (human consumption, irrigation, etc.), but also in groundwater-dependent ecosystems (Kløve et al. 2014; Quevauviller 2007). Since 2000, after Water Framework Directive (WFD, EU 2000) came into effect, there has been an increase in the number of groundwater quality assessment studies, and, consequently, in the development of methodologies to quantify groundwater pollution. These methodologies intend to contribute in the identification of the groundwater bodies in risk of not achieving the WFD objectives (Ballesteros et al. 2016). Moreover, the protection of groundwater resources is a priority issue to be considered to achieve the sustainable management and maintenance of the good status of water bodies according to the WFD. The required degree of protection of groundwater resources from contaminants mainly depends on intrinsic vulnerability and pollution risk due to anthropogenic activity.

Both groundwater quality and vulnerability are affected by the climate. The future potential scenarios of Climate Change (CC) will also produce significant impacts on groundwater levels due to a decrease of the recharge and an increase in water requirements to supply agricultural and urban demand (Green et al. 2011; Pulido-Velazquez et al. 2018). The analysis of the impacts of CC on groundwater resources helps to identify and assess adaptation measures and to identify strategic groundwater bodies to define sustainable management strategies.

The target of this thesis is to develop methodologies to analyse the lumped global status and vulnerability of groundwater at aquifer scale. It intends to contribute in the harmonization of methods to assess groundwater vulnerability and risk to pollution. This thesis also introduces an analyses of potential impacts of future CC scenarios on the global status, vulnerability and risk to pollution. The contributions generated in the framework of this thesis has been published in the next SCI papers, which are summarised below:

(1) Global Assessment of Seawater Intrusion Problems (Status and Vulnerability). Water Resources Management. https://doi.org/10.1007/s11269-018-1952-2
(2) Summarizing the impacts of future potential global change scenarios on seawater intrusion at the aquifer scale. Environmental Earth Sciences. https://doi.org/10.1007/s12665-020-8847-2
(3) GIS-SWIAS: tool to summarize seawater intrusion status and vulnerability at aquifer scale. Scientific Programming. Accepted (awaiting publication)
(4) A Novel Approach to Harmonize Vulnerability Assessment in Carbonate and Detrital Aquifers at Basin Scale. Water. https://doi.org/10.3390/w12112971
(5) A Preliminary Lumped Assessment of Pollution Risk at Aquifer Scale by Using the Mean Residence Time. Analyses of Potential Climate Change Impacts. Water. https://doi.org/10.3390/w13070943

(1) A novel method to analyse the status and vulnerability of coastal aquifers to seawater intrusion (SWI) was proposed. It is based on a conceptual approach of intrusion that allows to summarised results in a visual way at aquifer scale. The results are presented as steady pictures (corresponding to instantaneous or mean values in a period), including maps and 2D conceptual cross-sections, and temporal series of lumped indices. This method allows coastal groundwater bodies at risk of not achieving good chemical status according to the Water Framework Directive to be identified. The indices are obtained from available information about aquifer geometry and historical monitoring data

(chloride concentration and hydraulic head data). This method does not require complex modelling and it may be applied even in cases where a reduced number of data are available. This approach requires to estimate distributed maps of chloride concentration in the historical period. Fields (maps) of chloride concentration and hydraulic head can be obtained by applying simple interpolation techniques in each date with enough available information. 3D maps of the saturated thickness (with a finite number of cells) can be obtained by combining hydraulic head maps with the geometry and the storage coefficient. Vertical aquifer geometry and storage coefficient can be obtained from previous 3D models and hydrogeological studies, respectively. If there is insufficient information to assess the vertical distribution of chloride concentration, an invariant concentration with depth is assumed at each point, thus obtaining 2D fields of chloride concentration. From chloride concentration and saturated thickness maps, we can define the affected and non-affected zone (areas where the chloride concentration level is above a reference level). 2D representative cross-sections can be deduced to summarise the mean geometry of the aquifer (thickness of the affected volume, T_{ha}, and penetration of the intrusion, P). The intensity of the intrusion is represented by the increment in concentration, which is defined as the difference between the chloride concentration in the affected volume and the threshold value of chloride. The lumped index Ma is defined as the total additional mass of chloride that causes the concentration in some areas to exceed the natural threshold. It is obtained multiplying the increment of concentration (IC) by Penetration (P) and affected Thickness (T_{ha}). While 2D maps and cross sections summarize the extent and magnitude of SWI in an aquifer at a specific time, Ma index shows the intensity and temporal evolution of the problem. The evolution of the Ma index can give an overall assessment of the resilience (R) and trend (T) of the aquifer status according to the SWI problem. We propose calculating Resilience as the maximum relative change of the Ma index (relative difference between maximum and minimum value) over six-year periods, which is the horizon defined to update management plans. Thus, Resilience shows the potential change for a short-term period, taking into account the measures occurred in this period. Trend is also calculated for six-year periods. It is defined as the relative difference between the values of Ma at the beginning and end of the period. A positive trend indicates the mass of water affected is increasing, while a negative trend indicates an improvement in aquifer status. The combination of Mass of affected water body (Ma), Resilience of the water body and Trend of SWI defines the MART index, which summarize SWI evolution in the aquifer. While SWI status is calculated using only physical variables (chloride concentration and hydraulic head), vulnerability employs weighted qualitative characteristics. In this study, we summarise vulnerability status based on the application of the GALDIT method (Aquifer type; aquifer hydraulic conductivity; height of groundwater head above sea level; distance from the shore; impact of existing status of SWI; thickness of aquifer being mapped). The GALDIT scores are classified into three vulnerability classes: High (GALDIT Index range ≥ 7.5), Moderate (between 5 and 7.5) and Low (< 5). These vulnerability classes are used to define the thresholds to identify the affected zone (area where vulnerability is higher than the adopted reference threshold (moderate or high vulnerability)). A lumped global value of GALDIT (L_GALDIT) is defined by weighting the GALDIT score for each point with the storage. This method to summarise SWI can be also useful to compare intrusion problemsin different aquifers and temporal periods. It has been applied to Plana de Oropesa-Torreblanca and Plana de Vinaroz aquifers, two Mediterranean coastal aquifers that present SWI problems. The results showed that Plana de Oropesa-Torreblanca aquifer has a worse status than Plana de Vinaroz. Resilience indicates that this aquifer has more potential to recover a good status, although it would require great changes in the current pumping management. Plana de Oropesa-Torreblanca aquifer is also the most vulnerable of the two aquifers, both in terms of its extent and magnitude.

(2) The impacts of future CC and Global Change (GC) scenarios on SWI are assessed in Plana de Oropesa-Torreblanca aquifer. Some adaptation measures have been integrated

in the definition of future GC scenarios. Measures to reduce aquifer demands (adaptation strategies are mainly focused on LULC changes in the area) and measures on the offer (eg. Water reuse) are applied to obtain complementary resources to supply demands. In order to assess the hydrological impacts of those climatic and management scenarios we simulate them within a modelling framework based on a density-dependent SEAWAT model whose inputs are defined by a sequential coupling of different models (rainfall-recharge models, crop irrigation requirements and irrigation return models). It allows to estimate hydraulic head and chloride concentration fields within the aquifer from the historical period and other potential scenarios. Representative future CC scenarios were generated by ensembles of different local projections and a future LULC scenario was defined in accordance with the plan approved by the local government. Four GC scenarios were defined by combining the LULC scenario and the CC scenarios. These GC scenarios have been propagated by simulating with the cited calibrated chain of models. The methodology proposed in the previous objective (1) and the results from the SEAWAT model are combined to summarize the impacts of potential GC scenarios in terms of SWI status and vulnerability at the aquifer scale through steady pictures (maps and conceptual 2D cross sections for specific dates or statistics of a period) and time series for lumped indices. The dynamic of the lumped indices is analyzed taking into account the particularities of the future scenarios. In an historical assessment we have a single real climatic series that allows to draw conclusions about the resilience and trend in the aquifer. But in the assessment of future scenarios infinite potential future series could be feasible (although we finally considered a limited number of them), and, therefore, the summary of the time series analyses should not be performed in the same way. In this work we propose to use a new index, the recovery rate, which can be obtained from the evolution of the global indices Ma and L_GALDIT. It is defined as the mean reduction in the index value in a given period. The impacts of CC are analysed though a sensitivity analysis in order to quantify the influence of the CC on the simulated GC scenarios. We compare results obtained for the GC scenarios, which include both, future LULC and potential future CC scenarios, and a future LULC scenario defined assuming that there is not CC. The results show that GC scenarios will produce higher variability of SWI status and vulnerability. The analysis of the impacts of future GC scenarios shows the effect of adaptation measures in order to cope with the growing water requirements. It reveals that complementary adaptation strategies are needed in order to cope with CC.

(3) The proposed methodology to assess and summarise SWI and vulnerability at aquifer scale has been implement in GIS-SWIAS (SeaWater Intrusion status and vulnerability at Aquifer Scale), a novel generalized ArcGIS ArcToolbox. It is a user-friendly tool that can be applied to any aquifer and is fully integrated in the ArcGIS environment, which is a widely available software. It is the first ArcGIS tool with these characteristics focussing on SWI analyses that we can find in the literature. GIS-SWIAS is able to deal with geo-referenced information, it is easy to introduce the required data (inputs) and to efficiently perform the demanding computational operations required. Its outputs are in the form of shapefiles, reports and images (maps, conceptual cross sections and time series of lumped indices) to summarize the magnitude, intensity and temporal evolution of SWI within an aquifer for specific dates or by showing statistics for a chosen time period. GIS-SWIAS is an ArcGIS ArcToolbox composed by three models programmed in ModelBuilder. These models have been compiled by adding different tools from ArcToolbox to produce a complete lumped assessment of the SWI at aquifer scale. GIS-SWIAS can be shared with other users and it can be added as a Toolbox in ArcGIS. The first model, “Chloride concentration map” model, generates a classified chloride concentration shapefile from a point feature table in text format by using Inverse Distance Weighting (IDW)

interpolation technique (other interpolation techniques could be implemented in this tool). The second one, "Hydraulic head map" model, generates a classified hydraulic head shapefile from a point feature table in text format. It also generates a shapefile containing aquifer variables (chloride concentration and hydraulic head values) and aquifer parameters (storage coefficient and bottom of the aquifer). Finally, the "Summarizing SWI" model, generates Excel® tables containing statistics that summarizing SWI at aquifer scale. It also generates conceptual cross sections (.shp), where the mean affected and non-affected volume are drawn for the aquifer (average values over a time period or instantaneous values on a specific date). If different dates are analyzed, it shows graphs representing the temporal evolution of Pa and Ta variables, percentage of affected volume, chloride concentration within the aquifer and Ma index (or lumped vulnerability index). GIS-SWIAS can be applied to assess historical SWI dynamic in cases where there is no groundwater flow model. In those cases, the spatial distribution is assessed by applying simple interpolation techniques. Nevertheless, if we want a rational quantitative analysis of the sustainability of alternative management scenarios to SWI problem, the GIS-SWIAS tool requires that information on hydraulic head and chloride concentration distribution are generated from simulations of their impacts by a calibrated density-dependent flow model. In such cases, adaptation strategies to potential future scenarios-whose distributed impacts have to be propagated within the previously calibrated models-could usefully be analyzed and compared using this tool. Given all these ways that the GIS-SWIAS tool can be applied, it provides a valuable tool for both researcher and technician to assess SWI dynamics and aquifer resilience under different scenarios. It can support the decision-making process by helping to make a rational selection of sustainable management strategies. Its performance for the analyses of historical and potential future scenarios were tested and confirmed in Plana de Oropesa-Torreblanca and Plana de Vinaroz aquifers.

(4) A novel method was proposed in order to harmonise the vulnerability assessment in different aquifer typologies. Two well-known vulnerability methods, DRASTIC and COP, were applied in five carbonate aquifers in the Upper Guadiana Basin. The validation analyses demonstrated a higher confidence in the vulnerability assessment provided by the COP method in the carbonate aquifers. An adaptation of DRASTIC index is made in order to obtain reliable vulnerability assessments in carbonate aquifers. This approach is analogous to the hypothesis of "equivalent porous medium", which applies to karstic aquifers the numerical solution developed for detrital aquifers. The proposed method solves an optimization problem to minimize the differences between the assessments provided by the modified DRASTIC and COP methods. Decision trees and spatial statistics analyses were combined to identify the ranges and weights of DRASTIC parameters to produce an optimal solution. Two objective functions were tested: (A) to maximize the percentage of spatial coincidence between DRASTIC and COP vulnerability classes; and (B) to minimize the distance between the vulnerability classes in DRASTIC and COP. The decision variables in this optimization problem are (1) the ranges (of the DRASTIC index and its parameters) and (2) the weights of the DRASTIC parameters. The ranges of the DRASTIC parameters and index are proposed based on the available data in the study area and covering a wide range of hypothetical cases. Only weights between 1 to 5 are considered, following the original proposal of DRASTIC method. The optimal solution is sought following two steps. First, DRASTIC vulnerability maps are calculated modifying only the ranges of parameters and the classification of the DRASTIC index. All the DRASTIC maps are evaluated through the objective functions. In order to reduce the number of calculations, we employ data mining techniques (decision trees) to select the values of the variables domain to be tested.

Decision trees are applied in order to find out the ranges for each parameter that gives the highest coincidence and a lowest distance between vulnerability classes assigned using DRASTIC and COP. In this second step, the weights of parameters are introduced as new variables to compute all the feasible combinations of weights and parameter ranges selected in the previous step. The DRASTIC index is calculated for all the combinations of weights and selected classifications in step 1. The optimal solution (O-DRASTIC) matches the COP vulnerability classification for carbonate aquifers in 75% of the area, while maintaining a reliable assessment of the detrital aquifers in the Upper Guadiana Basin.

(5) A new method was proposed to make a preliminary estimation of the risk for groundwater pollution at the aquifer scale in the Upper Guadiana Basin through the lumped turnover time index (T index). A new lumped index (L-RISK index) was defined to assess the significance of the risk for pollution at the aquifer scale. Both L-RISK and T indices were employed to calibrate a linear regression model based on the assumption that a higher groundwater vulnerability is related to a shorter residence time. A simple linear regression model was defined in order to approximate the L-RISK as a function of the mean residence time, calculated as the T index, in the studied aquifers. Different transformations of the analyzed variables (y = L-RISK and x = T) were performed in order to determine the model that provided the better correlation. The regression model showed a good inverse correlation in the eight aquifers of the Upper Guadiana Basin. This novel method can be applied to analyze a wide range of aquifers with limited information in order to identify potential strategic aquifers. It also allows one to make a preliminary assessment of the impacts of climate change on L-RISK. The results showed a high variability of the T index in the eight aquifers (8–76 years). Three of them had significant greater mean T values, which could be considered to be the main strategic groundwater resources. In the future, the T index will increase between 8 and 44%, and the L-RISK will decrease in all aquifers (1–18%). These results are useful to identify strategic groundwater bodies to define sustainable management measures of groundwater resources.

Keywords: Hydrology; water resources; climate change impacts; groundwater pollution; groundwater vulnerability to contamination; seawater intrusion; index-based methods;

References

Ballesteros BJ, Morell I, García-Menéndez O, Renau-Pruñonosa A (2016) A standardized index for assessing seawater intrusion in coastal aquifers: the SITE index. Water Resour Manag 30(13):4513–4527. https://doi. org/10.1007/s11269-016-1433-4

EU, 2000. Water framework directive, 2000, Directive 2000/60/EC of the European parliament and the council of 23 October 2000. Establishing a framework for community action in the field of water policy. In: E. Commission (Ed.), Official Journal of the European Communities, pp. L 327/1.

Green, T.R.; Taniguchi, M.; Kooi, H.; Gurdak, J.J.; Allen, D.M.; Hiscock, K.M.; Treidel, H.; Aureli, A. Beneath the surface of global change: Impacts of climate change on groundwater. J. Hydrol. 2011, 405, 532–560, doi:10.1016/j.jhydrol.2011.05.002.

Kløve, B.; Ala-Aho, P.; Bertrand, G.; Gurdak, J.J.; Kupfersberger, H.; Kværner, J.; Muotka, T.; Mykrä, H.; Preda, E.; Rossi, P.; et al. Climate change impacts on groundwater and dependent ecosystems. J. Hydrol. 2014, 518, 250–266, doi:10.1016/j.jhydrol.2013.06.037.

Pulido-Velazquez, D.; Renau-Pruñonosa, A.; Llopis-Albert, C.; Morell, I.; Collados-Lara, A.-J.; Senent-Aparicio, J.; Baena-Ruiz, L. Integrated assessment of future potential global change scenarios and their hydrological impacts in coastal aquifers—A new tool to analyse management alternatives in the Plana Oropesa-Torreblanca aquifer. Hydrol. Earth Syst. Sci. 2018, 22, 3053–3074, doi:10.5194/hess-22-3053-2018.

Quevauviller, P. Chapter 1. General Introduction: The Need to Protect Groundwater. In Groundwater Science and Policy; Roy-al Society of Chemistry (RSC): London, UK, USA, 2007; pp. 1–18.

Capítulo 1: Introducción

En este capítulo se exponen los principales motivos que han llevado al desarrollo de esta tesis doctoral. Tras una breve exposición de la problemática de la contaminación y escasez de los recursos hídricos subterráneos y su relación con el cambio climático, se enumeran los principales objetivos de esta tesis, la metodología seguida para la consecución de dichos objetivos, así como los casos de estudio que han servido de aplicación de las metodologías propuestas. Finalmente se resume la organización del resto de la tesis y el contenido de cada uno de los capítulos.

1. Motivación

El agua subterránea juega un papel importante en el suministro de agua a nivel mundial, especialmente en zonas semiáridas. La distribución de los recursos hídricos subterráneos, así como la cantidad y sus características químicas dependen de la interacción entre la hidrosfera, actividad antrópica y el clima, que puede producir impactos negativos no sólo en la disponibilidad de agua para los diferentes usos (consumo, regadío, etc) sino también en los ecosistemas dependientes (Kløve et al. 2014; Quevauviller 2007).

La contaminación de las masas de agua subterráneas está relacionada con los usos del suelo, y depende tanto de la vulnerabilidad de los acuíferos a la contaminación, como del funcionamiento del sistema y la capacidad de renovación del mismo (Zwahlen 2003). Además, en zonas costeras, los acuíferos pueden experimentar problemas de contaminación por intrusión marina asociada normalmente con la sobreexplotación de los mismos (Custodio 2010; García-Menéndez et al. 2016). La intrusión marina incrementa la salinidad del agua subterránea disminuyendo la disponibilidad de agua dulce y deteriorando los ecosistemas dependientes.

En las últimas décadas, especialmente desde los años 70 con la extensión de la agricultura y el incremento de la urbanización, se observó un claro empeoramiento de la calidad de los sistemas hídricos en España, así como un significativo descenso de los niveles piezométricos (Sahuquillo 1991; Conan et al. 2003). El deterioro de los recursos hídricos creó alarma en distintos grupos de la sociedad produciendo un incremento de la concienciación sobre la necesidad de proteger los sistemas hídricos. Actualmente es una cuestión de prioridad en todos los planes de cuenca alcanzar una gestión sostenible y el mantenimiento del buen estado de las masas de agua para cumplir con los objetivos de la Directiva Marco del Agua (DMA, EU 2000).

A partir de la entrada en vigor de la DMA aumentó la necesidad de desarrollar metodologías que permitan caracterizar de una manera rápida y sencilla las masas de agua subterráneas con el fin de identificar aquellas que se encuentren en riesgo por algún tipo de presión (Ballesteros et al. 2016). Así mismo, se requiere el seguimiento y evaluación del estado y la vulnerabilidad de las masas de agua subterráneas para garantizar el cumplimiento de los objetivos marcados mediante estrategias de gestión sostenibles. La DMA tiene como objeto no sólo mejorar el estado de los sistemas acuáticos si no también la protección de los mismos a largo plazo contribuyendo a un uso del agua sostenible.

Además de la caracterización del estado global de las masas de agua, conocer la vulnerabilidad de las mismas a la contaminación ayuda al correcto diseño de estrategias de adaptación sostenibles. El grado de protección natural de las masas de agua subterráneas depende de la vulnerabilidad intrínseca, que se define como la susceptibilidad de los acuíferos a la contaminación por acción antrópica (Foster 1987). Cuando en la evaluación de la vulnerabilidad se introducen factores relativos a un contaminante determinado se habla de vulnerabilidad específica (Vrba and Zaporozec 1994).

Para apoyar en el proceso de toma de decisiones es importante contar con resultados procedentes de métodos generales que sean comparables y fácilmente aplicables, que permitan evaluar tanto el estado global como la vulnerabilidad del sistema, con el fin de identificar aquellos que necesitan una actuación prioritaria. Los métodos agregados, aunque menos precisos que los distribuidos, resultan adecuados para este fin, ya que permiten realizar una evaluación preliminar en amplias

zonas mediante aproximaciones sencillas que requieren datos fácilmente disponibles. Para que los resultados en los distintos acuíferos sean comparables, se precisa armonizar criterios y metodologías de evaluación. Por otro lado, para la planificación futura es imprescindible la consideración de los impactos del CC sobre la distribución espacio temporal de las variables climáticas e hidrológicas.

Esta investigación pretende contribuir al avance del conocimiento en algunas lagunas identificadas en la literatura en relación con la caracterización del estado global, vulnerabilidad y riesgo a la contaminación de las masas de agua subterráneas.

2. Objetivos

De acuerdo con la motivación expuesta en el apartado anterior, la finalidad de esta tesis es el desarrollo de metodologías que permitan analizar, de forma agregada, el estado global y la vulnerabilidad de las masas de agua subterránea a escala de acuífero y evaluar el impacto de potenciales escenarios del CC con el fin de poder establecer medidas de gestión sostenibles en el futuro. Para demostrar su utilidad, estas metodologías se aplican a varios casos de estudio, a escala de acuífero y de cuenca. Dentro de este objetivo general se pueden distinguir los siguientes objetivos específicos:

(1) Propuesta de metodología basada en índices para sintetizar el estado global y vulnerabilidad al problema de intrusión de acuíferos costeros.
(2) Análisis del impacto de escenarios futuros de CG en el estado global y vulnerabilidad en zonas costeras.
(3) Desarrollo de una herramienta automática en entorno ArcGIS para la aplicación de la metodología de análisis y síntesis del estado global y la vulnerabilidad a la intrusión.
(4) Estudio de la vulnerabilidad a la contaminación de masas de agua subterráneas a escala de cuenca y armonización de una metodología aplicable a acuíferos detríticos y kársticos.
(5) Análisis agregado del riesgo a la contaminación a escala de acuífero a partir del tiempo de renovación medio del acuífero y análisis de impactos del CC en la sostenibilidad de la explotación de los sistemas analizados.

3. Metodología

A continuación, se resume el enfoque metodológico seguido en esta tesis para cumplir los objetivos anteriormente descritos. Los capítulos 2-6 contienen las cinco publicaciones que se han desarrollado en el marco de esta tesis, donde se explica de manera detallada el método seguido para alcanzar cada uno de los cinco objetivos expuestos. Además, en cada publicación se incluye un diagrama de flujo con los pasos necesarios para aplicar dichas metodologías.

El primer objetivo marcado en esta tesis surge de la necesidad de establecer una metodología que permita identificar acuíferos vulnerables a la contaminación y en riesgo de no cumplir los objetivos establecidos por la DMA en relación con la intrusión marina. Para ello se plantea una conceptualización del proceso de intrusión a escala de acuífero o masa de agua subterránea que permite, de una manera sencilla y visual, representar su dinámica en forma de mapas, secciones conceptuales 2D e índices agregados. Dicha aproximación requiere estimar previamente mapas con la distribución de la concentración media del ion cloruro en el acuífero en el periodo histórico a considerar. Estos mapas se pueden obtener mediante interpolación espacial de datos procedentes de las redes de observación o, de forma más precisa, mediante un modelo de densidad variable. Para identificar la zona afectada por intrusión se precisa fijar un umbral de concentración de cloruros, que, dependiendo del objetivo perseguido, puede ser el fondo geoquímico natural, o cualquier umbral definido como aceptable para usos específicos del agua (el límite considerado para consumo humano, o incluso cualquier otro valor de referencia establecido por las autoridades competentes). Combinando el mapa de concentración de cloruros con el espesor saturado en el acuífero, y teniendo en cuenta el umbral establecido, se puede calcular el volumen de recurso afectado y no afectado por intrusión. Estos volúmenes se representan en forma de sección conceptual mediante rectángulos definidos por el espesor medio y la distancia media

perpendicular a la costa. En concreto, el volumen afectado queda definido por el Espesor afectado (T_{ha}) y la Penetración (P) de la intrusión en sentido perpendicular a la costa. La intensidad de la intrusión en esa zona queda definida por el Incremento de concentración (IC) por encima del umbral establecido, calculado como la diferencia entre la concentración de cloruros en el volumen afectado y dicho valor de referencia. El producto de espesor afectado, penetración de la intrusión e incremento de concentración da como resultado la Masa de la zona afectada (Ma), que se define como la masa total adicional de cloruros que tiene una concentración por encima del umbral establecido. Este índice agregado (Ma) permite analizar la evolución del estado global de intrusión en un acuífero, así como comparar el estado de diferentes acuíferos con el fin de establecer medidas prioritarias en la gestión. A partir del índice Ma se puede analizar la Resiliencia y Tendencia del acuífero en relación con la intrusión. La Resiliencia se ha definido como el máximo cambio relativo del índice Ma en un periodo de seis años, de acuerdo con los horizontes de los planes de gestión. La Tendencia se calcula como la diferencia relativa entre los valores de Ma al principio y final del periodo de seis años. Así, la Resiliencia muestra el cambio potencial a corto plazo, mientras que la Tendencia indica la evolución de la masa afectada en el periodo temporal considerado. El análisis de la vulnerabilidad a la intrusión se realiza de manera análoga, pero en lugar de emplear la concentración de cloruros como indicador, se utiliza el valor de la vulnerabilidad previamente calculado mediante el método GALDIT. En este caso se propone usar como umbral el valor de vulnerabilidad a partir del cual la vulnerabilidad es alta (esto es, GALDIT≥7,5). El índice de vulnerabilidad agregado L_GALDIT se define como el valor de vulnerabilidad (índice GALDIT) ponderado por el volumen en cada celda o zona del acuífero.

El segundo objetivo de esta tesis es el análisis del impacto de escenarios futuros de CC y CG en el estado y vulnerabilidad a la intrusión de acuíferos costeros. Para ello es necesario contar con un modelo de flujo previamente calibrado que permita realizar la propagación de impactos de potenciales escenarios futuros en la concentración de cloruros y nivel piezométrico. Los escenarios de CG se definen mediante la combinación de potenciales escenarios locales de CC previamente generados y usos del suelo. La metodología basada en índices desarrollada para sintetizar la dinámica de la intrusión en un acuífero (primer objetivo descrito) se combina con los resultados del modelo para evaluar el impacto de los potenciales escenarios de CG en términos de intrusión y vulnerabilidad a escala de acuífero, teniendo en cuenta que, en lugar de una única serie histórica, tenemos múltiples potenciales series equiprobables. Esta metodología permite comparar el impacto medio sobre la intrusión de los diferentes escenarios futuros para un determinado horizonte temporal. Se analiza además la influencia del CC en los escenarios de CG mediante un análisis de sensibilidad comparando los escenarios de CG con un escenario que sólo incluye las medidas de adaptación suponiendo que no hay CC. Para analizar la dinámica temporal en el futuro del índice agregado que sintetiza el estado global (Ma) se propone un nuevo índice, Recovery rate, definido como la reducción media del índice Ma en un periodo determinado, que representa la velocidad de recuperación media del sistema en el horizonte temporal fijado.

Esta metodología basada en índices para el análisis agregado del estado global y vulnerabilidad a la intrusión se ha implementado en una herramienta desarrollada en ArcGIS, llamada GIS-SWIAS. GIS-SWIAS permite realizar los cálculos necesarios de una manera rápida y sencilla en un entorno amigable, proporcionando resultados en forma de mapas y secciones transversales, series temporales y estadísticos para mostrar la intensidad, magnitud y evolución temporal de la intrusión en un acuífero en instantes de tiempo determinados o para un periodo de temporal. El desarrollo de esta aplicación se corresponde con el tercer objetivo de esta tesis. La herramienta se compone de tres modelos desarrollados en Model Builder de ArcGIS: el primer modelo realiza los cálculos para obtener el mapa distribuido de concentración de cloruros en el acuífero; el segundo modelo realiza los cálculos para obtener un mapa distribuido de nivel piezométrico; el tercer modelo genera la sección representativa del acuífero identificando la zona afectada y una tabla en formato .xlsx con los estadísticos de las variables que resumen el estado global del acuífero ante el problema de intrusión (T_{ha}, P, Ma, entre otros). Además, si se analizan diferentes instantes de tiempo, este modelo también proporciona un gráfico mostrando la evolución de las variables P, T_{ha}, porcentaje de volumen afectado, concentración de cloruros en el acuífero y el índice Ma. Esta herramienta se puede utilizar para analizar la intrusión en casos en los que no hay

disponible un modelo de flujo, mediante la interpolación de datos de monitoreo, aunque si se dispone de información de concentración de cloruros y nivel piezométrico de un modelo previamente calibrado, la herramienta permite también analizar la sostenibilidad de escenarios de gestión futuros. Dada su versatilidad, GIS-SWIAS es una herramienta útil tanto para investigadores como técnicos para analizar la intrusión a escala de acuífero bajo diferentes escenarios, lo que puede ser de ayuda en el proceso de toma de decisiones para la selección de estrategias de gestión sostenibles

Los dos últimos objetivos de esta tesis surgen como necesidad de avanzar en la armonización de metodologías de análisis de la vulnerabilidad y riesgo a la contaminación, así como su validación de manera agregada a escala de acuífero.

Se propone realizar una adaptación del método DRASTIC para obtener un método armonizado que permita analizar la vulnerabilidad a la contaminación de manera homogénea tanto en acuíferos detríticos como carbonatados. Esto permite comparar los resultados entre distintos acuíferos en una cuenca con el fin de valorar adecuadamente las medidas de gestión en relación con la protección de la calidad de los recursos hídricos subterráneos. La adaptación del método DRASTIC se realiza mediante la resolución de un problema de optimización cuya función objetivo es maximizar la coincidencia en la clasificación de la vulnerabilidad con el método COP y minimizar la distancia entre las clases de vulnerabilidad de DRASTIC y COP. Aunque el método COP muestra resultados más satisfactorios en los acuíferos carbonatados de la cuenca de estudio de acuerdo con la validación realizada, éste método no se puede aplicar en acuíferos detríticos. Sin embargo, el método DRASTIC se ha aplicado en numerosos estudios en acuíferos de cualquier tipología. Por este motivo se propone realizar una adaptación de DRASTIC para obtener unos resultados fiables en una cuenca compuesta por acuíferos de diferente tipología. Las variables de decisión en el problema de optimización son (1) los rangos del índice DRASTIC y de sus parámetros numéricos y (2) los pesos de los parámetros de DRASTIC. El dominio de búsqueda de la solución óptima se compone de un número finito de combinaciones de la clasificación de DRASTIC y de cada uno de sus parámetros numéricos. Las distintas clasificaciones se establecen en función de criterios estadísticos según la distribución de los datos en el área de estudio. El valor de los pesos para cada parámetro varía entre 1 y 5, siguiendo la propuesta original del método DRASTIC. El problema se divide en dos pasos para su resolución. Primero se realiza una optimización de los rangos de DRASTIC y de sus parámetros mediante la combinación de todas las clasificaciones posibles definidas anteriormente. Debido a la gran cantidad de combinaciones posibles que se generan al variar uno a uno los parámetros del índice DRASTIC, se aplica un algoritmo sencillo de árboles de decisión para delimitar el dominio del problema en el segundo paso. En este segundo paso se realiza una optimización del peso de cada parámetro de DRASTIC para aquellas combinaciones seleccionadas en el paso anterior. Mediante la resolución de este problema de optimización se obtiene un método de vulnerabilidad (O-DRASTIC) que mejora notablemente los resultados de la validación de los mapas tanto en acuíferos carbonatados como en detríticos en la zona de estudio.

Finalmente, continuando con la propuesta de armonización de metodologías a escala de acuífero, se propone un nuevo método que permite realizar una primera estimación y/o validación agregada del riesgo a la contaminación de un acuífero a partir del tiempo medio de residencia del agua subterránea en el mismo. El riesgo a la contaminación se calcula combinando el mapa de vulnerabilidad (obtenido aplicando el método DRASTIC optimizado anteriormente, O-DRASTIC) y los usos del suelo que determinan la potencial amenaza de contaminación. El mapa de riesgo distribuido en el acuífero se pondera por la superficie del mismo para obtener el índice agregado L-RISK. El tiempo de residencia medio (T), que es un indicador de la susceptibilidad a la contaminación del agua subterránea, se aproxima mediante un índice agregado sencillo: T=Almacenamiento/Recarga media. Estos dos índices agregados se emplearon para calibrar un modelo de regresión lineal basado en la hipótesis de que un tiempo de residencia corto está relacionado con un mayor riesgo a la contaminación. Se probaron diferentes transformaciones de las variables L-RISK y T para determinar el modelo que ofrece una mejor correlación. Este modelo se utiliza para realizar un análisis preliminar del impacto del CC en el índice L-RISK. El

método propuesto permite analizar un gran número de acuíferos utilizando datos frecuentemente disponibles. Además, resulta útil para identificar potenciales acuíferos estratégicos para establecer medidas de gestión sostenibles de los recursos hídricos subterráneos, especialmente durante periodos de sequía.

4. Casos de estudio

Los casos de estudio seleccionados en esta tesis incluyen acuíferos sobreexplotados y con graves problemas de contaminación, tanto por intrusión marina como por la actividad agrícola. La aplicación de las metodologías propuestas a estos casos de estudio permite demostrar la utilidad de las mismas. Los casos de estudio seleccionados para el análisis del estado global y vulnerabilidad a la intrusión son dos acuíferos costeros Mediterráneos, situados en Castellón, con graves problemas de salinización debido a la sobreexplotación. La armonización de metodologías de evaluación de la vulnerabilidad y el análisis agregado del riesgo a la contaminación se ha realizado en la Cuenca del Alto Guadiana, que integran acuíferos de diferente tipología, con graves problemas de contaminación por nitratos, algunos de ellos sometidos también a una explotación intensiva, que ha provocado el deterioro de ecosistemas dependientes de alto valor ecológico como son las Lagunas de Ruidera, entre otros. Estos casos de estudio se describen de manera más detallada en los distintos capítulos de la tesis.

5. Organización de la tesis

Esta tesis se organiza en siete capítulos, cuyo contenido se resume a continuación.

En el capítulo 1 se introduce la motivación de esta tesis, los objetivos y casos de estudio analizados. Los cinco objetivos principales expuestos se corresponden con cinco artículos científicos publicados en revistas indexadas de alto impacto (una publicación Q1, tres publicaciones Q2 y una publicación Q4).

Cada una de estas publicaciones se incluyen en los capítulos 2-6 durante el desarrollo de la tesis.

Finalmente, en el capítulo 7 se exponen las conclusiones generales y posibles líneas futuras de investigación que han sido identificadas durante el desarrollo de esta tesis.

Referencias

Ballesteros BJ, Morell I, García-Menéndez O, Renau-Pruñonosa A (2016) A standardized index for assessing seawater intrusion in coastal aquifers: the SITE index. Water Resour Manag 30(13):4513–4527. https://doi. org/10.1007/s11269-016-1433-4

Conan, C.; De Marsily, G.; Bouraoui, F.; Bidoglio, G. A long-term hydrological modelling of the Upper Guadiana river basin (Spain). Phys. Chem. Earth Parts A/B/C 2003, 28, 193–200, doi:10.1016/s1474-7065(03)00025-1.

Custodio E (2010) Coastal aquifers of Europe: an overview. Hydrogeol J 18:269–280

EU, 2000. Water framework directive, 2000, Directive 2000/60/EC of the European parliament and the council of 23 October 2000. Establishing a framework for community action in the field of water policy. In: E. Commission (Ed.), Official Journal of the European Communities, pp. L 327/1.

Foster, S.S.D. Fundamental concepts in aquifer vulnerability, pollution risk and protection strategy. Hydrol. Resour. Proc. Inf. 1987, 38, 69–86.

García-Menéndez O, Morell I, Ballesteros BJ, Renau-Pruñonosa A, Esteller MV (2016) Spatial characterization of the seawater upconing process in a coastal Mediterranean aquifer (Plana de Castellón, Spain): evolution and controls. Environ Earth Sci 75:728. https://doi.org/10.1007/s12665-016-5531-7

Kløve, B.; Ala-Aho, P.; Bertrand, G.; Gurdak, J.J.; Kupfersberger, H.; Kværner, J.; Muotka, T.; Mykrä, H.; Preda, E.; Rossi, P.; et al. Climate change impacts on groundwater and dependent ecosystems. J. Hydrol. 2014, 518, 250–266, doi:10.1016/j.jhydrol.2013.06.037.

Quevauviller, P. Chapter 1. General Introduction: The Need to Protect Groundwater. In Groundwater Science and Policy; Royal Society of Chemistry (RSC): London, UK, USA, 2007; pp. 1–18.

Sahuquillo, A., 1991. La utilización conjunta de aguas superficiales y subterráneas en la litigación de los efectos de las sequías [Joint use of surface and ground waters in mitigating drought effects]. Revista de la Real Academia de Ciencias Exactas, Físicas y Naturales de Madrid. Jornadas sobre las sequías [Drought] 85, 275–291.

Vrba J, Zaporozec A (1994) Guidebook on mapping groundwater vulnerability. IAH Int Contrib to Hydrogeol 16, Heise, Hannover, Germany, 131 pp

Zwahlen, F. COST Action 620 Vulnerability and Risk Mapping for the Protection of Carbonate (Karst) Aquifers Final Report; Office of the Official Publications of the European Communities: Brussels, Belgium, 2003; ISBN 928946416X

Capítulo 2: Global Assessment of Seawater Intrusion Problems (Status and Vulnerability)

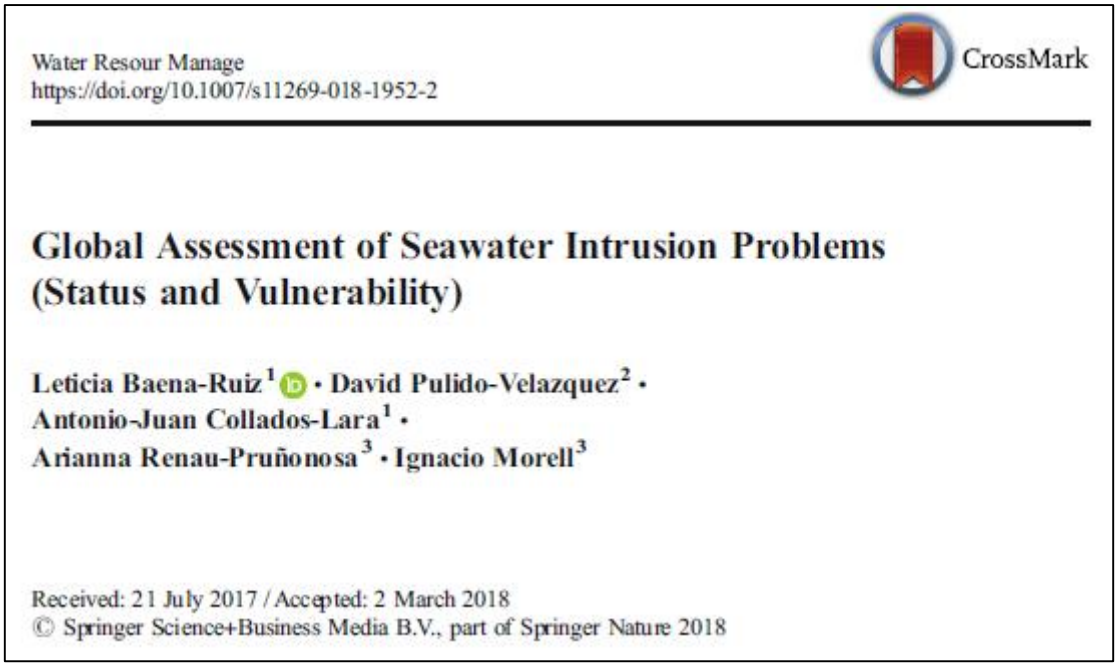

Water Resour Manage
https://doi.org/10.1007/s11269-018-1952-2

CrossMark

Global Assessment of Seawater Intrusion Problems (Status and Vulnerability)

Leticia Baena-Ruiz[1] · David Pulido-Velazquez[2] · Antonio-Juan Collados-Lara[1] · Arianna Renau-Pruñonosa[3] · Ignacio Morell[3]

Received: 21 July 2017 / Accepted: 2 March 2018

Reference: Baena-Ruiz, L., Pulido-Velazquez, D., Collados-Lara, AJ. et al. Global Assessment of Seawater Intrusion Problems (Status and Vulnerability). Water Resour Manage 32, 2681–2700 (2018). https://doi.org/10.1007/s11269-018-1952-2

Authors and affiliations:

LETICIA BAENA RUIZ(1,*), DAVID PULIDO-VELAZQUEZ(2), ANTONIO-JUAN COLLADOS-LARA(1), ARIANNA RENAU-PRUÑONOSA(3), IGNACIO MORELL(3)

(1) IGME, Granada, Spain. lbaenar@gmail.com; ajcollados@gmail.com

(2) IGME and UCAM, Granada, Spain. d.pulido@igme.es

(3) Jaume I University, Castellón, Spain. arenau@guest.uji.es; morell@uji.es

* Corresponding author

Abstract

In this research paper we propose a novel method to perform an integrated analysis of the status and vulnerability of coastal aquifers to seawater intrusion (SWI). The method is based on a conceptual approach of intrusion that allows to summarised results in a visual way at different spatial scales, moving from steady pictures (corresponding to instantaneous or mean values in a period) including maps and 2D conceptual cross-sections and temporal series of lumped indices. Our aim is to help in the identification of coastal groundwater bodies at risk of not achieving good chemical status according to the Water Framework Directive. The indices are obtained from available information about aquifer geometry and historical monitoring data (chloride concentration and hydraulic head data). This method may be applied even in cases where a reduced number of data are available. It does not require complex modelling and has been implemented in a GIS tool that encourages its use in other cases. Analysis of the evolution of historical time series of these indices can be used to assess resilience and trends with respect to SWI problems. This method can be also useful to compare intrusion problemsin different aquifers and temporal periods.

Keywords Global change; Seawater intrusion; Coastal aquifer; Lumped indices; Vulnerability

1. Introduction

Seawater intrusion affects a great number of coastal aquifers all over the world, and this is a problem often due to the intense economic activity in these zones and the consequent exploitation of their groundwater resources. Several authors have highlighted this problem in Africa (Steyl and Dennis 2010; Bouderbala 2015), America (Barlow and Reichard 2010, Boschetti et al. 2015), Asia (Parck et al. 2012; Pratheepa et al. 2015), Oceania (Werner and Gallagher 2006; Werner 2010) and Europe (Custodio 2010; García-Menéndez et al. 2016). In Mediterranean Europe, seawater intrusion (SWI) is a common problem in Spain (Guhl et al. 2006; García-Menéndez et al. 2016), Italy (Barrocu 2003; Benini et al. 2016), Greece (Petalas and Lambrakis 2006; Kazakis et al. 2016), and Turkey (Günay 1997; Arslan et al. 2012). It is due to several factors such as a high summer population density and the intensification of irrigated croplands, which increment the risk of SWI. These factors have led to an increasing water demand since the 1970s. Since 2000, after Water Framework Directive (2000) came into effect, there has been an increase in the number of groundwater quality assessment studies, and consequently in the development of methodologies to quantify groundwater pollution in an aquifer.

Many different distributed approaches have been applied to assess spatio-temporal distribution of GW quality issues in coastal regions, depending on the aim of the investigation. They can be classified into two main groups: physical quantitative assessment of aquifer status and mixed quantitative-qualitative assessment of vulnerability to seawater intrusion.

The spatio-temporal distribution of the aquifer status can be estimated from available information by applying different modelling approaches (simple interpolation methods or sharp interface solutions and density dependent approaches). The flow models have been extensively applied to study SWI problems (Smith 2004; Eeman et al. 2011). They attempt to determine the position of the seawater-freshwater interface and to simulate SWI processes using analytical or numerical procedures. Several authors have discussed the advantages and limitations of different quantitative flow approaches (Llopis-Albert and Pulido-Velazquez 2014). Numerical approaches can simulate complex intrusion processes under transient conditions, but they require numerical approaches and excessive data to obtain a parsimonious approach with enough data to calculate representative parameters on a large scale (with significantly greater requirements in density-dependent flow approaches) (Wriedt and Bouraoui 2009).

On the other hand, qualitative methods can be applied to assess vulnerability and/or risk mapping in coastal regions. They aim to identify the parts of a groundwater body that could be contaminated as a result of human activities, taking into account physiographic characteristics such as geology or piezometric level. A numerical index or score is assigned to the different attributes, which are then weighted. The numerical scores cluster similar areas into classes of vulnerability (e.g., low, moderate and high), which are then displayed on a map. They can be used to define hydrogeological subregions with different levels of severity (Kumar et al. 2015). Due to their easy implementation, many index-based techniques have been applied to assess vulnerability. Several authors have criticised the roughness of these index-based methods, however they also reveal the easy implementation and interpretation of these techniques to get a preliminary assessment of vulnerability of groundwater bodies (Werner et al. 2012).

The groundwater vulnerability assessment technique was started in 1987 by Aller et al. (1987) through the development of DRASTIC, though this system has undergone several modifications over time (Kumar et al. 2015). Several indices have been developed to assess vulnerability to pollution (SINTAC (Civita 1994), EPIK (Doerfliger et al. 1999) and AVI (Stempvoort et al. 1993)) but they are not usually employed to evaluate vulnerability to SWI. The GALDIT method was developed by Chachadi and Lobo-Ferreira (2001) with the aim of assessing the spatial vulnerability of hydrogeological settings to SWI. GALDIT has been mostly used to perform large-scale assessments of SWI (Benini et al. 2016). The major drawback of this method is that the effect of pumping on the SWI process is not considered (Trabelsi et al. 2016). Despite this

limitation, this model shows many advantages, such as its low computational cost. Moreover, it requires few, easy to collect historical variables and parameters, and it can be applied over large areas. However, vulnerability methods only highlight specific areas in the aquifer that are at risk or prone to pollution due to their intrinsic characteristics, whereas it might be interesting to adopt measures in order to improve them. In the literature, there are examples of works developed to provide a global assessment of aquifer status (e.g., Ballesteros et al. 2016), but none that address aquifer vulnerability.

In this paper we propose a new systematic method to analyse status and vulnerability to SWI at different spatial scales. The method is based on a conceptual approach that allows to define steady pictures (representing instantaneous or mean values in a period) to move from maps to 2D schematic cross sections, and temporal series of lumped indices. The analysis of these temporal series of the indices, which summarize global status and vulnerability, allows to study the SWI dynamic, resilience and trend. The proposed method can be useful to identify aquifers in risk of not achieve the objective defined in the Water Framework Directive (2000). The paper is structured as follows. Section 2 describes the method, defining the proposed indices and specifying the steps to obtain them. Section 3 describes the case studies and the available data, while Section 4 outlines the results and discussion. Section 5 gives our main conclusions.

2. Methodology

The inputs required and the steps to be followed to apply the method are represented in Figure 2.1. The inputs include variables (to characterise the historical evolution of hydraulic head and chloride concentration) and parameters (to define aquifer geometry and hydrodynamic behaviour) to determine the overall status of the aquifer. The data describing the historical evolution could come from direct observation (monitoring network) or other techniques (geophysical applications, etc.). For the vulnerability assessment, other intrinsic information is also needed as inputs to apply the proposed method.

The steps proposed in order to summarize status and vulnerability to SWI through visual pictures and time series are described in the next subsections.

2.1. Assessment of Seawater Intrusion (SWI) Status

The described inputs will be employed to assess SWI status according to the following steps:

2.1.1. Maps of Chloride Concentration

Fields (maps) of chloride concentration and hydraulic head can be obtained by applying simple interpolation techniques in each date with enough available information. 3D maps of the saturated thickness (with a finite number of cells) can be obtained by combining hydraulic head maps with the geometry and the storage coefficient. Vertical aquifer geometry and storage coefficient can be obtained from previous 3D models and hydrogeological studies respectively. If there is insufficient information to assess the vertical distribution of chloride concentration, an invariant concentration with depth is assumed at each point, thus obtaining 2D fields of chloride concentration.

From chloride concentration and saturated thickness maps, we can define the affected and non-affected zone (areas where the chloride concentration level is above the natural background level). This threshold, which depends on the geochemistry of the aquifer, is difficult to determine. Some European projects ("BBRIDGE") (Dahlstrom and Müller 2006) have provided recommendations for its calculation, based on methodologies applied in some countries. Some of them determine. Some European projects ("BBRIDGE") (Dahlstrom and Müller 2006) have provided recommendations for its calculation, based on methodologies applied in some countries. Some of them determine the background level as the concentration in non- contaminated areas. Other define the threshold as 90 percentile of the concentration measured in the groundwater monitoring network, while sometimes they only use data from monitoring networks to define a background concentration. In other cases the threshold is based on the typical background level, the origin of

the chloride (natural or anthropogenic) and the possible impacts on ecosystems or human health. For this area we can calculate the affected volume taking into account the storage coefficient and the aquifer geometry.

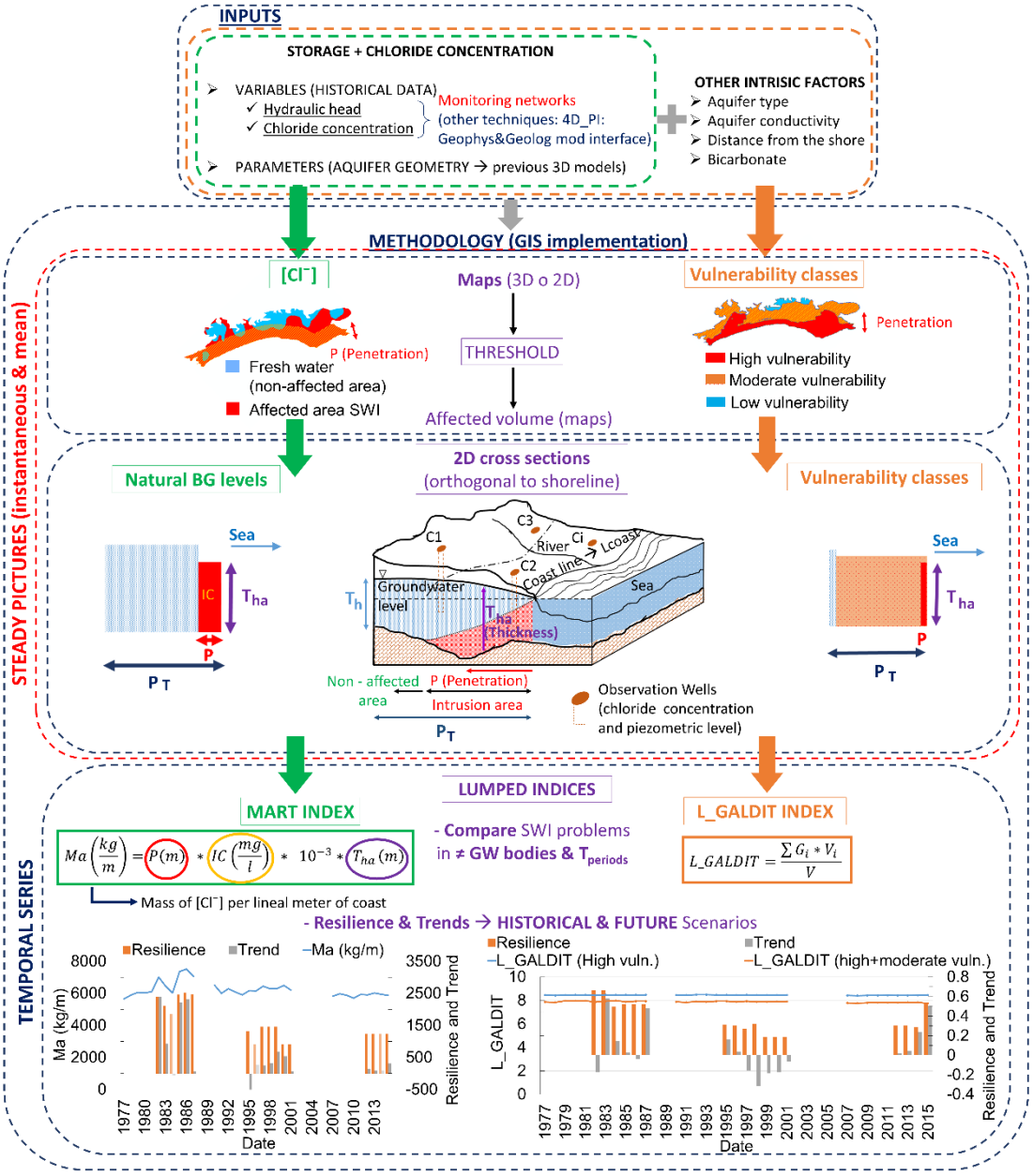

Figure 2.1. Flow chart of methodology

2.1.2. 2D Cross-Sections: Penetration and Thickness. Increment in Concentration

2D representative cross-sections can be deduced to summarise the mean geometry (thickness and penetration) and intensity of the intrusion (increment in concentration). The average affected thickness (T_{ha}) and inland penetration (P) of intrusion can be calculated as follow:

$$T_{ha}(m) = \frac{\sum V_{i(>V_r)}}{\sum S_{i(>V_r)}} \quad (1)$$

$$P(m) = \frac{\sum V_{i(>V_r)}}{T_{ha} * L_{coast}} \quad (2)$$

$$V_{i(>V_r)}(m^3) = S_i(m^2) * b_i(m) * \alpha \quad (3)$$

where:

- $V_{i(>Vr)}$ is the storage in each cell (m^3) with a concentration greater than V_r;
- S_i is the surface area of each cell (m^2);
- b_i is the saturated thickness at each instant considered (m);
- α is the storage coefficient;
- L_{coast} is the length of coastline (m);

The chloride concentration (C) of the affected area is:

$$C\left(\frac{mg}{l}\right) = \frac{\sum(C_{i(>V_r)} * V_{i(>V_r)})}{V_{(>V_r)}} \quad (4)$$

$$V_r(\frac{mg}{l}) = Reference\ threshold \quad (5)$$

where:

- C_i is the concentration (mg/l) in each cell;
- $V_{(>Vr)}$ is the total storage (m^3) with a concentration greater than V_r;

The increment of concentration (IC) above the threshold (V_r) in the affected volume is:

$$IC\left(\frac{mg}{l}\right) = C - V_r \quad (6)$$

Cross sections give an overview of the magnitude and intensity of the intrusion process per linear metre of coast at a specific time. Mean cross sections can also be obtained for a time period.

2.1.3. Global Index: Mass of Affected Area (Ma)

The index Ma is defined as the total additional mass of chloride that causes the concentration in some areas to exceed the natural threshold. It is obtained multiplying the increment of concentration (IC) by Penetration (P) and affected Thickness (T_{ha}) from Eqs. 1 and 2.

$$Ma\left(\frac{kg}{m}\right) = P(m) * IC\left(\frac{mg}{l}\right) * 10^{-3} * T_{ha}(m) \quad (7)$$

The concept of Ma involves some simplifications, which are schematised in Figure 2.1.

While 2D maps and cross sections summarize the extent and magnitude of SWI in an aquifer at a specific time, Ma index show the intensity and temporal evolution of the problem.

2.1.4. Resilience and Trend (MART)

The evolution of the Ma index can give an overall assessment of the resilience (R) and trend (T) of the aquifer status according to the SWI problem.

We propose calculating Resilience as the maximum relative change of the Ma index (relative difference between maximum and minimum value) over six-year periods, which is the horizon defined to update management plans in the Water Framework Directive (2000). Thus, Resilience shows the potential change for a short-term period, taking into account the measures occurred in this period.

Trend is also calculated for six-year periods. It is defined as the relative difference between the values of Ma at the beginning and end of the period. A positive trend indicates the mass of water affected is increasing, while a negative trend indicates an improvement in aquifer status. The combination of Mass of affected water body (Ma), Resilience (R) of the water body and Trend (T) of SWI defines the MART index, which summarize SWI evolution in the aquifer.

2.2. Assessment of Vulnerability to SWI

While SWI status is calculated using only physical variables (chloride concentration and hydraulic head), vulnerability employs weighted qualitative characteristics. In this study, we

summarise vulnerability status based on the application of the GALDIT method (Aquifer type; aquifer hydraulic conductivity; height of groundwater head above sea level; distance from the shore; impact of existing status of SWI; thickness of aquifer being mapped) (Chachadi and Lobo-Ferreira 2005).

2.2.1. Maps of Vulnerability

Vulnerability maps are displayed from GALDIT method. The GALDIT Index is obtained by applying the expression:

$$GALDIT\ Index = \frac{\sum_{i=1}^{6} W_i * R_i}{\sum_{i=}^{6} W_i} \quad (8)$$

where Wi is the weight of the i^{th} indicator and R_i is the importance rating of the i^{th} indicator. The GALDIT scores are then classified into three vulnerability classes: High (GALDIT Index range ≥ 7.5), Moderate (between 5 and 7.5) and Low (< 5). These vulnerability classes are the threshold to define the affected zone (area where vulnerability is higher than the adopted reference threshold (moderate or high vulnerability)).

For this area we can calculate the affected volume taking into account the storage coefficient and the aquifer geometry.

2.2.2. 2D Cross-Sections: Penetration and Thickness. Vulnerability Classes

2D cross sections can be deduced to summarise the mean geometry and intensity of the GALDIT vulnerability score. Penetration (PL_GALDIT) and Thickness (T_{haL_GALDIT}) can be calculated from formulas 9 and 10:

$$T_{ha\ L\_GALDIT}(m) = \frac{\sum V_{i(>V_{r\ GALDIT})}}{\sum S_{i(>V_{r\ GALDIT})}} \quad (9)$$

$$P_{L\_GALDIT}(m) = \frac{\sum V_{i(>V_{r\ GALDIT})}}{T_{ha\ L\_GALDIT} * L_{coast}} \quad (10)$$

$$V_{i(>V_{r\ GALDIT})}(m^3) = S_i(m^2) * b_i(m) * \alpha \quad (11)$$

$$V_{r\ GALDIT} = GALDIT\ threshold\ (G \geq 7{,}5;\ G \geq 5) \quad (12)$$

where:

- $V_{i(>Vr\ GALDIT)}$ the storage in each cell (m^3) with a concentration greater than $V_{r\ GALDIT}$;
- S_i is the surface area of each cell (m^2);
- b_i is the saturated thickness at each instant considered (m);
- α is the storage coefficient;
- L_{coast} is the length of coastline (m).

The intensity of vulnerability is the GALDIT score in each zone for the thresholds established.

2.2.3. Global Index: L_GALDIT

A lumped global value of GALDIT (L_GALDIT) is defined by weighting the GALDIT score for each point with the storage (Eq. 13). This weighted value of GALDIT assesses the overall vulnerability of the aquifer. On the other hand, a lumped affected value of GALDIT can be obtained for the different thresholds (Eqs. 14 and 15).

$$L\_GALDIT = \frac{\sum(G_i * V_i)}{V} \quad (13)$$

$$L\_GALDIT_{high} = \frac{\sum(G_{i(\geq 7,5)} * V_{i(\geq 7,5)})}{V_{(\geq 7,5)}} \quad (14)$$

$$L\_GALDIT_{high+moderate} = \frac{\sum(G_{i(\geq 5)} * V_{i(\geq 5)})}{V_{(\geq 5)}} \quad (15)$$

- G_i is the value of GALDIT in each cell;
- V_i is the storage in each cell;
- V is the total storage in the aquifer;
- $G_{i(\geq 7,5)}$ is the value of GALDIT of each cell greater or equal to 7,5;
- $G_{i(\geq 5)}$ is the value of GALDIT of each cell greater or equal to 5;
- $V_{i(\geq 7,5)}$ is the volume of each cell with a value of GALDIT ≥7,5;
- $V_{i(\geq 5)}$ is the volume of each cell with a value of GALDIT ≥5;
- $V_{(\geq 7,5)}$ is the total volume with a value of GALDIT ≥7,5;
- $V_{(\geq 5)}$ is the total volume with a value of GALDIT ≥5;

2.2.4. Resilience and Trend

An analogous procedure to the one described for the MART index is applied to determine the evolution over time of the L_GALDIT index, the Resilience and Trend of aquifer vulnerability. The method employs the spatial distribution of the storage coefficient to obtain affected volume in the lumped indices (MART and L_GALDIT) and hydrogeological parameters as the transmissivity are implicitly considered in the spatial distribution of the hydraulic head, which considers effects of the aquifer system. Even so it does not require complex modelling approaches and has been implemented in a GIS tool that encourages its application to other cases.

3. Study Area

3.1. Geological and Hydrogeological Characterisation

The study area is situated on the Mediterranean coast of Spain, in Castellon province. Two different aquifers were studied: the Plana de Oropesa-Torreblanca and Plana de Vinaroz (Figure 2.2). The increasing population since 1970 and the continuing agricultural exploitation have produced SWI problems of different entity in these aquifers.

Both aquifers are unconfined, heterogeneous, detrital and multilayer aquifers composed of gravel and sand levels in a silty clay matrix (Ballesteros et al. 2016). Figure 2.2 also shows the hydrogeology of these aquifers. The transmissivity in the Plio-Quaternary Plana de Oropesa Torreblanca aquifer ranges from 300 to 1000 m2/day (García-Menéndez et al. 2016) and the storage coefficient varies between 2 and 12%, while in Plana de Vinaroz these parameters take the value of 250–1200 m2/day and 5–15% respectively.

3.1. Data

Historic data for the variables of chloride concentration and hydraulic head were provided by the Confederación Hidrográfica del Júcar. There are no data for this study area from 1988 to 1989 or from 2001 to 2005. The number of observation wells varies over time and also from one aquifer to another. The number of monitoring points of chloride concentration in Plana de Oropesa-Torreblanca and Plana de Vinaroz aquifers varies between 12 and 34 and 9–58 respectively, while the monitoring points of hydraulic head ranges between 9 and 19 and 6– 28 in both aquifers.

The number of data available was also variable for each observation point over the period. Observation points were considered if they had data for at least 20% of the study period.

The chloride concentration exceeds 1000 mg/l in zones close to the coast in both aquifers. Points inland exhibit lower concentrations that are more stable through time. Concentrations increased over the 1980s as a consequence of the expansion in irrigated croplands, associated with a period of scarce rainfall. Subsequently, there was a drop in mean chloride concentrations due to the reduction in pumping, together with improved hydrological planning (Figure 2.3).

Groundwater flow in both aquifers approximately follows a NW-SE direction before discharging to the sea. The range of piezometric levels varies significantly depending on the aquifer: in the

Plana de Oropesa-Torreblanca the piezometric level at points furthest from the coast is about 3 m a.s.l., while in the Plana de Vinaroz it reaches 50 m a.s.l. The piezometric level is depressed in both aquifers at certain times in zones close to the coast.

Aquifer geometry is derived from previous 3D models (Renau Pruñonosa 2013). The Plana de Oropesa-Torreblanca aquifer is wedge-shaped being the maximum thickest located near to the coastline, where it can reach 90 m thick. The Plana de Vinaroz has a lenticular geometry and its thickness varies between 30 m and 160 m in the inland zones.

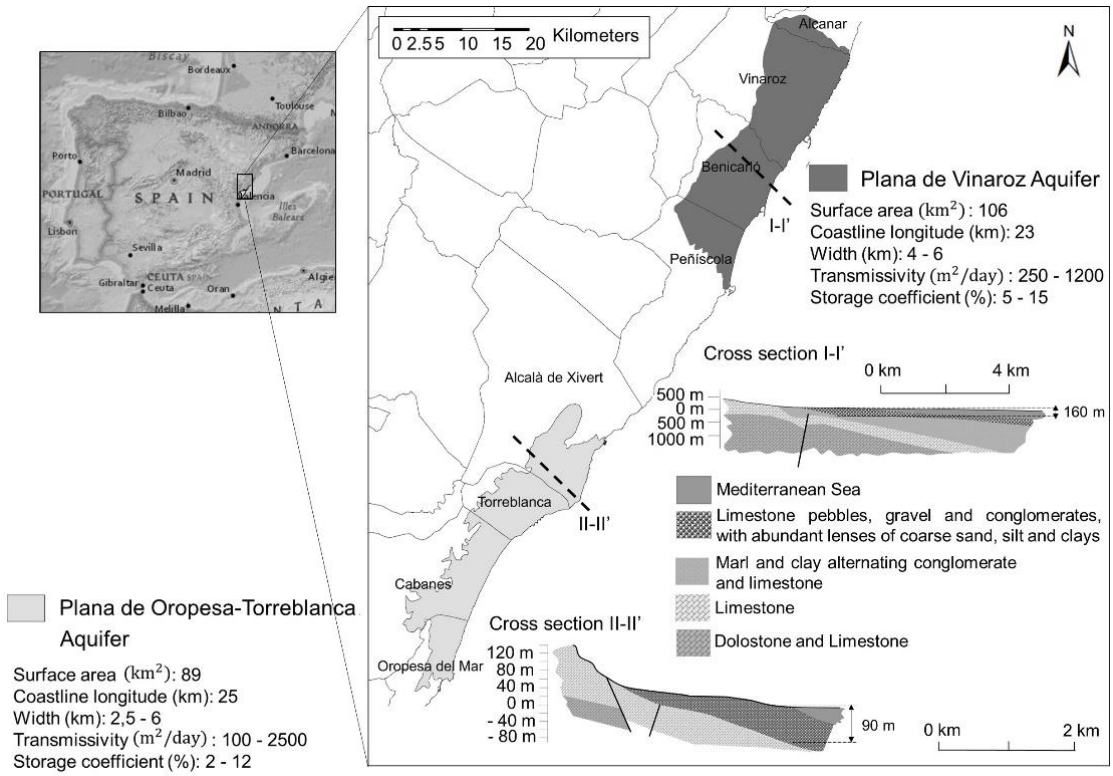

Figure 2.2. Situation of the study area and hydrogeology

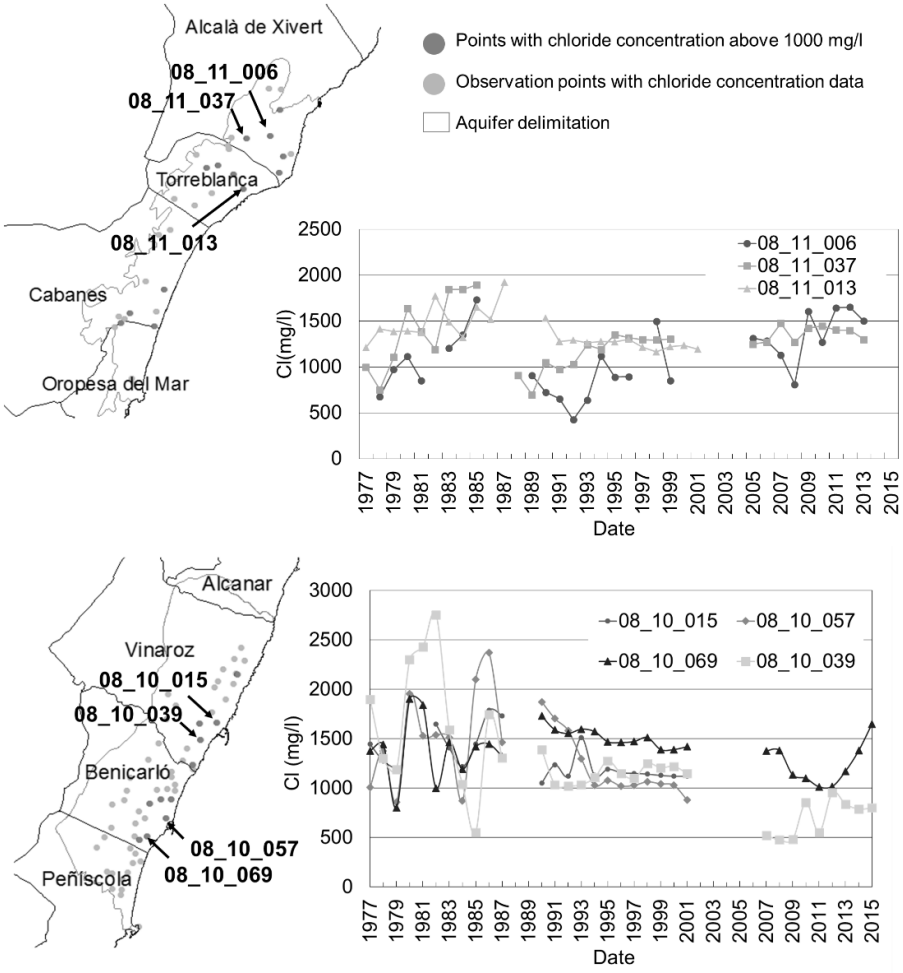

Figure 2.3. Observation points for chloride concentration and evolution of the chloride concentrations in monitoring points in Plana de Oropesa-Torreblanca (top) and Plana de Vinaroz (down) aquifers

4. Results

Here we present the results obtained when the proposed methodology was applied to the two case studies.

4.1. MART Index

4.1.1. 2D – 3D Maps. Evolution of Chloride Concentration and Affected Volume (Graphics)

In terms of the natural background, two different chloride thresholds were used for the calculations. First, a chloride concentration level is established according to the natural background for each aquifer. In CHJ (2016) a reference value of 1100 mg/l is established for both Plana de Oropesa-Torreblanca and Plana de Vinaroz aquifers. In order to analyse the sensitivity to the threshold value, we also tested a threshold of 250 mg/l, which is the default value for all aquifers set in other previous studies (Ballesteros et al. 2016).

Figure 2.4 shows an example of the chloride concentration map obtained, with the affected and unaffected zones for both thresholds.

The 2D maps of chloride concentration show that the zone of SWI in Plana de Oropesa-Torreblanca aquifer grew. However Plana de Vinaroz aquifer has undergone a slight improvement in the study period. Moreover the affected zone in the Plana de Oropesa is significantly greater than for Plana de Vinaroz (Figure 2.5a).

The mean concentration in the zone affected for each aquifer, based on the natural background threshold concentration, lies between 2000 and 2500 mg/l in both aquifers over almost the entire period (Figure 2.5b). Although a fall in mean chloride concentration of the affected zone is observed in Plana de Oropesa-Torreblanca aquifer from 1977 to 1983, it does not indicate an improvement in the water quality in this period since the affected volume increased in this period (Figure 2.5a). Chloride concentration is spread over a wider area although the mean concentration in the impacted zone diminished.

The mean chloride concentration in the entire aquifer shows an increasing trend until 1987 (Figure 2.5b), which may be explained by the increased abstractions made during this period; after this date, chloride concentrations fell again. The greater the distance between the mean aquifer concentration and the mean concentration in the affected zone, the better the overall status of the aquifer. This does not mean that the aquifer does not suffer grave SWI problems in certain zones. In the Plana de Oropesa-Torreblanca these curves are very close, and so there are significant SWI problems over almost all of the aquifer, the difference being much greater than in the Plana de Vinaroz.

Lastly, we analysed the sensitivity of the results to variations in the reference value used. The volume affected using a threshold of 250 mg/l for the two aquifers is much greater than when using a threshold corresponding to the natural background of each aquifer (Figure 2.5a). In contrast, of course, the mean concentration of the zone affected using the natural background threshold (Figure 2.5b) is much larger. This phenomenon highlights the need to determine the natural background of each aquifer precisely, since the assessment of whether there are SWI problems is quite sensitive to this threshold value.

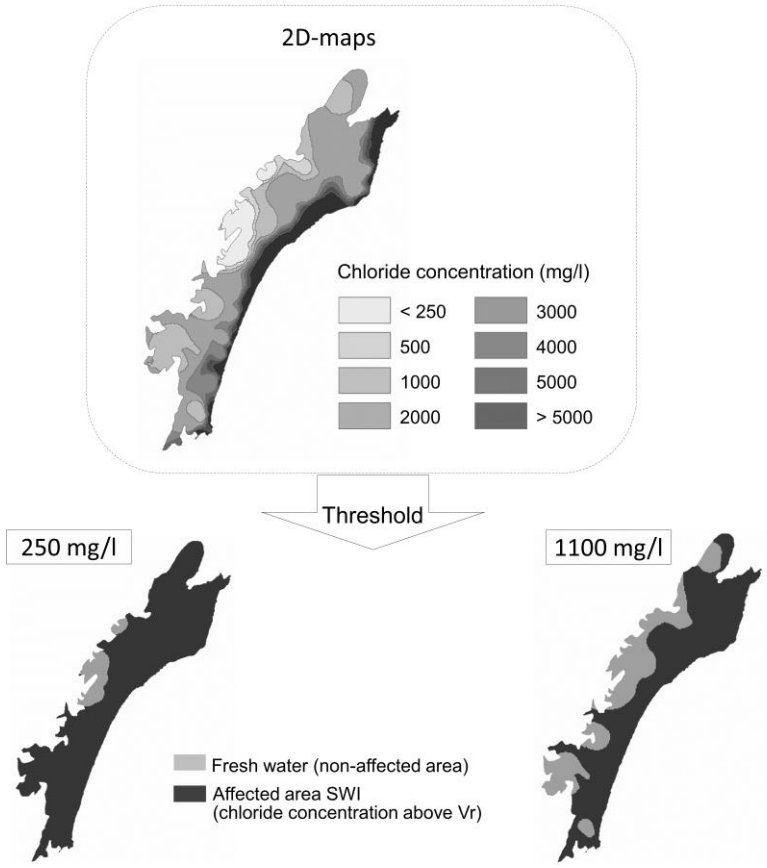

Figure 2.4. Chloride concentration maps in Plana de Oropesa-Torreblanca for October 1985

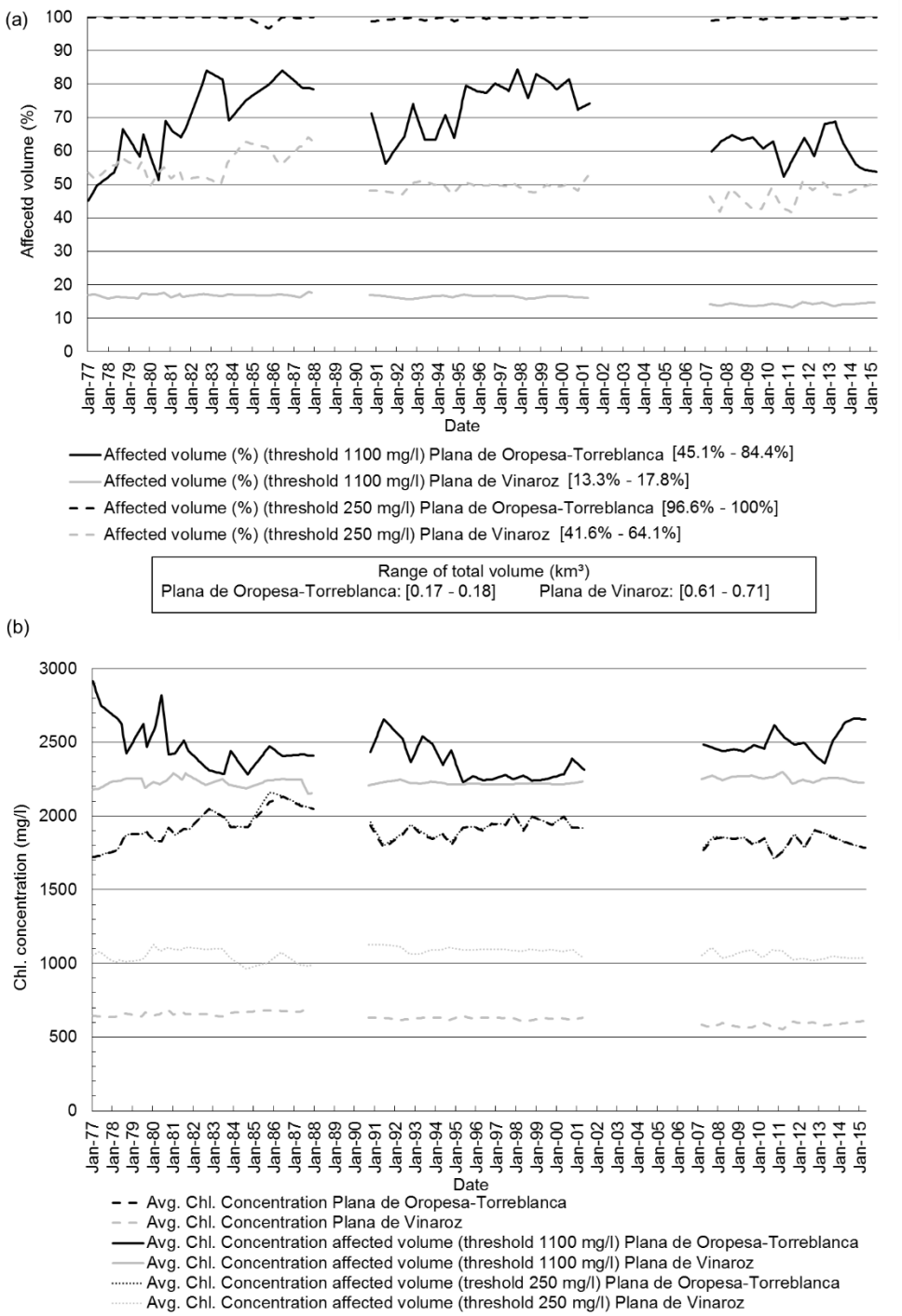

Figure 2.5. Evolution of (a) affected volume (rg (%)) and (b) average chloride concentration in total aquifer and in the affected volume for the two aquifers

4.1.2. 2D Cross-Sections: Penetration and Thickness. Increase in Concentration

The volume of the Plana de Vinaroz aquifer is significantly larger than the Plana de Oropesa-Torreblanca (Figure 2.6). In both aquifers, the thickness affected is greater than the mean thickness of the aquifer. These results are consistent with the aquifer geometry and the location of affected areas.

Again, the sensitivity of the results to the reference value used can be seen. The lower the value of the threshold, the further the affected zone extends inland. For example, using the 250 mg/l threshold, the entire Plana de Oropesa-Torreblanca aquifer is affected during certain years.

Both penetration and thickness reveal the proportion of the aquifer affected.

4.1.3. Global Index: Mass of Affected Area (Ma)

The trend of the index Ma in the two aquifers is similar for both thresholds tested (Figure 2.7). In general, there was a period when the water quality in the aquifers fell continuously (1977–1986), with Ma rising until 1986. In subsequent years, there was a generalised improvement in both aquifers, particularly after 2007. This improvement could be the result of the wet period from 2002 to 2004 (García-Menéndez et al. 2016) and the effect of newly implemented policies to comply with the Water Framework Directive (2000).

The value of Ma (Figure 2.7) in the Plana de Oropesa-Torreblanca for the natural background is greater than in the Plana de Vinaroz, indicating that the Plana de Oropesa-Torreblanca is in a more critical state than the Plana de Vinaroz. This index, Ma, provides information about the overall importance of SWI in each aquifer and its evolution over time. For a more detailed description of the problem, this index can be combined with the mean concentration of the affected zone (to give an idea of the intensity of the problem) and the 2D section (which informs about the size of the zone affected). For example, comparing the mean concentration of the affected zone when considering the natural background level as the threshold for identifying the presence of SWI in each of the two aquifers (Figure 2.5b), it can be seen that they take similar values (2000–2500 mg/l); however, the section affected in the Plana de Oropesa-Torreblanca (Figure 2.6) and the proportion of its volume affected (Figure 2.5a) are much greater than in the Plana de Vinaroz. These results indicate that the Plana de Oropesa-Torreblanca aquifer suffers grave problems due to SWI over almost all its entirety.

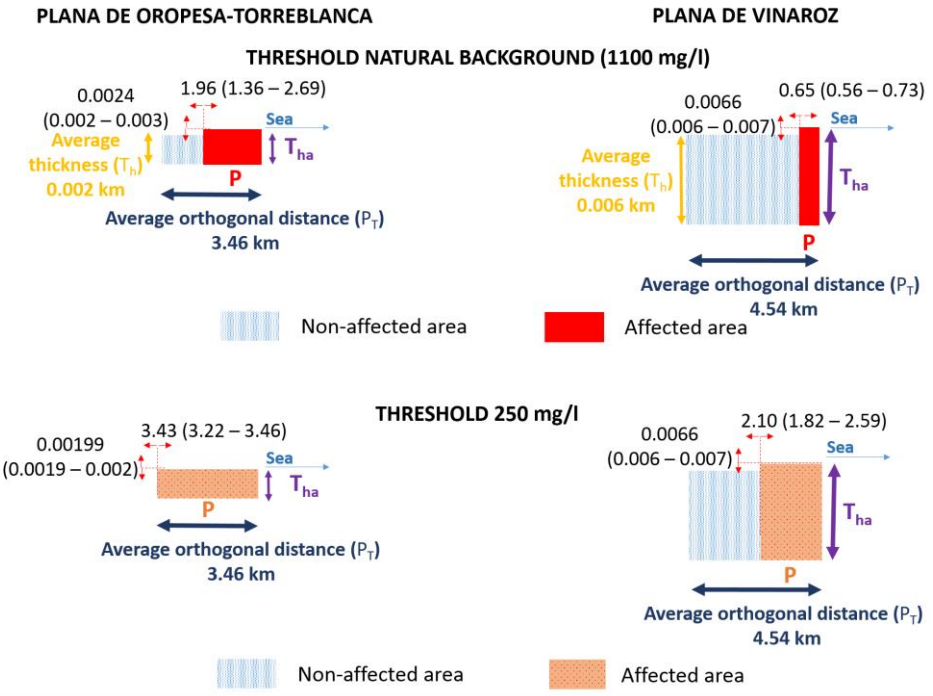

Figure 2.6. Average cross-sections for two thresholds (natural background and 250 mg/l) (MART index) over the period 1977–2015 (vertical exaggeration scale: 500)

4.1.4. Resilience and Trend (MART)

Higher values of Resilience were obtained for the period up to 1987 (Figure 2.8), which indicates that changes in the intrusion were more significant. The value of Trend in the Plana de Oropesa-Torreblanca is positive and also elevated, showing that the change has been a deterioration in the state of the aquifer; while in the Plana de Vinaroz there are periods of improvement (negative trend) though the changes are not significant (low resilience values).

Although changes have decreased in the last period, the values of Resilience in Plana de Oropesa-Torreblanca aquifer are higher than in Plana de Vinaroz aquifer.

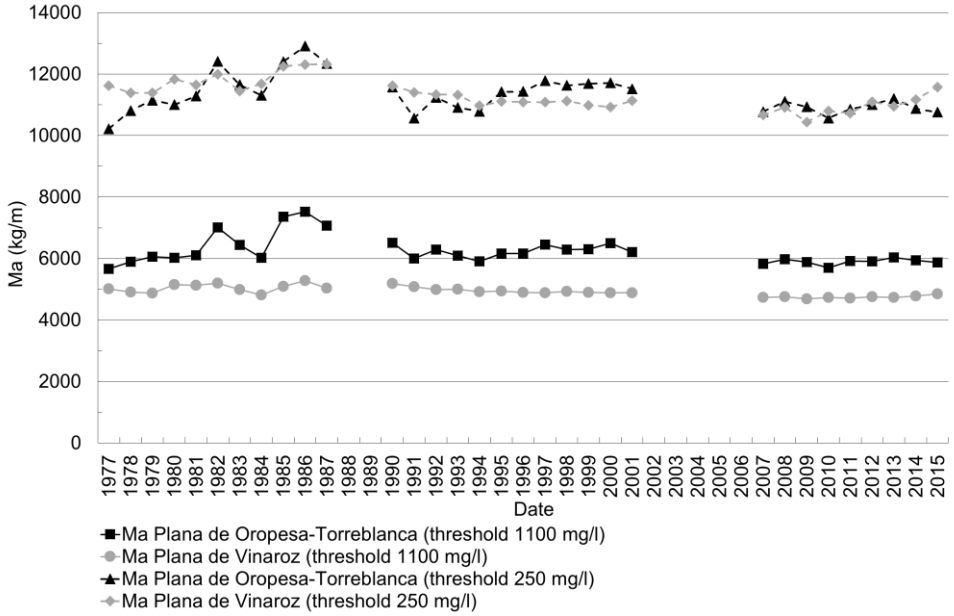

Figure 2.7. Evolution of the global index, Ma, in the two aquifers studied

The results are represented only for the threshold established by the natural background (1100 mg/l).

Due to the geometry and hydrodynamics of each aquifer, it is more complicated in some aquifers to recover good water quality than in others. In this way, the geometry is more of an obstructing factor in the case of Plana de Oropesa-Torreblanca, which is thickest close to the coastline.

4.2. GALDIT Index

4.2.1. Maps. Vulnerability and Identification of Affected Volume (Graphics)

Figure 2.9 shows examples of vulnerability maps from GALDIT for a specific date in both aquifers studied. The red circles indicate zones where changes occurred during the study period (1977–2015).

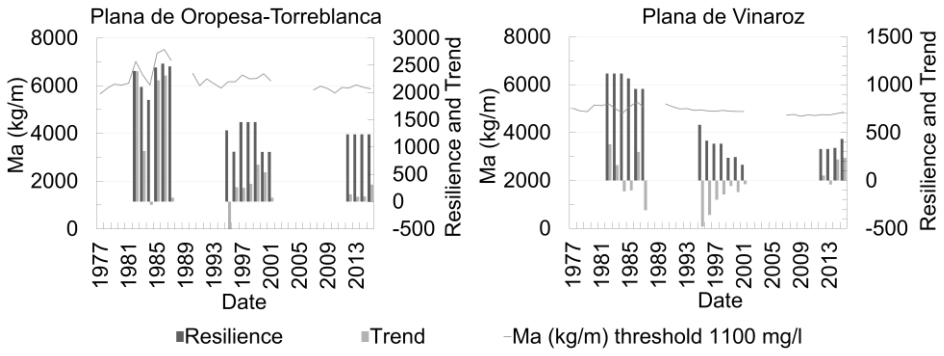

Figure 2.8. Ma, Resilience and Trend in Plana de Oropesa-Torreblanca and Plana de Vinaroz aquifers (scale exaggeration Resilience and Trend: 10000)

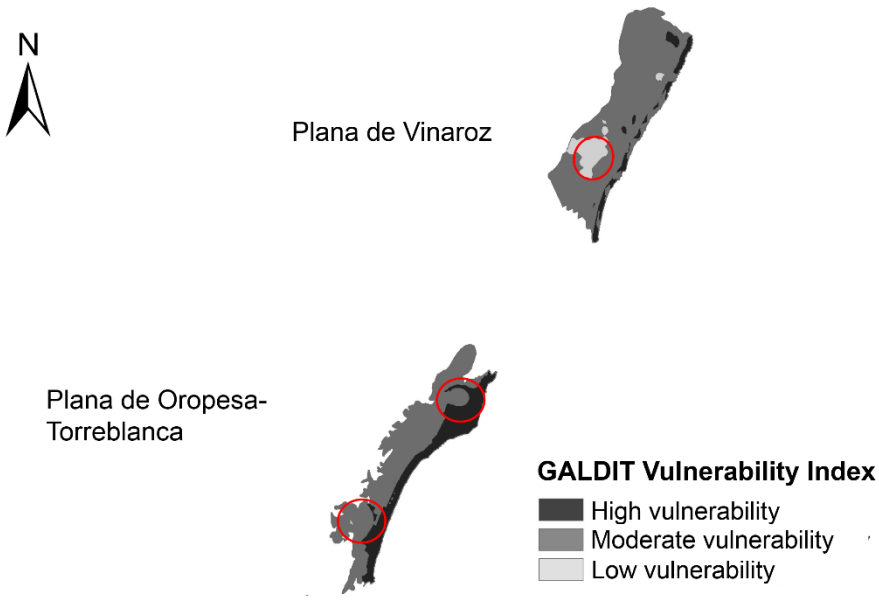

Figure 2.9. L_GALDIT maps in Plana de Oropesa-Torreblanca for April 2015

This leads to several conclusions. In the Plana de Vinaroz aquifer the zone of mean vulnerability occupies almost the whole aquifer while the zone of low vulnerability is very small since conductivity is greatly elevated in almost the entire aquifer.

The Plana de Oropesa-Torreblanca aquifer is highly vulnerable due to the charac- teristics of its formation (it is an aquifer lying parallel to the coast with a wedge shaped geometry, very shallow inland, thicker close to the coastline, and with high conductivity) and to the elevated chloride concentration along the coastline. Further- more, the concentration of bicarbonates is low, which is an indicator of the presence of seawater (Chachadi and Lobo-Ferreira 2005).

The volume affected when considering each vulnerability threshold shows little temporal variability over the period of study (1977–2015).

4.2.2. 2D Cross Sections: Penetration and Thickness. Vulnerability Classes

There are certain similarities in the cross-sections of L_GALDIT (Figure 2.10) and MART. In the Plana de Oropesa-Torrebanca aquifer, the sections obtained for MART for both threshold are similar as those obtained for GALDIT though less so for the Plana de Vinaroz.

It should be borne in mind that the vulnerability and the overall state of the aquifer do not have to concur. Poor quality is not necessarily found in a vulnerable zone. The zone affected by intrusion can be small, even if a large part of the aquifer is classed as vulnerable due to its intrinsic characteristics.

4.2.3. Lumped Index: L_GALDIT. Resilience and Trend

The aggregated index, L_GALDIT (Figure 2.11), exhibits little variability compared to the Ma Index (Figure 2.8). This is due to the various factors that are used in calculating vulnerability (Benini et al. 2016), especially those factors that have greater weight and less spatial variability (conductivity and distance from the coast), which help to smooth out the results.

Almost the entire extension of both aquifers has moderate+high vulnerability. Nevertheless, in the Plana de Oropesa-Torreblanca, the mean vulnerability is higher. These results indicate that the Plana de Oropesa-Torreblanca aquifer is much more vulnerable quantitatively, and second, that the vulnerable zone occupies a much larger extension.

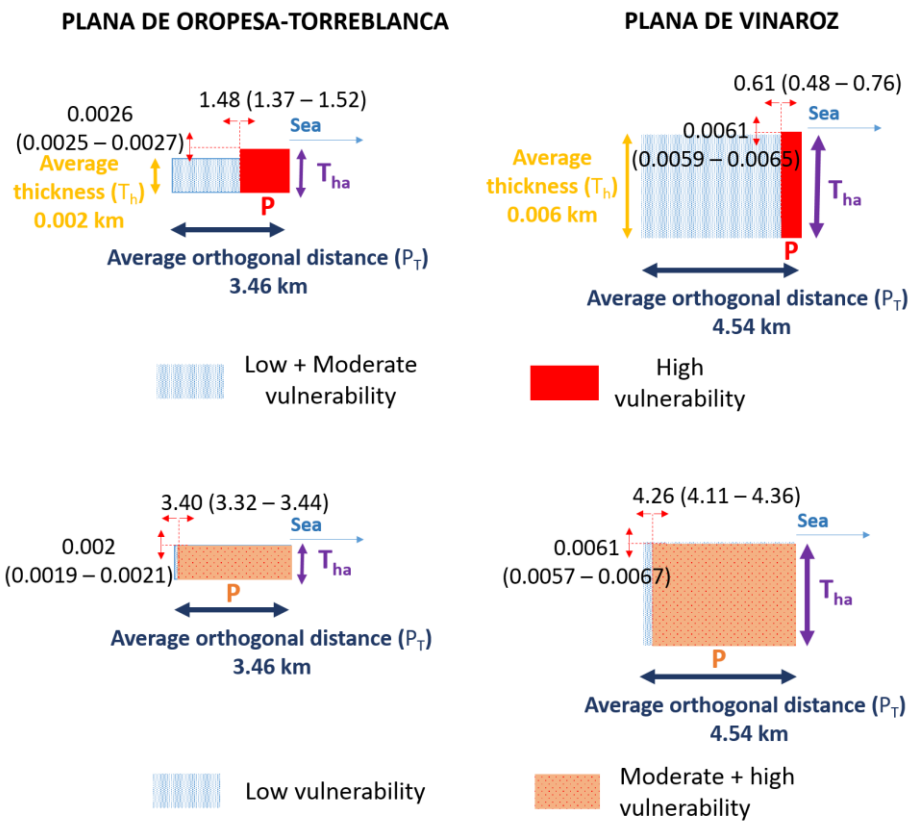

Figure 2.10. Average cross-sections in two aquifers (L_GALDIT index) for the period 1977–2015 (vertical exag- geration scale: 500)

Resilience and Trend are represented only for the threshold delimiting high vulnerability (GALDIT = 7.5). The Resilience values are low and very similar in both the Plana de Vinaroz and Plana de Oropesa-Torreblanca (values less than 0.01). Such low values are due to the fact that the values of the index L_GALDIT vary within a narrow range, as well as to the fact that the index has low variability due to the reasons commented above.

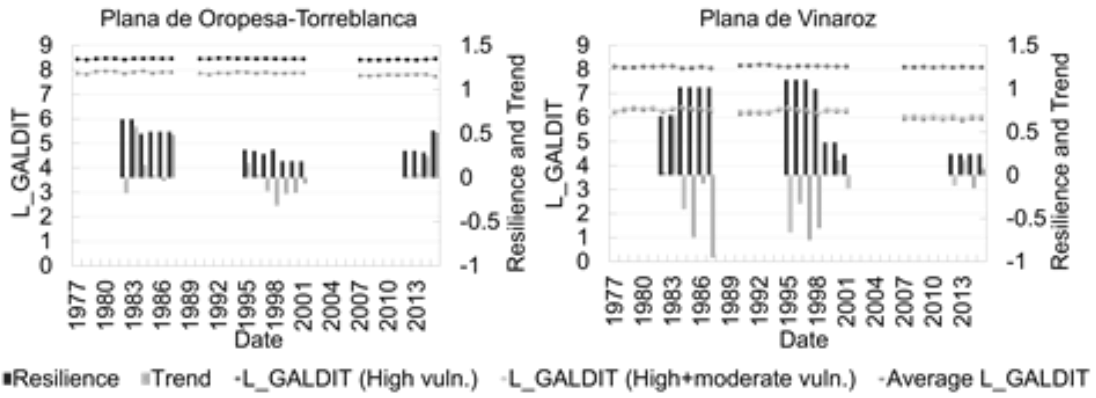

Figure 2.11. L_GALDIT, Resilience and Trend in Plana de Oropesa-Torreblanca and Plana de Vinaroz aquifers (scale exaggeration Resilience and Trend: 100)

5. Conclusions

This paper presents a novel methodology for assessing the overall status of seawater intrusion and vulnerability in coastal aquifers using a mixed lumped-distributed analysis. The problem of chloride contamination is represented in coastal aquifers on different spatial scales, obtaining 2D maps, mean cross-sections and an aggregated index of overall state. In addition, we propose an aggregated index for assessing vulnerability, L_GALDIT, based on the GALDIT method that is already known. The method allows the significance of intrusion and vulnerability to be compared across different aquifers and time periods. Moreover, it can be used to assess resilience and trend respect to SWI.

In terms of the overall status of the two aquifers studied, we deduce that the Plana de Oropesa-Torreblanca aquifer has a worse state and it needs more important changes in groundwater use. Resilience indicates that this aquifer has more potential to recover a good status, although it would require great changes in the current pumping management. In addition, due to its intrinsic characteristics it has a high vulnerability and is susceptible to contamination. With respect to vulnerability, again the Plana de Oropesa-Torreblanca is the more vulnerable of the two aquifers, both in terms of its extent and magnitude. Though the Plana de Vinaroz is also vulnerable over almost all of it extent, the value for vulnerability is moderate. Bearing in mind the overall status and vulnerability conjointly, we can say that the aquifer affected in the Plana de Oropesa-Torreblanca (47.6–86.7%) is similar to the aquifer classified as vulnerable (56.6–99.8%) for both thresholds. However, in the Plana de Vinaroz, though the majority of the aquifer is vulnerable (94.1% with an index of moderate vulnerability), no all of it exhibits SWI problems (the aquifer affected by high chloride concentration is less than 66% of the total aquifer).

Acknowledgments This work have been partially supported by the CGL2013-48424-C2-2-R project and the Plan de Garantía Juvenil from Mineco, co-financing by BEI and FSE.

References

Aller L, Bennett T, Lehr JH, Perry RJ, Hackett G (1987) DRASTIC: a standardized system for evaluating groundwater pollution potentials using hydrogeological settings. Environmental Protection Agency, EPA 600/2–87-035; pp 622

Arslan H, Cemek B, Demir Y (2012) Determination of seawater intrusion via hydrochemicals and isotopes in Bafra plain, Turkey. Water Resour Manag 26(13):3907–3922. https://doi.org/10.1007/s11269-012-0112-3

Ballesteros BJ, Morell I, García-Menéndez O, Renau-Pruñonosa A (2016) A standardized index for assessing seawater intrusion in coastal aquifers: the SITE index. Water Resour Manag 30(13):4513–4527. https://doi. org/10.1007/s11269-016-1433-4

Barlow PM, Reichard EG (2010) Saltwater intrusion in coastal regions of North America. Hydrogeol J 18(1): 247–260. https://doi.org/10.1007/s10040-009-0514-3

Barrocu G (2003) Seawater intrusion in coastal aquifers in Italy. Coastal Aquifers Intrusion Technology: Mediterranean Countries. IGME (ed). ISBN:84–7840–470-8

Benini L, Antonellini M, Laghi L (2016) Assessment of water resources availability and groundwater salinization in future climate and land use change scenarios: a case study from a coastal drainage basin in Italy. Water Resour Manag 30:731–745. https://doi.org/10.1007/s11269-015-1187-4

Boschetti T, González-Hernández P, Hernández-Díaz R, Naclerio G, Celico F (2015) Seawater intrusion in the Guanahacabibes Peninsula (Pinar del Río Province, western Cuba): effects on karst development and water isotope composition. Environ Earth Sci 73:5703–5719. https://doi. org/10.1007/s12665-014-3825-1

Bouderbala A (2015) Groundwater salinization in semi-arid zones: an example from Nador plain (Tipaza, Algeria). Environ Earth Sci 73:5479–5496. https://doi.org/10.1007/s12665-014-3801-9

Chachadi AG, Lobo-Ferreira JP (2001) Sea water intrusion vulnerability mapping of aquifers using GALDIT method. In: Proc. Workshop on Modelling in Hydrogeology (Anna University, Chennai), 143–156, and in COASTIN A Coastal Policy Research Newsletter, Number 4, March 2001. New Delhi, TERI, 7–9, cf. http://www.teriin.org/-teri-wr/coastin/newslett/coastin4.pdf

Chachadi AG, Lobo-Ferreira JP (2005) Assessing aquifer vulnerability to sea-water intrusion using GALDIT method: part 2 – GALDIT indicator descriptions. IAHS and LNEC, Proceedings of the 4th The Fourth Inter Celtic Colloquium on Hydrology and Management of Water Resources, held at Universidade do Minho, Guimarães, Portugal, July 11–13, 2005

CHJ (2016) (Júcar Water Agency) Júcar River Basin Plan. Demarcación hidrográfica del Júcar. Confederación Hidrográfica del Júcar. Ministry of Agriculture, Food and Environment, Spain

Civita MV (1994) Le carte della vulnerabilità degli acquiferi all'inquinamento: Teoria & pratica (Groundwater vulnerability maps to contamination: Theory and practice). Pitagora, Bologna

Custodio E (2010) Coastal aquifers of Europe: an overview. Hydrogeol J 18:269–280

Doerfliger N, Jeannin PY, Zwahlen F (1999) Water vulnerability assessment in karst environments: a new method of defining protection areas using a multi-attribute approach and GIS tools (EPIK method). Environ Geol 39:165–176

Dahlstrom K, Müller D (2006) D14: Report on National Methodologies for Groundwater Threshold Values. BRIDGE project, Background Criteria for the Identification of Groundwater Thresholds, 6th Framework Programme Contract, 6538

Eeman S, Leijnse A, Raats PAC, Van Der Zee SEATM (2011) Analysis of the thickness of a fresh water lens and of the transition zone between this lens and upwelling saline water. Adv Water Resour 34:291–302. https://doi.org/10.1016/j.advwatres.2010.12.001

García-Menéndez O, Morell I, Ballesteros BJ, Renau-Pruñonosa A, Esteller MV (2016) Spatial characterization of the seawater upconing process in a coastal Mediterranean aquifer (Plana de Castellón, Spain): evolution and controls. Environ Earth Sci 75:728. https://doi.org/10.1007/s12665-016-5531-7

Guhl F, Pulido-Bosch A, Pulido-Leboeuf P, Gisbert J, Sánchez-Martos F, Vallejos A (2006) Geometry and dynamics of the freshwater-seawater interface in a coastal aquifer in southeastern Spain. Hydrol Sci J 51(3): 543–555. https://doi.org/10.1623/hysj.51.3.543

Günay G (1997) Solutions of seawater intrusion problems in Turkey. Chap. 15 of Seawater intrusion in coastal aquifers. Guidelines for study, monitoring and control. FAO. 153 pp. ISBN:92–5–103986-0

Kazakis N, Pavlou A, Vargemezis G, Voudouris KS, Soulios G, Pliakas F, Tsokas G (2016) Seawater intrusion mapping using electrical resistivity tomography and hydrochemical data. An application in the coastal area of eastern Thermaikos Gulf, Greece. Sci Total Environ 543:373–387. https://doi.org/10.1016/j. scitotenv.2015.11.041

Kumar P, Bansod BK, Debnath SK, Thakur PK, Ghanshyam C (2015) Index-based groundwater vulnerability mapping models using hydrogeological settings: a critical evaluation. Environ Impact Assess Rev 51:38–49

Llopis-Albert C, Pulido-Velazquez D (2014) Discussion about the validity of sharp-interface models to deal with seawater intrusion in coastal aquifers. Hydrol Process 28:3642–3654. https://doi.org/10.1002/hyp.9908

Parck Y, Lee JY, Kim JH, Song SH (2012) National scale evaluation of groundwater chemistry in Korea coastal aquifers: evidences of seawater intrusion. Environ Earth Sci 66:707–718. https://doi.org/10.1007/s12665- 011-1278-3

Petalas C, Lambrakis N (2006) Simulation of intense salinization phenomena in coastal aquifers of Thrace. J Hydrol 324:51–64. https://doi.org/10.1016/j.hjydrol.2005.09.031

Pratheepa V, Ramesh S, Sukumaran N, Murugesan AG (2015) Identification of the sources for groundwater salinization in the coastal aquifers of Southern Tamil Nadu, India. Environ Earth Sci 74:2819–2829. https://doi.org/10.1007/s12665-015-4303-0

Renau Pruñonosa A (2013) Nueva herramienta para la gestión de las aguas subterráneas en acuíferos costeros. Volumen ecológico de remediación (VER). Metodología y aplicación a la Plana de Oropesa-Torreblanca (MASub 080.110), Universitat Jaume I

Smith AJ (2004) Mixed convection and density-dependent seawater circulation in coastal aquifers. Water Resour Res 40:W083091–W.083091. https://doi.org/10.1029/2003WR002977

Stempvoort DV, Ewert L, Wassenaar L (1993) Aquifer vulnerability index: a GIS-compatible method for groundwater vulnerability mapping. Can Water Resour J 18:25–37

Steyl G, Dennis I (2010) Review of coastal-area aquifers in Africa. Hydrogeol J 18:217–225. https://doi. org/10.1007/s10040-009-05459

Trabelsi N, Triki I, Hentati I, Zairi M (2016) Aquifer vulnerability and seawater intrusion risk using GALDIT, GQISWI and GIS: case of a coastal aquifer in Tunisia. Environ Earth Sci 75:1–19

Water Framework Directive (WFD) (2000) Directiva 2000/60/CE del Parlamento Europeo y del Consejo de 23 de Octubre de 2000. Diario Oficial de las Comunidades Europeas de 22/12/2000. L 327/ 1–327/32

Werner AD (2010) A review of seawater intrusion and its management in Australia. Hydrogeol J 18:281–285.

Werner AD, Gallagher MR (2006) Characterisation of sea-water intrusion in the Pioneer Valley, Australia using hydrochemistry and three-dimensional numerical modelling. Hydrogeol J 14:1452–1469

Werner AD, Ward JD, Morgan LK, Simmons CT, Robinson NI, Teubner MD (2012) Vulnerability indicators of sea water intrusion. Ground Water 50(1):48–58

Wriedt G, Bouraoui F (2009) Large scale screening of seawater intrusion risk in Europe – methodological development and pilot application along the Spanish Mediterranean coast. Luxembourg: European Commission, Joint Research Centre, Institute for Environment and Sustainability. https://doi.org/10.2788/19371

Capítulo 3: Summarizing the impacts of future potential global change scenarios on seawater intrusion at the aquifer scale

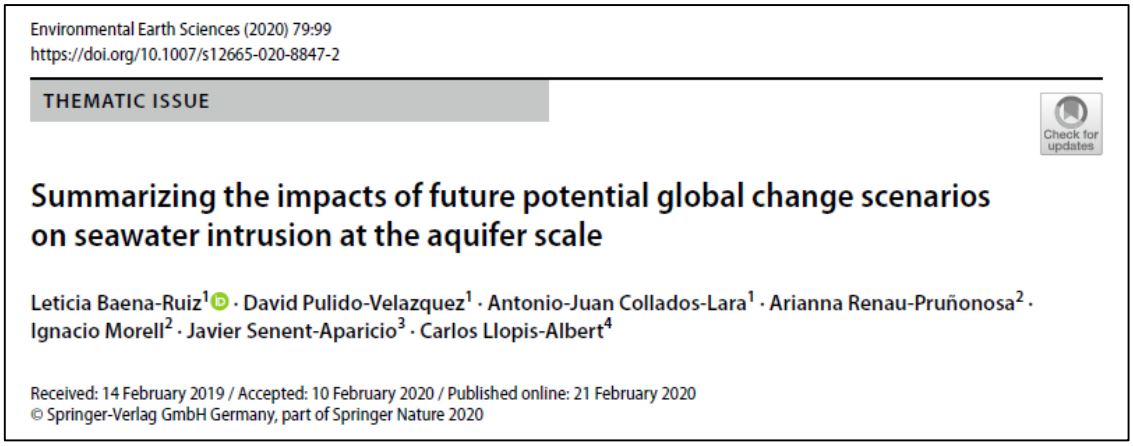
Environmental Earth Sciences (2020) 79:99
https://doi.org/10.1007/s12665-020-8847-2

THEMATIC ISSUE

Summarizing the impacts of future potential global change scenarios on seawater intrusion at the aquifer scale

Leticia Baena-Ruiz[1] · David Pulido-Velazquez[1] · Antonio-Juan Collados-Lara[1] · Arianna Renau-Pruñonosa[2] · Ignacio Morell[2] · Javier Senent-Aparicio[3] · Carlos Llopis-Albert[4]

Received: 14 February 2019 / Accepted: 10 February 2020 / Published online: 21 February 2020

Reference: Baena-Ruiz, L., Pulido-Velazquez, D., Collados-Lara, AJ. et al. Summarizing the impacts of future potential global change scenarios on seawater intrusion at the aquifer scale. Environ Earth Sci 79, 99 (2020). https://doi.org/10.1007/s12665-020-8847-2

Authors and affiliations:

Leticia Baena Ruiz[(1,*)], David Pulido-Velazquez[(1)], Aantonio-Juan Collados-Lara[(1)], Arianna Renau-Pruñonosa[(4)], Ignacio Morell[(2)] Javier Senent-Aparicio[(3)], Carlos Llopis-Albert[(4)]

[(1)] IGME, Granada, Spain. lbaenar@gmail.com; d.pulido@igme.es; ajcollados@gmail.com

[(2)] Jaume I University, Castellón, Spain. arenau@guest.uji.es

[(3)] Catholic University of Murcia (UCAM), Campus de los Jerónimos, 30107 Guadalupe (Murcia), Spain. jsenent@ucam.edu

[(4)] Centro de Investigación en Ingeniería Mecánica (CIIM), Universitat Politècnica de València, Camino de Vera s/n, 46022 Valencia, Spain. cllopisa@upvnet.upv.es

*Corresponding author

Abstract

Climate change affects rainfall and temperature producing a breakdown in the water balance and a variation in the dynamic of freshwater–seawater in coastal areas, exacerbating seawater intrusion (SWI) problems. The target of this paper is to pro- pose a method to assess and analyze impacts of future global change (GC) scenarios on SWI at the aquifer scale in a coastal area. Some adaptation measures have been integrated in the definition of future GC scenarios incorporating complementary resources within the system in accordance with urban development planning. The proposed methodology summarizes the impacts of potential GC scenarios in terms of SWI status and vulnerability at the aquifer scale through steady pictures (maps and conceptual 2D cross sections for specific dates or statistics of a period) and time series for lumped indices. It is applied to the Plana de Oropesa-Torreblanca aquifer. The results summarize the influence of GC scenarios in the global status and vulnerability to SWI under some management scenarios. These GC scenarios would produce higher variability of SWI status and vulnerability.

Keywords Global change impacts; Adaptation measures; Seawater intrusion; Status and vulnerability; Coastal aquifer; Lumped index

1. Introduction

It is a fact that climate change (CC) would imply a variation in the patterns of temperature and precipitation in the future. In general, in the Mediterranean area an increase in temperature and a decrease in precipitation is expected. The available potential future scenarios show higher evapotranspiration, a lower groundwater (GW) recharge and an increase of the sea level. In coastal areas, the problem is exacerbated due to overexploitation, intensifying SWI. Therefore, maintaining acceptable quantity and quality characteristics of GW reserves is important to ensure demand water supply (Sola et al. 2013; Renau-Pruñonosa et al. 2016).

Many investigations have focused on sea-level rise as an important effect of GC on SWI in coastal aquifers (Werner and Simmons 2009; Ferguson and Gleeson 2012; Loáiciga et al. 2012; Benini et al. 2016), but many aquifers are more vulnerable to CC effects on GW recharge and pumping than to sea-level rise (Ferguson and Gleeson 2012; Rasmussen et al. 2013).

An increase in temperature and a decrease in precipitation will force a greater use of available water resources, especially GW. It is due to the recharge decrease and the increase in crop water requirements and, therefore, in the pumping rates. Overexploitation is the main problem in most coastal aquifers, since it produces inland penetration of the saltwater. Therefore, to reduce the impacts of GC on SWI, different adaptation strategies could be applied. They include measures to reduce aquifer demands such as land use and land cover (LULC) changes, modernization and adaptation of irrigation areas and/or economic instruments (Escriba-Bou et al. 2017; Grundmann et al. 2012; Robins et al. 1999). Different measures focused on the offer could be also applied to obtain complementary resources to supply demands, as for example water reuse, desalinations, water transfers and conjunctive use measures (Trinh et al. 2012; McEvoy and Wilder 2012; Pulido-Velazquez et al. 2011).

Many authors have assessed hydrological impacts of CC and/or LULC changes in the SWI phenomenon using sharp interface or density-dependent flow models to simulate hydraulic head and salinity in the aquifer (Pulido-Velazquez et al. 2018; Romanazzi et al. 2015; Klove et al. 2014; Rajan et al. 2006). Potential climate scenarios are defined by simulating future emission scenarios within physically based climatic models [general circulation models (GCMs) and regional climatic models (RCMs)]. Due to the significant bias that usually appears between the historical information and the control simulation of the model, to make this climate information relevant for case study, we need to translate them to the regional local scale by applying some statistical corrections (Collados-Lara et al. 2018). Distributed hydrological models are useful tools to propagate scenarios to assess the impacts on hydrological variables at the specific time and location. Nevertheless, they do not allow drawing direct conclusions about the impacts on SWI (status and vulnerability) at the aquifer scale. For this purpose, an approach such as an index-based method, defined from the output of the model, is a useful tool to analyze this issue. It can also help to summarize SWI problems at the aquifer scale in different periods and identify aquifers in risk of not achieving good chemical status according to the Water Framework Directive (WFD 2000; CHJ 2015).

The vulnerability to contamination in coastal aquifers under future climate scenarios has been previously studied by several authors by employing different vulnerability indices. Li and Merchant (2013) employed a modified DRASTIC index to model GW vulnerability under future climate and LULC scenarios. Benini et al. (2016) used the GALDIT method to assess vulnerability in the Quinto Basin by employing some CC and LULC change scenarios in a long-term period. They did not use a flow model to simulate salinity and hydraulic head variables. Luoma et al. (2017) assessed the potential impacts of CC on the vulnerability to pollution of an aquifer comparing AVI, SINTACS and GALDIT methods. Although the assessment of vulnerability under future scenarios using an index-based method has been applied by different authors (Huang et al. 2017; Koutroulis et al. 2018), none of them have summarized and analyzed this issue at the aquifer scale.

In Baena-Ruiz et al. (2018), a novel index-based method was proposed to perform an integrated assessment of the global status and vulnerability to SWI in coastal aquifers. The methodology was applied in the Plana de Oropesa- Torreblanca and Plana de Vinaroz aquifers. It was obtained from hydraulic head and chloride concentration data avail- able in observation wells for the historical period from 1977 to 2015. In that approach, the distributed fields of variables required to define the indices were obtained by applying a simple interpolation method.

This paper intends to achieve a novel objective, to assess the impacts of future GC and CC scenarios on the global status and vulnerability to SWI at the aquifer scale. We propose to perform it by combining a method to summarize SWI at the aquifer scale and the outputs of an integrated method to propagate the impacts of GC scenarios (including adaptation strategies). It intends to contribute to the definition of methods to harmonize the assessment of GC impacts on SWI problems (status and vulnerability) at the aquifer scale. It would not only allow to compare the significance of SWI in different historical and future periods in an aquifer, but also to compare results between different aquifers. The method proposed by Baena-Ruiz et al. (2018) will be adapted to analyze future potential scenarios, since, instead of having a single well-known series (as in the historical period), an infinite number of potential future series are feasible and we analyze some of them. The method will be applied to the Plana de Oropesa-Torreblanca case study, where the impacts of different future GC scenarios are compared. A sensitivity analysis is conducted to assess the influence of CC on the simulated scenarios.

2. Methodology

Figure 3.1 shows the inputs and the method that we propose to follow to achieve the novel objective. It allows to identify the steps to follow to assess the analyses of impacts of future GC and CC scenarios at the aquifer scale (considering adaptation strategies to CC).

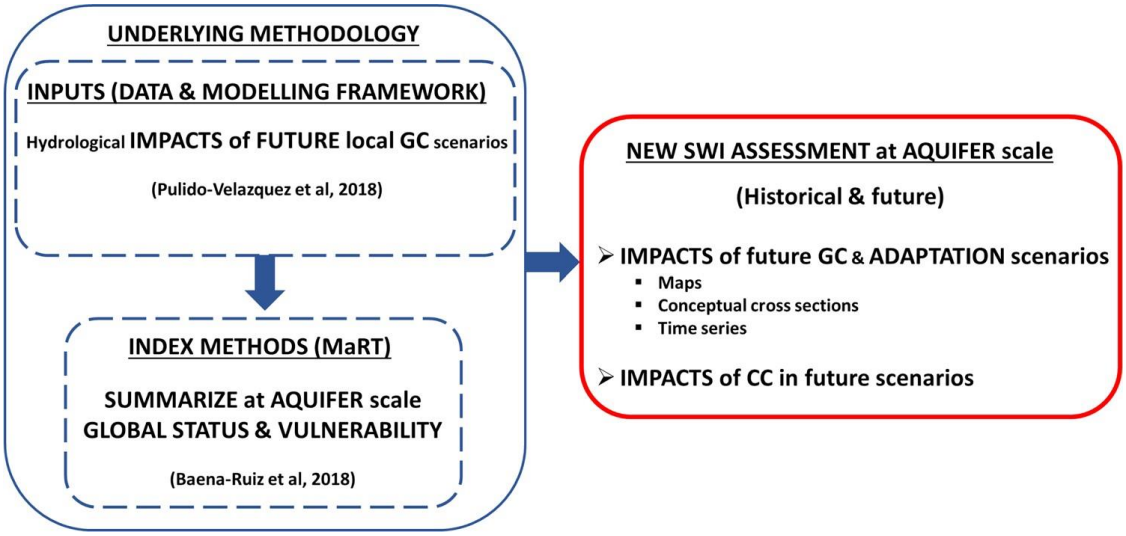

Figure 3.1.Flowchart of the proposed methodology

2.1. Impacts of future GC scenarios and adaptation scenarios at the aquifer scale

Baena-Ruiz et al. (2018) proposed a method to summarize the dynamic of the historical status and vulnerability to SWI at the aquifer scale. It was applied to the Plana de Oropesa Torrablanca aquifer, with the required distributed fields (hydraulic head and chloride concentration) obtained by using a simple interpolation method, which was applied to the in situ measurements. These interpolation approaches cannot be employed to assess future scenarios in which we need physical models to propagate the potential future conditions to obtain the cited variable fields. In these cases, the use of a chain of models, which includes a density- dependent flow model, will be required to assess those fields (Pulido-Velazquez et al. 2018).

To summarize the outputs of the models developed in Pulido-Velazquez et al. (2018) in terms of future SWI results (status and vulnerability) at the aquifer scale, we propose to adapt the Baena-Ruiz et al. (2018) method to deal with the particularities of these future potential scenarios. The method will be also employed to analyze future SWI vulnerability, taking into account other intrinsic aquifer parameters (aquifer type and conductivity). In order to summarize the results, steady pictures (maps of affected area and 2D conceptual cross sections) and lumped indices will be employed. The method will be implemented in a GIS tool that helps to apply it to other case studies.

The maps of chloride concentration are directly obtained from the physical model from Pulido-Velazquez et al. (2018) both for the historical and future periods.

We will also use the definition of affected volume provided by Baena-Ruiz et al. (2018), which is the volume where the chloride concentration level is above the natural background level.

A conceptual cross-section orthogonal to the coastline will be defined to summarize the SWI status at aquifer scale. It can be calculated for a specific time and/or for the statistics (eg. mean, minimum, and maximum values) of a period (historical and/or future). It represents average affected geometry, including the Penetration (P) and the Affected Thickness (Th_a).

$$P(m) = \frac{\sum V_{i(>V_r)}}{T_{ha} * L_{coast}} \quad (1)$$

Where:

- $V_{i(>Vr)}$ is the storage in each cell (m^3) with a concentration greater than V_r $V_{i(>V_r)}(m^3) = S_i(m^2) * b_i(m) * \alpha$;
- V_r = Reference threshold (natural background of the aquifer or vulnerability class);
- L_{coast} is the length of coastline (m);
- S_i is the surface area of each cell in the model (m^2);
- b_i is the saturated thickness at each instant considered (m);
- α is the specific yield;
- T_{ha} is the affected thickness (m). It can be calculated as follow:

$$T_{ha}(m) = \frac{\sum V_{i(>V_r)}}{\sum S_{i(>V_r)}} \quad (2)$$

The affected zone has an increment of concentration (IC) above the natural threshold.

$$IC\left(\frac{mg}{l}\right) = C - V_r \quad (3)$$

Where:

- C=Concentration in the affected volume

$$C\left(\frac{mg}{l}\right) = \frac{\sum(C_{i(>V_r)} * V_{i(>V_r)})}{V_{(>V_r)}} \quad (4)$$

Vulnerability maps were also obtained by applying the GALDIT method (Chachadi and Lobo-Ferreira 2005), which is described in detail in an Appendix. The affected volume is defined as the areas in which the vulnerability is higher than a specific vulnerability class or value (eg. High vulnerability). A conceptual cross section to summarize vulnerability at aquifer scale could be defined following an analogous reasoning to those applied to assess the status (Baena-Ruiz et al. 2018).

The maps and conceptual cross sections will allow to identify the impacts of future GC scenarios on the aquifer in terms of affected volume by a chloride concentration above the natural background or by a high vulnerability, regarding to the historical status. It also allows to compare impacts of different future scenarios on the status and/or vulnerability to SWI.

In order to assess the dynamic-of global status and vulnerability at aquifer scale we analyse time series for two lumped indices: "Ma" and "L_GALDIT" respectively. The "Ma" index is defined as "the total additional mass of chloride that causes the concentration in some areas to exceed the natural threshold" (Baena-Ruiz et al. 2018).

$$Ma\left(\frac{kg}{m}\right) = P(m) * IC\left(\frac{mg}{l}\right) * 10^{-3} * T_{ha}(m) \quad (5)$$

In an analogous way, the "L_GALDIT" is defined as the weighted GALDIT index by the aquifer storage:

$$L\_GALDIT = \frac{\sum(G_i * V_i)}{V} \quad (6)$$

where:

- G_i is the value of GALDIT index in each cell (calculated following the GALDIT method explained in Appendix);
- V_i is the storage in each cell;
- V is the total storage in the aquifer;

In this paper the dynamic of the lumped indices is analyzed taking into account the particularities of the future scenarios. In an historical assessment we have a single real climatic series that allows to draw conclusion about the resilience and trend in the aquifer (Baena-Ruiz et al. 2018). But in the assessment of future scenarios infinite potential future series could be feasible (although we finally considered a limited number of them), and, therefore, the summary of the time series analyses should not be performed in the same way.

In this work we propose to use a new index, the recovery rate, which can be obtained from the evolution of the global indices Ma and L_GALDIT. It is defined as the mean reduction in the index value in a given period. It may be represented in a box-whisker plot in order to provide a statistical assessment of the SWI dynamic in future horizons. The recovery rate for Ma index, which represents the mean recovery velocity of the system, is defined as follow:

$$Recovery\ rate = \frac{Ma_t - Ma_{t-n}}{n} \quad (7)$$

Where:

- Ma_t is the global status (Ma index) in a specific date "t";
- Ma_{t-n} is the global status (Ma index) in a specific date "t-n";
- n is the difference between the date "t" and "t-n" (at monthly scale);

2.2. Impacts of CC in future scenarios

The impacts of CC are analysed though a sensitivity analysis in order to quantify the influence of the CC on the simulated GC scenarios. We compare results obtained for the GC scenarios, which include both, future LULC and potential future CC scenarios, and a future LULC scenario defined assuming that there is not CC. The relative differences in the global status (Ma%) and GW vulnerability (L_GALDIT%) for those scenarios are obtained with the next expressions:

$$Ma\% = \left(\frac{Ma(x) - Ma}{Ma}\right) * 100 \quad (8)$$

$$L\_GALDIT\% = \left(\frac{L\_GALDIT(x) - L\_GALDIT}{L\_GALDIT}\right) * 100 \quad (9)$$

Where:

- Ma% is the variation of the global status (Ma index) due to CC, expressed as a percentage;
- Ma(x) is the average global status (Ma index) for each GC scenario;
- Ma is the average global status index (Ma index) for LULC scenario;

- L_GALDIT% is the variation of the vulnerability (L_GALDIT index) due to CC, expressed as a percentage;
- L_GALDIT(x) is the average vulnerability (L_GALDIT index) for each GC scenario;
- L_GALDIT is the average vulnerability index (L_GALDIT) for LULC scenario;

3. Description of the study area and available information

The Plana de Oropesa-Torreblanca is a detrital Mediterranean aquifer which extends over 75 km^2 in the province of Castellon in Spain. It has a length of 21 km and a width of between 2.5 and 6 km. This Plio-Quaternary aquifer is unconfined and heterogeneous and consist on a silty clay matrix with gravel and sand levels. The aquifer is wedge-shaped and it can reach 90 m thick near to the coast. The transmissivity varies between 300-1000 m^2/day (Renau-Pruñonosa et al. 2016) and the storage coefficient ranges from 2-12%. Figure 3.2 show the location and hydrogeology of the aquifer.

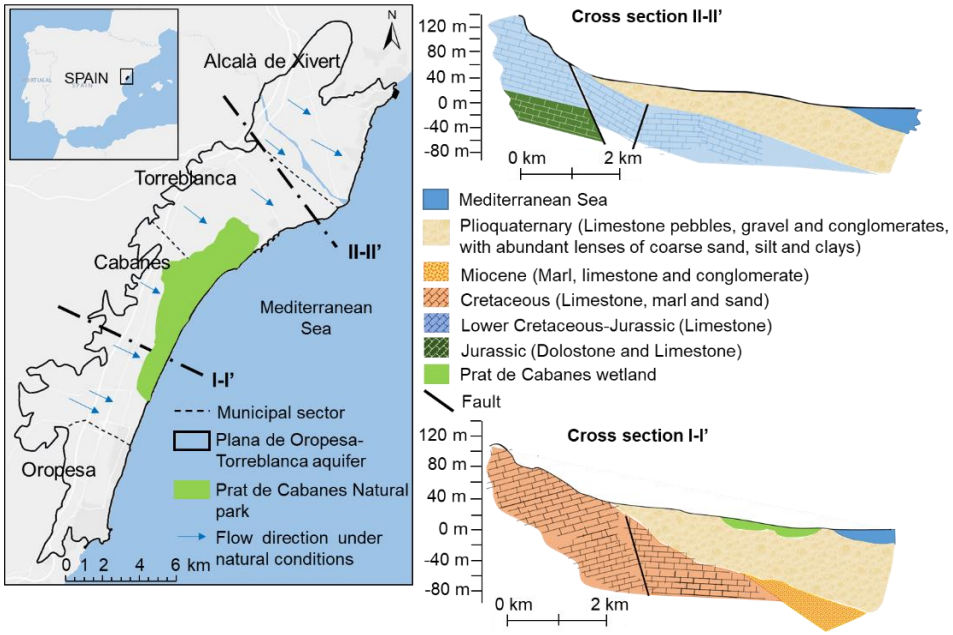

Figure 3.2. Situation of the study area and hydrogeological sections

The wetland Prat de Cabanes is situated in the central zone of the Plana, parallel to coastline. It extends approximately 9 km^2. Its formation is due to the clogging of an old lagoon that reaches several meters thick. This wetland is separated from the sea by a coastal bar of sorted pebbles.

The aquifer is laterally connected with adjacent aquifers which provide inflows to the system (Giménez and Morell 1997). In addition, the aquifer is fed by infiltration of precipitation and irrigation returns. Pumped abstractions, drains to the Prat de Cabanes wetland and GW discharges to sea compound the outflows to the system (Pulido-Velazquez et al. 2018). Groundwater follows a NW-SE direction under natural conditions (Giménez and Morell 1997; Renau-Pruñonosa et al. 2016).

3.1. Data: hydro-climatic conditions, LULC, and pumping data

Historical temperature and precipitation data come from the Spain02 project dataset (Herrera et al. 2012; Herrera et al. 2016). The monthly average precipitation in the period 1973-2010 varied between 20-30 mm in summer and it reached almost 80 mm in the rainiest month. The monthly average temperature went from 12ºC to 28ºC throughout the year.

In the study area there have been important land use changes from 70's. Until 1995 there was a transformation in the crop irrigation, turning it into irrigation lands. From this date to 2010 the

main change was an increase of artificial surfaces (mainly residential LULC along the coast) (Feranec et al. 2010) and an improvement in the efficiency of irrigation techniques (CHJ 2015).

Pumping was deduced from historical data. The mean annual pumping in the historical period is 22 hm^3/year approximately. The land use changes are reflected in the evolution of total pumping in the Plana de Oropesa-Torreblanca aquifer. First, the transformation into irrigated croplands from 1975 to 1995 produce an increase in pumping from 15 hm^3/year to a maximum of 35 hm^3/year. It produced a drop in GW level and higher SWI problems. Later the transformation of irrigation techniques and land uses led to a reduction in pumping to a minimum rate around 13 hm^3/year (Pulido-Velazquez et al. 2018).

3.2. Future LULC scenarios. Implementation of adaptation measures

The future LULC change scenarios are defined taking into account the urban development planning. It has projected land uses changes that are mainly the construction of golf courses and the transformation of the land use from agricultural to residential. The main changes in each municipality are the following (Figure 3.3):

- In Alcalà de Xivert there are not expected significant changes.
- The Urban Development Plan for Torreblanca contemplates the land use change from agricultural to residential (70% of the total area of municipality will be classified as buildable residential or industrial). In the coastal area, north of Prat de Cabanes Natural Park, Doña Blanca Golf Course has been projected.
- In Cabanes and Oropesa municipalities the integrated development plan Marina d'Or Golf has been approved. It will include three golf courses, private urbanization, hotels and landscapes areas.

In order to mitigate the impacts of CC on the GC scenarios, we have also considered the next adaptation measures to increase complementary resources. These adaptation measures were also requirements included in the Urban Development Plan: the irrigation in the golf courses must be supplied by reclaimed water from residential use and water from desalinization plant will be used for human consumption.

In order to make the model more realistic, we assume that these land use changes would be executed gradually from 2015 to 2035. Figure 3.3 shows the evolution of changes in time.

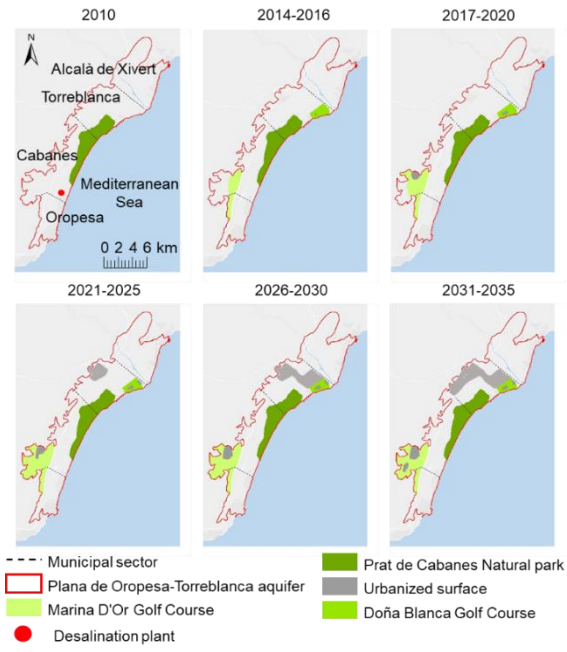

Figure 3.3. Expected land use changes in the Plana de Oropesa-Torreblanca aquifer (2010-2035)

3.3. Future GC scenarios and propagation of impacts

Pulido-Velazquez et al. (2018) generated four potential future climate scenarios (CC scenarios) for Plana de Oropesa-Torreblanca aquifer by employing control and future climatic series data simulated with RCMs in the framework of the CORDEX project (2013) for the most pessimistic emission scenario RCP8.5. All these climate scenarios showed an increase in mean temperature (≈ 1°C on average) with respect to the historical period (1973-2010). The future mean rainfall also showed a decrease (up to 24% monthly) for every month except September and October, in which a relative increase was predicted (up to 30%). These months are the rainiest in the study area and frequent storms occur. The local future scenarios show an increment in these extreme rainfall events (Pulido-Velazquez et al. 2018).

These climate scenarios were combined with a land use change scenario (Section 3.2), including some adaptation measures oriented to define more feasible/realistic future scenarios in accordance with the urban development planning, in which complementary resources will be incorporated within the system (water reuse and water from desalination plants for human consumption in the new urban areas).

The next scenarios were finally analyzed:

- Four GC scenarios (GC1, GC2, GC3, GC4) defined by combining four climate scenarios with the future LULC scenario;
- The LULC scenario was defined assuming that there is not CC;
- In the baseline scenario we assume that the LULC will be maintained as in 2010 and the historical hydro-climatic characteristics will be analogous to those of the period 2006-2010.

A modelling framework was defined with a chain of auxiliary models (rainfall-recharge models, crop irrigation requirements, and irrigation returns models) that provide the inputs to a density dependent flow model (SEAWAT). It was calibrated from the estimated historical pumping and recharge (deduced from the climate and land use data) (Section 3.1 and 3.2) in the aquifer and the hydraulic head and chloride concentration data available in the observation points during the period 1981-2010. Data from 1973 to 1981 were used to validate it. This model was used to propagate the impacts of the plausible future GC scenarios. It provided a spatio-temporal distribution of the chloride concentration and the hydraulic head evolution for the different GC scenarios. The available volume of resource can be estimated from the hydraulic head and the aquifer geometry. The water budget for each GC scenario was also calculated by using SEAWAT model with the Visual Modflow interface. It allows to understand the system dynamic due to CC and LULC changes.

4. Results and discussion

The proposed methodology is applied to Plana de Oropesa-Torreblanca aquifer in order to assess impacts of GC scenarios on SWI at aquifer scale.

4.1. Impacts of future GC scenarios and adaptation scenarios at aquifer scale

The six scenarios defined have been simulated by using SEAWAT model. Field maps of chloride concentration and hydraulic head were previously obtained as output of this model. The area affected by SWI in the aquifer has been identified taking into account the natural background in the aquifer, which is 1100 mg/l of chloride concentration (CHJ 2015; Baena-Ruiz et al. 2018). Figure 3.4 shows the largest affected areas in the historical period and in the future period for different scenarios (future baseline, LULC and GC4). The future baseline and LULC scenarios (defined including the cited adaptation measures) do not show a clear deterioration of the aquifer. The worst hypothetical scenario is the GC4, in which practically the whole aquifer would have a chloride concentration above 1100 mg/l. GC4 experiments an increment of 10% in the affected volume regarding to the baseline scenario in 2010 (the started point of the future period in this

study). As can be seen in Figure 3.4, the aquifer already had a large affected volume in 2010 (more than 80%) (Pulido-Velazquez et al, 2018).

The affected areas in terms of high vulnerability is pretty similar for the future LULC and baseline scenarios. The GC4 scenario shows a zone of high vulnerability at the north of the aquifer that corresponds with an area with high conductivity.

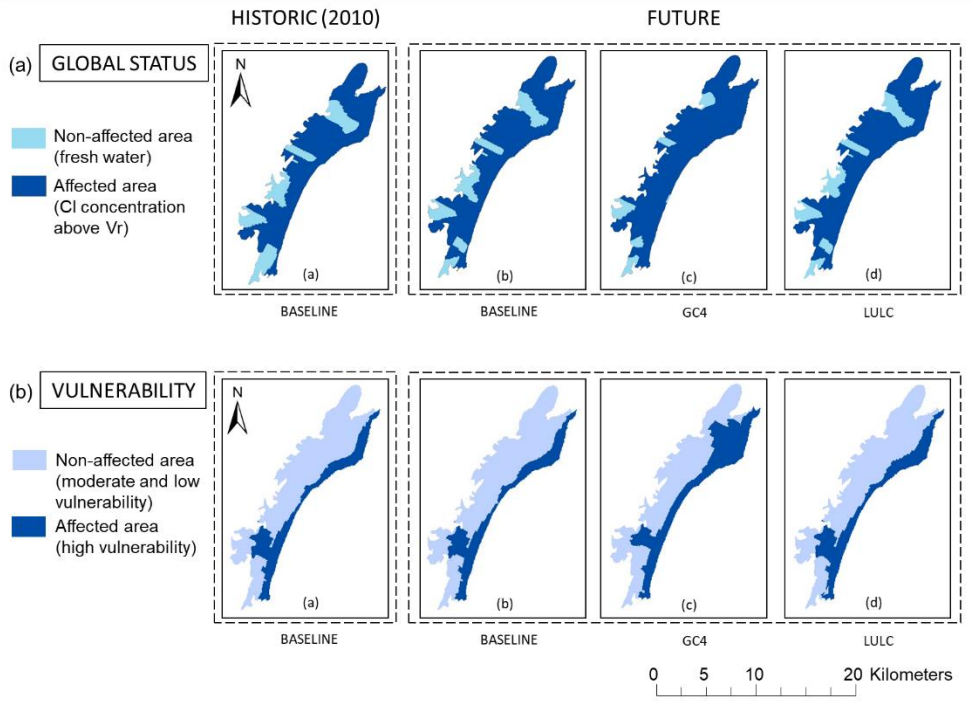

Figure 3.4. Maps of affected areas in the years with the largest affected volume (a) chloride concentration and (b) vulnerability

Due to the applied adaptation strategies, the considered changes in land use (LULC scenario) would not produce a high increase in the maximum values of affected volume. The reduction of pumping in this LULC scenario would reduce the amplitude of the fluctuations of the affected volumes within the aquifer (Figure 3.5(a) and 3.5(b)). Those non-distributed stresses cause that faster fluctuations on the aquifer status. Note that the LULC scenarios are defined assuming that the adaptation measures contemplated within the Urban Development Plan (reduction of pumping due to water reuse and water desalination) will be applied, which would help to reduce the potential impacts of these LULC scenario on SWI. On the other hand, the waterproofing due to the increase in the residential use contributes to a lower recharge (increasing slightly the mean sea water intrusion volume) in the future and the urbanized area in Torreblanca would continue being supplied with GW.

The GC scenarios (GC1, GC2, GC3, GC4) show an increase in their variability and in the affected volume regarding to the baseline scenario, which is obtained from the output of the calibrated SEAWAT model in the historical period and considering the LULC remains as in 2010 and there is not CC in the future. Taking into account that this increase is not observed in the LULC scenarios, it is mainly due to the impact of CC (Figure 3.5(a) and 3.5(b)). The decrease in pumping in GC scenarios is less significant than the reduction of the inflows in the aquifer (lateral GW inflow + recharge) producing an increase in the affected volume.

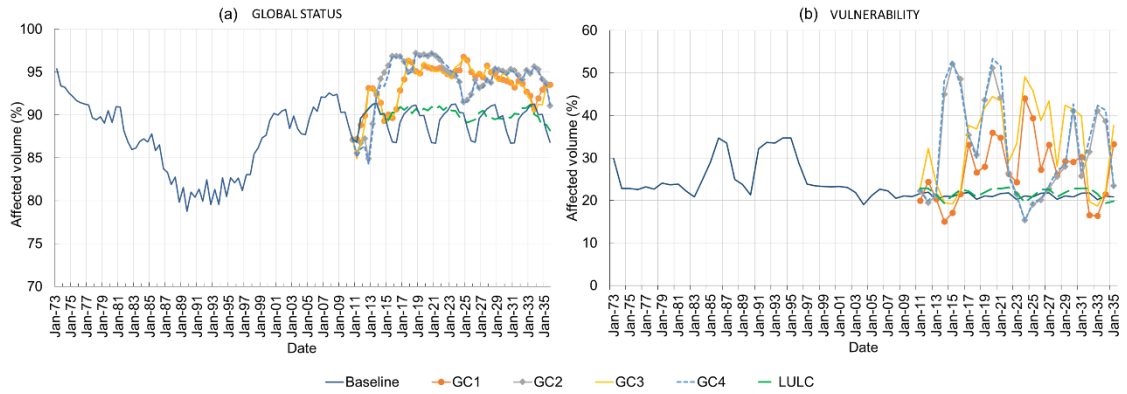

Figure 3.5. Evolution of (a) affected volume by a chloride concentration above 1100 mg/l and (b) affected volume by high vulnerability

All potential future GC scenarios would undergo an increase in average and maximum affected conceptual cross section, although the aquifer was largely affected in the historical period (Pulido-Velazquez et al. 2018). The LULC scenario (including adaptation measures) does not show substantial changes in the affected areas with respect the baseline scenario, while GC3 and GC4 scenarios involve the largest affected area in the aquifer (Figure 3.6). The expected future climatic conditions would have a negative impact in the salinization of the aquifer resources and in its vulnerability to SWI.

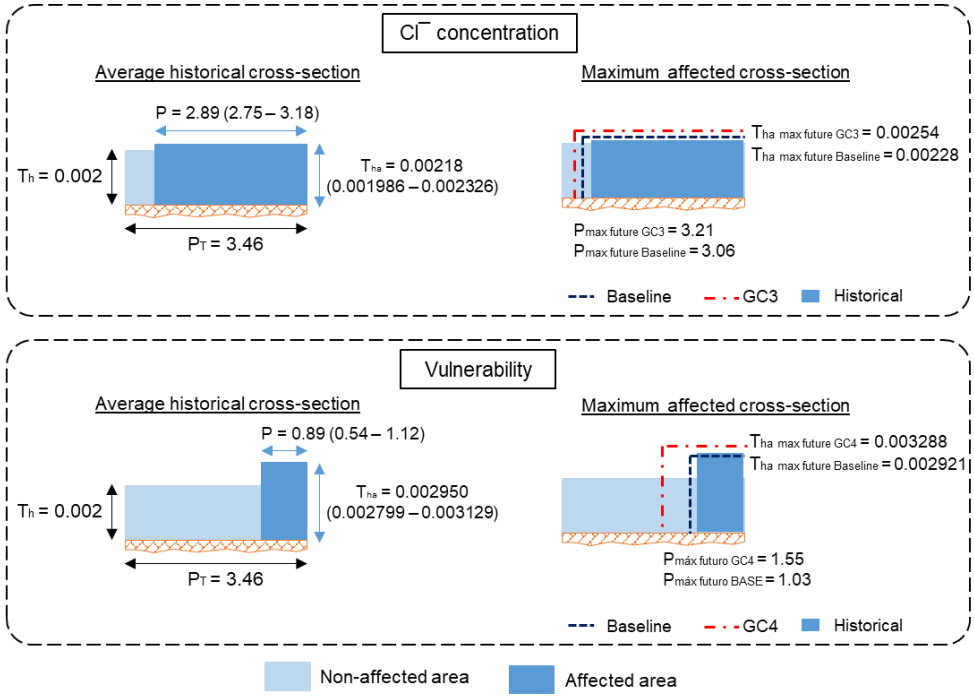

Figure 3.6. Average historical and maximum future affected cross-sections (linear dimensions in kilometers. Vertical exaggeration scale: 500)

The global indices (Ma and L_GALDIT) calculated for the baseline, LULC and the GC scenarios (Figure 3.7) show that LULC changes would not produce a clear deterioration of the global status and vulnerability of the aquifer. The continuous growing trend (in the LULC and GC scenarios) in the Ma index observed from 2025 (Figure 3.7(b)) are related with the impacts of the planned urbanization of a large area in Torreblanca, which produces an increase of chloride concentrations. GC scenarios forecast a large affected mass in the future, which is mainly due to the potential climatic conditions. The maximum values of the lumped indices (Ma and

L_GALDIT) during the GC scenarios are induced by periods with high temperature and low precipitation.

The LULC scenario does not produce significant changes in the vulnerability. The vulnerability is more sensitive to the GC scenarios. All of them show a significant increase in its variability and a mean increase in the vulnerability, but there are some periods in which the vulnerability even decreases. (Figure 3.7(a)).

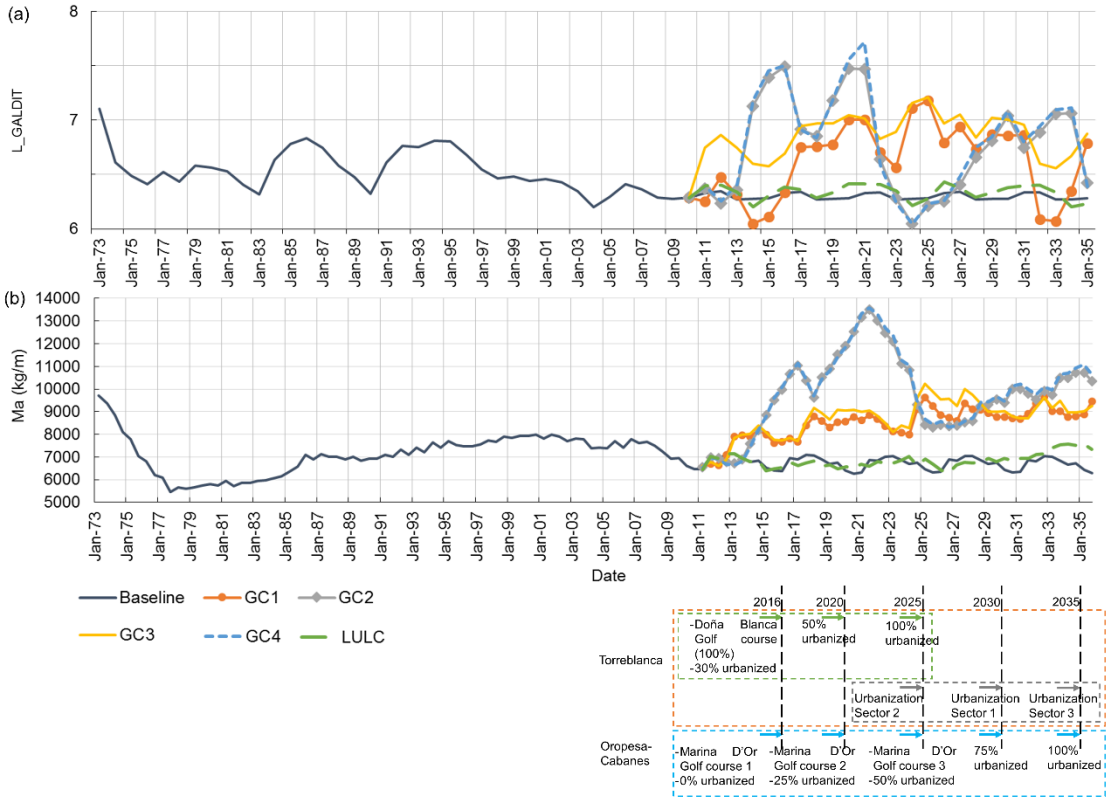

Figure 3.7. Lumped indices for vulnerability and global status: (a) L_GALDIT index; (b) Ma index

The resilience and trend of the lumped indices were analysed for the historical period in Baena-Ruiz et al. (2018). In CC studies we cannot analyze the trend of the indices due to the uncertainty of the chronological sequence. Instead the recovery rate is assessed as described in the methodology. Figure 3.8 shows that the aquifer is able to respond to the severe climatic conditions estimated in GC scenarios. Based on the calibrated model, GC2 and GC4 scenarios present more extreme values but also they show higher recovery rates.

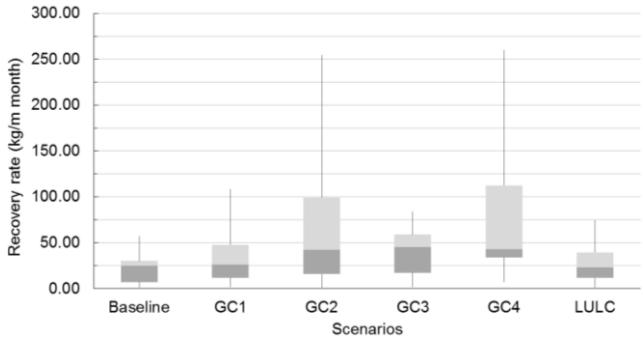

Figure 3.8. Statistics of recovery rate for baseline, LULC and GC scenarios

4.2. Impacts of CC in future scenarios

A sensitivity analysis is carried out to evaluate the impact of CC on global status and vulnerability to SWI at aquifer scale. The LULC (without CC) scenario provides us information about the sensitivity of the results to CC.

Figure 3.9 represents the increase (%) in Ma and L_GALDIT due to the CC. It shows that CC would have a significant impact in Ma index (related to global status of the aquifer). Vulnerability is less sensitive to CC due to other factors that are used in the index (conductivity and distance from the coast) which have greater weight and are invariant in time.

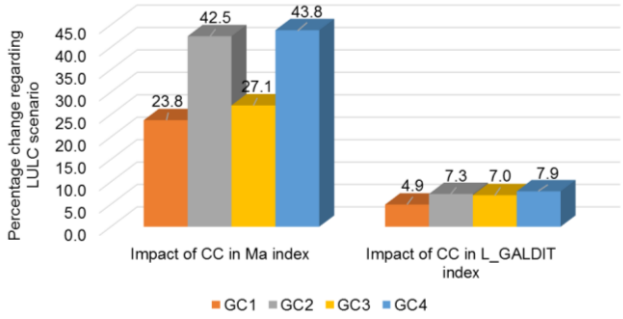

Figure 3.9. Sensitivity analysis of CC in lumped indices

Taking into account these results, CC would produce significant impacts in global status of the aquifer.

The mean annual values of the budget for the six scenarios was calculated running the density dependent flow model in Visual Modflow (Pulido-Velazquez et al. 2018). Figure 3.10 shows the mean annual values of the affected components of the budget for the six scenarios. It also includes the deficit in the resource produced in the system due to both GC and/or exploitation in this aquifer. Red bars in Figure 3.10 show the difference between total inflows and pumping.

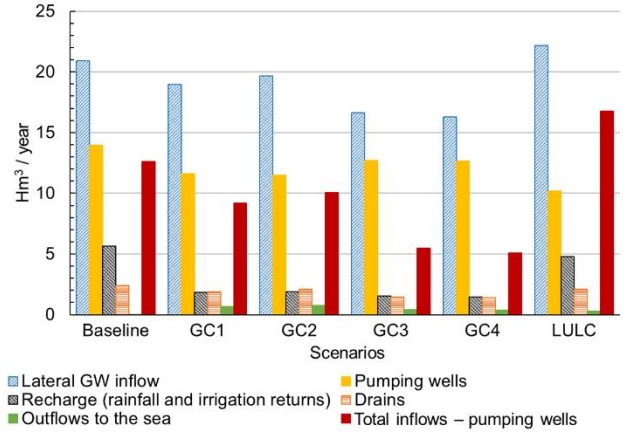

Figure 3.10. Mean annual values of the budget four GC, LULC and Baseline scenarios

In the future LULC scenario and the four GC scenarios, the pumping is reduced due to changes in land use and the proposed adaptation measures (water reuse for irrigation and water from desalinization plant for human consumption in the new urban areas) defined in accordance with the Urban Development Plan, but also the recharge (direct and lateral) decreases due largely to CC and waterproofing of the land in the Torreblanca area and urbanizations.

Figure 3.10 also shows that the GC scenarios (specially GC4) experiment a larger reduction in the total budget than the LULC scenario. Therefore, the impact of CC is greater than the improvement caused by LULC. This result is consistent with Figure 3.4, where GC4 would provide the largest affected area. It is due to GC4 scenario experiments a small decrease in

pumping due to LULC changes and adaptation measures, but the inflows (lateral and recharge) decrease still further (Figure 3.10).

Therefore, in summary, we have obtained results to analyse potential future impact of GC and LULC scenarios on SWI in a coastal aquifer. They show a significant increase in the magnitude and variability of the affected volume for the GC scenarios regarding to the baseline scenario. Pulido-Velazquez et al (2018) also highlighted the higher variability observed for these GC scenarios when they analysed the flow budget.

The potential future scenarios would produce a negative impact in the salinization of the aquifer resources and in its vulnerability to SWI, which is in agreement with results observed in previous studies in the Mediterranean area (Mabrouk et al. 2018). The decrease in recharge will exacerbate SWI problems (Liu et al. 2008; Petty 2011), producing a great effect in the affected mass of the aquifer, whose distribution and magnitude will depend on the scenarios (Van and Lee 2015).

The sensitivity analysis performed to assess the impacts of CC shows that it has a higher influence on aquifer status than in its vulnerability. It is due to GALDIT does not consider explicitly the recharge variable, although it controls aquifer salinization. These conclusions are in agreement with other previous study (Benini et al. 2016).

Finally, the comparison between LULC and baseline scenarios reveals that pumping is a key factor in SWI problem in coastal areas. This conclusion is supported by other authors (Van and Lee 2015).

4.3. Hypothesis and limitations

In this section we summarise the hypothesis assumed in this analysis. They have been classified in two categories:

Inputs for the method:

- Historical climatic data are taken from Spain02 dataset. They are considered to properly fit the historical period (1973-2010).
- LULC is supposed to be executed gradually from 2015 to 2035.
- CC scenarios data for the period (2011-2035) were taken considering the most pessimistic emission scenario published by the IPCC in the AR5 report (RPC8.5) and many assumptions were performed in Pulido-Velazquez et al. (2018).
- The generation of local CC scenarios and the propagation of its impacts has been assessed through a chain of auxiliary models and a SEAWAT model whose reliability depends on assumptions and data considered in calibration (Pulido-Velazquez et al. 2018). We consider as inputs of the proposed method the local CC scenarios and their impacts obtained by propagating with the modelling framework (Pulido-Velazquez et al. 2018).

Method:

- The natural background or reference level to identify SWI where taken from CHJ (2015). Results are sensitive to the adopted value (Baena-Ruiz et al. 2018).
- This general method provides lumped results and information about local potential impacts may be lost in the aggregation process.

5. Conclusions

In this paper an integrated methodology is applied in order to assess the hydrological impacts of GC scenarios on the global status and vulnerability to SWI at aquifer scale.

The novelty of this paper consists on the harmonization of the impacts of GC scenarios in the global status and vulnerability to SWI at aquifer scale including some management strategies. It allows to compare the significance of the SWI problems in different historical and future periods

for an aquifer and between different aquifers. The effect of CC in the GC scenarios is also analysed. The method has been implemented in a GIS tool that helps to apply it to any case study.

Results show that GC scenarios would imply a greater deterioration in the aquifer than LULC scenario. The adaptation strategies will produce a reduction of pumping in some areas of the aquifer, which would reduce the impacts of the potential future LULC and GC scenarios. The lumped indices reveal that GC would involve more variability in SWI problems (global status and vulnerability) and CC would increase the degradation of the aquifer. On average it is expected a greater area affected by intrusion and an extreme climatic conditions might produce an increase of the aquifer more vulnerable. GC would produce a greater impact in SWI global status than in the aquifer vulnerability. Nevertheless the resilience capacity of the aquifer would allow to recover from the impacts of the extreme climatic conditions.

The main contribution of this paper is the analysis of impacts of future GC scenarios in the SWI problem at aquifer scale. It allows to obtain general conclusions about the global status and vulnerability and to assess the effects of CC and adaptation strategies. Due to the sensitivity of the method to the natural background, a proper assessment of it is important to achieve realistic results. This method also helps to understand the effect of adaptation measures in order to cope with the growing water requirements. It reveals that complementary adaptation strategies are needed in order to cope with CC.

References

Baena-Ruiz L, Pulido-Velazquez D, Collados-Lara AJ, Renau-Pruñonosa A, Morell I (2018) Global Assessment of Seawater Intrusion Problems (Status and Vulnerability). Water Resources Management 32:2681-2700. https://doi.org/10.1007/s11269-018-1952-2

Benini L, Antonellini M, Laghi L (2016) Assessment of water resources availability and groundwater salinization in future climate and land use change scenarios: A case study from a coastal drainage basin in Italy. Water Resources Management 30:731–745. https://doi.org/10.1007/s11269-015-1187-4

Chachadi AG, Lobo-Ferreira JP (2005) Assessing aquifer vulnerability to sea-water intrusion using GALDIT method: part 2 – GALDIT indicator descriptions. IAHS and LNEC, Proceedings of the 4th The Fourth Inter Celtic Colloquium on Hydrology and Management of Water Resources, held at Universidade do Minho, Guimarães, Portugal, July 11–13, 2005

CHJ (Júcar Water Agency) (2015) Júcar River Basin Plan. Confederación Hidrográfica del Júcar https://www.chj.es/es-es/medioambiente/planificacionhidrologica/Paginas/PHC-2015-2021-Plan-Hidrologico-cuenca.aspx. Accessed 21 October 2019

Collados-Lara A.-J, Pulido-Velazquez D, Pardo-Igúzquiza E (2018) An Integrated Statistical Method to Generate Potential Future Climate Scenarios to Analyse Droughts. Water 10:1224-1248. https://doi.org/10.3390/w10091224

CORDEX PROJECT (2013) The Coordinated Regional Climate Downscaling Experiment CORDEX. Program sponsored by 20 World Climate Research Program (WCRP). http://wcrp-cordex.ipsl.jussieu.fr/. Accessed 21 October 2019

Escriva-Bou A, Pulido-Velazquez M, Pulido-Velazquez D (2017). Economic value of climate change adaptation strategies for water management in Spain's Jucar basin. Journal of Water Resources Planning and Management, 143(5), 04017005. https://doi.org/10.1061/(ASCE)WR.1943-5452.0000735

Feranec J, Jaffrain G, Soukup T, Hazeu G (2010) Determining changes and flows in European landscapes 1990–2000 using CORINE land cover data. Applied Geography, 30(1):19-35. https://doi.org/10.1016/j.apgeog.2009.07.003

Ferguson G, Gleeson T (2012) Vulnerability of coastal aquifers to groundwater use and climate change. Nature Climate Change, 2(5):342-345

Giménez E, Morell I (1997) Hydrogeochemical analysis of salinization processes in the coastal aquifer of Oropesa (Castellón, Spain). Environmental Geology, 29(1-2):118–131. https://doi.org/10.1007/s002540050110

Grundmann J, Schütze N, Schmitz G. H, Al-Shaqsi S (2012) Towards an integrated arid zone water management using simulation-based optimisation. Environmental Earth Sciences, 65(5):1381-1394

Herrera S, Gutiérrez J.M, Ancell R, Pons M.R, Frías M.D, Fernández J (2012) Development and Analysis of a 50 year high-resolution daily gridded precipitation dataset over Spain (Spain02). International Journal of Climatology, 32:74-85. https://doi.org/10.1002/joc.2256

Herrera S, Fernández J, Gutiérrez J. M (2016) Update of the Spain02 Gridded Observational Dataset for Euro-CORDEX evaluation: Assessing the Effect of the Interpolation Methodology. International Journal of Climatology, 36:900–908. https://doi.org/10.1002/joc.4391

Huang L, Zeng G, Liang J, Hua S, Yuan Y, Li X, Liu J (2017) Combined impacts of land use and climate change in the modeling of future groundwater vulnerability. Journal of Hydrologic Engineering, 22(7):05017007. https://doi.org/10.1061/(ASCE)HE.1943-5584.0001493

Kløve B, Ala-Aho P, Bertrand G, Gurdak J. J, Kupfersberger H, Kværner J, Uvo C. B (2014) Climate change impacts on groundwater and dependent ecosystems. Journal of Hydrology, 518:250-266. https://doi.org/10.1016/j.jhydrol.2013.06.037

Koutroulis A. G, Papadimitriou L. V, Grillakis M. G, Tsanis I. K, Wyser K, Betts R. A (2018) Freshwater vulnerability under high end climate change. A pan-European assessment. Science of the Total Environment, 613:271-286. https://doi.org/10.1016/j.scitotenv.2017.09.074

Li R, Merchant J. W (2013) Modeling vulnerability of groundwater to pollution under future scenarios of climate change and biofuels-related land use change: A case study in North Dakota, USA. Science of the Total Environment, 447:32-45. https://doi.org/10.1016/j.scitotenv.2013.01.011

Liu J, Rich K, Zheng C (2008) Sustainability analysis of groundwater resources in a coastal aquifer, Alabama. Environmental Geology, 54(1):43-52. https://doi.org/10.1007/s00254-007-0791-x

Loáiciga H. A, Pingel T. J, Garcia E. S (2012) Sea Water Intrusion by Sea-Level Rise: Scenarios for the 21st Century. Groundwater, 50(1):37-47. https://doi.org/10.1111/j.1745-6584.2011.00800.x

Luoma S, Okkonen J, Korkka-Niemi K (2017) Comparison of the AVI, modified SINTACS and GALDIT vulnerability methods under future climate-change scenarios for a shallow low-lying coastal aquifer in southern Finland. Hydrogeology Journal, 25(1):203-222. https://doi.org/10.1007/s10040-016-1471-2

Mabrouk M, Jonoski A, HP Oude Essink G, Uhlenbrook S (2018) Impacts of Sea Level Rise and Groundwater Extraction Scenarios on Fresh Groundwater Resources in the Nile Delta Governorates, Egypt. Water, 10(11):1690. https://doi.org/10.3390/w10111690

McEvoy J, Wilder M, 2012. Discourse and desalination: potential impacts of proposed climate change adaptation interventions in the Arizona–Sonora border region. Global Environmental Change 22 (2012):353–363. https://doi.org/10.1016/j.gloenvcha.2011.11.001

Petty K (2011) The Effects of Land Cover, Climate, and Urbanization on Groundwater Resources in Dauphin Island. Dissertation, Auburn University (Alabama).

Pulido-Velazquez D, Garrote L, Andreu J, Martin-Carrasco FJ, Iglesias A (2011) A methodology to diagnose the effect of climate change and to identify adaptive strategies to reduce its impacts in conjunctive-use systems at basin scale. Journal of Hydrology 405:110–122. https://doi.org/10.1016/j.jhydrol.2011.05.014

Pulido-Velazquez D, Renau-Pruñonosa A, Llopis-Albert C, Morell I, Collados-Lara A. J, Senent-Aparicio J, Baena-Ruiz L (2018) Integrated assessment of future potential global change scenarios and their hydrological impacts in coastal aquifers–a new tool to analyse management alternatives in the Plana Oropesa-Torreblanca aquifer. Hydrology and Earth System Sciences, 22(5):3053. https://doi.org/10.5194/hess-22-3053-2018

Ranjan S. P, Kazama S, Sawamoto M (2006) Effects of climate and land use changes on groundwater resources in coastal aquifers. Journal of Environmental Management, 80(1):25-35. https://doi.org/10.1016/j.jenvman.2005.08.008

Rasmussen P, Sonnenborg T.O, Goncear G, Hinsby K (2013) Assessing impacts of climate change, SLR, and drainage canals on saltwater intrusion to coastal aquifer, Hydrology and Earth System Sciences, 17:421-443. https://doi.org/10.5194/hess-17-421-2013

Renau-Pruñonosa A, Morell I, Pulido-Velazquez D (2016) A methodology to analyse and assess pumping management strategies in coastal aquifers to avoid degradation due to seawater intrusion problems, Water Resources Management, 30(13):4823-4837. http://dx.doi.org/10.1007/s11269-016-1455-y

Robins N.S, Jones H.K, Ellis J (1999) An aquifer management case study- The Chalk of the English South Downs, Water Resources Management, 13(3):205-218. https://doi.org/10.1023/A:1008101727356

Romanazzi A, Gentile F, Polemio M (2015) Modelling and management of a Mediterranean karstic coastal aquifer under the effects of seawater intrusion and climate change. Environmental Earth Sciences, 74(1):115-128. https://doi.org/10.1007/s12665-015-4423-6

Sola F, Vallejos A, Moreno L, López-Geta J.A, Pulido-Bosch A (2013) Identification of hydrogeochemical process linked to marine intrusion induced by pumping of a semi-confined Mediterranean coastal aquifer, International Journal of Environmental Science and Technology, 10(1):63-76. https://doi.org/10.1007/s13762-012-0087-x

Trinh L.T, Nguyen G, Vu H, Van Der Steen P, Lens R.N.L (2012) Climate change adaptation indicators to assess wastewater management and reuse options in the Mekong Delta, Vietnam. Water Resour. Manag. 27 (5):1175–1191. https://doi.org/10.1007/s11269-012-0227-6

Van Pham H, Lee S. I (2015) Assessment of seawater intrusion potential from sea-level rise and groundwater extraction in a coastal aquifer. Desalination and Water Treatment, 53(9):2324-2338. https://doi.org/10.1080/19443994.2014.971617

Werner A. D, Simmons C. T (2009) Impact of sea-level rise on sea water intrusion in coastal aquifers. Groundwater, 47(2):197-204. https://doi.org/10.1111/j.1745-6584.2008.00535.x

Water Framework Directive (WFD) (2000) Directiva 2000/60/CE del Parlamento Europeo y del Consejo de 23 de Octubre de 2000. Diario Oficial de las Comunidades Europeas de 22/12/2000. L 327/ 1–327/32

Appendix 3.1

GALDIT METHOD

GALDIT was proposed by Chachadi and Lobo-Ferreira (2005) to assess the vulnerability to SWI.

This method considers that there are six parameters/variables influencing the vulnerability to SWI: aquifer type, hydraulic conductivity, height of GW level above sea level, distance from the shore, impact of existing status of SWI and thickness of aquifer.

A rate of importance is assigned to the parameters according to the value or characteristics of each parameter.

The values of the parameters are weighted by a factor to obtain the GALDIT index.

$$GALDIT\ index = \frac{\sum_{i=1}^{6}(W_i * R_i)}{\sum_{i=1}^{6} W_i} \quad \text{(A1)}$$

Where W_i is the weight of the i^{th} indicator and R_i is the importance rating of the i^{th} indicator.

The GALDIT index is classified into three vulnerability levels:

- GALDIT≥7,5 → High vulnerability
- 7,5>GALDIT≥5 → Moderate vulnerability
- GALDIT<5 → Low vulnerability

Capítulo 4: GIS-SWIAS: tool to summarize seawater intrusion status and vulnerability at aquifer scale

Hindawi
Scientific Programming
Volume 2021, Article ID 8818634, 15 pages
https://doi.org/10.1155/2021/8818634

Research Article

GIS-SWIAS: Tool to Summarize Seawater Intrusion Status and Vulnerability at Aquifer Scale

Leticia Baena-Ruiz and David Pulido-Velazquez

Department of Research on Geological Resources, Geological Survey of Spain (IGME), Urb. Alcázar del Genil, 4-Edif. Bajo, Granada 18006, Spain

Correspondence should be addressed to Leticia Baena-Ruiz; l.baena@igme.es

Received 13 March 2020; Accepted 26 April 2021; Published 12 May 2021

Reference: Baena-Ruiz, L.; Pulido-Velazquez, D. "GIS-SWIAS: Tool to Summarize Seawater Intrusion Status and Vulnerability at Aquifer Scale," Scientific Programming, vol. 2021, Article ID 8818634, 15 pages, 2021. https://doi.org/10.1155/2021/8818634.

Authors and affiliations:

Leticia Baena-Ruiz,[1*] David Pulido-Velazquez[1]

[(1)] Department of Research on Geological Resources, Geological Survey of Spain (IGME), Urb. Alcázar del Genil, 4-Edif. Bajo, 18006 Granada, Spain

[(*)]Corresponding author

Abstract

In this paper we introduce GIS-SWIAS, a novel generalized ArcGIS ArcToolbox that helps to analyze SeaWater Intrusion (SWI) status and vulnerability at Aquifer Scale (SWIAS). It is a user-friendly tool that can be applied to any aquifer and is fully integrated in the ArcGIS environment, which is a widely available software. It is the first ArcGIS tool with these characteristics focussing on SWI analyses that we can find in the literature. GIS-SWIAS is able to deal with geo-referenced information, it is easy to introduce the required data (inputs) and to efficiently perform the demanding computational operations required. Its outputs are in the form of shapes, reports and images (maps, conceptual cross sections and time series of lumped indices) to summarize the magnitude, intensity and temporal evolution of SWI within an aquifer for specific dates or by showing statistics for a chosen time period.

It can be applied to assess historical SWI dynamic in cases where there is no groundwater flow model. In those cases, the spatial distribution is assessed by applying simple interpolation techniques. Nevertheless, if we want a rational quantitative analysis of the sustainability of alternative management scenarios to SWI problem, the GIS-SWIAS tool requires that information on hydraulic head and chloride concentration distribution are generated from simulations of their impacts by a calibrated density-dependent flow model. In such cases, adaptation strategies to potential future scenarios-whose distributed impacts have to be propagated within the previously calibrated models- could usefully be analyzed and compared using this tool.

Given all these ways that the GIS-SWIAS tool can be applied, it provides a valuable tool for both researcher and technician to assess SWI dynamics and aquifer resilience under different scenarios.

It can support the decision-making process by helping to make a rational selection of sustainable management strategies. Its performance for the analyses of historical and potential future scenarios has been tested and confirmed in two case studies described in previous research works.

1. Introduction

Seawater intrusion (SWI) in coastal aquifers is a worldwide problem affecting groundwater-dependent ecosystems and human health. In recent decades, society's awareness of this issue has grown and this has been reflected in the legal framework of many countries. For example, the European Union's Water Framework Directive (WFD) requires that river basin plans address the achievement of a good qualitative and quantitative status of groundwater bodies [1]. In coastal groundwater bodies, intrusion is one of the main issues that need to be considered to achieve or maintain good groundwater status.

The impacts of SWI on groundwater have a heterogeneous distribution. Analyses of spatio-temporal distribution of SWI requires salinity or chloride concentration to be mapped for different dates. Depending on the issue to be addressed and the available information, SWI can be approximated using various models. SWI can be mapped either by applying simple interpolation models [2, 3] to existing point data or by simulating the physical processes using transient density-dependent groundwater flow models [4, 5]. The results obtained with these physical process models can be applied to assess sustainable management strategies, *i.e.*, strategies that prevent deterioration of the aquifer resource due to SWI [6]. They can even be employed to propagate impacts of potential local climate change (CC) [7] or global change (GC) scenarios and to identify adaptation strategies [8].

Based on the salinity or chloride concentration maps at different dates, some authors have defined indices to summarize SWI [9, 10, 11, 12]. These indices provide an overview of the intensity and spatial distribution or percentage SWI at aquifer scale. Such indices need to offer descriptive and synthetic results so that the status of SWI in different aquifers and over different periods can be compared. These index-methods [9, 13] establish threshold values for chloride to define the basis of SWI have been defined in various ways: by referencing natural background levels and/or by taking into account the concentrations required to protect dependent ecosystems or human health [14].

When simple interpolation is used to draw the maps used to define the indices, analyses must be limited to the historical period for which there are data. In contrast, physical process models can be applied to propagate various potential conditions and so maps can be obtained for different scenarios (e.g., alternative managements scenarios or future potential CC scenarios); in this latter case, the output can be used to determine the optimum strategy and therefore support the decision-making process [15].

In addition to the SWI status and dynamics, another important issue to take into account in identifying sustainable management strategies for coastal aquifers, is the aquifer's vulnerability to SWI. In the literature we found various methods for mapping SWI vulnerability, such as the GALDIT method [16]. Then, by applying a method to express vulnerability as an index, we can also get an overview of the intensity and spatial distribution or percentage of SWI at aquifer scale [13].

1.1. Related works

In the literature we find many tools to assess and analyse water resource problems [17, 18, 19]. The success of these software tools lies in their usability. A user-friendly environment and the implementation in a commonly-used software are key factors for their success and popular use. For example, groundwater studies usually employ Geographic Information Systems (GIS) since they are powerful, widely-available tools that can deal with large amounts of spatial geo-referenced information [20], and make calculations in an efficient way to provide quick results [21]. The analysis and mapping of hydrogeological data provides useful spatiotemporal information to decision makers [22].

GIS tools have been widely used for different purposes related to groundwater issues [23, 24]. Several authors have developed different source codes within GIS environment [25Alcaraz et al., 2017; 26Bhatt et al., 2014] for hydrogeological modelling. A free and open source module included in FREEWAT was developed by [27Criollo et al 2019] to analyse hydrochemical and hydrogeological data in order to simplify the characterization of the groundwater bodies at chemical risk. [28Almeida et al. 2013] coupled a groundwater flow model into a GIS environment to simulate transient flow in a confined aquifer. [29Akbar et al. (2011) and 30Ríos et al. (2013)] presented GIS-based models to simulate contaminants leaching into groundwater.

In coastal areas, a three-dimensional GIS-based groundwater flow model was developed [31] to simulate the aquifer's response to past climate changes. A new ArcGIS tool for groundwater flow simulation and visualization of results was also implemented by [32]. Other authors [33De Filippis et al 2019] applied a previously developed GIS-based tool (AkvaGIS), in addition to a groundwater flow model, to study the impacts of pumping on seawater intrusion in coastal aquifers in Malta and Italy. This tool was used in other studies [34Perdikaki et al 2020] to analyse hidrochemical parameters in a coastal aquifer that presented seawater intrusion problems.

Nevertheless, as far as we know, there is no ArcGIS tool focussing on analysing seawater intrusion (SWI) status and vulnerability at aquifer scale.

In this paper we describe the development of a new ArcGIS tool called GIS-SWIAS, which is the implementation of the index-based method for assessing aquifer status and vulnerability to SWI proposed by [13, 15]. It helps to analyze SWI status and/or vulnerability at aquifer scale using a mixed lumped-distributed analysis. It is a user-friendly ArcGIS® toolbox that performs all the required calculations for specific dates or temporal periods inside a GIS environment. The data inputs to the model are hydraulic head and chloride concentration maps. The tool provides two options to map these variables: the first is to use point data by applying interpolation techniques integrated within GIS-SWIAS; while the second is to take these data from existing external distributed models. The second approach allows different climatic and/or management scenarios to be assessed and compared. From those maps, extensive calculations have been fully automatized in GIS-SWIAS to display the results as distributed maps of affected and non-affected volumes (at a specific moment or over a period of time); mean conceptual cross sections; and a lumped index (Ma and L_Vul) to analyze the global intensity and the dynamics of SWI.

Although there are many GIS-based tools in the literature that allow to simulate groundwater flow and analyse groundwater quality, none of them perform spatial and temporal analysis on groundwater quality and vulnerability issues. Moreover, this new tool provides simple pictures that summarise the proportional affected area within the aquifer according to a chloride threshold. For this purpose, GIS-SWIAS has been applied to analyse the seawater intrusion problem but this tool could be applied to represent the global status of an aquifer to any contaminant. The main objective of GIS-SWIAS is to provide an easy-to-use tool through a user-friendly interface that can be used by users at different levels of expertise to summarize the SWI problem at aquifer scale. It allows to analyse long time periods with a low computing cost.

2. Description of GIS-SWIAS tool. Models, inputs and outputs

GIS-SWIAS is an ArcGIS ArcToolbox that contains the models required to analyze SWI status and vulnerability at aquifer scale, according to the methodology described in previous works [13, 15]. Figure 4.1 shows the structure of the tool, which includes inputs, steps and models, as well as the outputs generated.

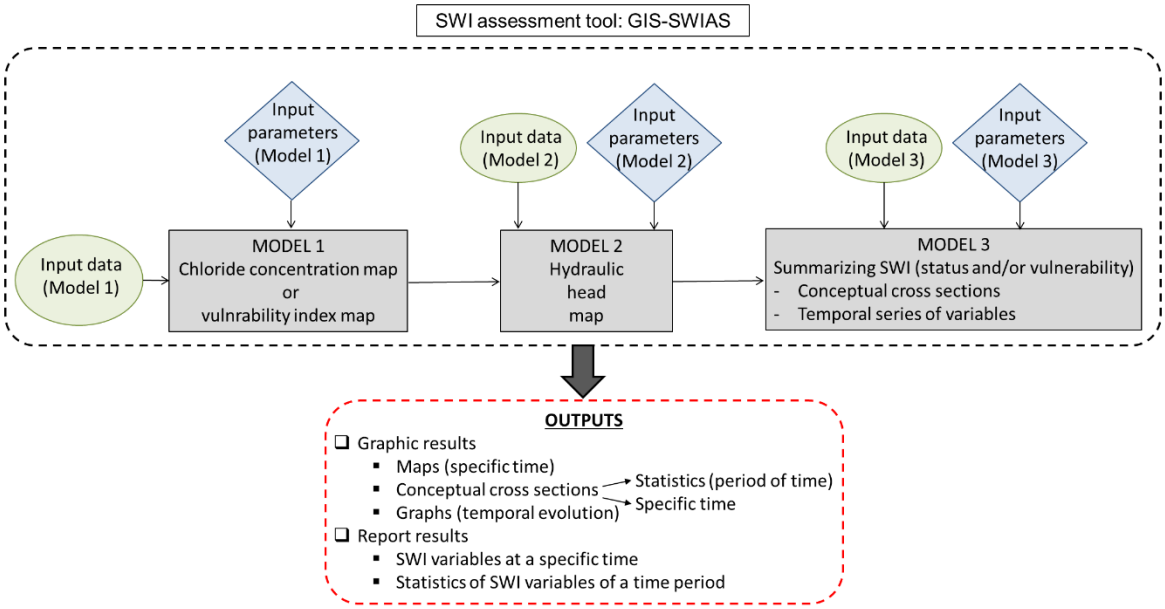

Figure 4.1. Workflow of the GIS-SWIAS ArcToolbox

To determine the overall status of the aquifer, the **inputs** to the tool include variables (to characterize the historical evolution of hydraulic head and chloride concentration) and parameters (to define aquifer geometry and hydrodynamic behaviour). Data describing the historical evolution can come from direct observations (monitoring network) or other techniques (geophysical applications, etc). For the vulnerability assessment, an additional input is required: a distributed vulnerability index map, which comes from other intrinsic information (aquifer type, conductivity, distance from the shoreline, bicarbonate concentration).

The results/**outputs** produced to summarize status and vulnerability to SWI through visual displays and time series are: 1. Maps of aquifer volumes affected by SWI; 2. 2D conceptual cross-sections (with mean penetration inland and mean thickness on specific dates, or mean values over a period of time); 3. Lumped Index (mass of chloride that causes the concentration in some areas to exceed the SWI threshold and lumped vulnerability index) to summarize the global dynamic of SWI within the aquifer.

2.1. Description of the outputs. Theoretical background

In order to assess the maps of SWI-affected aquifer volumes for different dates we need to compile: A) maps of chloride concentration or vulnerability to SWI; B) maps of groundwater volumes for specific dates; C) threshold of chloride concentration or vulnerability that will be used to tag which parts of the aquifer are impacted (areas with chloride concentration or vulnerability index exceeding the threshold). The tool provides two options with respect to the input maps (A (chloride or vulnerability maps) and B): either calculating the maps internally from point data by applying interpolation techniques integrated within GIS-SWIAS; or to taking the maps from existing external distributed models; the second option means that various potential climatic and/or management scenarios can be compared and assessed. Maps of groundwater volume are calculated by combining hydraulic head, geometry and the storage coefficient. The maps of groundwater volume and chloride concentration are combined to assess the aquifer volume affected by using a chloride threshold (V_t). This threshold is assumed to be equal to the natural background level of the aquifer, or the reference quality standard determined by authorities in order to maintain a good groundwater status. The affected volume is defined as the groundwater volume of resource whose chloride concentration is above the stablished threshold.

2D conceptual cross-section depicts the magnitude of the intrusion process in the aquifer at a specific moment, or the mean values in a period of time. The cross-section is defined orthogonal to the shoreline. It summarizes the mean geometry of the affected volume, i.e., the mean thickness

and inland penetration of the aquifer volume with chloride concentration above the threshold. The average affected thickness T_{ha}(m) and inland penetration P(m) of the intrusion can be calculated by summing the values in each cell i of the aquifer mesh where the chloride concentration exceeds the threshold:

$$T_{ha}(m) = \frac{\sum V_{i(>V_r)}}{\sum S_{i(>V_r)}} \quad (1)$$

$$P(m) = \frac{\sum V_{i(>V_r)}}{T_{ha} * L_{coast}} \quad (2)$$

$$V_{i(>V_r)}(m^3) = S_i(m^2) * b_i(m) * \alpha_i \quad (3)$$

where:

- $V_{i(>Vr)}$ is the groundwater volume (m^3) in the cell i with a chloride concentration (or vulnerability) exceeding V_r;
- S_i is the surface area (m^2) of the cell i with chloride concentration (or vulnerability) exceeding V_r;
- b_i is the saturated thickness (m) within the cell i with Cl concentration (or vulnerability) above V_r;
- α_i is the storage coefficient in the cell i;
- L_{coast} is the length of coastline (m);

The mean chloride concentration (C) of the affected volume is:

$$C\left(\frac{mg}{l}\right) = \frac{\sum(C_{i(>V_r)} * V_{i(>V_r)})}{V_{(>V_r)}} \quad (4)$$

where:

- $C_{i(>V_r)}$ is the chloride concentration (mg/l) in cell i;
- $V_{i(>Vr)}$ is the groundwater volumes (m^3) in cell i with a concentration exceeding V_r;
- $V_{(>Vr)}$ is the total groundwater volume (m^3) of the affected area;

The increment of chloride concentration (IC) above the threshold (V_r) in the affected volume is:

$$IC\left(\frac{mg}{l}\right) = C - V_r \quad (5)$$

Both variables, the conceptual cross section and IC index give an overview of the magnitude and intensity of the intrusion process per linear metre of coast at a specific moment in time.

The lumped index Ma (mass of chloride that causes the concentration in some areas to exceed the threshold) to summarize the global dynamic of SWI within the aquifer is obtained multiplying the increment of concentration (IC) by Penetration (P) and affected Thickness (T_{ha}) from equations 1, 2 and 5.

$$Ma\left(\frac{kg}{m}\right) = P(m) * IC\left(\frac{mg}{l}\right) * 10^{-3} * T_{ha}(m) \quad (6)$$

The vulnerability to SWI (or vulnerability to contamination in general) is assessed and summarized following the same steps to assess the SWI status. In this case, instead of chloride concentration values, a distributed map of groundwater vulnerability has to be generated by applying any index-based method (e.g. GALDIT) and the threshold applied to identify the affected area is defined by a specific vulnerability class (e.g. high or very high vulnerability).

The affected volume corresponds to the groundwater that present vulnerability values above the threshold (e.g. very high vulnerability). The average affected thickness T_{ha}(m) and inland penetration P(m) are calculated by applying Equations 1 and 2.

The lumped index to assess vulnerability is:

$$L\_Vul\ (-)=\frac{\sum(Vul_{i(>V_r)}*V_{i(>V_r)})}{V_{(>V_r)}} \quad (7)$$

where:

- $Vul_{i(>V_r)}$ is the value of the vulnerability index (-) in cell i;

The concept of Ma and L_Vul involves some simplifications, in accordance with the definition of the conceptual cross sections. While 2D maps and cross sections summarize the extent and magnitude of SWI and vulnerability in an aquifer at a specific time, Ma and L_Vul indices show the lumped intensity and temporal dynamic of the SWI and vulnerability to SWI at aquifer scale.

2.2. Tool programming in ArcGIS

GIS-SWIAS is an ArcGIS ArcToolbox composed by a chain of models programmed in ModelBuilder. ModelBuilder is a visual programming language that allows to chain and sequence several geoprocessing ArcGIS tools through a user-friendly interface. ModelBuilder is available within the tool bar in ArcGIS. It allows to add any geoprocessing tool of ArcGIS by linking and providing its output and transferring it to another tool as input.

Programming in ModelBuilder allows us to automate a workflow to create a model, which can be documented and shared as a ArcGIS tool. ModelBuilder contains a script tool to link with Python scripts and other models. It also allows to iterate a workflow, so it can be very useful to analyse the evolution of the historical hydrogeological processes.

The three models that compose GIS-SWIAS have been compiled by adding different tools from ArcToolbox to create shapes from point data, to interpolate, etc. Figure 4.2 shows the workflow of one of the three models.

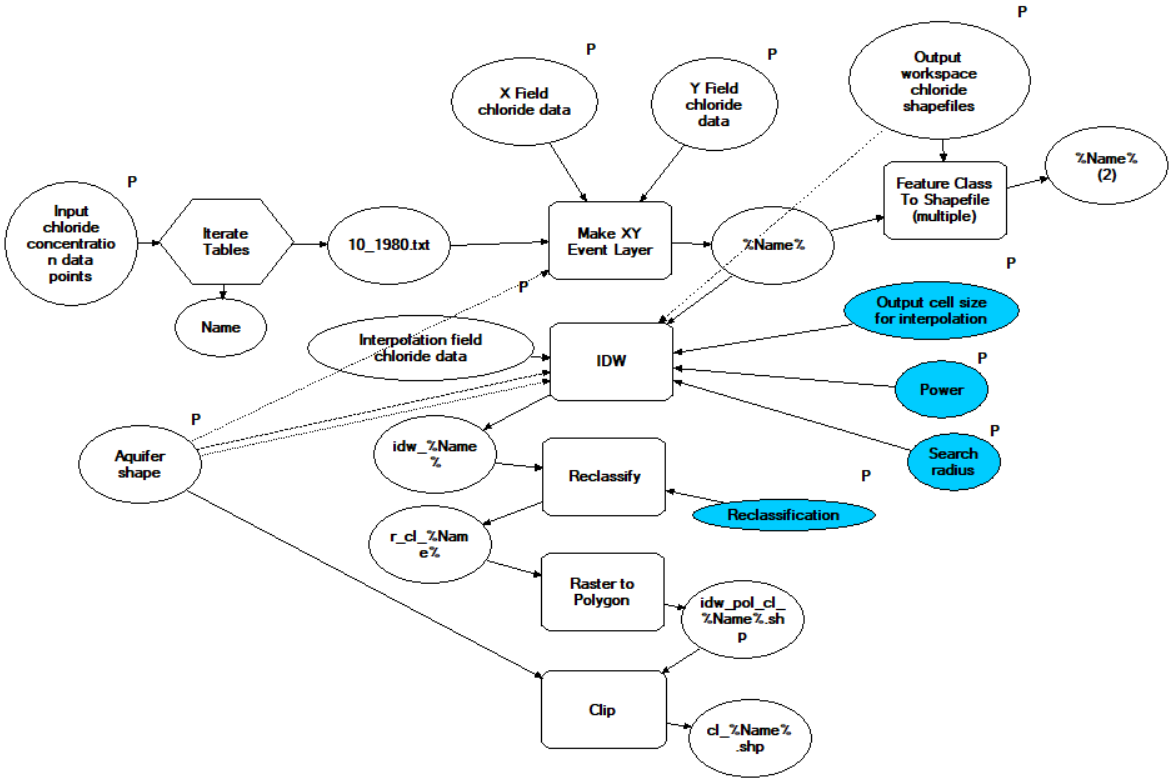

Figure 4.2. Workflow of "Chloride concentration map" model

Although ModelBuilder is an intuitive and easy-to–use tool, the integration of lots of geoprocesses in the same model may be difficult. Due to several geoprocesses have dynamic parameters and the user interaction is necessary, GIS-SWIAS was divided into three steps (models) that have to be executed following the workflow shown in Figure 4.1.

2.3. Description of the models within GIS-SWIAS

GIS-SWIAS contains three ModelBuilder models (Figure 4.2) that can be applied individually or used sequentially to produce a complete lumped assessment of the SWI at aquifer scale. GIS-SWIAS can be shared with other users and it can be added as a Toolbox as shown in Figure 4.3. The run sequence follows the order shown in the workflow (Figure 4.1): "Chloride concentration map", "Hydraulic head map" and "Summarizing SWI". These models can be run within the ArcToolbox window providing a user-friendly graphical user interface.

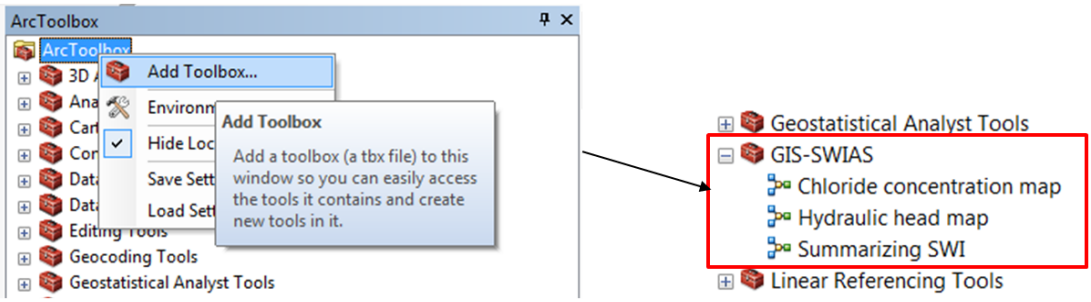

Figure 4.3. GIS-SWIAS in the ArcToolbox

2.3.1. "Chloride concentration map" model

The "Chloride concentration map" model generates a classified chloride concentration shapefile from a point feature table in text format by using Inverse Distance Weighting (IDW) interpolation technique (other interpolation techniques could be implemented in this tool). It can also import chloride concentration fields from Visual Modflow files. The dialog box shown in Figure 4.4 is opened by double-clicking the model tool on the ArcToolbox window.

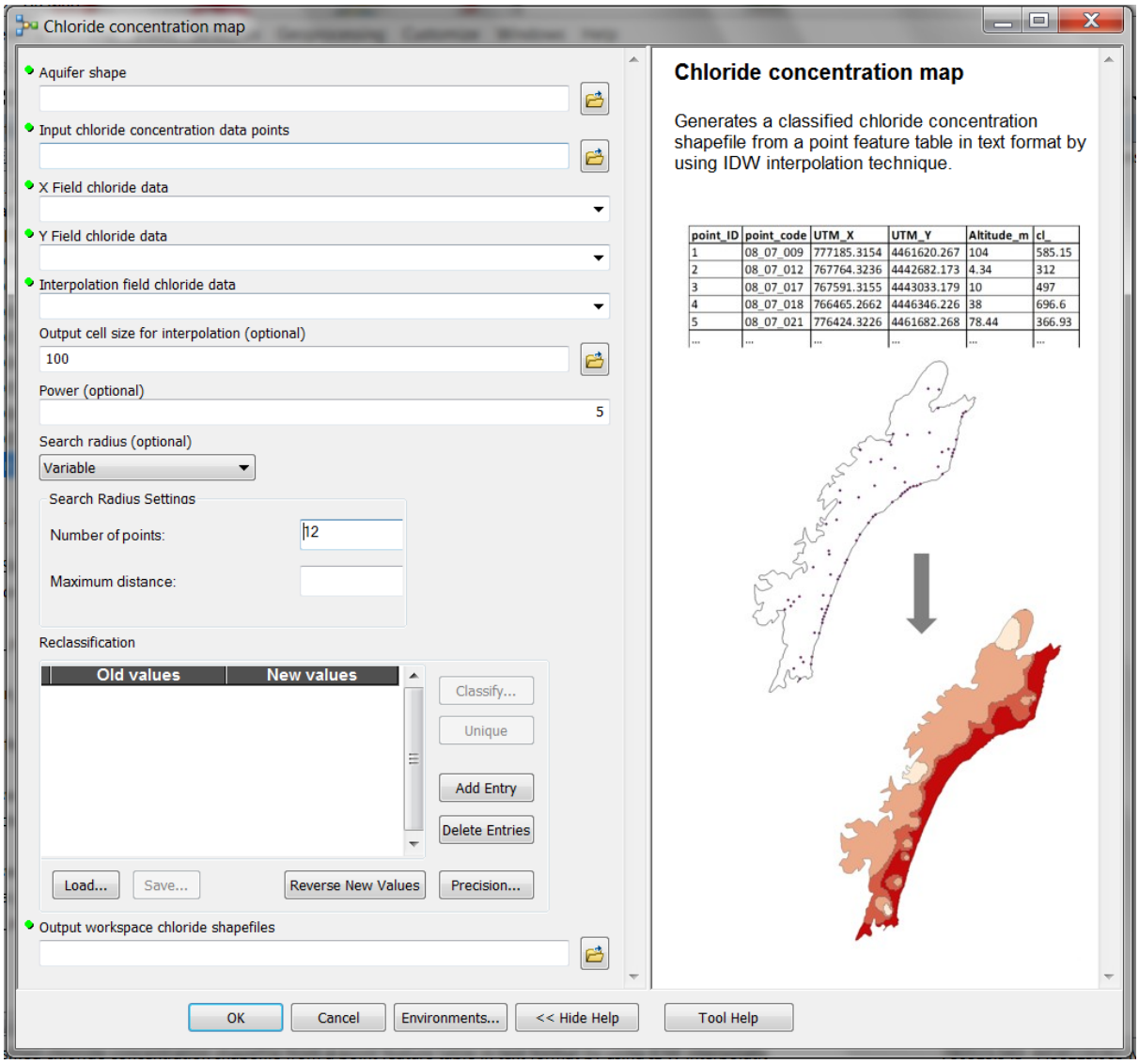

Figure 4.4. Dialog box of the "Chloride concentration map" model

The model requires a polygon shapefile of the aquifer and the workspace containing a text file for each date to be analyzed. The text files have to include X and Y UTM coordinates that define the locations of the point features and chloride concentration values (mg/l) in the observation wells. Text files also have to include column header, as shown in Figure 4.4. The text filename cannot exceed eight characters nor include blank spaces or special characters (underscore can be used as a substitute). It is not necessary that all points contain data every date of the period to be analyzed.

The user has to indicate the fields (columns) in the input table that contain the X and Y coordinates and the chloride concentration value for each point (Figure 4.5). Optional settings concerning IDW interpolation techniques can be changed by the user. A reclassification of the values after interpolation is also required. Finally, the user has to choose a folder where the output shapefiles will be saved.

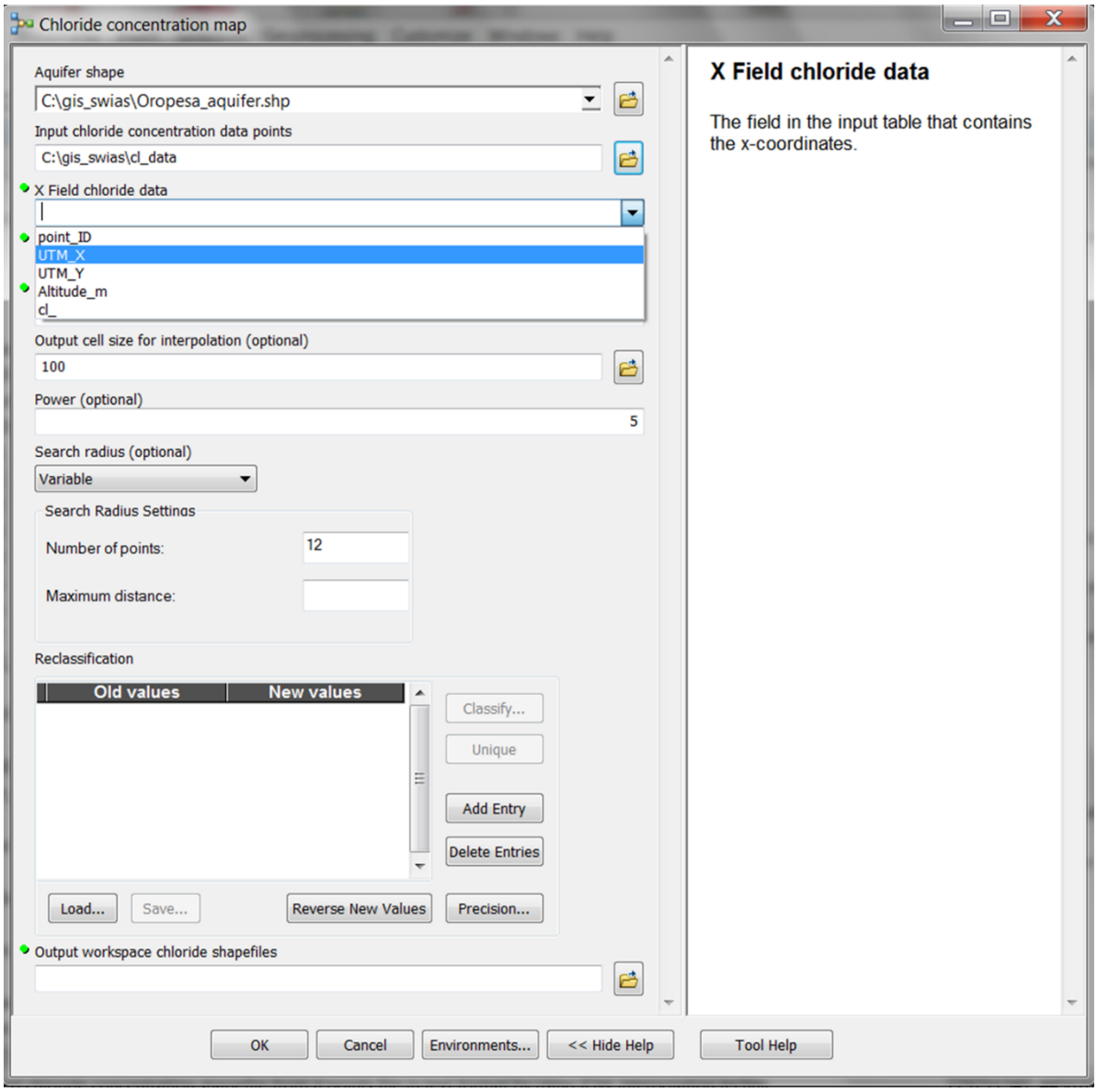

Figure 4.5. Setting options defined by the user

When all the required parameters are filled out, the model can be executed by clicking "OK" at the bottom of the dialog box. The execution screen (Figure 4.6) shows the running processes and it can be closed when the execution has successfully completed.

The "Chloride concentration map" model provides the following shapefiles for each date analyzed: (1) point shapefile of chloride concentration data; (2) raster from data interpolation; (3) polygon shapefile from interpolation covering the default extension; and (4) polygon shapefile from interpolation clipped to the shape of the aquifer.

2.3.1. "Hydraulic head map" model

The "Hydraulic head map" model generates a classified hydraulic head shapefile from a point feature table in text format. It also generates a shapefile containing aquifer variables (chloride concentration and hydraulic head values) and aquifer parameters (storage coefficient and bottom of the aquifer). The dialog box is showed in Figure 4.7.

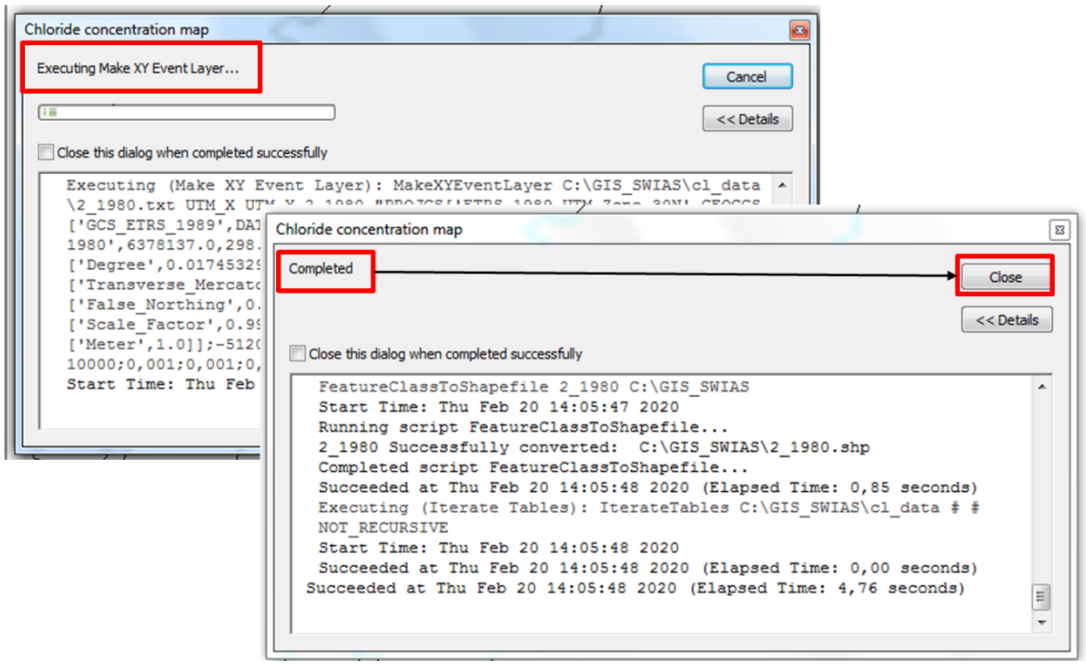

Figure 4.6. Execution screen of the model

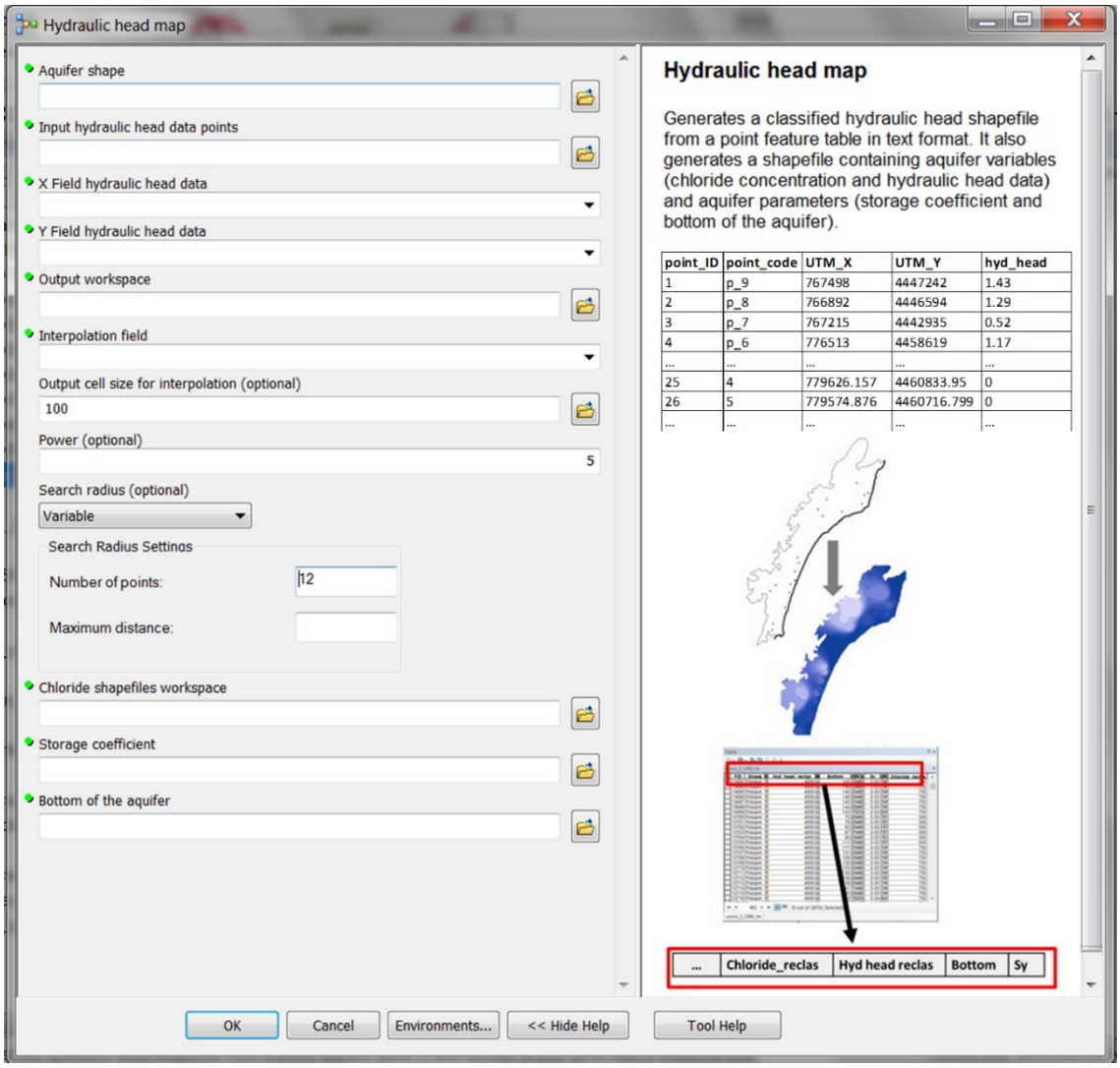

Figure 4.7. Dialog box of the "Hydraulic head map" model

This model has the same input requirements as for the "Chloride concentration map" model but focuses on hydraulic head data (m.a.s.l.). It also allows hydraulic head fields to be imported from Visual Modflow. The name of hydraulic head text files must be the same as the chloride concentration text files for each time period analyzed.

The user has to indicate the location of the chloride shapefiles generated in the previous model ("Chloride concentration map" model). It also requires polygon shapefiles of storage coefficient and bottom (m) of the aquifer as inputs.

The model generates shapefiles of hydraulic head data in an analogous way to the "Chloride concentration map" model. Moreover, it provides a polygon shapefile containing variables for each date analyzed (chloride concentration and hydraulic head values) and parameters (bottom and storage coefficient) of the aquifer. This shapefile is named "union_%name of the hydraulic head text file%_hh.shp", where "% name of the hydraulic head text file%" is variable if different dates are analyzed.

2.3.2. "Summarizing SWI" model

For the "Summarizing SWI" model, the methodology proposed in Baena-Ruiz et al. [13, 15] and described in Section "Description of the outputs. Theoretical background" have been implemented in the ArcGIS environment. This tool generates Excel® tables containing statistics that summarizing SWI at aquifer scale. It also generates conceptual cross sections (.shp), where the mean affected and non-affected volume are drawn for the aquifer (average values over a time period or instantaneous values on a specific date). If different dates are analyzed, it shows graphs representing the temporal evolution of Pa and Ta variables, percentage of affected volume, chloride concentration within the aquifer and Ma index (or lumped vulnerability index). The dialog box for global status assessment is showed in Figure 4.8.

The "Summarizing SWI" model requires the folder path where the results of the "Hydraulic head model" have been previously saved to be specified. In this folder, the shapefiles named "union_%name of the hydraulic head text file%_hh.shp" contains chloride concentration, hydraulic head, bottom of the aquifer and storage coefficient fields. The user has to select from the pull-down list the corresponding column in the input shapefile for each field, as shown in Figure 4.9.

The next required parameter in this tool is the "Chloride threshold". It is defined as the chloride concentration value above which the aquifer is considered to be affected by SWI. This threshold may be set as the natural background level of the aquifer or as the relevant environmental quality standards. [14] proposed a method to calculate groundwater thresholds values based on these criteria.

The shoreline length (m) is also required for subsequent calculations.

X and Y axes establish the coordinate system of the conceptual cross sections. The GIS-SWIAS tool provides polyline shapefiles for X and Y axes located at (0,0), but the user can translate them to another coordinate origin or create new ones.

The vertical scale factor is used to rescale the vertical magnitude (Ta) of the conceptual cross section if the factor Ta/Pa is too small. If vertical scale factor = 1, the conceptual cross section will maintain the real size ratio.

Finally, two paths where the output results will be saved are required. "Output workspace statistic" will contain lumped-variables reports in Excel table format for each date analyzed (Figure 4.10) and mean statistics for the entire period. Four graphs will be also saved in this path: (1) temporal evolution of Pa and Ta variables; (2) percentage volume affected; (3) Ma index; and (4) chloride concentration within the aquifer (mean chloride concentration in the aquifer, mean chloride concentration in the affected volume and the increment of concentration within the affected volume above the threshold).

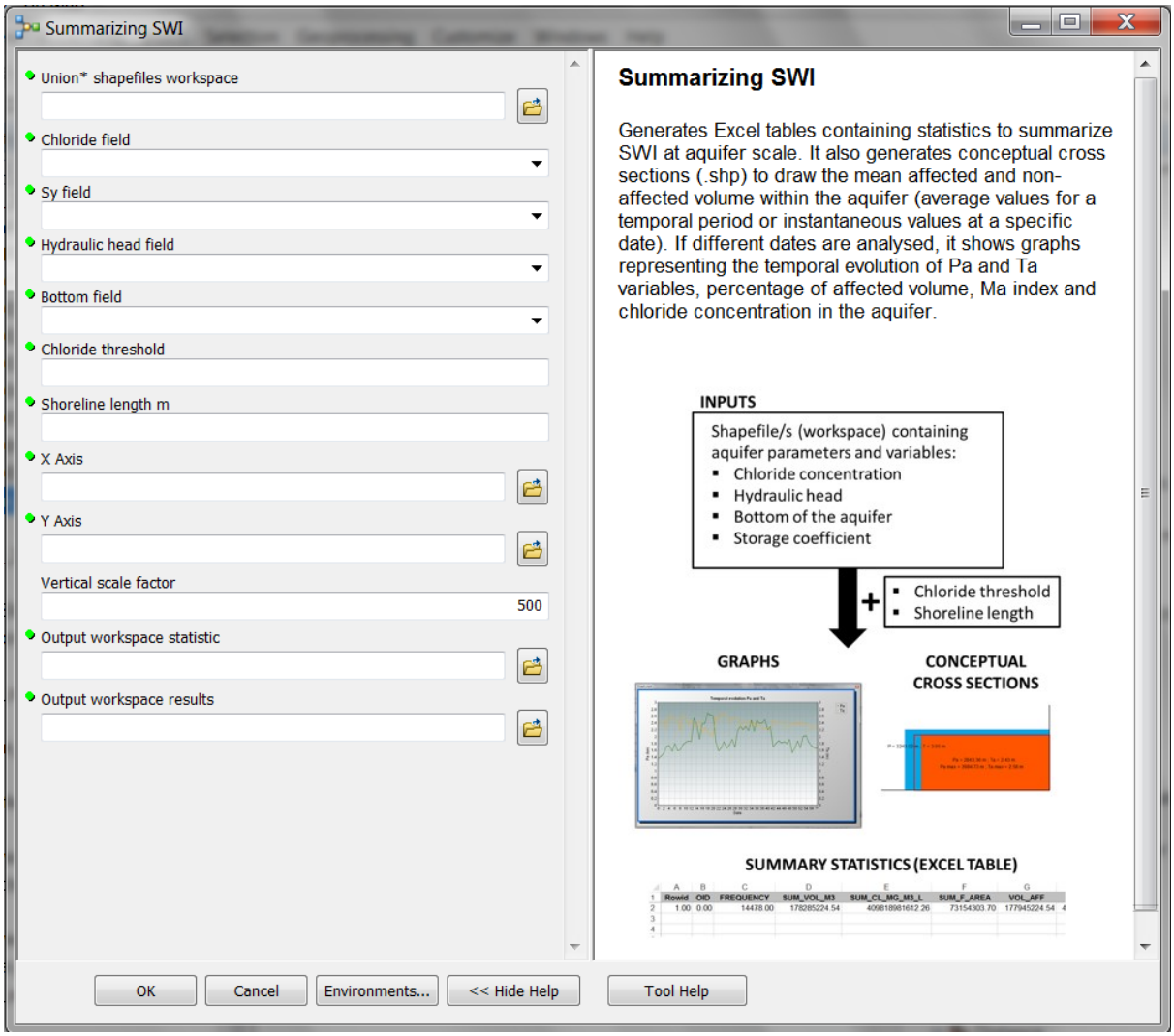

Figure 4.8. Dialog box of the "Summarizing SWI" model

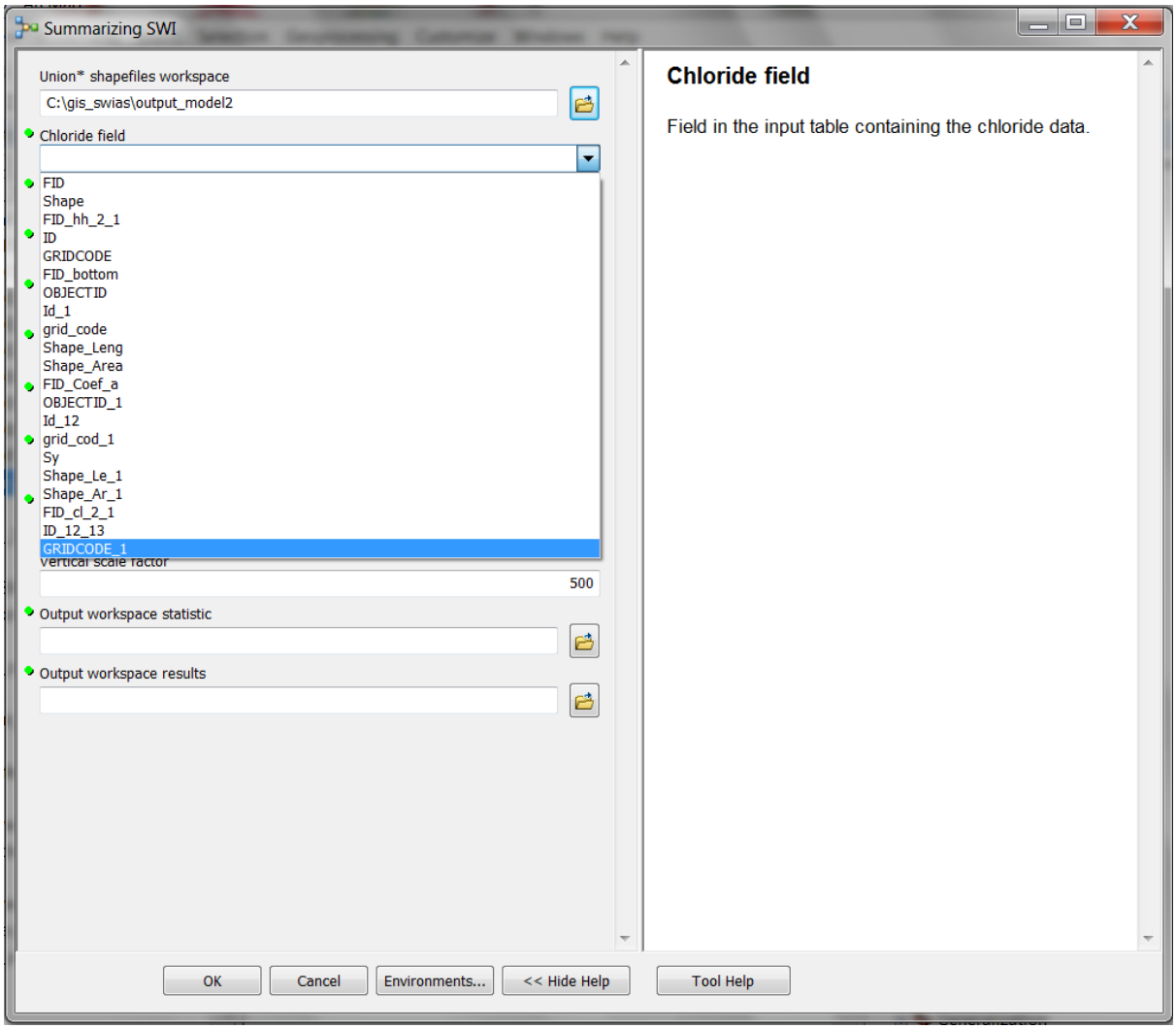

Figure 4.9. Selection of chloride field from the input table

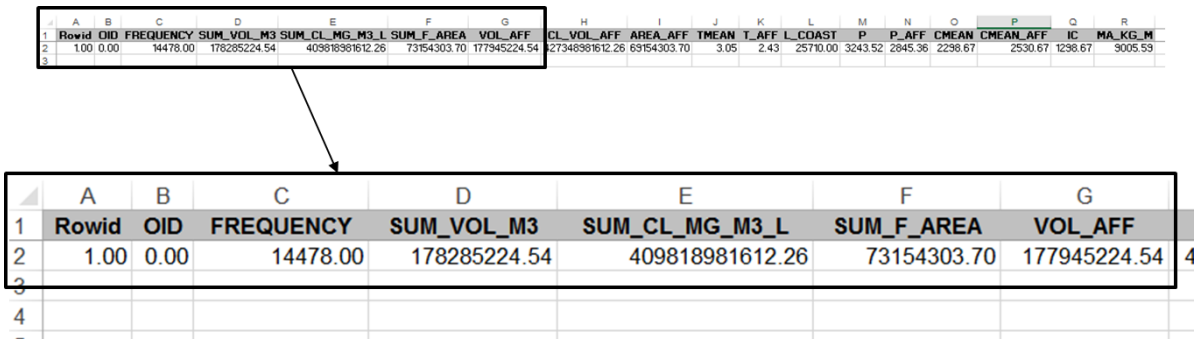

Figure 4.10. Summary statistics for a date

"Output workspace results" will contain the polygon shapefiles that allow the (1) mean affected and (2) non-affected conceptual cross section within the aquifer for each date analyzed to be drawn, (3) the mean affected and (4) non-affected conceptual cross section within a time period and the (5) maximum affected cross section for a time period. These two paths can be the same for all results, but they have to be different from the output paths of the previous models.

Figure 4.11 and Table 4.1 show the graphical and statistical summaries, respectively, from the GIS-SWIAS tool.

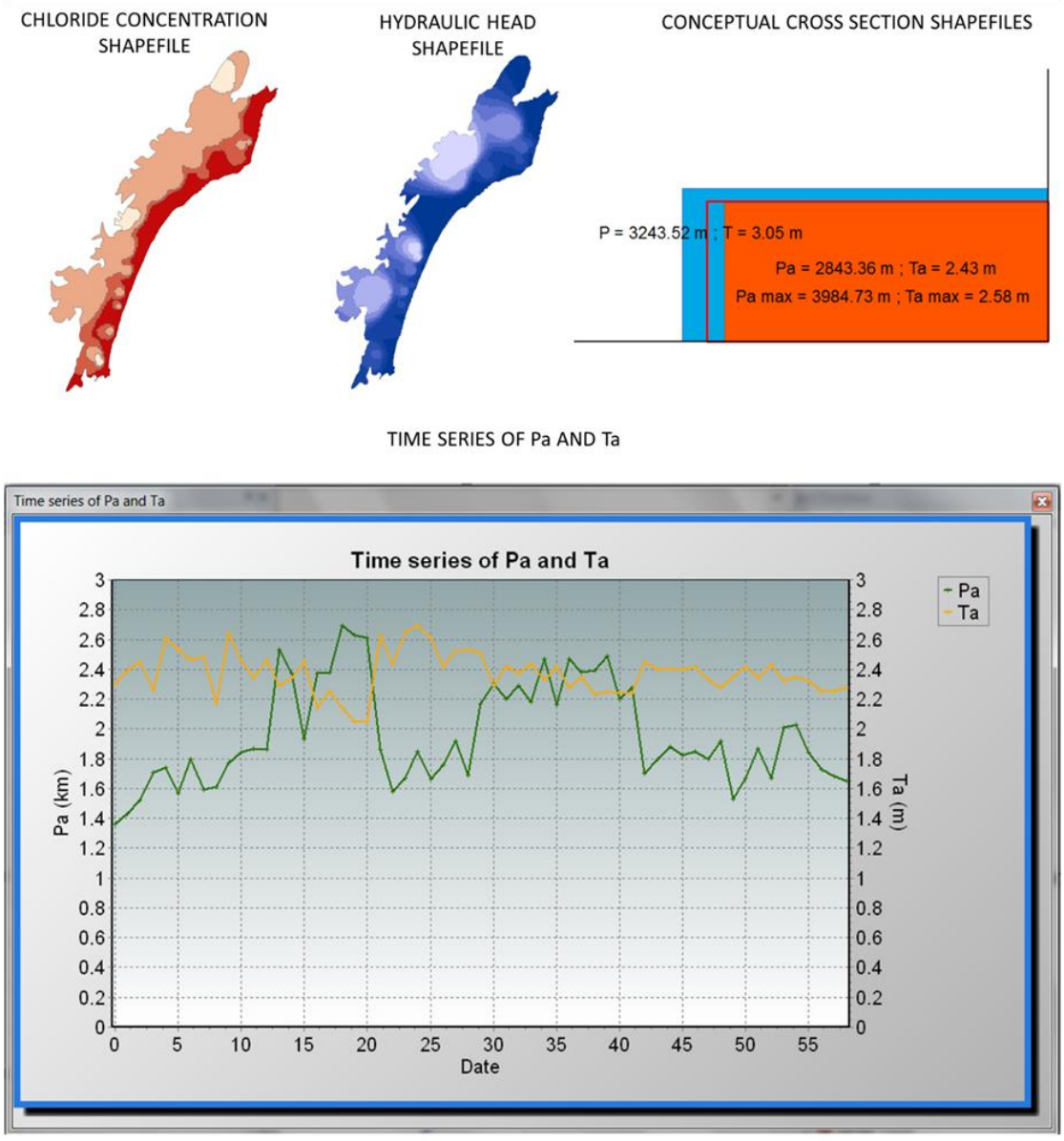

Figure 4.11. Graphical output from the GIS-SWIAS tool

The GIS-SWIAS tool can provide results for each date where information is available; these are obtained by iterative application of the described method. GIS-SWIAS allows historical [13] and future periods [15] to be analyzed if the hydraulic head and chloride maps come from a density-dependent flow model. By this means, GIS-SWIAS can be used to analyze adaptation strategies [15] in terms of reducing SWI, taking into account future potential scenarios that might include CC and/or GC, also considering projected land use change scenarios (new urbanized areas, crop transformations) [15].

Moreover, this tool may be also used to summarize SWI vulnerability, for any index method applied to assess it. In this case, instead of the chloride concentration maps, generated by executing the "Chloride concentration map" model, polygon shapefiles of the vulnerability index (previously prepared by the user) would be used as inputs of the model "Summarizing SWI vulnerability" (Figure 4.12), which also will require the "Hydraulic head map" shapefile generated by the tool, as previously described.

Table 4.1. Lumped variables output (Excel® table format) from the GIS-SWIAS tool

LUMPED VARIABLES (EXCEL TABLE)	
At a specific moment in time	Statistics for a time period
Total aquifer volume	Average aquifer volume
Total aquifer affected volume	Average aquifer affected volume
Total chloride concentration * aquifer volume	Average chloride concentration * aquifer volume
Total chloride concentration * aquifer volume in the affected volume	Average chloride concentration * aquifer volume in the affected volume
Total aquifer area	Average aquifer area
Total aquifer affected area	Average aquifer affected area
Shoreline length	Shoreline length
Average aquifer thickness	Average aquifer thickness within the period
Average affected aquifer thickness	Average affected aquifer thickness within the period
Average orthogonal distance of the aquifer to the shoreline	Average orthogonal distance of the aquifer to the shoreline within the period
Average orthogonal distance of the affected aquifer to the shoreline	Average orthogonal distance of the affected aquifer to the shoreline within the period
Average chloride concentration within the aquifer	Average chloride concentration within the aquifer within the period
Average chloride concentration within the affected volume	Average chloride concentration within the affected volume within the period
Increment of chloride concentration above the threshold value	Increment of chloride concentration above the threshold value within the period
Ma index	Average Ma index within the period
Percentage of affected volume	Average percentage of affected volume within the period

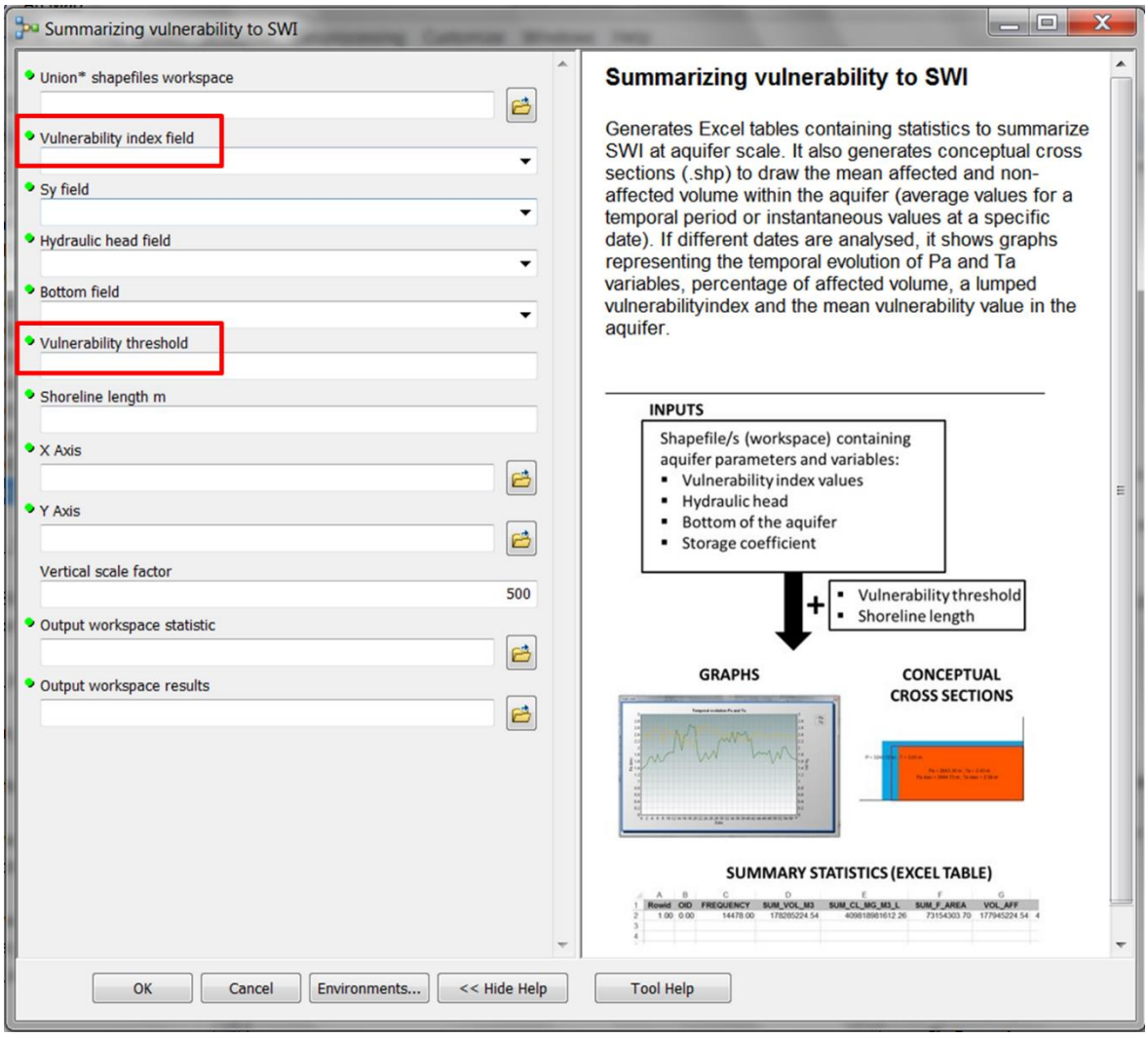

Figure 4.12. Dialog box of the "Summarizing SWI vulnerability" model

The vulnerability index maps must be included as numerical fields (values obtained before defining the vulnerability classes). In order to generate the conceptual cross sections that summarize the "affected" aquifer volume, i.e., where the vulnerability to SWI is identified, the tool requires a vulnerability threshold to be input that represents the reference value chosen to distinguish between affected and non-affected volumes. This threshold will be also used to assess the lumped vulnerability index.

Just as in the definition of the Ma index, the lumped global value of vulnerability in the aquifer on a specific date is obtained by weighting the vulnerability score in each cell with its water storage. This lumped index also allows an analysis of the dynamic of SWI vulnerability of the system at aquifer scale to be performed. The lumped index can be also obtained using different threshold values [13, 15].

3. Discussion

GIS-SWIAS is a user-friendly polyvalent ArcGIS tool that provides a comprehensive overview of SWI status and vulnerability at aquifer scale. It integrates three models, which are documented in order to briefly explain the tool's description, its utility and the data required for each item. This tool can be applied by scientific and decision makers, who may not be advanced users of GIS, to summarize SWI problems. Many GIS-based tools have demonstrated to be powerful and cost-effective to analyse groundwater issues [19; 34]. Moreover, GIS models as ModelBuilder models, can be integrated into other platforms by using the Python script tool [35].

Due to the heterogeneous distribution of seawater intrusion, distributed information and assessments are required to study its impacts [31, 32]. For this reason, the methods for modelling [36, 37] SWI impacts, and the user-friendly tools developed based on them [38, 39, 40] also require distributed inputs and calculations. The GIS-SWIAS is a tool that could be classified as a post-processing tool to summarize and help in the analysis of SWI impacts at aquifer scale. This tool produces both distributed and lumped results at aquifer scale but, logically, it also requires distributed inputs and assessments, as described in the previous sections. In this group of post-processing tools, we find in the literature, for example [41]. GIS-SWIAS is a new tool, in which the method proposed by [13, 15] has been implemented. A significant novelty of this method with respect to other previously developed methods is that the proposed lumped index to summarise SWI status at aquifer scale is based on a variable with physical meaning (mass of chloride that causes the concentration in some areas to exceed the natural threshold). On the other hand, a novel aspect of this tool is that, from the distributed information and calculations, GIS-SWIAS allows easy computation of the affected volume containing a chloride concentration above a threshold. This tool also helps to produce lumped SWI outputs (indices) at aquifer scale. It produces valuable information that help draw conclusions about the dynamic at aquifer scale, in terms of affected volume and global SWI intensity. Thus it also provides insight into aquifer resilience and trends. Therefore, it will help to identify coastal groundwater bodies that requires new management strategies to be implemented to achieve a good status.

The identification of SWI (the phenomenon that we want to analyze) requires a threshold value is established that defines the inflection point beyond which the aquifer begins to register an impact. Previous research shows that the impact of SWI is significantly sensitive to the choice of the threshold value adopted [13]. The significant uncertainties around determining these threshold values [14] and the sensitivity of whether the aquifer is reported as being impacted by SWI or not, increase the practical interest of the GIS-SWIAS tool: it is capable of performing the extensive calculations required to summarize SWI at aquifer scale, for the analyses of both historical and potential scenarios, considering different threshold values, which allow to compare the results.

With respect to the maps employed as inputs, the tool allows two options: to generate maps from available data using different interpolation techniques integrated in the tool, or to take the maps directly from SEAWAT files. This functionality -which allows maps to be generated from point data or to be loaded from other commonly employed tools- has also been implemented in other SWI assessment tools [38, 39]. However, as far as we know, it is not available in post-processing tools. In cases where map inputs are taken from density-dependent models, a comparative assessment of different scenarios (climatic conditions and/ or management strategies) could be performed. The physical-process approach can be applied to propagate and compare various potential conditions, and so in this case maps can be obtained and compared for different scenarios (e.g., managements scenarios or future potential CC scenarios), this means that the output of the tool can support the decision-making process [15]. In contrast, when the maps employed to define the indices are obtained by applying simple interpolation approaches, analysis is limited to the historical period for which the data are available.

The tool also helps to analyze the vulnerability to seawater intrusion at aquifer scale. In the literature we find different methods to assess groundwater vulnerability depending on the drivers of pollution [42, 43, 44] Baena-Ruiz and Pulido-Velazquez 2020], pumping [45, 46] and SWI [12, 16]. User-friendly tools have appeared to assist in this assessment, some of them developed in a GIS environment [47]. Nevertheless, there is no tools that helps in the assessment of SWI vulnerability with that focus on post-processing. Therefore, this is the first post-processing tool described that integrates SWI status and vulnerability assessment, which is very valuable information to help identify the significance of SWI problems in aquifers and potential sustainable solutions.

The GIS-SWIAS tool has been applied to two different case studies in the Mediterranean area of Spain (Plana de Oropesa Torreblanca and Plana de Vinaroz), obtaining the results described in previous papers [13, 15].In [13], the process automation to generate the interpolated maps enabled

authors to analyze SWI status and vulnerability over an extended time period (1977-2015) and to prove the sensitivity of results to the chloride threshold value (two threshold values were analyzed: 250 mg/l and 1100 mg/l) in Plana de Oropesa-Torreblanca and Plana de Vinaroz aquifers. In [15] the impacts of future GC scenarios were analyzed in Plana de Oropesa-Torreblanca aquifer. The methodology from [13] was adapted to compare six potential future scenarios including adaptation strategies. The historical period came from 1973 to 2010 and the six future scenarios covered the period 2011-2035.

The underlying methodology implemented in GIS-SWIAS was applied in the cited paper [13] by interpolating chloride maps and hydraulic head from observation points, whereas the information to generate the field maps in [15] was loaded from SEAWAT model. The results of these studies for the Plana de Oropesa-Torreblanca aquifer show differences that reveal the physical-process SWI approximations obtained using the density-dependent flow model give a more accurate representation. Despite these differences, the results are in the same order of magnitude. Other authors who have developed indices related to SWI [9, 48], have also proved that results do not differ considerably by including three-dimensional salinity data. Furthermore, the approximation obtained using interpolation will depend on the number of observations and the distribution of these points within the aquifer.

Despite this tool has been developed to analyse SWI problem, it could be applied to study the lumped impact of any contaminant on groundwater and/or the groundwater vulnerability by applying any vulnerability index. In this case, instead of the “Shoreline length” parameter to generate the cross section, other equivalent length (e.g. the aquifer length orthogonal to the groundwater flow direction) should be considered. Therefore, GIS-SWIAS fulfils the requirements of flexibility, sturdiness, easy interaction and user-friendly, which make it a useful tool in the decision making process. It will allow to use them as “share vision models/tools” to help in the discussion of management alternatives between stakeholders, and administration representatives [49]. Many Decision Support Systems tools were not successful due to they were not user-friendly [50; 51].

3.1. Assumptions and limitations

In this section we summarize the main assumptions/limitations of the GIS-SWIAS tool and in the implemented methodology.

3.1.1. Underlying methodology

- The methodology implemented [13] provides lumped results at aquifer scale. An analysis based exclusively on these lumped results would lose information about the heterogeneity of SWI in the system.
- Although the method can be applied in cases where a distributed flow models is not available, a proper assessment for a specific date requires sufficient distributed data about hydraulic head, chloride concentration and aquifer bottom. On the other hand, to generate the required fields from the data it needs to apply an interpolation approach whose parameters influence on the results. It is recommended that the user tests different interpolation approaches and parameters in order to obtain results in agreement with expert opinion.
- In order to assess the dynamic of SWI and the resilience of the aquifer, there is need to have data for several dates over a long period.
- If the aim is to assess sustainable management strategies, appropriate hydrological models to propagate the impacts are required, not only of the climatic conditions, but also of the management strategies.

3.1.2. GIS-SWIAS tool

- This tool has been implemented in ArcGIS and is licensed GIS software. Future implementations may be developed in an open environment.

- The GIS-SWIAS tool had to be divided into three models due to some difficulties arose to implement all the geoprocesses into one model. Nevertheless, in the future, we plan to combine these three steps into one, improving the usability of the model.
- Graphic results are based on a pre-defined template. Although graphs in ArcGIS are customizable, there is not so much potential.
- Output report are generated automatically in Excel format and lack a refined style.

4. Conclusions

In this paper we describe a new general tool, GIS-SWIAS. It is an ArcGIS-based tool, designed to analyze SWI status and vulnerability at aquifer scale by applying the method presented by [13, 15]. It is a user-friendly tool that allows geo-referenced information to be dealt with, and it is easy to introduce the required data (inputs) and to efficiently perform the demanding computational operations required. Its outputs are in the form of reports and images to summarize the magnitude, intensity and temporal evolution of SWI within an aquifer.

The GIS-SWIAS tool can be applied to assess historical SWI dynamic in case studies where we do not have a previous model. Nevertheless, if we want to analyze in a rational quantitative analysis of the various alternative management scenarios to manage SWI in a sustainable manner, the GIS-SWIAS tool will need to take information on hydraulic head and chloride concentration distribution generated from simulations of their impacts by a calibrated density-dependent flow model. In such cases, adaptation strategies to potential future scenarios, whose distributed impacts have to be propagated within the previously calibrated models, could usefully be analyzed and compared using this tool. GIS-SWIAS can be applied to assess not only SWI status at aquifer scale, but also vulnerability to any contaminant.

Given all these ways that the GIS-SWIAS tool can be applied, it provides a valuable tool for both researcher and technician to assess SWI dynamics and aquifer resilience under different management scenarios. It can support the decision-making process in the rational selection of sustainable management strategies. The tool's performance has been tested and confirmed in two case studies described in previous research works.

It can be applied to any case study. The easy-to-use workflow and the few input data required facilitates its application to a large number of case studies in order to compare SWI.

Data Availability

The software developed in this study may be available for research purposes on application to the authors.

Conflicts of Interest

The authors declare that there are no conflicts of interest regarding the publication of this paper.

Funding Statement

This work has been supported by the GeoE.171.008-TACTIC and GeoE.171.008-HOVER projects from GeoERA organization funded by European Union's Horizon 2020 research and innovation program; and SIGLO-AN (RTI2018-101397-B-I00) project from the Spanish Ministry of Science, Innovation and Universities (Programa Estatal de I+D+I orientada a los Retos de la Sociedad).

Acknowledgments

This paper is presented within the framework of the GeoE.171.008-TACTIC and GeoE.171.008-HOVER projects from GeoERA organization funded by European Union's Horizon 2020 research and innovation program; Plan de Garantía Juvenil from MINECO (Ministerio de Economía y Competitividad), co-inancing by BEI (Banco Europeo de Inversiones) and FSE (Fondo Social Europeo); and SIGLO-AN (RTI2018-101397-B-I00) project from the Spanish

Ministry of Science, Innovation and Universities (Programa Estatal de I+D+I orientada a los Retos de la Sociedad).

References

[1] Water Framework Directive (WFD) (2000) Directiva 2000/60/CE del Parlamento Europeo y del Consejo de 23 de Octubre de 2000. Diario Oficial de las Comunidades Europeas de 22/12/2000. L 327/ 1–327/32

[2] Momejian, N., Najm, M. A., Alameddine, I., & El-Fadel, M. (2019). Groundwater vulnerability modeling to assess seawater intrusion: a methodological comparison with geospatial interpolation. Water resources management, 33(3), 1039-1052.

[3] Elumalai, V., Brindha, K., Sithole, B., & Lakshmanan, E. (2017). Spatial interpolation methods and geostatistics for mapping groundwater contamination in a coastal area. Environmental Science and Pollution Research, 24(12), 11601-11617.

[4] Llopis-Albert C, Pulido-Velazquez D (2014) Discussion about the validity of sharp-interface models to deal with seawater intrusion in coastal aquifers. Hydrol Process 28:3642–3654. https://doi.org/10.1002/hyp.9908

[5] Llopis-Albert, C. and Pulido-Velazquez, D., 2015. Using MODFLOW code to approach transient hydraulic head with a sharp-interface solution. Hydrol. Process 29, Issue 8, pages 2052–2064, 15. DOI: 10.1002/hyp.10354.

[6] Renau-Pruñonosa, A.; Morell, I., Pulido-Velazquez, D., 2016. A methodology to analyse and assess pumping management strategies in coastal aquifers to avoid degradation due to seawater intrusion problems. Water Resources Management 30 (4827-4837). DOI: 10.1007/s11269-016-1455-y

[7] Collados-Lara A-J, Pulido-Velazquez D, Pardo-Igúzquiza E (2018) An integrated statistical method to generate potential future climate scenarios to analyse droughts. Water 10:1224–1248. https ://doi.org/10.3390/w1009 1224

[8] Pulido-Velazquez D, Renau-Pruñonosa A, Llopis-Albert C, Morell I, Collados-Lara AJ, Senent-Aparicio J, Baena-Ruiz L (2018) Integrated assessment of future potential global change scenarios and their hydrological impacts in coastal aquifers—a new tool to analyse management alternatives in the Plana Oropesa-Torreblanca aquifer. Hydrol Earth Syst Sci 22(5):3053. https//doi.org/10.5194/hess-22-3053-2018

[9] Ballesteros BJ, Morell I, García-Menéndez O, Renau-Pruñonosa A (2016) A standardized index for assessing seawater intrusion in coastal aquifers: the SITE index. Water Resour Manag 30(13):4513–4527. https://doi.org/10.1007/s11269-016-1433-4

[10] Tomaszkiewicz, M., Najm, M. A., & El-Fadel, M. (2014). Development of a groundwater quality index for seawater intrusion in coastal aquifers. Environmental Modelling & Software, 57, 13-26.

[11] Babiker, I.S., Mohamed, M.A.A. & Hiyama, T. Assessing groundwater quality using GIS. Water Resour Manage 21, 699–715 (2007). https://doi.org/10.1007/s11269-006-9059-6

[12] Zeynolabedin, A., & Ghiassi, R. (2019). The SIVI index: a comprehensive approach for investigating seawater intrusion vulnerability for island and coastal aquifers. Environmental Earth Sciences, 78.

[13] Baena-Ruiz L, Pulido-Velazquez D, Collados-Lara AJ, Renau-Pruñonosa A, Morell I (2018) Global assessment of seawater intrusion problems (status and vulnerability). Water Resour Manage 32:2681–2700. https ://doi.org/10.1007/s1126 9-018-1952-2

[14] Hinsby, K., Melo, M.T., & Dahl, M. (2008). European case studies supporting the derivation of natural background levels and groundwater threshold values for the protection of dependent ecosystems and human health. The Science of the total environment, 401 1-3, 1-20.

[15] Baena-Ruiz, L., Pulido-Velazquez, D., Collados-Lara, A. et al. Summarizing the impacts of future potential global change scenarios on seawater intrusion at the aquifer scale. Environ Earth Sci 79, 99 (2020). https://doi.org/10.1007/s12665-020-8847-2

[16] Chachadi AG, Lobo Ferreira JP (2007) Assessing aquifer vulnerability to sea-water intrusion using GALDIT method: Part 2—GALDIT indicator descriptions. In: Water in celtic countries: quantity, quality and climate variability (ed. by J. P. Ferreira), Proceedings of the fourth inter-celtic colloquium on hydrology and management of water resources. Guimarães, Portugal, 11–13 July, 2005, pp 172–180

[17] Andreu, J., Capilla, J., & Sanchís, E. (1996). AQUATOOL, a generalized decision-support system for water-resources planning and operational management. Journal of hydrology, 177(3-4), 269-291.

[18] Vázquez-Suñé, E., Abarca, E., Carrera, J., Capino, B., Gámez, D., Pool, M., ... & Ibáñez, X. (2006). Groundwater modelling as a tool for the European Water Framework Directive (WFD) application: The Llobregat case. Physics and Chemistry of the Earth, Parts A/B/C, 31(17), 1015-1029.

[19] Criollo, R., Velasco, V., Nardi, A., Vries, L.M., Riera, C., Scheiber, L., Jurado, A., Brouyère, S., Pujades, E., Rossetto, R., & Vázquez-Suñé, E. (2019). AkvaGIS: An open source tool for water quantity and quality management. Comput. Geosci., 127, 123-132.

[20] Machiwal, D., Jha, M. K., Singh, V. P., & Mohan, C. (2018). Assessment and mapping of groundwater vulnerability to pollution: Current status and challenges. Earth-Science Reviews, 185, 901-927.

[21] Rikalovic, A., Cosic, I., & Lazarevic, D. (2014). GIS based multi-criteria analysis for industrial site selection. Procedia Engineering, 69(12), 1054-1063.

[22] Machiwal D, Jha MK (2014) Role of geographical information system for water quality evaluation. In: Nielson D (ed) Geographic information systems (GIS): techniques, applications and technologies. Nova Science Publishers, New York, USA, pp 217–278

[23] Gossel, W., Ebraheem, A. M., & Wycisk, P. (2004). A very large scale GIS-based groundwater flow model for the Nubian sandstone aquifer in Eastern Sahara (Egypt, northern Sudan and eastern Libya). Hydrogeology Journal, 12(6), 698–713. doi:10.1007/s10040-004-0379-4

[24] Wang, L., Jackson, C. R., Pachocka, M., & Kingdon, A. (2016). A seamlessly coupled GIS and distributed groundwater flow model. Environmental Modelling & Software, 82, 1–6. doi:10.1016/j.envsoft.2016.04.007

[25] Alcaraz, M., Vázquez-Suñé, E., Velasco, V., & Criollo, R. (2017). A loosely coupled GIS and hydrogeological modeling framework. Environmental Earth Sciences, 76(11), 382.

[26] Bhatt G, Kumar M, Duffy CJ (2014) A tightly coupled GIS and distributed hydrologic modeling framework. Environ Model Softw 62:70–84. doi:10.1016/j.envsoft.2014.08.003

[27] Criollo, R., Velasco, V., Nardi, A., De Vries, L. M., Riera, C., Scheiber, L., ... & Vázquez-Suñé, E. (2019). AkvaGIS: An open source tool for water quantity and quality management. Computers & Geosciences, 127, 123-132.

[28] Almeida, C. N., Roehrig, J., & Wendland, E. (2014). Development and integration of a groundwater simulation model to an open geographic information system. JAWRA Journal of the American Water Resources Association, 50(1), 101-110.

[29] Akbar, T. A., Lin, H., & DeGroote, J. (2011). Development and evaluation of GIS-based ArcPRZM-3 system for spatial modeling of groundwater vulnerability to pesticide contamination. Computers & geosciences, 37(7), 822-830.

[30] Rios, J. F., Ye, M., Wang, L., Lee, P. Z., Davis, H., & Hicks, R. (2013). ArcNLET: A GIS-based software to simulate groundwater nitrate load from septic systems to surface water bodies. Computers & Geosciences, 52, 108-116.

[31] Ali, R., McFarlane, D., Varma, S., Dawes, W., Emelyanova, I., and Hodgson, G.: Potential climate change impacts on the water balance of regional unconfined aquifer systems in south-western Australia, Hydrol. Earth Syst. Sci., 16, 4581–4601, https://doi.org/10.5194/hess-16-4581-2012, 2012.

[32] Pulido-Velazquez, D., Renau-Pruñonosa, A., Llopis-Albert, C., Morell, I., Collados-Lara, A.-J., Senent-Aparicio, J., and Baena-Ruiz, L.: Integrated assessment of future potential global change scenarios and their hydrological impacts in coastal aquifers – a new tool to analyse management alternatives in the Plana Oropesa-Torreblanca aquifer, Hydrol. Earth Syst. Sci., 22, 3053–3074, https://doi.org/10.5194/hess-22-3053-2018, 2018.

[33] De Filippis, G., Pouliaris, C., Kahuda, D., Vasile, T. A., Manea, V. A., Zaun, F., ... & Rossetto, R. (2020). Spatial Data Management and Numerical Modelling: Demonstrating the Application of the QGIS-Integrated FREEWAT Platform at 13 Case Studies for Tackling Groundwater Resource Management. Water, 12(1), 41.

[34] Perdikaki, M., Manjarrez, R. C., Pouliaris, C., Rossetto, R., & Kallioras, A. (2020). Free and open-source GIS-integrated hydrogeological analysis tool: an application for coastal aquifer systems. Environmental Earth Sciences, 79(14), 1-16.

[35] Menezes, G. B., & Inyang, H. I. (2009). GIS-based Contaminant Transport Model for Heterogeneous Hydrogeological Settings. Journal of Environmental Informatics, 14(1).

[36] McDonald, M.G. and Harbaugh, A.W. 1988. A modular three-dimensional finite-difference ground-water flow model: U.S. Geological Survey Techniques of Water-Resources Investigations, book 6, chap. A1, 586 p.

[37] Bakker, Mark, Schaars, Frans, Hughes, J.D., Langevin, C.D., and Dausman, A.M., 2013, Documentation of the seawater intrusion (SWI2) package for MODFLOW: U.S. Geological Survey Techniques and Methods, book 6, chap. A46, 47 p., https://pubs.usgs.gov/tm/6a46/.

[38] HYDROGEOLOGIC, W. (2005). Visual MODFLOW User's Manual. Waterloo Hydrogeologic. Inc. Canada.

[39] Chiang, W.H., 2001, 3D-Groundwater modeling with PMWIN: A simulation system for modeling groundwater flow and transport processes, 2 (New York: Springer).

[40] Winston, R. B. (2009). ModelMuse: a graphical user interface for MODFLOW-2005 and PHAST (p. 52). Reston, VA: US Geological Survey.

[41] Criollo, R., Velasco, V., Vázquez-Suñé, E. et al. An integrated GIS-based tool for aquifer test analysis. Environ Earth Sci 75,391 (2016). https://doi.org/10.1007/s12665-016-5292-3

[42] Aller L, Bennett T, Lehr J, Petty R, Hackett G (1987) DRASTIC: a standardized system for evaluating groundwater pollution potential using hydrogeologic settings: U.S. environmental protection agency report 600/2- 87/035, p 622

[43] Vías, J.M., Andreo, B., Perles, M.J. et al. Proposed method for groundwater vulnerability mapping in carbonate (karstic) aquifers: the COP method. Hydrogeol J 14, 912–925 (2006). https://doi.org/10.1007/s10040-006-0023-6

[44] Baena-Ruiz, L., & Pulido-Velazquez, D. (2020). A Novel Approach to Harmonize Vulnerability Assessment in Carbonate and Detrital Aquifers at Basin Scale. Water, 12(11), 2971.

[45] Pulido-Velazquez, D., Collados-Lara, A-J., Baena-Ruiz, L., Fernández-Chacón, F., Alcalá, F. J. Assessment of present and future vulnerability to pumping in Spanish groundwater bodies using a natural turnover time index. IAH 2017, Dubrovnik, Croatia.

[46] Pulido-Velazquez, David; Romero, Javier; Collados-Lara, Antonio-Juan; Alcalá, Francisco J.; Fernández-Chacón, Francisca; Baena-Ruiz, Leticia. 2020. "Using the Turnover Time Index to Identify Potential Strategic Groundwater Resources to Manage Droughts within Continental Spain" Water 12, no. 11: 3281.

[47] Duarte, L., Teodoro, A. C., Gonçalves, J. A., Dias, A. J. G., & Marques, J. E. (2014, June). Assessing groundwater vulnerability to pollution through the DRASTIC method. In International Conference on Computational Science and Its Applications (pp. 386-400). Springer, Cham.

[48] Renau-Pruñonosa, A., Morell, I. & Pulido-Velazquez, D. A Methodology to Analyse and Assess Pumping Management Strategies in Coastal Aquifers to Avoid Degradation Due to Seawater Intrusion Problems. Water Resour Manage 30, 4823–4837 (2016). https://doi.org/10.1007/s11269-016-1455-y

[49] Loucks, D. P., & Van Beek, E. (2017). Water resource systems planning and management: An introduction to methods, models, and applications. Springer.

[50] Reitsma, R. F. (1996). Structure and support of water-resources management and decision-making. Journal of Hydrology, 177(3-4), 253-268.

[51] Atta, M. T. (2017). The Effect of Usability and Information Quality on Decision Support Information System (DSS). Arts Social Sci J, 8, 257.

Capítulo 5: A novel approach to harmonize vulnerability assessment in carbonate and detrital aquifers at basin scale

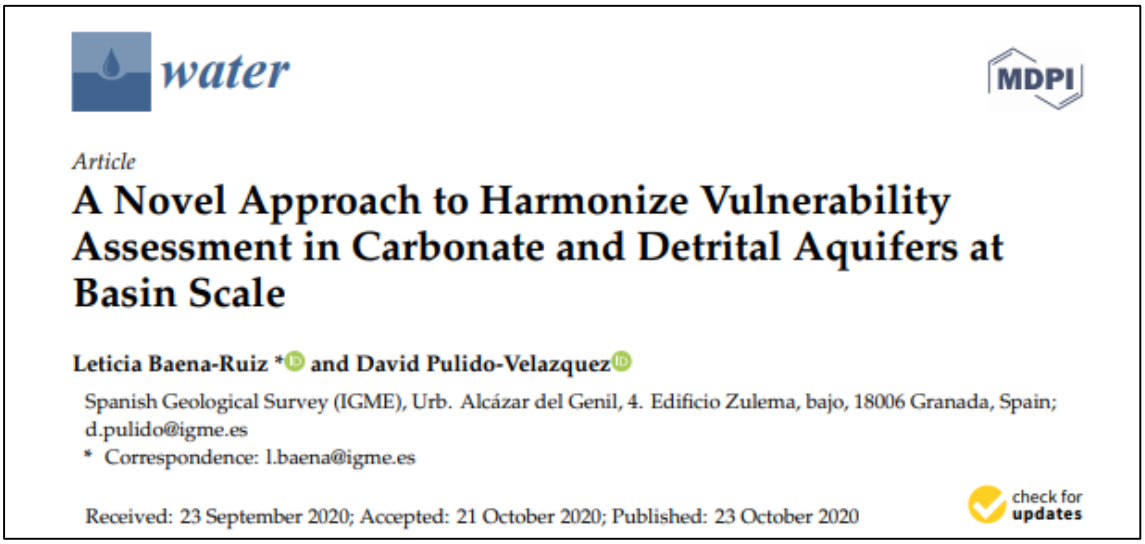

Reference: Baena-Ruiz, L.; Pulido-Velazquez, D. A Novel Approach to Harmonize Vulnerability Assessment in Carbonate and Detrital Aquifers at Basin Scale. Water 2020, 12, 2971. https://doi.org/10.3390/w12112971

Authors and affiliations:

Leticia Baena-Ruiz * and David Pulido-Velazquez

Spanish Geological Survey (IGME). Urb. Alcázar del Genil, 4. Edificio Zulema, bajo, 18006 Granada, Spain; d.pulido@igme.es

*****Correspondence: l.baena@igme.es

Received: 23 September 2020; Accepted: 21 October 2020.

Abstract

The DRASTIC (D: Depth to water; R: Net recharge; A: Aquifer media; S: Soil media; T: Topography; I: Impact of vadose zone; C: Hydraulic conductivity) index is usually applied to assess intrinsic vulnerability in detrital and carbonate aquifers, although it does not take into account the particularities of karst systems as the COP (C: Concentration of flow; O: Overlying layers above water table; P: precipitation) method does. In this paper we aim to find a reasonable correspondence between the vulnerability maps obtained using these two methods. We adapt the DRASTIC index in order to obtain reliable assessments in carbonate aquifers while maintaining its original conceptual formulation. This approach is analogous to the hypothesis of "equivalent porous medium", which applies to karstic aquifers the numerical solution developed for detrital aquifers. We applied our novel method to the Upper Guadiana Basin, which contains both carbonate and detrital aquifers. Validation analysis demonstrated a higher confidence in the vulnerability assessment provided by the COP method in the carbonate aquifers. The proposed method solves an optimization problem to minimize the differences between the assessments provided by the modified DRASTIC and COP methods. Decision trees and spatial statistics analyses were combined to identify the ranges and weights of DRASTIC parameters to produce an optimal solution that matches the COP vulnerability classification for carbonate aquifers in 75% of the area, while maintaining a reliable assessment of the detrital aquifers in the Basin.

Keywords: groundwater vulnerability; carbonate aquifers; optimized DRASTIC; COP; decision trees; nitrate validation

1. Introduction

Groundwater pollution is a widespread problem affecting most aquifers all over the world due to the increasing agricultural and industrial human activity [1,2]. It is the result of the interaction between the anthroposphere and the hydrosphere, where substances from the different land uses penetrate the groundwater, leading to impacts on environmental water quality and human health. The protection of the groundwater resources has become a priority due to the importance of groundwater for human supply, irrigation and dependent ecosystems, especially in semi-arid regions [3–5]. The degree of protection depends on intrinsic groundwater vulnerability, which is defined as the susceptibility of aquifers to pollution arising from anthropogenic activity [6]. Several methods have been proposed to assess intrinsic vulnerability by using conceptual groundwater flow models and taking transport processes into account [7,8]. The most frequently employed methods are the index-based approaches [9,10] of which DRASTIC (D: Depth to water; R: Net recharge; A: Aquifer media; S: Soil media; T: Topography; I: Impact of vadose zone; C: Hydraulic conductivity) [9] is the most common. DRASTIC has been applied to various types of aquifer, though some authors have revealed that it is not suitable for assessing vulnerability in some karstic aquifers [10–13].

Karstic aquifers present physical particularities that, in general, make them more sensitive to contamination [14,15]. Specific approaches, such as the COP (C: Concentration of flow; O: Overlying layers above water table; P: precipitation) method [10], have been developed specifically to assess groundwater vulnerability in carbonate (karstic) aquifers. The COP method has been extensively applied in different research studies to this type of aquifer [16–21].

However, despite significant physical differences between detrital and karstic aquifers, the same approaches are often applied to simulate groundwater processes in both types of aquifers. In numerical groundwater flow models, the "equivalent porous medium" assumes the validity of the Darcy's law in karstic aquifers, which is the most frequent numerical approach deduced for detrital aquifers. We find many examples of application of this approach both for detrital aquifers [22–24] and karstic aquifers [25,26]. In the same way, index methods such as DRASTIC could be suited to assessing vulnerability in both detrital and karstic aquifers.

In this context, recent research studies have attempted to adapt the DRASTIC method to karst aquifers in recent years [12,27–30]. Some of these [12,28,29] modified DRASTIC by including and/or removing parameters to account for karst characteristics. Other studies [27,30] adapted DRASTIC by modifying the classic assessment according to the distribution of nitrate concentration, although the most contaminated areas do not always imply higher vulnerability [31,32]. A detailed review of different approaches proposed to modify the DRASTIC method is given in [13].

These modifications of the DRASTIC method were performed using different methodologies/approaches: single-parameter sensitivity analysis [3,5,33], calibration by correlation analysis with pollutants [4,34,35], analytic hierarchy process [36–38] amongst others. Different data mining algorithms have also been applied to improve DRASTIC performance [39–42], predict areas vulnerable to groundwater contamination or to identify hydrogeological factors influencing groundwater contamination [39,43,44]. Data mining algorithms aim to extract knowledge from previously unknown and indistinguishable data, and are used as operational tools to find optimal solutions in high-dimension problems. Although many authors have employed these techniques for different purposes, more research is needed to explore the potential of the statistical techniques—including data mining—to deal with the uncertainties in the weights and ratings of index-based methods in the groundwater vulnerability assessments [45].

In general, the aforementioned index-based methods have been proven to provide satisfactory vulnerability assessment in a variety of regions. However, different index methods often provide dissimilar results in a single study area, making it difficult to compare and validate results [46–48]. In complex groundwater systems containing various aquifers types, an integrated vulnerability assessment is needed to homogenize criteria and compare results at basin scale and between different case studies. In general, a harmonized method that is applicable to all aquifer types would be more likely to be implemented worldwide [12,49]. Previous work [12] has aimed at developing a new

method (DRISTPI; Depth to water, Recharge, Impact of vadose zone, Soil, Topography, Preferential Infiltration) by adding and removing certain parameters from the classic DRASTIC method that can be applied to any type of aquifer. It was tested in karstic aquifers, but not in detrital aquifers.

In this paper we propose a novel approach to standardize the DRASTIC method to assess vulnerability in a basin composed by both, detrital and carbonate aquifers. We proposed an adaptation of the most commonly applied method for detrital aquifers—the DRASTIC method—to obtain a reliable vulnerability assessment for carbonate aquifers. The DRASTIC method can be applied in both detrital and carbonate aquifers, though it does not always provide appropriate vulnerability assessment in carbonate aquifers. In contrast, the COP method is specific to carbonate aquifers and it yielded better results in the validation analysis in our case study. Therefore, we proposed to adapt DRASTIC to harmonize the vulnerability assessment for different aquifer typologies, in order to make the results comparable in a basin that contains a wide variety of geological formations. Harmonization of criteria in the vulnerability assessment would allow the dissimilarities provided by different vulnerability methods to be dealt with. Although in the literature we can find several attempts to adapt the DRASTIC method to the particularities of each case study, none of them have proved the applicability of the modified DRASTIC in different aquifer typologies.

In this study, an optimization problem is solved to establish a correspondence between DRASTIC and COP by maintaining the original formulation of the DRASTIC method. It aims to find the weights and ranges of the DRASTIC parameters that maximize the correspondence between the qualitative vulnerability classes obtained using DRASTIC and COP methods. The optimization problem is solved through a new approach that combines spatial statistics analysis and data mining (decision trees). Although decision trees have been applied to predict the sensitivity to contaminants based on groundwater vulnerability [50,51], they have not been used to adapt/improve the DRASTIC method.

The optimization methodology was applied to five carbonate aquifers in the Upper Guadiana Basin, where the validation analysis demonstrated that COP method produces better vulnerability assessment than the original DRASTIC one. The optimal solution obtained for carbonate aquifers (O-DRASTIC) was also tested in the three detrital aquifers within the basin and the validation analysis also shows significant improvement in the results comparing with the original DRASTIC. A sensitivity analysis of the changes introduced to define the optimum DRASTIC reveals the influence of the various intrinsic characteristics on the severity of vulnerability for different aquifer typologies.

2. Materials and Methods

2.1. Study Area and Data

The Upper Guadiana Basin (Figure 5.1) is located in the central part of Spain. It is composed of eight groundwater bodies including five unconfined mixed (carbonate and detrital) and three unconfined detrital aquifers extending over approximately 14000 km^2.

The climate in this area is typically continental and semiarid. Mean annual precipitation over the period 1974–2015 was 445 mm and the mean annual temperature is 14.7 °C. Mean potential evapotranspiration is 700 mm/year.

The area is predominantly flat, bounded by mountain landscapes to the north (Sierra de Altomira) and south (Campo de Montiel).

Connectivity between groundwater bodies is structurally complex, with strong natural interaction between groundwater and surface water. Under natural conditions groundwater flow discharges into the central aquifer of the system (Mancha Occidental Aquifer) [52] which flows eastwards.

The predominantly dry climate and the prevalence of irrigated agriculture means that the Upper Guadiana Basin has been intensively pumped, and this has led to some of its aquifers being declared overexploited [53]. The water table is highly variable, lying at less than 1 m to more than 250 m, though over most of the basin it lies below 15 m.

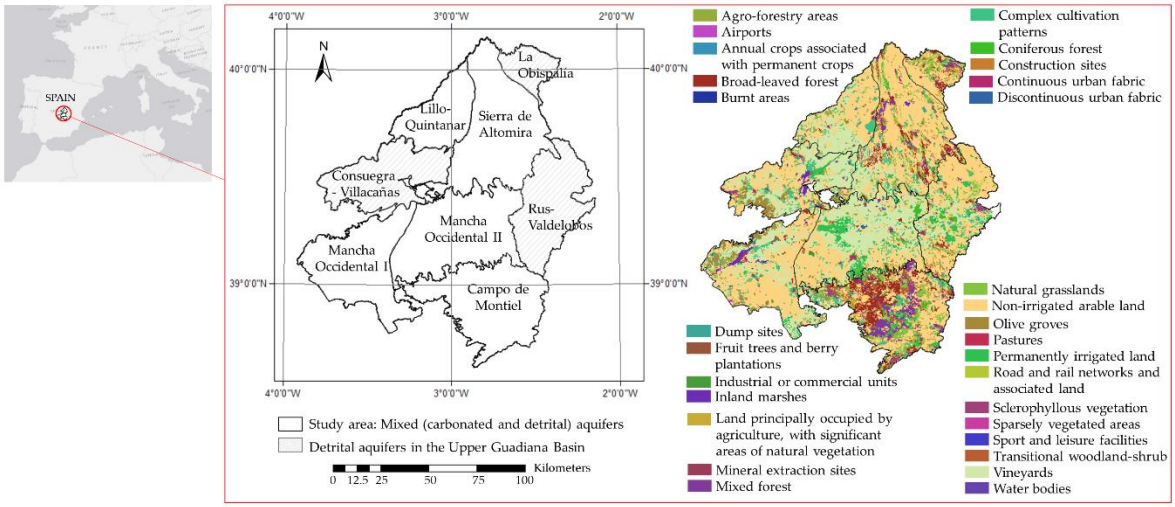

Figure 5. 1. Location of study area within the Upper Guadiana Basin (Spain).

Rainfall is the main source of aquifers' recharge. Mean annual recharge varies between 45 and 70 mm/year, although there is disagreement about these values [52–54].

The soils in the basin mainly belong to the cambisol group according to the FAO (Food and Agriculture Organization of the United Nations) classification [54,55]. Regosol and others, such as luvisol and podzol, can be found in the southeast [54]. Soil texture in the northern part of the basin is predominantly silty-loam, whereas the soil in the southern part it is peaty.

The geology is complex, including mixed carbonate–detrital aquifers. In the southern half of the Upper Guadiana Basin, the aquifers are predominantly composed of limestones, with many karstified zones [53]. In general, the karst is not very developed and there are no swallow holes in these aquifers. Many parts of the central aquifer are formed by Tertiary detrital deposits [53]. The northern aquifers are more heterogeneous. There are no large karstified areas and other formations of metamorphic materials can be found. The detrital aquifers are mainly composed of Tertiary and Quaternary alluvial materials.

The unsaturated zone is formed by poorly permeable lithology in the northern part of the basin, with higher permeability in the southern part [54].

Conductivity in the Upper Guadiana Basin varies widely. To the north, conductivity is low (below 1.5×10^{-4} m/s); in the central part there are zones with values higher than 5×10^{-4} m/s, while conductivity to the southern is mainly in the range 3.5×10^{-4}–5×10^{-4} m/s [56].

2.2. DRASTIC and COP Vulnerability Maps

DRASTIC and COP vulnerability maps were calculated in the five mixed aquifers following the proposal made in [9,10], respectively (Figure 5.2). A detailed explanation of these methods can be found in the Appendix A. Tables A4 and A5 (Appendix B) summarizes the data sources and the methodology applied to calculate the parameters of DRASTIC (hereinafter, we will call it "original DRASTIC") and COP, respectively.

The "original DRASTIC" values vary between 41 and 171 within the study area. The final index was reclassified into five qualitative classes (Very low: <100; Low: 100–120; Moderate: 120–160; High: 160–180; Very high: ≥180) by grouping the original categories proposed in [9] to obtain the same number of classes as the COP vulnerability map. The values of parameters Aquifer media, Soil media, Impact of vadose zone and Conductivity (Figure 5.2(a3,a4,a6,a7)) show significant heterogeneity, with clear differences between the northern and central–southern areas. These differences are finally reflected in the vulnerability map (Figure 5.2(a8)).

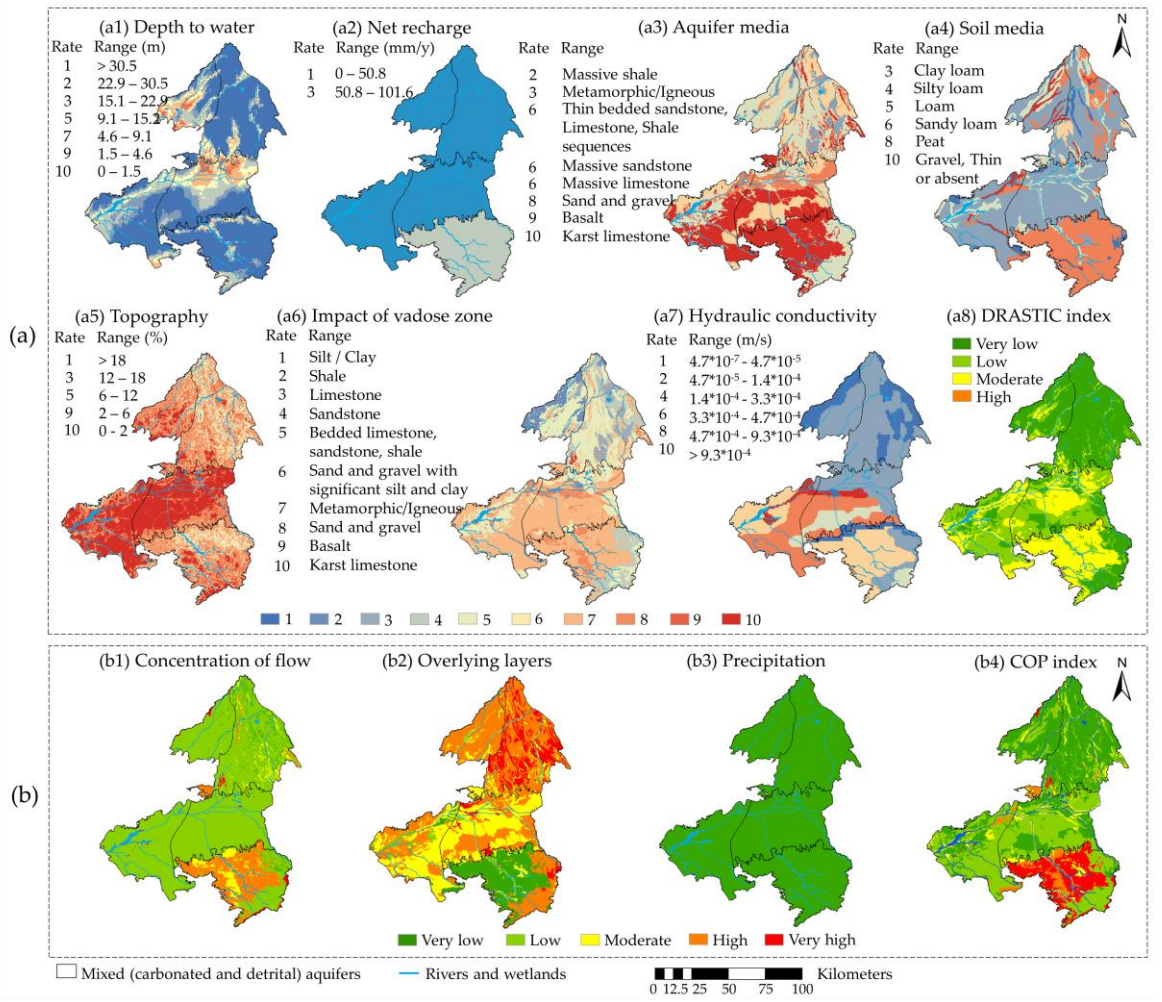

Figure 5.2. (a) DRASTIC (D: Depth to water; R: Net recharge; A: Aquifer media; S: Soil media; T: Topography; I: Impact of vadose zone; C: Hydraulic conductivity) maps: (a1) Depth to water; (a2) Net recharge; (a3) Aquifer media; (a4) Soil media; (a5) Topography; (a5) Topography; (a6) Impact of vadose zone; (a7) Hydraulic conductivity; (a8) Vulnerability map; (b) COP(C: Concentration of flow; O: Overlying layers above water table; P: precipitation) maps: (b1) Reduction of protection due to Concentration of flow; (b2) Degree of protection from Overlying layers; (b3) Reduction of protection due to the precipitation factor; (b4) Vulnerability map.

Figure 5.2b shows the results of applying the COP method as proposed by [10]. The protection conferred by Overlaying the layers (Figure 5.2(b2)) generally decreases from north to south. It is very low in the southern part due to the presence of limestones and dolomites outcrops. The surface features related to the Concentration of flow (Figure 5.3(b1)) produce only a slight reduction of protection over 80% of the area, except in the southern Campo de Montiel aquifer, where the protection from Overlying layers is greatly reduced.

While the highest values of the DRASTIC index are located in the center and southern part of the basin (classified as “Moderate vulnerability”), the highest values of the COP index appear in the southern zone (Campo de Montiel aquifer). Both indices give their lowest values in the north area (Sierra de Altomira and Lillo Quintanar aquifers).

The percentage overlap between the vulnerability classes obtained using COP and DRASTIC is 55.75%. There is a significant coincidence in the “Very low” and “Low” vulnerability classes, which cover nearly 80% of the area in the COP map. However, the coincidence in “High” and “Very high” classes is almost null. A misclassification of the highest vulnerability areas of groundwater dependent ecosystems such as the Upper Guadiana Basin would lead to erroneous planning and management decisions, possibly leading to significant environmental impacts.

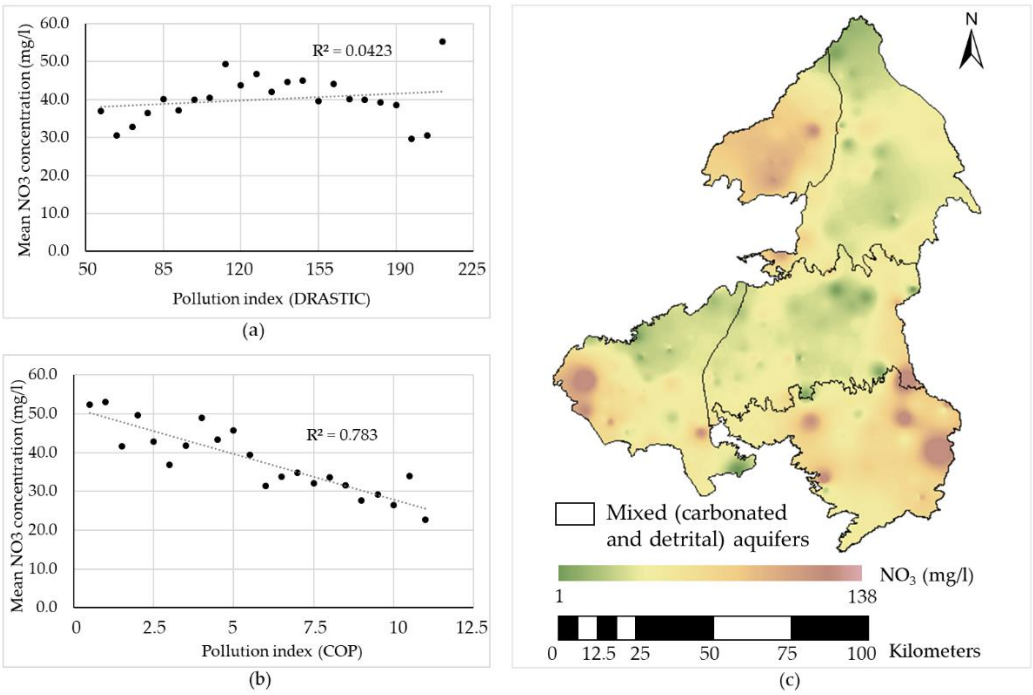

Figure 5.3. Validation of vulnerability maps in mixed aquifers: (a) DRASTIC + 5 × land use (LU); (b) COP + 5/LU; (c) mean nitrate concentration map (1975–2015).

2.3. Validation of Vulnerability Maps

Contaminant loads are linked to human activities and land use (LU). Therefore, in addition to aquifer vulnerability, these are a key factor in determining groundwater contamination [3,57]. In the study area, the intensive agriculture and the use of nitrogen fertilizers has provoked high levels of nitrates in many groundwater areas. Since nitrate is not naturally found in groundwater, it is considered to be a good indicator of contamination by human impact, especially in agricultural zones. The DRASTIC vulnerability map is validated by adding an LU factor to the DRASTIC index (Equation (1)), as proposed in other studies [27,58,59]. Making an analogy, the index defining protection against pollution could be based on the COP vulnerability (Equation (2)). In this case the inverse of the LU factor is considered since a higher COP index indicates lower vulnerability levels. Since the principal land use is agriculture, the pollution index and the protection-against-pollution index will maintain the factor of 5 used to weight the LU term, as was originally included in the DRASTIC pollution index by other authors [27,60]:

$$Pollution\ index\ (DRASTIC) = DRASTIC\ index + 5 \times LU \quad (1)$$

$$Protection - \text{against} - Pollution\ index\ (COP) = COP\ index + \frac{5}{LU} \quad (2)$$

The rates assigned to LU [3,27,33,34] are shown in Table 5.1.

The correlations (R-squared coefficient) with the pollution index derived from DRASTIC and COP methods (Figure 5.3) were determined from the 214 observation points where nitrate concentration data was available (1974 to 2015 provided by the Spanish Geological Survey and the River Basin Authority). The DRASTIC pollution index (Figure 5.3a) is weakly correlated with the mean nitrate concentration ($R^2 = 0.04$) in the carbonate aquifers. However, the protection-against-pollution index linked to the COP map (Figure 5.3b) shows strong correlation ($R^2 = 0.78$). Accordingly, in this validation analysis, the COP vulnerability assessment for the study area provides a more reliable assessment than the DRASTIC index one.

Table 5.1. Rates of LU

LU	Rate
Agro-forestry areas	7
Airports	2
Annual crops associated with permanent crops	8
Broad-leaved forest	2
Burnt areas	2
Complex cultivation patterns	8
Coniferous forest	2
Construction sites	2
Continuous urban fabric	10
Discontinuous urban fabric	10
Dump sites	9
Fruit trees and berry plantations	7
Industrial or commercial units	8
Inland marshes	1
Land principally occupied by agriculture, with significant areas of natural vegetation	5
Mineral extraction sites	3
Mixed forest	3
Natural grasslands	3
Non-irrigated arable land	5
Olive groves	6
Pastures	5
Permanently irrigated land	8
Road and rail networks and associated land	2
Sclerophyllous vegetation	3
Sparsely vegetated areas	3
Sport and leisure facilities	2
Transitional woodland-shrub	2
Vineyards	5
Water bodies	1

As can be observed in Figures 5.2 and 5.3, both DRASTIC and COP indices suggest low vulnerability in some zones with high nitrate concentration (in the western part of the basin) that results from the intensive agricultural exploitation since early 1970′s. Thus, groundwater contamination not only depends on intrinsic vulnerability, but also the land use, type of crops, type of irrigation, etc. For this reason, the most contaminated areas do not always correspond to the most vulnerable ones [31,32].

2.4. Methodology: Optimization of DRASTIC Method

In this paper we adapt the DRASTIC method to minimize differences with the COP vulnerability map for the five carbonate aquifers in the Upper Guadiana Basin, which has been proven to provide better results in those aquifers according to the validation analysis. The main objective is to obtain a harmonized method that allows vulnerability in carbonate and detrital aquifers to be assessed in a homogenous way, in a system comprising varying geological formations. The harmonization of criteria to assess groundwater vulnerability will make the results comparable at basin scale. To this end, the DRASTIC index is recalculated by varying the ranges and weights of its parameters (fulfilling certain constraints to maintain a rational definition), in order to minimize the differences with the COP vulnerability map for the five mixed (carbonate and detrital) aquifers in the Upper Guadiana Basin. Data mining techniques are then applied to identify the ranges and weights that provide an optimal solution.

Figure 5.4 shows the flowchart of the proposed optimization problem and the methodology applied. Two objective functions (O.F.) were tested: (A) to maximize the percentage of spatial coincidence (area, Si) between DRASTIC and COP vulnerability classes; and (B) to minimize the distance (di; see Equation (3)) between the vulnerability classes in DRASTIC and COP. The decision variables in this optimization problem are (1) the ranges (of the DRASTIC index and its parameters) and (2) the weights of the DRASTIC parameters.

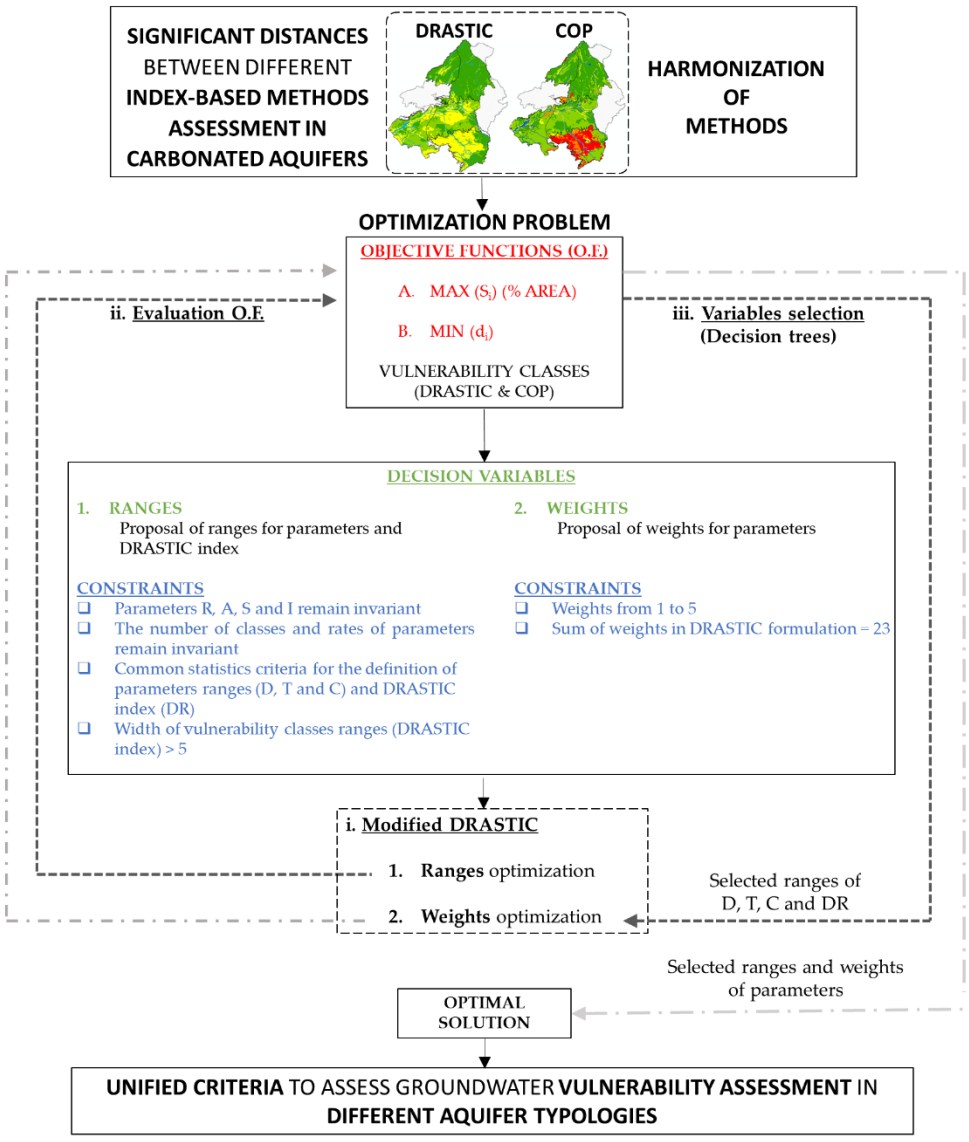

Figure 5.4. Flowchart of methodology.

The ranges of the DRASTIC parameters and index are proposed based on the available data in the study area and covering a wide range of hypothetical cases. The following constraints regarding the ranges proposal are imposed:

- The ranges of non-continuous parameters (A, S and I) were assumed to be invariant and we classify these parameters as proposed in [9]. We modify the DRASTIC index classification (DR) and the ranges of only three numerical parameters in DRASTIC: Depth to water (D), Topography (T) and Conductivity (C). The proposed ranges are shown in Table 5.2. Due to the narrow variability of the data in the study area the recharge ranges were not modified.
- The number of classes and rates adopted for all parameters are as proposed in [9]. We change only the distribution of numerical data within the ranges in order to adapt them to the characteristics of the case study.

- The modification of ranges is based on statistical criteria according to the distribution of data in the study area (quantile method, equal intervals, natural clusters in ArcGIS and increasing the limit of the ranges by a constant value) [32,61].
- We established a minimum range amplitude of 5 for the DRASTIC vulnerability classes.

We also established certain **constraints** in the weights of parameters:

- Only weights between 1 to 5 are considered;
- The sum of the weights had to be 23 for each combination (as the original proposal in [9]).

For each combination of parameter ranges and weights used to generate a DRASTIC map, the distance (d_i) or difference between vulnerability classes reported by DRASTIC and COP is calculated by Equation (3):

$$d_i = \sum \alpha_{jk} \times x_{jk} \tag{3}$$

where

- α_{jk} is the total area of "*j*" vulnerability class of COP overlapping with the "*k*" vulnerability class of DRASTIC;
- x_{jk} is a weight from 0 to 4 depending on the number of jumps from one vulnerability class to another.

In order to establish a dimensionless threshold to quantify the distance (d_i), it is expressed as a percentage of the maximum calculated distance (d_{max}) over all calculated DRASTIC indices:

$$d_i(\%) = \frac{d_i}{d_{max}} \times 100 \tag{4}$$

Table 5.2. Proposed classifications for the parameters and DRASTIC index.

Vulnerability	DR1	DR2	DR3	DR4	DR5	DR6	DR7	DR8	DR9	DR10	DR11	DR12
Very low	<70	<70	<70	<80	<80	<90	<90	<90	<100	<100	<100	<100
Low	80	90	100	90	100	100	100	110	110	115	120	130
Moderate	90	110	130	100	120	110	115	130	120	125	140	140
High	100	130	160	110	140	120	130	150	130	140	160	150
Very high	>100	>130	>160	>110	>140	>120	>130	>150	>130	>140	>160	>150
D (m) rate	D*	D1	D2	D3	D4	D5	D6	D7	D8	D9	D10	D11
10	1.5	5	5	10	10	13	15	15	20	20	25	25
9	5	10	10	15	20	21	20	30	25	40	30	50
7	10	15	20	20	30	30	25	45	30	60	35	75
5	15	20	40	25	40	37	30	60	35	80	40	100
3	23	25	80	30	50	54	35	75	40	100	45	125
2	30	30	160	35	60	88	40	90	45	120	50	150
1	>30	>30	>160	>35	>60	>88	>40	>90	>45	>120	>50	>150
T (%) rate	T*	T1	T2	T3	T4							
10	2	1	<3	4	9							
9	6	2	7	8	18							
5	12	4	14	12	27							
3	18	8	22	20	36							
1	>18	>8	>22	>20	>36							
C (m/day)	C*	C1	C2	C3	C4	C5	C6	C7	C8			

1	0.04–4	≤0.1	≤2	≤2	≤3	≤3	≤5	≤6	≤15
2	4 a 12	3	5	6	6	12	12	15	30
4	12 a 28	6	12	15	15	25	25	30	45
6	28 a 40	15	25	30	30	40	40	75	60
8	40–80	30	40	40	75	80	80	80	75
10	>80	>30	>40	>40	>75	>80	>80	>80	>75

* Original classification of DRASTIC parameters.

In order to reduce the number of calculations, we employ data mining techniques (decision trees) to select the values of the variables domain to be tested. The optimal solution is sought following two steps:

1. Ranges optimization:

   i. First, DRASTIC vulnerability maps are calculated modifying the ranges of parameters and the classification of the DRASTIC index. The weights of parameters are the same as proposed in [9].

   ii. All the DRASTIC indices are evaluated through the objective functions and the results are classified intro three categories (Table 5.3).

   iii. Decision trees are applied in order to find out the ranges for each parameter that gives the highest coincidence ($Max(S_i)$) and a lowest distance ($Min(d_i)$) between vulnerability classes assigned using DRASTIC and COP.

Table 5.3. Classification criteria of objective functions for the decision trees algorithm.

Objective Function	Value	Class
Si (spatial coincidence)	<30%	1
	30–50%	2
	>50%	3
Di (distance)	<30%	1
	30–50%	2
	>50%	3

2. Weights optimization:

   i. In this second step, the weights of parameters are introduced as new variables to compute all the feasible combinations of weights and parameter ranges selected in the previous step. The DRASTIC index is calculated for all the combinations of weights and selected classifications in step 1.

   ii. The new set of DRASTIC maps are evaluated by means of the objective functions.

   iii. For each parameter, decision trees are applied again to determine the weight that yields greatest similarity between the DRASTIC and COP maps.

The main objective of decision trees in this study is to identify the ranges and weights for each DRASTIC parameter involved in any combination that yields the maximum spatial coincidence (Si) and the minimum distance between vulnerability classes (di) ($S_i = 3$ or $d_i = 1$ according to Table 5.3). We establish these threshold values according to the distribution of results in the first set of combinations. Decision trees reduce the computational cost of the optimization problem and allow the most relevant variables to be identified in the vulnerability assessment in carbonate aquifers.

The CHAID (Chi-square Automatic Interaction Detection) algorithm [62,63] is applied in decision trees, considering the objective functions of the optimization problem (Si and di) as dependent variables. The proposed ranges and weights of parameters and classifications of DRASTIC are the independent variables, and the chi-squared test of significance is used as the splitting criterion in the CHAID algorithm. Each dataset generated in steps 1 and 2 is partitioned into a training set (70%) and a testing set (the remaining 30%) in order to assess the performance of the models. The goodness-of-fit of the classification is evaluated using the precision index [51,64]:

$$Precision = \frac{\sum_{n=1}^{n=3} TP_n}{\sum_{n=1}^{n=3}(TP_n + FP_n)} \quad (5)$$

where:

- n = number of classes;
- TP_n = number of correctly recognized class examples in the class n;
- FP_n = number of examples incorrectly assigned to the class n;

Decision trees can represent the relationship between variables and output class using specific rules following the pathway from the root node to the terminal node [63,65,66]. A priori, the number of terminal nodes on the tree can determine the number of rules but it may generate a large number of irrelevant pieces of information. Only the most relevant variables (rules with the highest population for each decision tree with precision above 50%) whose terminal nodes in the tree are classified as $S_i = 3$ or $d_i = 1$ are selected to generate all the feasible combinations to compute the DRASTIC indices.

3. Results

3.1. Optimization of the DRASTIC Method

3.1.1. Ranges Optimization

In the first optimization step, we obtained a total of 11,520 different DRASTIC maps. The spatial coincidence (Si) of the vulnerability classes between the DRASTIC and COP maps rose to 61.31% (from 55.75% in "original DRASTIC") and the minimum distance between vulnerability classes (di) fell to 20.85% ($d_{\text{original DRASTIC}} = 24.72\%$).

The selected ranges (from Table 5.2) for each parameter extracted from decision trees were as follows:

- DR11, DR12, DR14, DR15 and DR16 for DRASTIC classification;
- D*, D1, D2, D3 and D4 for Depth to water;
- T* and T1 for Topography;
- C7 and C8 for Conductivity.

The ranges proposed in [9] were selected for parameters D and T in the decision tress. For conductivity, the selected classifications (C7 and C8) assign lower rates to conductivity values.

3.1.2. Weights Optimization

The selected ranges for parameters and the DRASTIC index were combined, varying the weights of parameters between one and five. Due to a large number of generated combinations, we first considered weights one, three and five. This resulted in 35,700 new DRASTIC maps. The spatial coincidence (Si) between vulnerability classes increased to 70.34% and the minimum distance between vulnerability classes (di) fell to 8.45%.

Decision trees were applied again to determine the optimum weight for each parameter. We aimed to determine if the value of the weight for each parameter provides relevant information in the optimization problem. We found that a weight equal to five did not appear in relevant rules in parameters D and T, whereas a weight equal to one did not appear for parameters R and S. All weights (one, three, and five) were found in rules for parameters A, I and C.

A new set of combinations of ranges and weights were computed to find an optimum between the gaps left due to constraints. We introduced the mid-weights for each parameter, discarding those

not found in the relevant rules. We included the following weights for each parameter: $W_D = 2$; $W_R = 4$; $W_A = 2$ and 4; $W_S = 4$; $W_T = 2$; $W_I = 2$ and 4; $W_C = 2$ and 4. The total of combinations provide two optimal solutions:

- Optimum of O.F. Min(di): di = 8.45; Si = 42.91;
- Optimum of O.F. Max(Si): di = 13.05; Si = 70.34;

The second solution was considered the best solution because the gain in S_i was higher than the loss in d_i. Finally, the best solution was refined by adjusting the classification of the DRASTIC index to increase the spatial coincidence with the COP map, obtaining the optimum DRASTIC. The classification of the optimum DRASTIC does not match with the ranges proposed originally in [9]. The objective functions take the following values for the optimum DRASTIC: $S_i = 76.75\%$; $d_i = 10.92\%$.

Figure 5.5 shows the dot-plot of the all the DRASTIC indices calculated. It reveals the efficacy of using decision trees in the methodology to reduce the number of combinations to be tested when seeking the optimal solution. Each set of combinations improves the objective functions. Black dots show those including the mid-weights for each parameter that produce improvement in the objective function "di", but not in "Si". Red dots indicate the DRASTIC indices that provide Max(Si) and Min(di).

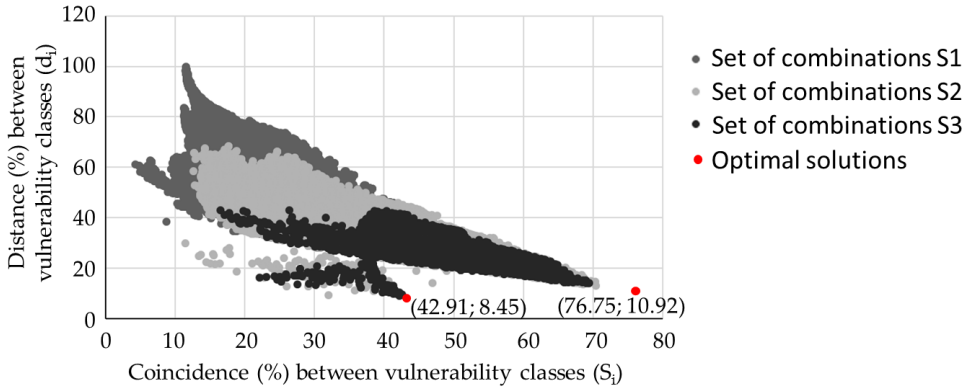

Figure 5.5. Results of objective functions for all DRASTIC combinations.

3.2. Analysis of Optimum DRASTIC (O-DRASTIC)

O-DRASTIC keeps the ranges proposed in [9] for parameters D and T. Only ranges of parameter C change in O-DRASTIC (C8 from Table 5.2). In general, the value of the conductivity rates is reduced in O-DRASTIC. The spatial distribution of conductivity ranges shows slight changes. The weights (W) of parameters of O-DRASTIC are shown in Table 5.4, compared with the original DRASTIC weights.

Table 5.4. Weights of parameters of original DRASTIC and optimum (O)-DRASTIC.

DRASTIC Parameters	D	R	A	S	T	I	C
W (original DRASTIC)	5	4	3	2	1	5	3
W (O-DRASTIC)	1	5	5	5	1	5	1

Results of O-DRASTIC reveal that Depth to water and Conductivity have no a significant impact on vulnerability for our case study area. The ranges of parameter C in O-DRASTIC also support this conclusion given that the new classification of this parameter reduces the rate assigned to conductivity values. This conclusion is confirmed by the single-parameter sensitivity analysis of O-DRASTIC, in which the parameter C takes a mean effective weight of 1.7% (compared to its empirical weight 4.3%). In general, in the study area, the carbonate aquifers have a scarcely

developed karst. In fact, approximately half the study area shows lower rates in the conductivity map. Although conductivity takes high values in some zones, the ranges of this parameter change in O-DRASTIC with respect to the original DRASTIC. The new classification in O-DRASTIC assigns lower rates to the conductivity values. Therefore, this parameter losses influence, which is also reflected in the weight. Moreover, conductivity can be considered as implicit in the aquifer media parameter (A), which increased in weight in O-DRASTIC in our case study. The reduced weight of parameter D may be due to the large depth to water table over most of the study area. The mean effective weight obtained in the sensitivity analysis was 3.2% (empirical weight = 4.3%) Aquifer media and Soil media gained great significance in the vulnerability assessment, as well as Recharge, albeit by a reduced amount. Impact of vadose zone continues to be an important factor in O-DRASTIC.

The weights in O-DRASTIC are consistent with the concept of COP methodology, where the vulnerability assessment is based mainly on the degree of protection afforded by overlying layers and the way in which the water percolates (recharges) into the aquifer.

The main changes between the original and optimum DRASTIC vulnerability maps mostly occur in areas of "Very low" and "Moderate" vulnerability of the original DRASTIC, since these are the predominant classes in this vulnerability map. Remarkably, those changes do not always occur in one direction. "Moderate" vulnerability shifts towards "Low" or "Very high" vulnerability depending on the zone, whereas other "Moderate" vulnerability areas remain with the same class. In the same way, some "Very low" vulnerability zones jump up a vulnerability class to "Low", while other maintain the same class. We analyzed the differences in the distribution of the parameter rates in these areas.

Figure 5.6a shows that the main factor causing the vulnerability to change from "Moderate" to "Low" is Depth to water. Since the weight of this parameter changed from five to one in O-DRASTIC, zones with higher rates of D report a greater fall in the vulnerability value, leading the vulnerability class to drop by one level. This graph also shows how some areas with rates of three, five and seven change from "Moderate" to "High" vulnerability, which demonstrates that other parameters influence the "Very high" vulnerability class.

On the other hand, we can observe in Figure 5.6a that the rate of parameter S (soil media) is equal to eight over more than 80% of the area where vulnerability increased from "Moderate" to "Very high", corresponding with soils with a high organic content, and outcrops of limestone and dolomites. Furthermore, the rate of S is equal to four over nearly 90% of the area where vulnerability fell from "Moderate" to "Low". Zones where no change in vulnerability class was observed have soils with medium values.

A similar conclusion regarding Soil media is drawn in the areas where vulnerability rose from "Very low" to "Low" (Figure 5.6b). In these zones we can also observe higher rates of parameters A (aquifer media) and I (impact of vadose zone). These zones correspond to karstified areas and highly permeable layers.

The results highlight the influence of Aquifer media, Soil media and Impact of vadose zone in the vulnerability of carbonate aquifers.

These conclusions are supported by the single-parameter sensitivity analysis carried out for O-DRASTIC, which yields higher effective weights in parameters A, S and I and lower effective weights for parameters D and C.

In general, the new ranges of Conductivity in O-DRASTIC contribute to an overall drop in vulnerability class, but the weights of parameters cause a sharp jump in vulnerability class, especially in the southern part of the basin, where Aquifer media and Soil media have the greatest influence (higher rates in this area).

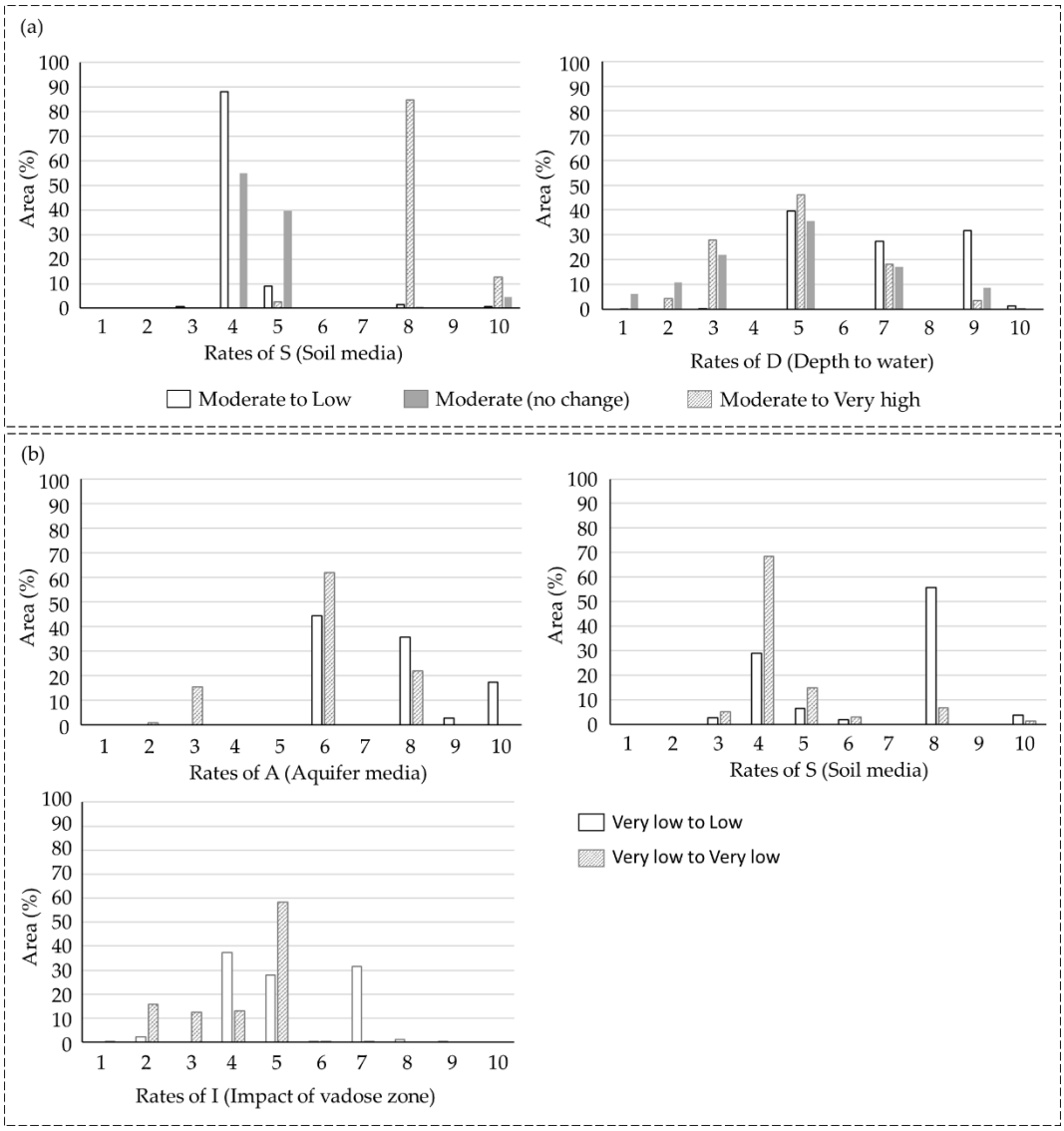

Figure 5.6. Distribution of rates of the different parameters within the area where significant changes are observed from (a) "Moderate" or from (b) "Very low" classes in the original DRASTIC to other vulnerability classes in O-DRASTIC.

The values of the optimum DRASTIC (O-DRASTIC) vary between 52 and 178 and the optimal vulnerability classes are the following:

- "Very low": 52–107;
- "Low": 107–130;
- "Moderate": 130–138;
- "High": 138–146;
- "Very high": ≥146;

Figure 5.7a shows a better distribution of vulnerability values in O-DRASTIC within the COP vulnerability classes (compared to the original DRASTIC). Close similarities can also be appreciated between the O-DRASTIC and COP vulnerability maps (Figure 5.7b). The vulnerability classes in O-DRASTIC overlap with COP over 76.75% of the basin, representing an improvement of 20% relative to the original DRASTIC. This spatial coincidence is particularly improved in the class of "Very high" vulnerability, with a 90% coincidence between COP and O-DRASTIC.

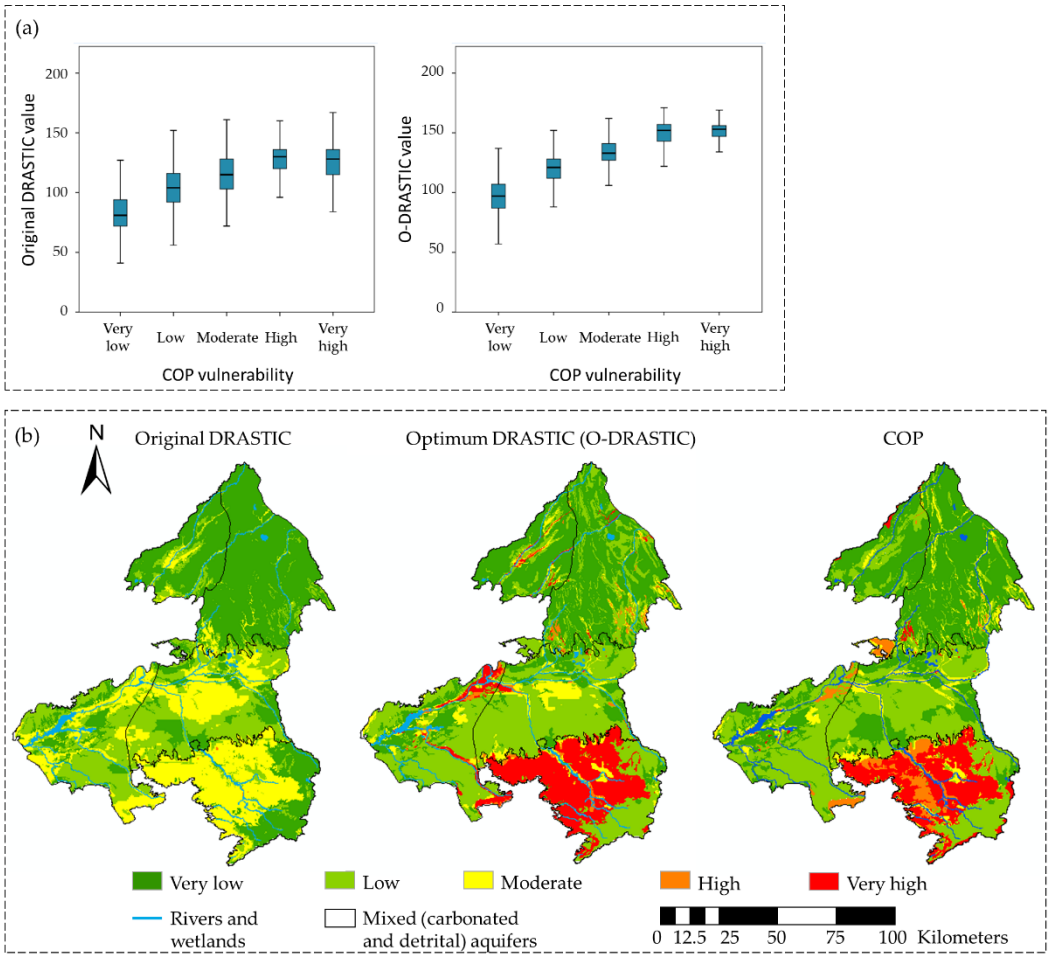

Figure 5.7. Distribution of vulnerability values of original DRASTIC and O-DRASTIC within vulnerability classes in COP (a); vulnerability maps for original DRASTIC, O-DRASTIC and COP (b).

O-DRASTIC was validated using the pollution index (Equation (1)) and the correlation with nitrate concentration (R^2 = 0.653) in carbonate aquifers improved with respect to the original DRASTIC).

Lastly, we assessed the vulnerability of the three detrital aquifers in the Upper Guadiana Basin by applying original DRASTIC and O-DRASTIC, and we validated the maps following Equation (1). Original DRASTIC showed a good correlation (R^2 = 0.765) in detrital aquifers but O-DRASTIC gave a significantly better correlation (R^2 = 0.862). Both methods (original DRASTIC and O-DRASTIC) perform a better vulnerability assessment in detrital aquifers than in carbonate aquifers.

Figure 5.8 shows the change that O-DRASTIC produces (compared to original DRASTIC) in terms of distance between vulnerability classes. Negative values mean the vulnerability class drops in O-DRASTIC compared to original DRASTIC, while positive values mean the vulnerability class in O-DRASTIC is higher than in original DRASTIC. Three zones are thus distinguished in the Upper Guadiana Basin: the southern area (Campo de Montiel) where vulnerability increases by one or two classes. This area is characterized by a higher recharge rate and a karstified aquifer. In the mid-basin (including Mancha Occidental I, Mancha Occidental II, Consuegra Villacañas and Rus-Valdelobos), vulnerability decreases generally by one class, although most of the area remains unchanged; in the northern zone (Lillo-Quintanar, Sierra de Altomira and La Obispalía) only small areas jump up a vulnerability class, and by only one level.

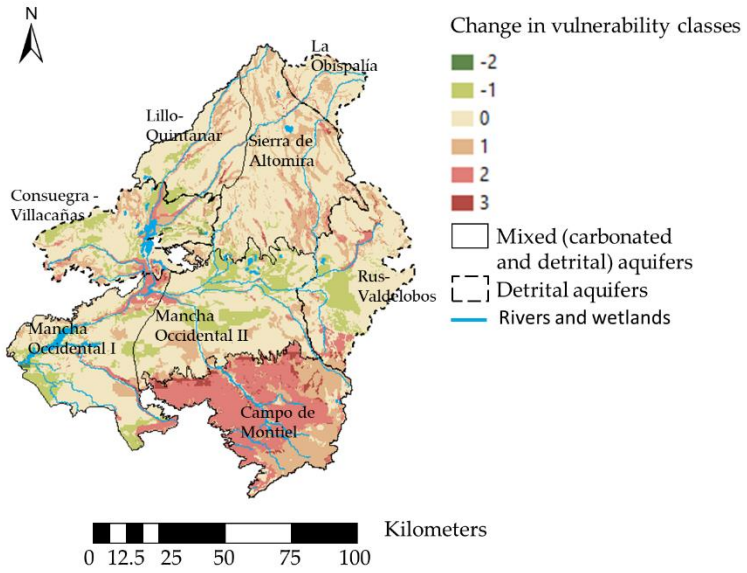

Figure 5.8. Spatial distribution of change in O-DRASTIC vulnerability classes in comparison to the original DRASTIC.

The largest difference in vulnerability class assigned is for carbonate aquifers. More than 17% of the carbonate aquifers area rises by two classes or more vulnerability classes. Only 7% of the detrital aquifers area jumps by this much, while 62% of the detrital aquifers show no change in the vulnerability class.

4. Discussion and Conclusions

This paper demonstrates that the DRASTIC method can be adapted to assess vulnerability in carbonate aquifers by undertaking some simple modifications of the weights and ranges of the parameters. Most recent studies to adapt the DRASTIC method to carbonate aquifers have aimed to transform DRASTIC by including and/or removing parameters that take the karst characteristics into account [12,28,29]. Other studies modified the classic assessment according to nitrate concentrations [27,30], though the most highly contaminated groundwater does not always imply higher vulnerability [31,32]. Instead of using either of these previous approaches, our study establishes a correspondence between DRASTIC and a vulnerability method that was specifically developed for karstic aquifers, the COP method, and therefore we avoid making conceptual changes in the original definition of DRASTIC method.

Our methodology is based on an optimization approach that identifies the ranges and weights of DRASTIC parameters that minimize the differences in the vulnerability assessment compared with the COP method, which was developed specifically for karstic aquifers. It allows us to identify the significance of the different DRASTIC parameters in the vulnerability assessment in karstic aquifers. Decision trees and spatial statistics analyses are combined to identify the ranges and weights of parameters that provide the optimal DRASTIC classes in terms of coincidence and distance with the COP vulnerability map. This optimization approach could be applied by minimizing the differences with respect to any other reference method for assessing vulnerability, whose results has been previously validated and considered as reasonable. Although many data mining techniques have been applied in groundwater vulnerability assessments [39,40,42], only a few studies have used decision trees in vulnerability studies [50,51]. They have been mainly used to assess other groundwater quality problems [65,67,68].

Our proposed method was applied in the Upper Guadiana Basin, an agricultural area that overlies carbonate and detrital aquifers. The socio-economic and hydrogeological particularities of the basin highlight the need to establish unified management measures at basin scale, not only

regarding groundwater exploitation but also in terms of protecting the good quality of the groundwater resource. Therefore, harmonization of criteria to assess groundwater vulnerability would allow comparison at basin scale and overcome the issue of dissonant results provided by contrasting vulnerability methods. Our approach assumes that the COP method provides a better approximation of the vulnerability in the case study. This assumption was tested by means of a validation analysis in which we show that the "protection-against-pollution" index (derived from COP and LU data) more closely correlates (R^2 = 0.78) with nitrate concentration than the DRASTIC "pollution index". The results of the validation show that the pollution index derived from the original DRASTIC for carbonate aquifers is not correlated with nitrates (R^2 = 0.04), whereas in detrital aquifers there is a close correlation ((R^2 = 0.76). Other authors have previously pointed out that the original DRASTIC method does not significantly correlate with nitrate concentration in agricultural areas [45,59,69]. In contrast, the pollution index derived from O-DRASTIC shows significant correlation with nitrates for both, carbonate and detrital aquifers (R^2 = 0.65 and R^2 = 0.86, respectively).

The optimal solution (O-DRASTIC) obtained in this optimization problem shows that changing the range of the Conductivity parameter produces a small drop in the vulnerability class compared with the original DRASTIC but does not lead to a significant improvement in the objective functions (coincidence and distance between vulnerability classes). The reduced significance of Conductivity is also confirmed by the much-reduced weight assigned to this parameter in O-DRASTIC. Other DRASTIC adaptation for carbonate aquifers also pointed the reduced significance of Conductivity to assess the potential "protection-against-pollution" in karstic systems [12]. We also observed a reduced significance of the Depth to water table in our case study (WD = 1). Other research studies that modified the weights of DRASTIC parameters [3,69,70] also found the Depth to water parameter to be insignificant. Specifically in karstic aquifers Depth to water is not so relevant in protecting an aquifer from contamination because of the high transit velocity through the vadose zone [12]. Moreover, the low significance of in our case study may be due to fact that the water table lies below 30 m over most of the basin. The same argument was also stated in another case study [3]. The reduced significance of Depth to water and Conductivity is confirmed by a sensitivity analysis. Topography and Impact of vadose zone maintain their weights (W_T and W_I) as defined in the original DRASTIC, while the remaining parameters (Recharge, Aquifer media and Soil media) are given maximum weights ($W_R = W_A = W_S = 5$). The large increments in the weights given to Aquifer media and Soil media in O-DRASTIC show that they are the most significant factors controlling the vulnerability in karstic aquifers. Other authors concur that these parameters are the most significant [3,70,71]. The principal change in O-DRASTIC with respect to the original DRASTIC is in the weights of parameters, which highlights that these parameters embrace most of the uncertainty in the DRASTIC vulnerability assessment [72].

Our optimal solution provides an improvement of 20% in terms of coincidence between the vulnerability classes assigned by DRASTIC and COP. This improvement was achieved by applying spatial statistical analyses and decision trees, which allowed potential solutions to be obtained by exploring only a 0.1% of the total dimensionality of the defined optimization problem. The proposed method also helps to achieve a better understanding of the parameters and variables of the "equivalent detrital approach" that really influence vulnerability in this karstic system. This optimal solution was tested for the carbonate and detrital aquifers in our case study, but it should also be tested in other different aquifers with similar hydrogeological characteristics in order to prove its applicability in a broader context under different management framework.

In summary, results show that COP and O-DRASTIC report higher vulnerability classes than the original DRASTIC method over 36% of the total area overlying carbonate aquifers. The greatest differences between the original DRASTIC and O-DRASTIC are produced for the carbonate aquifers rather than the detrital aquifers. This confirms that the reliability of DRASTIC vulnerability assessment is significantly better for detrital aquifers than for karst aquifers. These

underestimations of vulnerability in karstic aquifers when applying the classic DRASTIC is due to the physical particularities of these aquifers and their greater sensitivity to pollution [1,12,31].

4.1. Hypotheses, Limitations and Future Works

We have demonstrated the applicability of the method in the case of carbonate aquifers where the karst is not highly developed. Its applicability to well-developed karst aquifers also needs to be tested. The main adopted assumptions and limitations of the general methodology adopted are:

- The ranges of categorical non-continuous parameters (Aquifer media, Soil media and Impact of vadose zone) are not modified in this optimization procedure. We consider that the Delphi criteria proposed in [9] can be applied to establish the relative significance of each range with respect to potential pollution.
- Other algorithms and/or techniques (for example, a Random Forest algorithm) could be employed to achieve the goal in a more efficient way.
- We have not studied the whole domain of potential solutions, and a wider spectrum of parameter ranges could be tested to find other optimal solutions. Moreover, the optimization procedure provides local optimum solutions.
- Although decision trees help to reduce the dimensionality of the optimization problem, the methodology involves a large number of calculations, which might handicap extending the method to other case studies.
- The proposed methodology requires a previous validated vulnerability assessment in the study area in order to optimize the DRASTIC method.

Future work should be developed to verify the applicability of O-DRASTIC in other case studies, including aquifers with different physical (climatic and hydrogeological settings) and management particularities in order to withdrawal more generalized conclusions.

Author Contributions: Conceptualization, L.B.-R. and D.P.-V.; Data curation, L.B.-R.; Investigation, L.B.-R.; Methodology, L.B.-R. and D.P.-V.; Software, L.B.-R.; Supervision, D.P.-V.; Validation, L.B.-R.; Visualization, L.B.-R.; Writing—original draft, L.B.-R. and D.P.-V.; Writing—review and editing, L.B.-R. and D.P.-V. All authors have read and agreed to the published version of the manuscript.

Funding: This research did not receive any specific grant from funding agencies in the public, commercial, or not-for-profit sectors.

Acknowledgments: This paper was partially supported by the SIGLO-AN (RTI2018-101397-B-I00) project from the Spanish Ministry of Science, Innovation and Universities (Programa Estatal de I+D+I orientada a los Retos de la Sociedad), the GeoE.171.008-HOVER and the GeoE.171.008-TACTICproject from GeoERA organization funded by European Union's Horizon 2020 research and innovation program.

Conflicts of Interest: The authors declare that they have no known competing financial interests or personal relationships that could have appeared to influence the work reported in this paper.

Appendix 5.1. DRASTIC and COP Methods

A.5.1. DRASTIC Method

DRASTIC method was developed by [9] to assess intrinsic groundwater vulnerability in any type of aquifer.

This method considers that there are seven parameters/variables influencing the vulnerability to contamination: Depth to water table (D), Net recharge (R), Aquifer media (A), Soil media (S),

Topography (T), Impact of vadose zone (I) and Hydraulic conductivity (C). A rate of importance is assigned to the parameters according to the value or characteristics of each parameter (Table A5.1).

Table A5.1. Ranges and rates for DRASTIC parameters.

Groundwater Table Depth		
Original Ranges (ft)	**Transformed Ranges (m)**	**Original Ratings**
0–5	0–1.5	10
5–15	1.5–4.6	9
15–30	4.6–9.1	7
30–50	9.1–15.2	5
50–75	15.1–22.9	3
75–100	22.9–30.5	2
>100	>30.5	1
Net Recharge		
Original Ranges (inches)	**Transformed Ranges (mm)**	**Original Ratings**
0–2	0–50.8	1
2–4	50.8–101.6	3
4–7	101.6–177.8	6
7–10	177.8–254.0	8
>10	>254.0	9
Aquifer Media		
Original Ranges		**Original Ranges**
Massive shale		2
Metamorphic/Igneous		3
Weathered metamorphic/Igneous		4
Thin bedded sandstone, Limestone, Shale sequences		6
Massive sandstone		6
Massive limestone		6
Sand and gravel		8
Basalt		9
Karst limestone		10
Soil Media		
Original Ranges		**Original Ranges**
Thin or absent		10
Gravel		10
Sand		9
Peat		8
Shrinking and/or aggregated clay		7
Sandy loam		6
Loam		5
Silty loam		4
Clay loam		3
Muck		2
Nonshrinking and nonaggregated clay		1
Topography (% Slope)		
Original Ranges		**Original Ranges**
0–2		10
2–6		9
6–12		5
12–18		3
>18		1
Impact of Vadose Zone		

Original Ranges	Original Ranges
Silt/Clay	1
Shale	3
Limestone	6
Sandstone	6
Bedded limestone, sandstone, shale	6
Sand and gravel with significant silt and clay	6
Metamorphic/Igneous	4
Sand and gravel	8
Basalt	9
Karst limestone	10
Hydraulic Conductivity	
Original Ranges (GPD/FT^2)	**Transformed Ranges (m/s)**	**Original Ratings**
1–100	4.7×10^{-7}–4.7×10^{-5}	1
100–300	4.7×10^{-5}–1.4×10^{-4}	2
300–700	1.4×10^{-4}–3.3×10^{-4}	4
700–1000	3.3×10^{-4}–4.7×10^{-4}	6
1000–2000	4.7×10^{-4}–9.3×10^{-4}	8
>2000	$>9.3 \times 10^{-4}$	10

The values of the parameters are weighted to obtain the DRASTIC index, which is calculated following Equation (A1):

$$\text{DRASTIC index} = 5 \times D + 4 \times R + 3 \times A + 2 \times S + 1 \times T + 5 \times I + 3 \times C \quad \text{(A1)}$$

The DRASTIC index was originally classified into eight vulnerability levels according to some color codes [9] (Table A5.2) although it is usually grouped into five vulnerability classes that do not match with the original proposal in [9].

Table A5.2. Color codes for the DRASTIC index.

DRASTIC Index	Color Code
<79	Violet
80–99	Indigo
100–119	Blue
120–139	Dark Green
140–159	Light Green
160–179	Yellow
180–199	Orange
>200	Red

A.5.2. COP Method

The COP method was developed by [10] to assess intrinsic groundwater vulnerability in carbonate aquifers.

This method considers the properties of layers overlying the water table (O factor), the concentration of flow (C factor) and precipitation (P factor) as the main parameters influencing groundwater vulnerability in carbonate aquifers. The concept of this method is to assess the natural protection of groundwater determined by the overlying soils and the unsaturated zone, which may be modified by the infiltration process and climatic conditions.

Each factor is divided into subfactors, whose formulation is detailed explained in [10]. The factors are classified in ranges and the COP index calculated as the product of the three factors following the Equation (A2):

$$\text{COP index} = C \times O \times P \quad \text{(A2)}$$

The ranges of factors and the COP index are shown in Table A5.3.

Table A5.3. Values for COP parameters and vulnerability classes for the COP index.

C Factor		O Factor		*p* Factor		COP Index	
Ranges	**Reduction of Protection**	**Ranges**	**Protection Value**	**Ranges**	**Reduction of Protection**	**Ranges**	**Vulnerability Classes**
0–0.2	Very high	1	Very low	0.4–0.5	Very high	0–0.5	Very high
0.2–0.4	High	2	Low	0.6	High	0.5–1	High
0.4–0.6	Moderate	2–4	Moderate	0.7	Moderate	1–2	Moderate
0.6–0.8	Low	4–8	High	0.8	Low	2–4	Low
0.8–1.0	Very low	8–15	Very high	0.9–1	Very low	4–15	Very low

Appendix 5.2. Data Source and Methodology to Calculate DRASTIC and COP

Table A5.4. Data source and methodology to calculate DRASTIC parameters.

Factor	Data Source	Methodology
D	Data from simulation flow model (River Basin Authority) (mean of the simulated data for each grid point from 1974 to 2015).	Spatial interpolation using IDW (Inverse Distance Weighted)of groundwater level data and reclassification into D index values.
R	Recharge time series calculated from SACRAMENTO model. Mean recharge value in the period 1974–2015.	Estimation of the mean net recharge taking into account the different hydrology cycle variables in the period 1974–2015.
A	Hydrogeological map of Spain 1:200,000.	Direct assignment of A index values for each hydrogeological unit delimitated.
S	Soil Map of Spain 1:1,000,000.	Direct assignment of S index values for each soil type.
T	Digital Terrain Model at 100 × 100 m cell size.	Calculation of the slope raster file and reclassification of values into T index values.
I	Lithostratigraphic map of Spain 1:200,000.	Direct assignment of I index values for each lithostratigraphic unit.
C	Flow model at 1000 × 1000 m cell size.	Spatial interpolation using IDW of conductivity data and reclassification into C index values.

Table A5.5. Data source and methodology to calculate COP parameters.

Factor	Subfactor	Data Source	Methodology
C	-	-	There are no catchment areas to swallow holes in these aquifers.
	Scenario 2	Vegetation from CORINE LAND COVER and slope from Digital Terrain Model (100 × 100 m cell size) Karstic features from previous research works & fieldwork and	Carbonate lithologies with low karstification are considered as fissured formations. Limestones and dolomites with high or very high permeability are considered as scarcely developed karst. For sv factor, the vegetation cover is considered high when more than 30% of the surface is covered.

		litthostratigraphic map 1:200,000.	Assignment of the values for the karstic features, vegetation and slope according to COP methodology.
O	OS—Soil	Soil Map of Spain 1:1,000,000.	Assignment of the Os values after classify the different types of soil according to the COP methodology.
	OL—Lithology	Lithostratigraphic map of Spain 1:200,000.	Classification of each lithology according to COP methodology and determination of thickness of vadose zone from 3D flow model.
P	PQ—Precipitation quantity	Precipitation data from SPAIN02 [73] in the grid within the Upper Guadiana Basin (mean rainfall taking into account data above 0.5 mm/day).	Reclassification of the precipitation values into the PQ subfactor values, taking into account the average rainfall in the wet years. Precipitation series from SPAIN02 between 1974 and 2015 were used to extract the mean annual precipitation for wet years.
	PI—Temporal distribution	Precipitation data from SPAIN02 (number of rainy days in the grid within the Upper Guadiana Basin).	Counting of the number of rainy days above 0.5 mm for each cell in the SPAIN02 grid. For the estimate of the rainy days per year, meteorological historical series between 1974 and 2015 from SPAIN02 were analysed.

References

1. Kazakis, N.; Voudouris, K.S. Groundwater vulnerability and pollution risk assessment of porous aquifers to nitrate: Modifying the DRASTIC method using quantitative parameters. *J. Hydrol.* **2015**, *525*, 13–25, doi:10.1016/j.jhydrol.2015.03.035.
2. Kadkhodaie, F.; Moghaddam, A.A.; Barzegar, R.; Gharekhani, M.; Kadkhodaie, A. Optimizing the DRASTIC vulnerability approach to overcome the subjectivity: A case study from Shabestar plain, Iran. *Arab. J. Geosci.* **2019**, *12*, 527, doi:10.1007/s12517-019-4647-y.
3. Al-Hanbali, A.; Kondoh, A. Groundwater vulnerability assessment and evaluation of human activity impact (HAI) within the Dead Sea groundwater basin, Jordan. *Hydrogeol. J.* **2008**, *16*, 499–510, doi:10.1007/s10040-008-0280-7.
4. Javadi, S.; Kavehkar, N.; Mousavizadeh, M.H.; Mohammadi, K. Modification of DRASTIC model to map groundwater vulnerability to pollution using nitrate measurements in agricultural areas. *J. Agr. Sci. Tech.* **2011**, *13*, 239–249.
5. Neshat, A.; Pradhan, B.; Dadras, M. Groundwater vulnerability assessment using an improved DRASTIC method in GIS. *Resour. Conserv. Recycl.* **2014**, *86*, 74–86, doi:10.1016/j.resconrec.2014.02.008.
6. Foster, S.S.D. Fundamental concepts in aquifer vulnerability, pollution risk and protection strategy. *Hydrol. Resour. Proc. Inf.* **1987**, *38*, 69–86.
7. Sonnenborg, T.O.; Scharling, P.B.; Hinsby, K.; Rasmussen, E.S.; Engesgaard, P. Aquifer Vulnerability Assessment Based on Sequence Stratigraphic and 39 Ar Transport Modeling. *Ground Water* **2015**, *54*, 214–230, doi:10.1111/gwat.12345.
8. Seifert, D.; Sonnenborg, T.O.; Scharling, P.; Hinsby, K. Use of alternative conceptual models to assess the impact of a buried valley on groundwater vulnerability. *Hydrogeol. J.* **2007**, *16*, 659–674, doi:10.1007/s10040-007-0252-3.
9. Aller, L.; Bennett, T.; Lehr, J.H.; Petty, R.J.; Hackett, G. *DRASTIC: A Standardized System for Evaluating Groundwater Potential Using Hydrogeologic Settings*;

EPA/600/2-85/018; U.S.; Environmental Protection Agency: Washington, DC, USA, 1987.
10. Vías, J.M.; Andreo, B.; Perles, M.J.; Carrasco, F.; Vadillo, I.; Jiménez, P. Proposed method for groundwater vulnerability mapping in carbonate (karstic) aquifers: The COP method. *Hydrogeol. J.* **2006**, *14*, 912–925, doi:10.1007/s10040-006-0023-6.
11. Moratalla, A.; Gómez-Alday, J.; Sanz, D.; Castaño, S.; Heras, J.D.L. Evaluation of a GIS-Based Integrated Vulnerability Risk Assessment for the Mancha Oriental System (SE Spain). *Water Resour. Manag.* **2011**, *25*, 3677–3697, doi:10.1007/s11269-011-9876-0.
12. Jiménez-Madrid, A.; Carrasco, F.; Martínez, C.; Gogu, R.C. DRISTPI, a new groundwater vulnerability mapping method for use in karstic and non-karstic aquifers. *Q. J. Eng. Geol. Hydrogeol.* **2013**, *46*, 245–255, doi:10.1144/qjegh2012-038.
13. Barbulescu, A. Assessing Groundwater Vulnerability: DRASTIC and DRASTIC-Like Methods: A Review. *Water* **2020**, *12*, 1356, doi:10.3390/w12051356.
14. Vallejos, A.; Andreu, J.M.; Sola, F.; Pulido-Bosch, A. The anthropogenic impact on Mediterranean karst aquifers: Cases of some Spanish aquifers. *Environ. Earth Sci.* **2015**, *74*, 185–198, doi:10.1007/s12665-014-3994-y.
15. Goldscheider, N.; Chen, Z.; Auler, A.S.; Bakalowicz, M.; Broda, S.; Drew, D.; Hartmann, J.; Jiang, G.; Moosdorf, N.; Stevanovic, Z.; et al. Global distribution of carbonate rocks and karst water resources. *Hydrogeol. J.* **2020**, *28*, 1661–1677, doi:10.1007/s10040-020-02139-5.
16. Ravbar, N.; Goldscheider, N. Comparative application of four methods of groundwater vulnerability mapping in a Slovene karst catchment. *Hydrogeol. J.* **2008**, *17*, 725–733, doi:10.1007/s10040-008-0368-0.
17. Plan, L.; Decker, K.; Faber, R.; Wagreich, M.; Grasemann, B. Karst morphology and groundwater vulnerability of high alpine karst plateaus. *Environ. Earth Sci.* **2008**, *58*, 285–297, doi:10.1007/s00254-008-1605-5.
18. Polemio, M.; Casarano, D.; Limoni, P.P. Karstic aquifer vulnerability assessment methods and results at a test site (Apulia, southern Italy). *Nat. Hazards Earth Syst. Sci.* **2009**, *9*, 1461–1470, doi:10.5194/nhess-9-1461-2009.
19. Jiménez-Madrid, A.; Martínez-Navarrete, C.; Carrasco-Cantos, F. Groundwater Risk Intensity Assessment. Application to Carbonate Aquifers of the Western Mediterranean (Southern Spain). *Geodin. Acta* **2010**, *23*, 101–111, doi:10.3166/ga.23.101-111.
20. Marín, A.I.; Dörfliger, N.; Andreo, B. Comparative application of two methods (COP and PaPRIKa) for groundwater vulnerability mapping in Mediterranean karst aquifers (France and Spain). *Environ. Earth Sci.* **2011**, *65*, 2407–2421, doi:10.1007/s12665-011-1056-2.
21. Bagherzadeh, S.; Kalantari, N.; Nobandegani, A.F.; Derakhshan, Z.; Conti, G.O.; Ferrante, M.; Malekahmadi, R. Groundwater vulnerability assessment in karstic aquifers using COP method. *Environ. Sci. Pollut. Res.* **2018**, *25*, 18960–18979, doi:10.1007/s11356-018-1911-8.
22. Velázquez, D.P.; Sahuquillo, A.; Andreu, J. A two-step explicit solution of the Boussinesq equation for efficient simulation of unconfined aquifers in conjunctive-use models. *Water Resour. Res.* **2006**, *42*, 4205423, doi:10.1029/2005wr004473.
23. Pulido-Velazquez, D.; Sahuquillo, A.; Andreu, J.; Pulido-Velazquez, M. A general methodology to simulate groundwater flow of unconfined aquifers with a reduced computational cost. *J. Hydrol.* **2007**, *338*, 42–56, doi:10.1016/j.jhydrol.2007.02.009.
24. Llopis-Albert, C.; Pulido-Velazquez, D. Using MODFLOW code to approach transient hydraulic head with a sharp-interface solution. *Hydrol. Process.* **2014**, *29*, 2052–2064, doi:10.1002/hyp.10354.
25. Pulido-Velazquez, D.; Sahuquillo, A.; Andreu, J.; Pulido-Velazquez, M. An efficient conceptual model to simulate surface water body-aquifer interaction in conjunctive use management models. *Water Resour. Res.* **2007**, *43*, 07407, doi:10.1029/2006wr005064.
26. Velázquez, D.P.; Sahuquillo, A.; Andreu, J. Treatment on non-linear boundary conditions in groundwater modeling with Eigenvalue Methods. *J. Hydrol.* **2009**, *368*, 194–204, doi:10.1016/j.jhydrol.2009.02.002.

27. Panagopoulos, G.P.; Antonakos, A.K.; Lambrakis, N.J. Optimization of the DRASTIC method for groundwater vulnerability assessment via the use of simple statistical methods and GIS. *Hydrogeol. J.* **2006**, *14*, 894–911, doi:10.1007/s10040-005-0008-x.
28. Rózkowski, J. Evaluation of intrinsic vulnerability of an Upper Jurassic karst-fissured aquifer in the Jura Krakowska (southern Poland) to anthropogenic pollution using the DRASTIC method. *Geol. Q.* **2007**, *51*, 17–26.
29. Mimi, Z.A.; Mahmoud, N.; Abu Madi, M. Modified DRASTIC assessment for intrinsic vulnerability mapping of karst aquifers: A case study. *Environ. Earth Sci.* **2011**, *66*, 447–456, doi:10.1007/s12665-011-1252-0.
30. Pacheco, F.; Pires, L.; Santos, R.; Fernandes, L.S. Factor weighting in DRASTIC modeling. *Sci. Total. Environ.* **2015**, *505*, 474–486, doi:10.1016/j.scitotenv.2014.09.092.
31. Baalousha, H.M. Vulnerability assessment for the Gaza Strip, Palestine using DRASTIC. *Environ. Earth Sci.* **2006**, *50*, 405–414, doi:10.1007/s00254-006-0219-z.
32. Hamza, S.M.; Ahsan, A.; Imteaz, M.A.; Rahman, A.; Mohammad, T.A.; Ghazali, A.H. Accomplishment and subjectivity of GIS-based DRASTIC groundwater vulnerability assessment method: A review. *Environ. Earth Sci.* **2014**, *73*, 3063–3076, doi:10.1007/s12665-014-3601-2.
33. Saidi, S.; Bouri, S.; Ben Dhia, H. Groundwater vulnerability and risk mapping of the Hajeb-jelma aquifer (Central Tunisia) using a GIS-based DRASTIC model. *Environ. Earth Sci.* **2009**, *59*, 1579–1588, doi:10.1007/s12665-009-0143-0.
34. Antonakos, A.; Lambrakis, N. Development and testing of three hybrid methods for the assessment of aquifer vulnerability to nitrates, based on the drastic model, an example from NE Korinthia, Greece. *J. Hydrol.* **2007**, *333*, 288–304, doi:10.1016/j.jhydrol.2006.08.014.
35. Huan, H.; Wang, J.; Teng, Y. Assessment and validation of groundwater vulnerability to nitrate based on a modified DRASTIC model: A case study in Jilin City of northeast China. *Sci. Total. Environ.* **2012**, *440*, 14–23, doi:10.1016/j.scitotenv.2012.08.037.
36. Thirumalaivasan, D.; Karmegam, M.; Venugopal, K. AHP-DRASTIC: Software for specific aquifer vulnerability assessment using DRASTIC model and GIS. *Environ. Model. Softw.* **2003**, *18*, 645–656, doi:10.1016/s1364-8152(03)00051-3.
37. Hailin, Y.; Ligang, X.; Chang, Y.; Jiaxing, X. Evaluation of Groundwater Vulnerability with Improved DRASTIC Method. *Procedia Environ. Sci.* **2011**, *10*, 2690–2695, doi:10.1016/j.proenv.2011.09.418.
38. Sener, E.; Davraz, A. Assessment of groundwater vulnerability based on a modified DRASTIC model, GIS and an analytic hierarchy process (AHP) method: The case of Egirdir Lake basin (Isparta, Turkey). *Hydrogeol. J.* **2012**, *21*, 701–714, doi:10.1007/s10040-012-0947-y.
39. Fijani, E.; Nadiri, A.A.; Asghari-Moghaddam, A.; Tsai, F.T.-C.; Dixon, B. Optimization of DRASTIC method by supervised committee machine artificial intelligence to assess groundwater vulnerability for Maragheh–Bonab plain aquifer, Iran. *J. Hydrol.* **2013**, *503*, 89–100, doi:10.1016/j.jhydrol.2013.08.038.
40. Barzegar, R.; Moghaddam, A.A.; Baghban, H. A supervised committee machine artificial intelligent for improving DRASTIC method to assess groundwater contamination risk: A case study from Tabriz plain aquifer, Iran. *Stoch. Environ. Res. Risk Assess.* **2015**, *30*, 883–899, doi:10.1007/s00477-015-1088-3.
41. Jang, W.S.; Engel, B.A.; Harbor, J.; Theller, L. Aquifer Vulnerability Assessment for Sustainable Groundwater Management Using DRASTIC. *Water* **2017**, *9*, 792, doi:10.3390/w9100792.
42. Nadiri, A.A.; Gharekhani, M.; Khatibi, R. Mapping Aquifer Vulnerability Indices Using Artificial Intelligence-running Multiple Frameworks (AIMF) with Supervised and Unsupervised Learning. *Water Resour. Manag.* **2018**, *32*, 3023–3040, doi:10.1007/s11269-018-1971-z.
43. Dixon, B. Groundwater vulnerability mapping: A GIS and fuzzy rule based integrated tool. *Appl. Geogr.* **2005**, *25*, 327–347, doi:10.1016/j.apgeog.2005.07.002.

44. Rodriguez-Galiano, V.F.; Luque-Espinar, J.; Chica-Olmo, M.; Mendes, M. Feature selection approaches for predictive modelling of groundwater nitrate pollution: An evaluation of filters, embedded and wrapper methods. *Sci. Total. Environ.* **2018**, *624*, 661–672, doi:10.1016/j.scitotenv.2017.12.152.
45. Machiwal, D.; Jha, M.K.; Singh, V.P.; Mohan, C. Assessment and mapping of groundwater vulnerability to pollution: Current status and challenges. *Earth Sci. Rev.* **2018**, *185*, 901–927, doi:10.1016/j.earscirev.2018.08.009.
46. Fusco, F.; Allocca, V.; Coda, S.; Cusano, D.; Tufano, R.; De Vita, P. Quantitative Assessment of Specific Vulnerability to Nitrate Pollution of Shallow Alluvial Aquifers by Process-Based and Empirical Approaches. *Water* **2020**, *12*, 269, doi:10.3390/w12010269.
47. Gogu, R.C.; Hallet, V.; Dassargues, A. Comparison of aquifer vulnerability assessment techniques. Application to the Nylon river basin (Belgium). *Environ. Earth Sci.* **2003**, *44*, 881–892, doi:10.1007/s00254-003-0842-x.
48. Worrall, F.; Besien, T.; Kolpin, D.W. Groundwater vulnerability: Interactions of chemical and site properties. *Sci. Total. Environ.* **2002**, *299*, 131–143, doi:10.1016/s0048-9697(02)00270-x.
49. Zwahlen, F. *COST Action 620 Vulnerability and Risk Mapping for the Protection of Carbonate (karst) Aquifers Final Report*; Office of the Official Publications of the European Communities: Brussels, Belgium, 2004; p. 297.
50. Rodriguez-Galiano, V.; Mendes, M.P.; Garcia-Soldado, M.J.; Chica-Olmo, M.; Ribeiro, L.F. Predictive modeling of groundwater nitrate pollution using Random Forest and multisource variables related to intrinsic and specific vulnerability: A case study in an agricultural setting (Southern Spain). *Sci. Total. Environ.* **2014**, 189–206, doi:10.1016/j.scitotenv.2014.01.001.
51. Yoo, K.; Shukla, S.K.; Ahn, J.J.; Oh, K.; Park, J. Decision tree-based data mining and rule induction for identifying hydrogeological parameters that influence groundwater pollution sensitivity. *J. Clean. Prod.* **2016**, *122*, 277–286, doi:10.1016/j.jclepro.2016.01.075.
52. Martínez-Santos, P.; Llamas, M.; Martinezalfaro, P. Vulnerability assessment of groundwater resources: A modelling-based approach to the Mancha Occidental aquifer, Spain. *Environ. Model. Softw.* **2008**, *23*, 1145–1162, doi:10.1016/j.envsoft.2007.12.003.
53. Yustres, Á.; Botti, V.; Asensio, L.; Candel-Pérez, M.; García, B. Groundwater resources in the Upper Guadiana Basin (Spain): A regional modelling analysis. *Hydrogeol. J.* **2013**, *21*, 1129–1146, doi:10.1007/s10040-013-0987-y.
54. Conan, C.; De Marsily, G.; Bouraoui, F.; Bidoglio, G. A long-term hydrological modelling of the Upper Guadiana river basin (Spain). *Phys. Chem. Earth Parts A/B/C* **2003**, *28*, 193–200, doi:10.1016/s1474-7065(03)00025-1.
55. FAO, U.; The FAO-Unesco Soil Map of the World; Legend and 9 volumes, UNESCO: Paris, France, 1981.
56. Confederación Hidrográfica del Guadiana. Actualización y calibración del modelo de flujo de agua subterránea de los acuíferos del Alto Guadiana (FLUSAG). Ref: TEC0004594, 2018, Published report, Dirección General del Agua, Madrid, Spain, 150p.
57. Ahmed, I.; Nazzal, Y.; Zaidi, F. Groundwater pollution risk mapping using modified DRASTIC model in parts of Hail region of Saudi Arabia. *Environ. Eng. Res.* **2017**, *23*, 84–91, doi:10.4491/eer.2017.072.
58. Babiker, I.S.; Mohamed, M.A.; Hiyama, T.; Kato, K. A GIS-based DRASTIC model for assessing aquifer vulnerability in Kakamigahara Heights, Gifu Prefecture, central Japan. *Sci. Total. Environ.* **2005**, *345*, 127–140, doi:10.1016/j.scitotenv.2004.11.005.
59. Stigter, T.Y.; Riberio, L.; Dill, A.M.M.C. Evaluation of an intrinsic and a specific vulnerability assessment method in comparison with groundwater salinization and nitrate contamination levels in two agricultural regions in the south of Portugal. *Hydrogeol. J.* **2006**, *14*, 79–99.

60. McLay, C.; Dragten, R.; Sparling, G.; Selvarajah, N. Predicting groundwater nitrate concentrations in a region of mixed agricultural land use: A comparison of three approaches. *Environ. Pollut.* **2001**, *115*, 191–204, doi:10.1016/s0269-7491(01)00111-7.
61. Mentzafou, A.; Panagopoulos, Y.; Dimitriou, E. Designing the National Network for Automatic Monitoring of Water Quality Parameters in Greece. *Water* **2019**, *11*, 1310, doi:10.3390/w11061310.
62. Kass, G.V. An Exploratory Technique for Investigating Large Quantities of Categorical Data. *J. R. Stat. Soc. Ser. C Appl. Stat.* **1980**, *29*, 119, doi:10.2307/2986296.
63. Rokach, L.; Maimon, O. *Data Mining with Decision Trees Theory and Applications*; World Scientific: Toh Tuck Link, Singapore, 2007.
64. Sokolova, M.; Lapalme, G. A systematic analysis of performance measures for classification tasks. *Inf. Process. Manag.* **2009**, *45*, 427–437, doi:10.1016/j.ipm.2009.03.002.
65. Jeihouni, M.; Toomanian, A.; Mansourian, A. Decision Tree-Based Data Mining and Rule Induction for Identifying High Quality Groundwater Zones to Water Supply Management: A Novel Hybrid Use of Data Mining and GIS. *Water Resour. Manag.* **2019**, *34*, 139–154, doi:10.1007/s11269-019-02447-w.
66. Quinlan, J. Simplifying decision trees. *Int. J. Man-Mach. Stud.* **1987**, *27*, 221–234, doi:10.1016/s0020-7373(87)80053-6.
67. Wheeler, D.C.; Nolan, B.T.; Flory, A.R.; Dellavalle, C.T.; Ward, M.H. Modeling groundwater nitrate concentrations in private wells in Iowa. *Sci. Total. Environ.* **2015**, *536*, 481–488, doi:10.1016/j.scitotenv.2015.07.080.
68. Bui, D.T.; Khosravi, K.; Karimi, M.; Busico, G.; Khozani, Z.S.; Nguyen, H.; Mastrocicco, M.; Tedesco, D.; Cuoco, E.; Kazakis, N. Enhancing nitrate and strontium concentration prediction in groundwater by using new data mining algorithm. *Sci. Total. Environ.* **2020**, *715*, 136836, doi:10.1016/j.scitotenv.2020.136836.
69. Almasri, M.N. Assessment of intrinsic vulnerability to contamination for Gaza coastal aquifer, Palestine. *J. Environ. Manag.* **2008**, *88*, 577–593, doi:10.1016/j.jenvman.2007.01.022.
70. Hasiniaina, F.; Zhou, J.; Guoyi, L. Regional assessment of groundwater vulnerability in Tamtsag basin, Mongolia using drastic model. *J. Am. Sci.* **2010**, *6*, 65–78.
71. Al Hallaq, A.H.; Abuelaish, B. Assessment of aquifer vulnerability to contamination in Khanyounis Governorate, Gaza Strip—Palestine, using the DRASTIC model within GIS environment. *Arab. J. Geosci.* **2011**, *5*, 833–847, doi:10.1007/s12517-011-0284-9.
72. Dizaji, A.R.; Hosseini, S.A.; Rezaverdinejad, V.; Sharafati, A. Groundwater contamination vulnerability assessment using DRASTIC method, GSA, and uncertainty analysis. *Arab. J. Geosci.* **2020**, *13*, 1–15, doi:10.1007/s12517-020-05650-x.
73. Herrera, S.; Fernández, J.; Gutiérrez, J.M. Update of the Spain02 gridded observational dataset for EURO-CORDEX evaluation: Assessing the effect of the interpolation methodology. *Int. J. Clim.* **2015**, *36*, 900–908, doi:10.1002/joc.4391.

Capítulo 6: A preliminary lumped assessment of pollution risk at aquifer scale by using the mean residence time. Analyses of potential climate change impacts

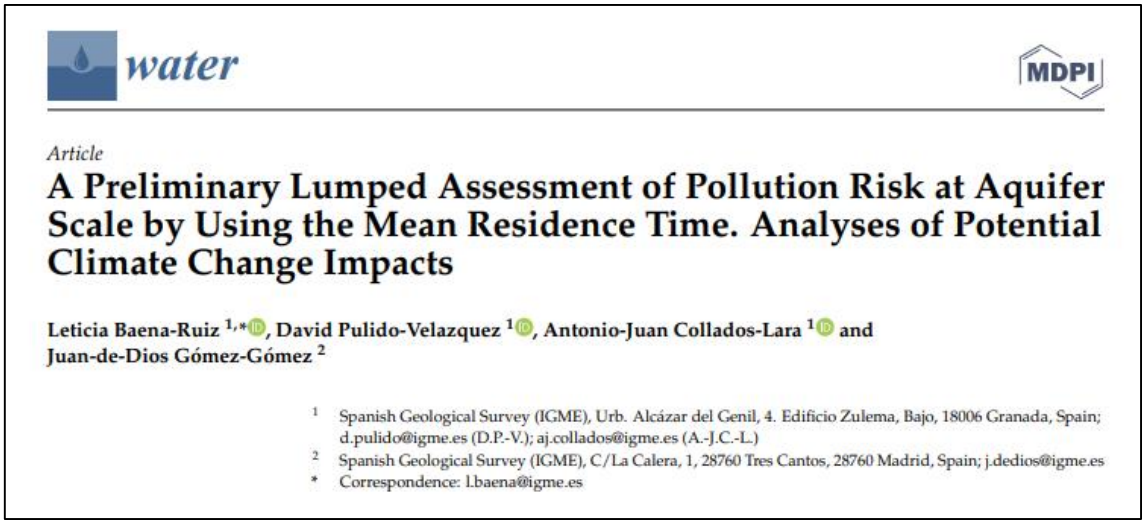

water

MDPI

Article

A Preliminary Lumped Assessment of Pollution Risk at Aquifer Scale by Using the Mean Residence Time. Analyses of Potential Climate Change Impacts

Leticia Baena-Ruiz [1,*], David Pulido-Velazquez [1], Antonio-Juan Collados-Lara [1] and Juan-de-Dios Gómez-Gómez [2]

[1] Spanish Geological Survey (IGME), Urb. Alcázar del Genil, 4. Edificio Zulema, Bajo, 18006 Granada, Spain; d.pulido@igme.es (D.P.-V.); aj.collados@igme.es (A.-J.C.-L.)
[2] Spanish Geological Survey (IGME), C/La Calera, 1, 28760 Tres Cantos, 28760 Madrid, Spain; j.dedios@igme.es
* Correspondence: l.baena@igme.es

Reference: Baena-Ruiz, L.; Pulido-Velazquez, D.; Collados-Lara, A.-J.; Gómez-Gómez, J.-d.-D. A Preliminary Lumped Assessment of Pollution Risk at Aquifer Scale by Using the Mean Residence Time. Analyses of Potential Climate Change Impacts. Water 2021, 13, 943. https://doi.org/10.3390/w13070943

Authors and affiliation:

Leticia Baena-Ruiz [1,*], David Pulido-Velazquez [1], Antonio-Juan Collados-Lara [1] and Juan de Dios Gómez-Gómez [2]

[1]Spanish Geological Survey (IGME), Urb. Alcázar del Genil, 4. Edificio Zulema, bajo, 18006 Granada, Spain; d.pulido@igme.es (D.P.-V.); aj.collados@igme.es (A.-J.C.-L.)

[2]Spanish Geological Survey (IGME), C/La Calera, 1, 28760 Tres Cantos, Madrid, Spain; j.dedios@igme.es

*Correspondence: l.baena@igme.es

Abstract

An assessment of the risk for groundwater pollution and vulnerability to pumping can help identify strategic groundwater bodies to define sustainable management measures of groundwater resources. In this paper, we propose a new method to make a preliminary estimation of the risk for groundwater pollution at the aquifer scale through the lumped turnover time index (T index). A new lumped index (L-RISK index) was defined to assess the significance of the risk for pollution at the aquifer scale. Both L-RISK and T indices were employed to calibrate a linear regression model that showed a good inverse correlation in the eight aquifers of the Upper Guadiana Basin (Spain). This novel method can be applied to analyze a wide range of aquifers with limited information in order to identify potential strategic aquifers. It also allows one to make a preliminary assessment of the impacts of climate change on L-RISK. The results showed a high variability of the T index in the eight aquifers (8–76 years). Three of them had significant greater mean T values, which could be considered to be the main strategic groundwater resources. In the future, the T index will increase between 8 and 44%, and the L-RISK will decrease in all aquifers (1–18%).

Keywords: groundwater pollution risk; residence time; vulnerability; droughts management; climate change impacts; adaptation strategies

1. Introduction

Groundwater is a valuable renewable resource that plays an important role in providing water supplies across the world, especially in semiarid areas where rivers are usually ephemeral. The interactions between anthropogenic activity, the hydrosphere, and climate affect groundwater resources and produce environmental impacts on human health, groundwater quality, and groundwater quantity depletion. This degradation produces negative effects—not only in exploitation for different uses (human consumption, irrigation, etc.) but also in groundwater-dependent ecosystems [1–3]. Therefore, the protection of groundwater resources is a priority issue to be considered to achieve the sustainable management and maintenance of the good status of water bodies according to the Water Framework Directive (WFD) [4].

The degree of protection of groundwater from contaminants mainly depends on intrinsic vulnerability and pollution risk due to anthropogenic activity. For many years, several approaches have been developed to assess intrinsic groundwater vulnerability [5–8]. Process-based methods [9] analyze pollutant movement in groundwater by using transport modelling. Statistical methods try to find a correlation between the influencing factors and contaminants [10]. Overlay and index methods [6,7] are based on the rating of hydrogeological factors that influence groundwater vulnerability. Index approaches are the most widely used through methods such as DRASTIC (D: Depth to water; R: Net recharge; A: Aquifer media; S: Soil media; T: Topography; I: Impact of vadose zone; C: Hydraulic conductivity) [6] due to its simple implementation [8]. All these methods provide distributed results that can be displayed on maps where different vulnerability levels are represented. Groundwater vulnerability can also be summarized at the aquifer scale through global indices that allow for lumped results between different aquifers to be compared [11–13]. In order to perform a risk assessment, we need to combine hazard and pollution vulnerability maps, with the hazard being defined as the potential source of contamination derived from the human activity at the land surface [14]. Pollution risk is usually assessed by considering different land uses as potential sources of contamination, as proposed in COST (European Cooperation in Science and Technology) action 620 [14], although pollution risk assessment can also be focused on the risk from only one source of contamination, e.g., landfills [15,16]. For that purpose, some contamination indices have been developed and widely applied [15,17,18] to assess the impact of a pollution source in groundwater, but they are usually applied at specific sites because they require a detailed hydrochemical analysis.

In addition to the groundwater quality issues, the protection of groundwater resources should also take the quantitative status of the aquifer into account. Therefore, in general, the term groundwater vulnerability can be applied to both intrinsic vulnerability to pollution and renewable resources (or vulnerability to pumping) [19,20]. An estimation of renewability is essential for the sustainable exploitation of groundwater resources and it can be approached through mean residence time or the mean age of the water leaving a system [2,20]. The understanding of the timescales of groundwater resources helps to identify problems related to the qualitative and quantitative status, as well as to groundwater-dependent ecosystems [21].

Some authors have linked the concept of vulnerability to pollution and/or to pumping with the mean residence time [22–24] for different purposes. It has been employed to define groundwater source vulnerability and delineate protection zones in karstic aquifers [25,26]. Residence time has also been employed to validate distributed groundwater vulnerability maps in any type of aquifer by using different approaches, concluding that high vulnerability values are related to short residence times [27–29].

Different approaches have been used to estimate residence time (also called renewal time, groundwater age, or travel time through the saturated zone). Some authors have used contaminant

transport models [30,31] or environmental and artificial tracers [32,33]. Age dating is a valuable way to analyze changes in groundwater systems [34] and a quantitative measure of the renewable capacity of groundwater [35]. It is also an important indicator of groundwater susceptibility to anthropogenic contamination [36]. Residence time is usually assessed in a distributed way [37,38], but it can also be estimated in a lumped way by applying simple index approximations, such as the turnover time index (T index), which expresses the ratio between storage (S), and recharge (R) [20,39]. It is related to the resilience of groundwater bodies to temporal pumping increases.

Aquifers with a short residence time are more vulnerable to exploitation [20,40], which will be exacerbated in the future due to climate change. Climate change will not only affect the quantity of water resources but also their quality, especially in agricultural areas. Impacts of climate change on groundwater resources has been addressed in several studies, especially in semi-arid areas [34,41]. They conclude that climate change will involve a decline of groundwater levels due to a decrease of the recharge and an increase in water requirements to supply agricultural and urban demand. Groundwater vulnerability has also been analyzed under climate change scenarios. Some studies revealed that the vulnerability is not very sensitive to climate change [12,42] because many factors considered in the index-based assessment are static. However, other authors [43] found different patterns of groundwater vulnerability to contamination between drought, average, and wet periods. Groundwater vulnerability has also been proven to significantly shift under future land use change scenarios [44,45], although these changes vary from site to site [46].

Distributed approximations of residence time have been employed to assess and validate intrinsic groundwater vulnerability in several studies [22,23,37]. These distributed approaches, more precise and detailed than lumped approaches, demand higher computational efforts and need data that are not always available, which makes it impossible to use a single method to validate the vulnerability maps from different case studies [13,14]. This drawback usually makes the results of different sites scarcely comparable. However, lumped approaches provide preliminary evaluations that can be usually applied to large areas with limited information [47], thus allowing one to compare the status of many different groundwater bodies.

In this paper, we propose a new method to make a preliminary estimation and/or validation of the risk for groundwater pollution at the aquifer scale through a lumped index based on the mean residence time concept. A regression model was defined to assess the risk for pollution from the lumped mean residence time and to estimate potential impacts of climate change scenarios on pollution risk. The proposed methodology was applied to the Upper Guadiana Basin (Spain), which is composed of different aquifer typologies. The obtained results will be useful to identify potential strategic aquifers, where more exhaustive analyses should be performed to define conjunctive use measures for the sustainable management of water resources systems, especially during critical droughts.

The spatial distribution of groundwater residence time and groundwater vulnerability to contamination has been related in previous works [22,23]. Nevertheless, as far as we know, none of them assessed groundwater pollution risk from the mean residence time approximation, and none of them studied the potential impacts of climate change. The novel lumped approach proposed in this paper can be applied to extensive areas with limited information. In the literature, we found examples of lumped vulnerability indices (e.g., [11,13]), but none of these studies were about groundwater pollution risk. The use of this lumped approach, based on mean residence time and considering not only the resilience to periods of intensive pumping [20] but also the pollution risk, is also novel.

2. Materials and Methods

2.1. Methodology

The proposed methodology intended to demonstrate the utility of the lumped mean residence time as a preliminary approach to validate groundwater pollution risk at the aquifer scale.

The inputs to obtain the lumped indices included variables (physical and hydraulic properties) and parameters (overlying layers and hydrogeological characteristics) of the aquifer media that could come from direct observation (field measurements) or other techniques (geological and flow models). Climatic and socio-economic variables also impact (directly or indirectly) risk of groundwater pollution and mean residence time, and they should be considered in a risk of pollution assessment.

Figure 6.1 depicts the flowchart of the methodology including the modelling framework to assess the future impacts of climate change on risk assessment.

The analysis of future impacts required the generation of local climate scenarios and their propagation through previously calibrated recharge and groundwater flow models.

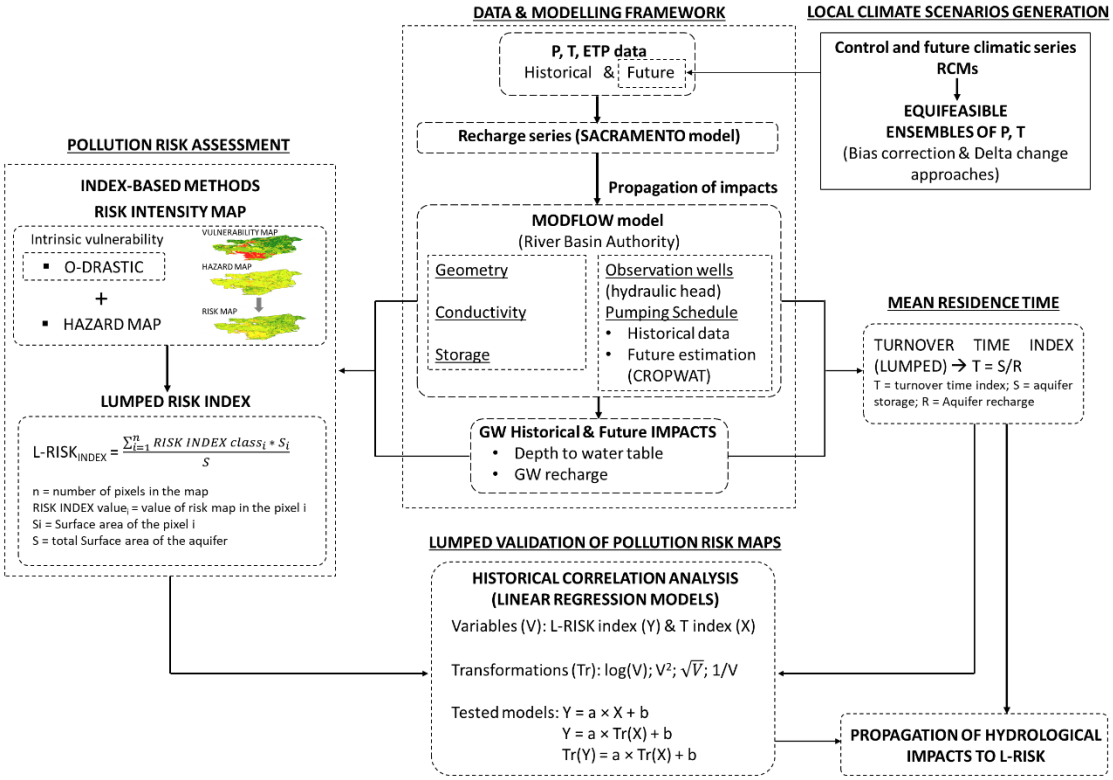

Figure 6.1. Flowchart of the methodology. L-RISK: lumped risk index; O-DRASTIC: Groundwater vulnerability assessment method based on DRASTIC method; CROPWAT: Computer program for irrigation planning and management.

2.1.1. Pollution Risk Assessment

Risk of groundwater contamination is defined as the probability that groundwater will become contaminated due to the anthropogenic activity in the overlying land surface [14,48]. A risk assessment considers the interaction between the contaminant load coming from the land use (hazard) and the groundwater vulnerability to pollution.

A hazard map can be obtained from a land use map at adequate detail in order to determine the contaminant load from different activities. Land uses change over time, especially in agricultural areas through crop rotation, as well as pollutants leaching from each type of crop. Pollutant

loading from crops is highly variable, depending on irrigation system and efficiency, soil characteristics (which also vary regarding the type of crop), crop management system, fertilizer management, climatic conditions, etc. [49,50]. The complex relationship between these variables requires a multi-disciplinary approach [51], and a real detailed approximation by crop patterns is not always feasible. Instead, a more general land use classification can be used to define different rates that approach the probability of contamination that reaches groundwater.

Groundwater vulnerability depends on the intrinsic hydrogeological characteristics that make an aquifer susceptible to contamination, such as aquifer media, hydraulic conductivity, and the type of soil above the aquifer. Groundwater vulnerability can be assessed by using index-based methods such as DRASTIC or other approaches that allow one to display different vulnerability classes in a map. A vulnerability map should be validated by expert criteria or by contrasting it with contaminant concentrations or other techniques.

Hazard and vulnerability maps are combined to define a risk map, considering that the highest risk will exist when the most dangerous hazard is located over the highest vulnerability zones [52,53].

The combination of hazard and vulnerability provides a risk class that must be previously defined, e.g., following a matrix concept [14].

The lumped risk index (L-RISK index) assesses the significance of each risk class at the aquifer scale by a weighted average. The L-RISK index is defined as:

$$\text{L-RISKINDEX} = \frac{\sum_{i=1}^{n} RISK\ INDEX\ class_i * S_i}{S}, \quad (1)$$

where n is the number of pixels (or zones with a unique value of risk) in the map, $RISK\ INDEX\ class_i$ is the value of risk class in the pixel or zone i, Si is the surface area in the pixel or zone i (m^2), and S is the total surface area of the aquifer (m^2).

The lumped index evaluates the overall pollution risk of an aquifer. It allows for the results of different aquifers to be compared in order to establish appropriate management measures regarding land use, type of crops, fertilization, and irrigation techniques.

2.1.2. Mean Residence Time

The mean residence time is an indicator of the susceptibility of the groundwater resource to pollution. It provides an approximation of the time that a contaminant event needs to reach a zone within the aquifer. The mean residence time can be approached by using tracers or particle tracking in flow models in order to obtain distributed results, but it can also be estimated as a T index [20] for a whole aquifer.

In this paper, we used the T index, defined as the ratio between the mean volume of a resource stored in an aquifer and the mean aquifer recharge in the studied period:

$$T = \frac{V}{R} \quad (2)$$

where T is the turnover time index (years), V is the volume of the groundwater resource (Mm^3), and R is the groundwater recharge (Mm^3/year).

The volume of a groundwater resource can be calculated from geological or flow models that provide accurate results, but it can also be obtained from existing data from river basin authorities. The aquifer recharge can be calculated by applying different approaches, from simple balance calculations to complex deterministic models previously calibrated in the studied area. Both of these variables (groundwater resource volume and recharge) can be considered as the mean values

in a large historical period or the mean values in a more recent period (e.g., a river basin management plan).

2.1.3. Lumped Validation of Pollution Risk Maps

Based on the assumption that a higher groundwater vulnerability is related to a shorter residence time, we attempted to establish a correlation between the T index and the L-RISK index at the aquifer scale.

A simple linear regression model was defined in order to approximate the L-RISK as a function of the mean residence time, calculated as the T index, in the studied aquifers. Different transformations of the analyzed variables (y = L-RISK and x = T) were performed (Table 6.1) in order to determine the model that provided the better correlation.

Table 6.1. Tested regression models and transformation of variables (* means the combinations of the target and explanatory variables).

TR(y) = a × TR (x) + b		**TR (x)**				
		-	x^2	$\sqrt{x}$	Log (x)	1/x
TR(y)	-	*	*	*	*	*
	y^2	-	*	-	-	-
	$\sqrt{y}$	-	-	*	-	-
	Log(y)	-	-	-	*	-
	1/y	-	-	-	-	*

2.1.4. Propagation of Hydrological Impacts to L-RISK

A future assessment allows one to analyze the mean change of a groundwater system due to exploitation and climate change. Climate change will affect groundwater recharge, stored resource volume, and, therefore, the T index. Groundwater vulnerability and, therefore, risk of pollution will also experience changes due to variations of mean groundwater levels and recharge.

The climatic series of the future potential scenarios must be downscaled in order to propagate them through previously calibrated recharge and flow models. Those models are used to calculate the future T index, and the calibrated regression model is used to estimate the future L-RISK index.

2.2. Study Area, Data and Modelling Framework

2.2.1. Location, Hydrogeology and Historical Climatic Data

The case study was the Upper Guadiana Basin, located in the center of the Iberian Peninsula. It covers an extension of approximately 14,000 km^2. The topography was found to be predominantly flat in the central area and undulating in the north (Sierra de Altomira) and south (Campo de Montiel) boundaries.

In general, the drainage network was found to be poorly defined, although it showed strong natural interaction between groundwater and surface water [54]. The Guadiana River and several tributaries have risen to over one hundred wetlands that make up UNESCO's "Mancha Húmeda Biosphere Reserve." Most of them were found to be groundwater-dependent wetlands and are also in the Ramsar Convention list [54]. The Upper Guadiana Basin is composed of eight groundwater bodies, including detrital and carbonated aquifers. Figure 6.2 shows the main geological formations (a) and hydrogeological characteristics (b). The northern aquifers are heterogeneous, mainly composed of Cretaceous and Neogene formations, and they consist of clays, sand, marls, calco-dolomitic, and Paramo limestone materials [55] from medium to high permeability. The central zone is characterized by the presence of Neogene–Quaternary materials, alternating detrital and carbonated formations with medium, high and very high permeability. The

southern are is predominantly composed of fractured and highly permeable Jurassic calco-dolomitic materials that mainly consist of dolomite and oolitic limestones, as well as thick levels of marls [55,56]. The hydraulic conductivity in the Upper Guadiana Basin is highly variable. In the northern area, the conductivity is low (below 1.5×10^{-4} m/s although there is a small area with a conductivity higher than 10^{-3}). The central area has values between 1.5×10^{-4} and 10^{-3} m/s, and the conductivity in the southern area is mainly in the range from 3.5×10^{-4} to 5×10^{-4} m/s [19].

The climate of the study area can be considered continental and semiarid. Historical climate data from 1974–2015 were collected from Spain 02 project [57]. The mean annual precipitation from this dataset was found to be 433 mm/year, and the mean temperature was 14.6 °C. Summer months are characterized by high temperature and scarce rainfall, causing the mean potential evapotranspiration to be notably high; therefore, the recharge and runoff are low in most cases [54,55]. The mean annual recharge obtained from the calibration of Sacramento model in the period of 1974–2015 was 46.8 mm/year.

The main land use in the Upper Guadiana Basin is agriculture, which covers approximately the 80% of the total area (Figure 6.2c). The use of nitrogen fertilizers has led to high levels of nitrate in many groundwater areas. Moreover, the expansion of irrigated agriculture resulted in an intensive groundwater withdrawal (mainly in the central aquifers), that caused the depletion of the water table by more than 20 m in some areas between the mid-1970s and the first decade of the new century, which led to a degradation of important wetlands such as Las Tablas de Daimiel Natural Park. Since the WFD came into effect, there has been a growing awareness regarding the consequences of overexploitation, and more sustainable policies have been applied in the last few decades.

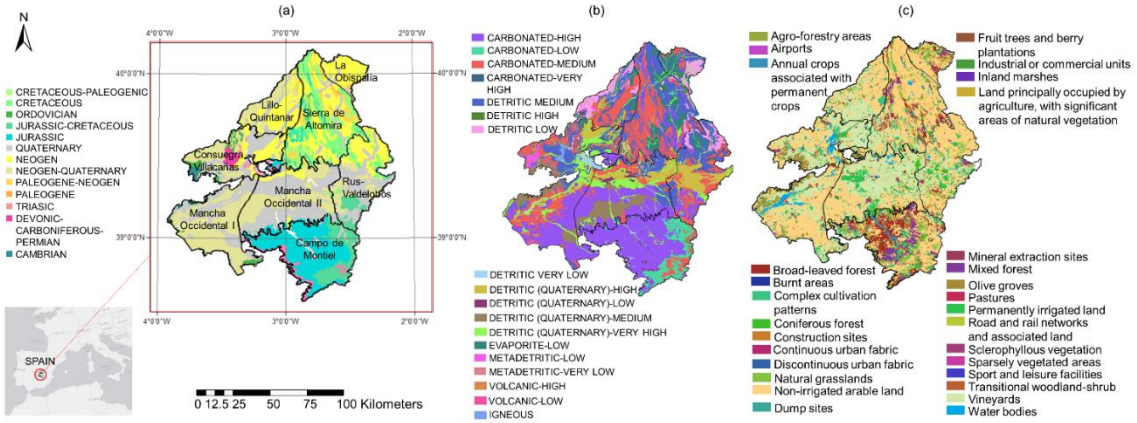

Figure 6.2. Case study: (a) geological map; (b) hydrogeological characteristics and permeability; (c) land use map.

2.2.2. Groundwater Flow (Modflow) Model

A numerical groundwater flow (Modflow) model from the river basin authority was used to obtain some necessary data to apply the proposed methodology. The model simulated the groundwater flow and river–aquifer relationship in the eight groundwater bodies in the Upper Guadiana Basin. It provided hydraulic head maps and the flow budget in the modelled groundwater bodies.

For input, the flow model required recharge series, which were obtained from a calibrated Sacramento Soil Moisture Accounting (SAC-SMA) model of the US National Weather Service River Forecast System in the study area.

The pumping schedule and distribution were defined from historical data in the period of 1974–2015.

2.2.3. Vulnerability Map

For the purpose of this paper, we employed a vulnerability map generated in a previous work [19]. That map was obtained from an optimization of the DRASTIC method in an attempt to harmonize the vulnerability assessments of different aquifer typologies. The new method, called O-DRASTIC (Optimum DRASTIC) (see Appendix A), maintains all the parameters from the original DRASTIC models while varying their weights and classification. Data to compute depth to water (D) and conductivity (C) were obtained from the Modflow model, and net recharge (R) data came from SAC-SMA model. Mean values of D and R in the historical period were considered to calculate O-DRASTIC. The other parameters came from official databases (A: hydrogeological map of Spain 1:200000; S: soil map of Spain 1:1000000; T: digital terrain model 100 × 100 m cell size; and I: lithostratigraphic map of Spain 1:200000). The O-DRASTIC vulnerability map (Figure 6.3a) was validated by using nitrate concentrations [19], and it provided better results than the original DRASTIC model in the study area.

2.2.4. Groundwater Resource Map

From the flow model simulation, we calculated the mean resource map of the upper aquifer for each groundwater body in the historical period (1974–2015). A combination of the geometry, hydraulic head, and storage coefficient provided a saturated resource for each cell within the aquifers (Figure 6.3b).

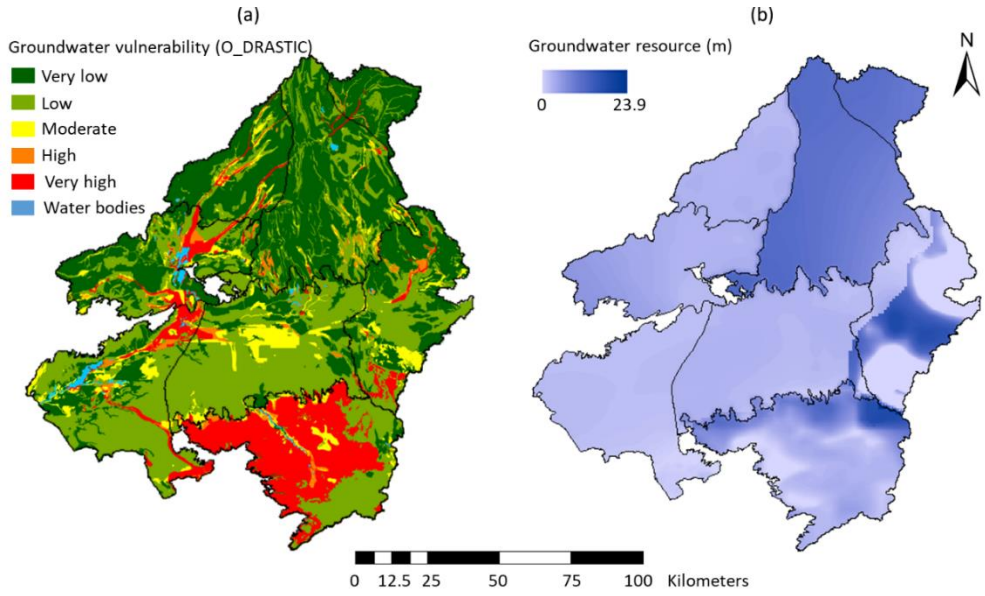

Figure 6.3. Groundwater vulnerability map (O-DRASTIC) and (b) mean historical groundwater resource (m).

2.2.5. Generation of Local Climate Scenarios

A statistical method was used to define local future climate change scenarios for the case study. It was based on the historical information (Spain02 dataset [57]; see Figure 6.4) for the adopted reference period (1976–2015) and nine regional climate model (RCM) simulations (CCLM4-8-17 and RCA4 nested to CNRM-CM5, EC-EARTH, and MPI-ESM-LR; HIRHAM5 and RACMO22E nested to EC-EARTH; and WRF331F nested to IPSL-CM5A-MR) available in the CORDEX project [58]. We used the most pessimistic emission scenario, RCP 8.5, and the future temporal horizon of 2016–2045. The future local scenarios were generated by applying the first and second moment correction techniques under the bias-correction approach. In this approach, a perturbation (transformation function) was applied to the control series of the RCM simulations to obtain another series with statistics (mean and standard deviation) more similar to the historical series. The same transformation function was applied to the future simulations of the RCM to

obtain the local climate change projections. Finally, an equally feasible ensemble of individual climate change projections was proposed in order to define more robust climate scenarios that were more representative than those based on a single model.

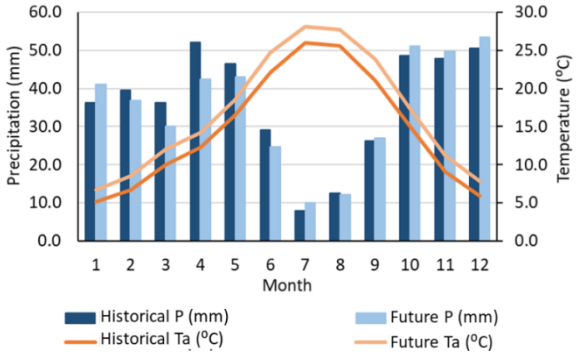

Figure 6.4. Monthly mean historical and future estimated climatic variables (precipitation (P; mm) and temperature (Ta; °C)). The historical (1974–2015) data were obtained from the Spain02 dataset, and the future (2016–2045) series was generated by applying the proposed methodology

3. Results and Discussion

3.1. Pollution Risk Assessment

The risk of pollution map was computed by combining the groundwater vulnerability map (O-DRASTIC) and the hazard map.

The hazards were defined by assigning a rate to the different categories of the land use and land cover (LULC) map. Though it did not provide detailed information about the crop typologies, the LULC map displayed the main agricultural uses in this area. Based on literature [59,60], rates were assigned to the different land use categories regarding irrigation, since irrigated agriculture is considered the major factor that contributes to the diffuse pollution of surface and groundwater bodies [49]. The leaching of nitrogen was not estimated, because the approach presented in this paper was based on mean values from a long historical period (1974–2015) and we decided that the uncertainties in crop rotation, the variables that influence the load of nitrates [49], and detailed climatic variability in this historical period would encumber the proposed assessment and be out of the scope of this paper. Therefore, for a preliminary lumped assessment, we decided that a rough classification could afford an approximation of the potential hazard. Previous studies [59] also considered land use as a potential variable to estimate the contaminant loading parameter. Table 6.2 shows the rates assigned to the land uses.

Table 6.2. Rates of land use (LU).

LU	Rate
Agroforestry areas	7
Airports	2
Annual crops associated with permanent crops	8
Broad-leaved forest	2
Burnt areas	2
Complex cultivation patterns	8
Coniferous forest	2
Construction sites	2
Continuous urban fabric	10
Discontinuous urban fabric	10
Dump sites	9
Fruit trees and berry plantations	7

Industrial or commercial units	8
Inland marshes	1
Land principally occupied by agriculture, with significant areas of natural vegetation	5
Mineral extraction sites	3
Mixed forest	3
Natural grasslands	3
Non-irrigated arable land	5
Olive groves	6
Pastures	5
Permanently irrigated land	8
Road and rail networks and associated land	2
Sclerophyllous vegetation	3
Sparsely vegetated areas	3
Sport and leisure facilities	2
Transitional woodland-shrub	2
Vineyards	5
Water bodies	1

The combination of groundwater vulnerability and hazard maps provided the risk of pollution map. The risk map was classified following the matrix technique displayed in Figure 6.5a, and the lumped risk index (L-RISK index) is summarized at the aquifer scale following Equation (1).

3.2. Mean Residence Time

The groundwater resource map (Figure 6.3b) and the output recharge for each aquifer from the flow model described in Section 2.2.2 were used to approximate the mean residence time at the aquifer scale as the T index following Equation (2) (Figure 6.5b).

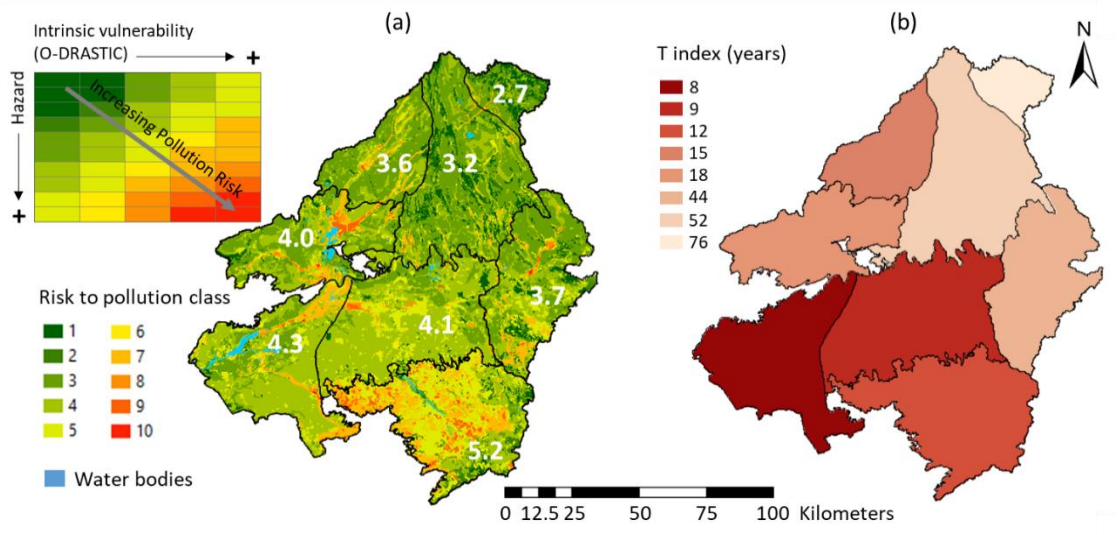

Figure 6.5. Pollution risk map (numbers indicate the L-RISK index for each aquifer) and (b) lumped mean residence time map in the historical period.

Figure 6.5 shows clear differences in the L-RISK and T indices between the different aquifers, although a higher heterogeneity is observed in the T index values due to the fact that nearly the 70% of the total area in the Upper Guadiana Basin is occupied by non-irrigated arable land and vineyards, which represent medium hazard (value 5); therefore, the risk map was smoothed.

The L-RISK index helped to determine the most vulnerable aquifers, overcoming the drawbacks of the subjective nature of visual analysis in a distributed map [13]. Vulnerability lumped indices have been shown to be useful to compare results between different aquifers in previous studies [11,13].

Two groups of aquifers could be distinguished with the T index, with each showing significant differences in their mean values in the historical period: aquifers had a T under 20 years, and others had a T value higher than 40 years (Figure 6.6). The aquifers that had lower T values showed lower volumes of resource than the recharge, which makes them extremely vulnerable to pumping [20,21] and suffering drastic variations due to exploitation [2].

We also analyzed the volume of resources, recharge, and the T index in dry and wet periods (1993–1995 and 2010–2014, respectively). We observed that some aquifers experienced large variations in the T index when comparing the dry and wet periods (bars in Figure 6.6), which was mainly driven by groundwater recharge. Despite the variation in groundwater recharge between dry and wet periods, this component was not significant compared to the groundwater volume in aquifers with higher T values. Therefore, these aquifers always maintain a higher residence time, which means that they are more resilient to climate variability [61] but might be susceptible to groundwater depletion over long dry periods if the withdrawals are not controlled. On the contrary, other aquifers showed lower T values in both wet and dry periods, with higher contributions of recent infiltration and, thus, higher risks for pollution [62].

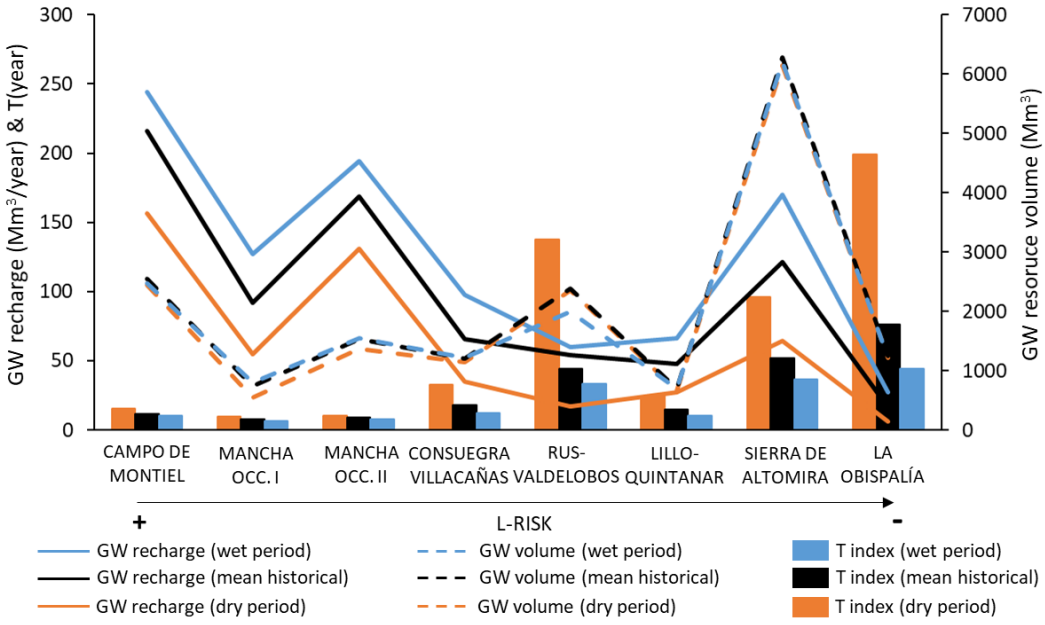

Figure 6.6. Groundwater recharge (Mm3/year), volume of resource (Mm3), and lumped turnover time index (T index) for each aquifer in the Upper Guadiana Basin in the historical period (mean, wet, and dry historical periods).

3.3. Lumped Validation of Pollution Risk Maps

Different regression models (Table 6.1) were tested in order to demonstrate the correlation between the T and L-RISK indices in the eight aquifers of the Upper Guadiana Basin. The coefficient of determination R^2 of the different models varied in the range of 0.51–0.69. The best combination of the model was the obtained for the transformation of square root in both variables ($\sqrt{L-RISK} = a \times \sqrt{T} + b$).

The results (Figure 6.7) showed that the T index can be a potential lumped approach to assess and/or validate the risk of pollution at the aquifer scale. This method can be useful in regional or

national studies in which several aquifers are analyzed at the same time in order to establish priority management measures to achieve the objectives of the WFD. The validation of risk (or vulnerability) maps is usually performed by employing different methods according to data availability and the type of aquifer. Previous studies [13,14] that analyzed and compared groundwater vulnerability in several aquifers employed a different distributed validation method for each aquifer, thus forfeiting the advantage of a harmonized methodology that makes the results comparable.

On the other hand, the T index as a lumped approach of groundwater risk for pollution can help to quantify the degradation of an aquifer due to groundwater vulnerability and recent contamination, but it would also allow for more efficient management measures to be established in order to remediate the contamination of groundwater. The renewal time of groundwater helps one to understand many problems related to groundwater supply and quality, as well as groundwater-dependent ecosystems [2,21].

The T index provides a preliminary estimation of the risk for pollution that only requires the volumes of resource and recharge. These data are usually available from river basin authorities. The use of the T index as vulnerability indicator may help to overcome the drawbacks of data availability when applying more complex methods and the ambiguity when different vulnerability methods are applied to the same pilot area.

In order to prove the potential suitability of this model to provide future estimations under climate change scenarios, we validated it in two historical periods with different climatic conditions (dry and wet historical periods). The recharge in the dry and wet periods varied between −60% and +40%, respectively, compared to the average. Figure 6.7 shows the relationship between the transformation of the T and L-RISK indices for the mean, dry, and wet historical periods and the fitted linear regression for the mean historical values. The R^2 was similar for the three periods, which showed that the model could be useful to estimate the future mean L-RISK index if the variation of the mean future recharge regarding the mean historical one is within the range of the dry and wet historical periods.

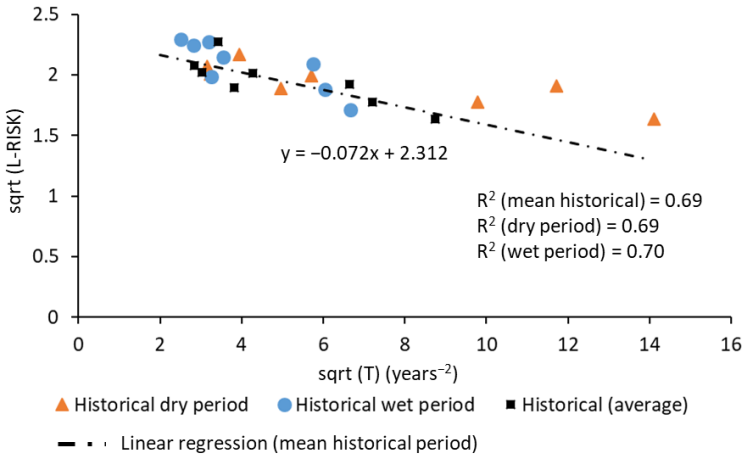

Figure 6.7. Relationship between the target and explanatory variables for the best linear regression model (√(L-RISK)=a×√T+b).

3.4. Impacts of Future Potential Climatic Scenarios

The estimated future climatic data allowed us to estimate the impacts of climate change through the SAC-SMA and Modflow models in order to obtain the recharge and groundwater resource volume to calculate the T index. The future pumping schedule was generated by using the CROPWAT model [63] to calculate net irrigation demands according to the climate change scenario. This tool allows one to estimate water requirements for each kind of crop from

precipitation and temperature data. Thus, the future climatic series was applied to a business-as-usual management scenario based on the assumption by maintaining the current (2015) spatial crop distribution in the future. The forecasted increase of mean temperature and decrease of mean precipitation in the climate change scenario implies higher crop water requirements according to CROPWAT calculations. Therefore, although the future scenario does not encompass land use changes, irrigation volume will have to increase in order to maintain crop exploitation, as in the last year of the historical period (2015).

The simulated climate change scenario showed a decrease in precipitation and an increase in temperature, which involved a lower recharge (33.4 mm/year in the simulated future scenario) and a decline in groundwater levels exacerbated by higher crop water requirements. This would be reflected in a reduction of groundwater vulnerability to contamination.

The T index was found to increase in the future regarding the mean historical for all the studied aquifers (Figure 6.8a). It showed a heterogeneous variation depending on the aquifer. The difference between future and historical T index values was found to vary in the range from 1 to 45 years (Figure 6.8b). It was observed that the lowest risk for pollution correlated to the largest the difference between future and historical T index values. The differences in the T index between historical and future assessment were mainly due to the reduction in the recharge, which was larger in the aquifers with high T values. The change in the mean recharge in the future with respect to the historical reflected a decrease between 15 and 56% depending on the aquifer, whereas the volume of resource showed a maximum variation of 23%.

These recharge changes were related to climate variables, which include precipitation and influence water crop requirements. However, the management of resources regarding exploitation due to a future pumping schedule was considered in the Modflow simulation (explained above in this section).

A linear regression model calibrated in the historical period was employed to predict the impacts of the potential future climate change scenario on risk of pollution (L-RISK index).

Risk for pollution will decrease in the future in all aquifers. Aquifers with a high risk in the historical period will continue having high risk of pollution in the future (if the sources of contaminants do not drastically) change. In relation with the potential sources of contamination, the T index have an idea of the time in which the prevention measures could be effective [64]. Aquifers with high T index values will become less vulnerable to pollution (provided that land uses do not entail a major hazard), but greater efforts will be needed in order to maintain the mean reserves due to drought exacerbation [20]. Nevertheless, if sustainable use and a good quantitative status remain over time, these aquifers could have great strategic potential in drought management because they offer high reliability to groundwater managers. They could provide significant pumping rates without varying their hydrological operations [2]. However, aquifers with younger water (lower T values) will continue to be the most impacted by contamination and climate change [21], and more efforts will be required to maintain a good qualitative status, although the effect of prevention measures is being rapidly reflected. In these aquifers, management strategies will require that the groundwater extractions are lower than the mean future recharge in order to preserve groundwater status and groundwater-dependent ecosystems [2].

In summary, the novel approach proposed in this paper can be useful in cases with limited information, even if we do not have a hydrological model. It can produce preliminary results, covering wide areas (national or regional assessment), that help to identify potential strategic aquifers where more exhaustive analyses should be performed to define conjunctive use measures for the sustainable management of water resources systems during drought-critical periods. If data are available to perform a future assessment, the obtained results can also be useful to define sustainable groundwater planning based on the potential exploitation and risk of pollution of the groundwater. This will help to contribute the sustainable management of groundwater resources and groundwater-dependent ecosystems.

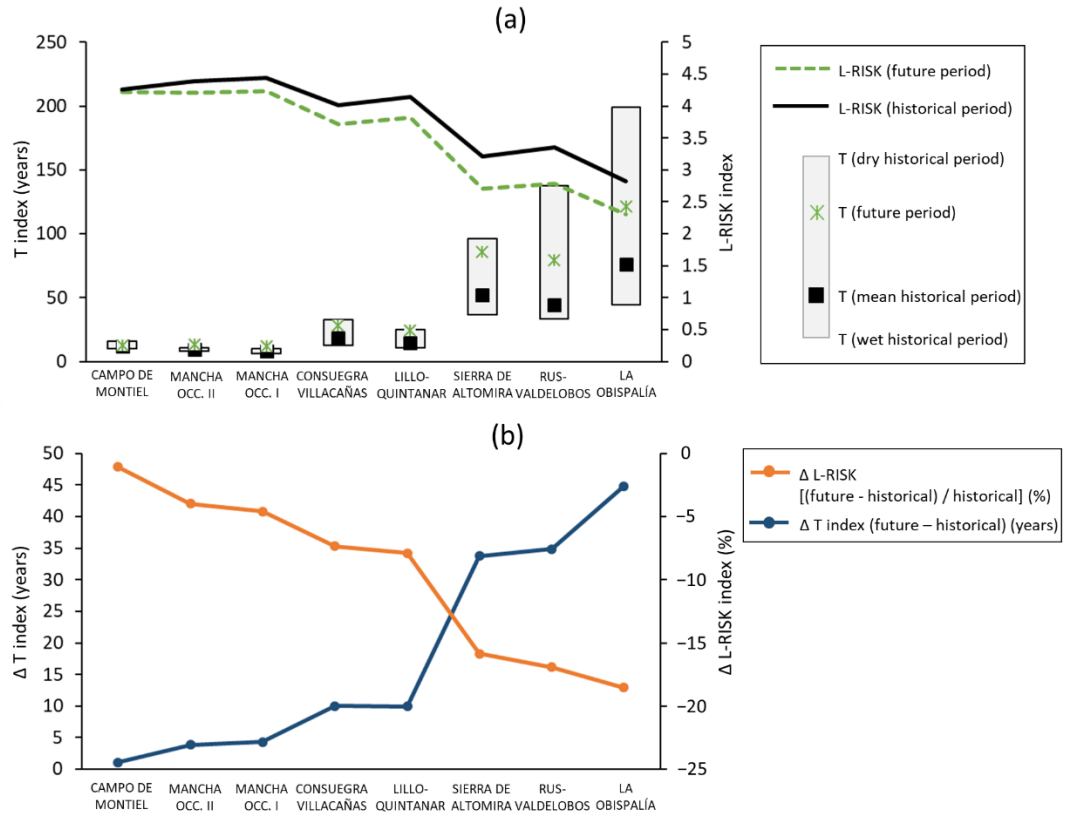

Figure 6.8. (a) Historical (medium, wet, and dry periods) and future T index and historical and future L-RISK for the best linear regression model; (b) change between future and historical T (years) and L-RISK (%) indexes.

3.5. Hypotheses and Limitations

The proposed approach presented in this paper involved some hypotheses and limitations regarding data and methodology.

Data:

- The hazard assessment considered the potential contamination from the different land uses based on the literature, but it did not consider the permissible quantity of fertilizers applicable according to the type of crop (which involves the potential load of nitrate into groundwater). This would require a complex analysis that was out of scope of this paper.
- The underlying vulnerability method may have involved some degree of subjectivity due to the own formulation of the method.
- Data to calculate the necessary variables for the T and L-RISK indices came from a calibrated flow model, which presented its own limitations.
- The climatic variables (precipitation and temperature) used in this study came from Spain 02 project dataset [57]. This dataset has been employed and validated in many research studies.

Method:

- The proposed method required a risk for pollution assessment, which could have involved some degree of subjectivity in the analysis. In this paper, a modification of the DRASTIC method (O-DRASTIC) was used to assess groundwater vulnerability, and it was combined with land uses to obtain the risk of pollution. Other vulnerability and/or risk assessment methods could be used to apply the proposed methodology.

- The T index could be obtained from available data from river basin authorities or by using a detailed groundwater model. The source of these data could influence the accuracy of results.
- We assumed a linear relationship between the mean residence time (T index) and the lumped risk of pollution (L-RISK index) in the studied aquifers. This allowed us to use a simple regression model.
- We assumed that the model was suitable in the range of variability of the future climatic variables.
- The method was demonstrated to be useful in the eight aquifers of the Upper Guadiana Basin, but it should be tested in a larger range of aquifers.
- The local climatic scenario used in this study was generated for the horizon of 2016-2045, assuming the most pessimistic emissions scenario (RCP 8.5). Observed biases were corrected by applying a simple statistical correction technique.
- The proposed method was useful to analyze the impacts of climate change on the risk of pollution at the aquifer scale, assuming that a business-as-usual management scenario was maintained in the future. Significant changes in the type of crops, which may involve higher fertilizer requirements, would have great impact on groundwater contamination, and the linear model would not allow one to approach a future assessment.

4. Conclusions

This paper presents a new method to make a preliminary assessment and/or validation of groundwater pollution risk maps at the aquifer scale by using a lumped approach of the mean residence time (T index). The study showed that the T index is a useful indicator to attempt a first approach of groundwater risk for pollution in order to determine which aquifers are in risk according to the WFD. The used method allowed us to identify potential hot spots (aquifers at risk) that will require further detailed risk assessments to analyze the most suitable management practices. The methodology assumed a linear relationship between the T and L-RISK indices, which was used to estimate the impacts of climate change under a future scenario. The methodology was applied to eight aquifers in the Upper Guadiana Basin. The results showed a good correlation between the T and L-RISK indices, not only in the mean historical period but also under variable historical climatic conditions (dry and wet historical periods). A regression model was used to estimate the future L-RISK index, which forecast a lower risk of pollution. Despite that, sustainable management will be necessary because the residence time of groundwater will also vary and involve a larger response time. The Mancha Occidental I, Mancha Occidental II, and Campo de Montiel aquifers presented the highest risk for groundwater pollution, and they were also found to have the lowest T index. Moreover, these aquifers have important associated groundwater-dependent ecosystems, and more efforts will therefore be required to maintain good qualitative and quantitative status. The T index is expected to increase in all aquifers under the future scenario. Aquifers with larger T values will become more resilient, and they could be identified as strategic aquifers in drought periods because they will allow for the maintenance of sustainable exploitation under climate change scenarios if the appropriate management measures are implemented.

In conclusion, the T index provides a rough assessment of the historical risk of pollution at the aquifer scale and gives an idea of the sustainability of groundwater resource exploitation under climate change scenarios. This index is a lumped index that can be calculated using easily available data, and it allows for results at the aquifer scale to be compared in order to establish priority measures in aquifers at risk.

Author Contributions: Conceptualization, L.B.-R. and D.P.-V.; data curation, L.B.-R., A.-J.C.-L. and J.d.D.G.-G.; investigation, L.B.-R.; methodology, L.B.-R., D.P.-V., and A.-J.C.-L.; software, L.B.-R.; supervision, D.P.-V.; validation, L.B.-R.; visualization, L.B.-R.; writing—

original draft, L.B.-R. and D.P.-V.; writing—review and editing, L.B.-R., D.P.-V., A.-J.C.-L., and J.d.D.G.-G. All authors have read and agreed to the published version of the manuscript.

Funding: This research did not receive any specific grant from funding agencies in the public, commercial, or not-for-profit sectors.

Acknowledgments: This paper was partially supported by the SIGLO-AN (RTI2018-101397-B-I00) project from the Spanish Ministry of Science, Innovation and Universities (Programa Estatal de I+D+I orientada a los Retos de la Sociedad), the GeoE.171.008-HOVER and the GeoE.171.008-TACTICproject from GeoERA organization funded by European Union's Horizon 2020 research and innovation program.

Conflicts of Interest: The authors declare that they have no known competing financial interests or personal relationships that could have appeared to influence the work reported in this paper.

Appendix 6.1. O-DRASTIC Method

The O-DRASTIC method was developed by the authors of [19] in an attempt to harmonize vulnerability assessments for different aquifer typologies. It was obtained by an optimization process, and it was validated in carbonated and detrital aquifers in the Up-per Guadiana Basin (Spain), ultimately showing better results than original DRASTIC [6].

This method considers the seven parameters/variables influencing the vulnerability to contamination as original DRASTIC: depth to water table (D), net recharge (R), aquifer media (A), soil media (S), topography (T), impact of vadose zone (I), and hydraulic conductivity (C). The classification and rate of importance assigned to the parameters are summarized in Table A6.1.

Table A6.1. Ranges and rates for O-DRASTIC parameters.

Groundwater Table Depth (m)	
Ranges	Ratings
0–1.5	10
1.5–4.6	9
4.6–9.1	7
9.1–15.2	5
15.1–22.9	3
22.9–30.5	2
>30.5	1
Net recharge (mm)	
Ranges	Ratings
0–50.8	1
50.8–101.6	3
101.6–177.8	6
177.8–254.0	8
>254.0	9
Aquifer media	
Ranges	Ratings
Massive shale	2
Metamorphic/Igneous	3
Weathered metamorphic/Igneous	4
Thin bedded sandstone, Limestone	6
Shale sequences	6

Massive sandstone	6
Massive limestone	8
Sand and gravel	9
Basalt	10
Karst limestone	
Soil media	
Ranges	Ratings
Thin or absent	10
Gravel	10
Sand	9
Peat	8
Shrinking and/or aggregated clay	7
Sandy loam	6
Loam	5
Silty loam	4
Clay loam	3
Muck	2
Non-shrinking and non-aggregated clay	1
Topography (% slope)	
Ranges	Ratings
0–2	10
2–6	9
6–12	5
12–18	3
>18	1
Impact of vadose zone	
Ranges	Ratings
Silt/Clay	1
Shale	3
Limestone	6
Sandstone	6
Bedded limestone, sandstone, shale	6
Sand and gravel with significant silt and clay	6
Metamorphic/Igneous	4
Sand and gravel	8
Basalt	9
Karst limestone	10
Hydraulic conductivity (m/d)	
Ranges	Ratings
15	1
30	2
45	4
60	6
75	8
>75	10

The values of the parameters are weighted by a weight to obtain the O-DRASTIC index, which is calculated following Equation (A1):

$$\text{O-DRASTIC index} = 1 \times D + 5 \times R + 5 \times A + 5 \times S + 1 \times T + 5 \times I + 1 \times C \quad \text{(A1)}$$

The O-DRASTIC index is classified into five vulnerability levels (Table A6.2):

Table A6.2. O-DRASTIC classes.

O-DRASTIC Index	Class Value
<107	Very low
107–130	Low
130–138	Moderate
138–146	High
>146	Very high

References

1. Quevauviller, P. Chapter 1. General Introduction: The Need to Protect Groundwater. In Groundwater Science and Policy; Roy-al Society of Chemistry (RSC): London, UK, USA, 2007; pp. 1–18.

2. Molina, J.-L.; Martos-Rosillo, S.; Martín-Montañés, C.; Pierce, S. The Social Sustainable Aquifer Yield: An Indicator for the Analysis and Assessment of the Integrated Aquifers Management. Water Resour. Manag. 2012, 26, 2951–2971, doi:10.1007/s11269-012-0058-5.

3. Kløve, B.; Ala-Aho, P.; Bertrand, G.; Gurdak, J.J.; Kupfersberger, H.; Kværner, J.; Muotka, T.; Mykrä, H.; Preda, E.; Rossi, P.; et al. Climate change impacts on groundwater and dependent ecosystems. J. Hydrol. 2014, 518, 250–266, doi:10.1016/j.jhydrol.2013.06.037.

4. Water Framework Directive Directive 2000/60/EC of the European Parliament and of the Council of 23 October 2000 estab-lishing a framework for Community action in the field of water policy. Off. J. Eur. Parliam. 2000. Available online: (accessed on).

5. Stigter, T.; Ribeiro, L.; Dill, A.C. Building factorial regression models to explain and predict nitrate concentrations in groundwater under agricultural land. J. Hydrol. 2008, 357, 42–56, doi:10.1016/j.jhydrol.2008.05.009.

6. Aller, L.; Bennett, T.; Lehr, J.H.; Petty, R.J.; Hackett, G. DRASTIC: A Standardized Method for Evaluating Ground Water Pollution Potential Using Hydrogeologic Settings; NWWA/Epa-600/2-87-035; Kerr Environmental Research Laboratory, Office of Research and Development, US Environmental Protection Agency: Washington, DC, USA, 1987.

7. Vías, J.M.; Andreo, B.; Perles, M.J.; Carrasco, F.; Vadillo, I.; Jiménez, P. Proposed method for groundwater vulnerability mapping in carbonate (karstic) aquifers: The COP method. Hydrogeol. J. 2006, 14, 912–925, doi:10.1007/s10040-006-0023-6.

8. Kumar, P.; Bansod, B.K.; Debnath, S.K.; Thakur, P.K.; Ghanshyam, C. Index-based groundwater vulnerability mapping models using hydrogeological settings: A critical evaluation. Environ. Impact Assess. Rev. 2015, 51, 38–49, doi:10.1016/j.eiar.2015.02.001.

9. Garcet, J.P.; Ordoñez, A.; Roosen, J.; Vanclooster, M. Metamodelling: Theory, concepts and application to nitrate leaching modelling. Ecol. Model. 2006, 193, 629–644, doi:10.1016/j.ecolmodel.2005.08.045.

10. Oke, S.A. An overview of aquifer vulnerability. In Aquifers: Properties, Roles and Research; Nova Science Publishers, Inc.: Hauppauge, NY, USA, 2017; ISBN 9781536110845.

11. Baena-Ruiz, L.; Pulido-Velazquez, D.; Collados-Lara, A.-J.; Renau-Pruñonosa, A.; Morell, I. Global Assessment of Seawater Intrusion Problems (Status and Vulnerability). Water Resour. Manag. 2018, 32, 2681–2700, doi:10.1007/s11269-018-1952-2.

12. Baena-Ruiz, L.; Pulido-Velazquez, D.; Collados-Lara, A.-J.; Renau-Pruñonosa, A.; Morell, I.; Senent-Aparicio, J.; Llo-pis-Albert, C. Summarizing the impacts of future potential global change scenarios on seawater intrusion at the aquifer scale. Environ. Earth Sci. 2020, 79, 1–13, doi:10.1007/s12665-020-8847-2.

13. Vías, J.; Andreo, B.; Ravbar, N.; Hötzl, H. Mapping the vulnerability of groundwater to the contamination of four carbonate aquifers in Europe. J. Environ. Manag. 2010, 91, 1500–1510, doi:10.1016/j.jenvman.2010.02.025.

14. Zwahlen, F. COST Action 620 Vulnerability and Risk Mapping for the Protection of Carbonate (Karst) Aquifers Final Report; Office of the Official Publications of the European Communities: Brussels, Belgium, 2003; ISBN 928946416X.

15. Dąbrowska, D.; Witkowski, A.J.; Sołtysiak, M. Application of pollution indices for the spatiotemporal assessment of nega-tive impact of a municipal landfill on groundwater (Tychy, southern Poland). Geol. Q. 2018, 62, 496, doi:10.7306/gq.1420.

16. Sołtysiak, M.; Dabrowska, D.; Jałowiecki, K.; Nourani, V. A multi-method approach to groundwater risk assessment: A case study of a landfill in southern Poland. Geol. Q. 2018, 62, 361, doi:10.7306/gq.1411.

17. Backman, B.; Bodiš, D.; Lahermo, P.; Rapant, S.; Tarvainen, T. Application of a groundwater contamination index in Finland and Slovakia. Environ. Earth Sci. 1998, 36, 55–64, doi:10.1007/s002540050320.

18. Kumar Singh, P.; Verma, P.; Tiwari, A.K.; Sharma, S.; Purty, P. Review of various contamination index approaches to evalu-ate groundwater quality with geographic information system (GIS). Int. J. Chem. Tech. Res. 2014, 7, 1920.

19. Baena-Ruiz, L.; Pulido-Velazquez, D. A Novel Approach to Harmonize Vulnerability Assessment in Carbonate and Detrital Aquifers at Basin Scale. Water 2020, 12, 2971, doi:10.3390/w12112971.

20. Pulido-Velazquez, D.; Romero, J.; Collados-Lara, A.-J.; Alcalá, F.J.; Fernández-Chacón, F.; Baena-Ruiz, L. Using the Turnover Time Index to Identify Potential Strategic Groundwater Resources to Manage Droughts within Continental Spain. Water 2020, 12, 3281, doi:10.3390/w12113281.

21. Newman, B.D.; Osenbrück, K.; Aeschbach-Hertig, W.; Solomon, D.K.; Cook, P.; Rozanski, K.; Kipfer, R.; Aeschbach, W. Da-ting of 'young' groundwaters using environmental tracers: Advantages, applications, and research needs. Isot. Environ. Health Stud. 2010, 46, 259–278, doi:10.1080/10256016.2010.514339.

22. Dedewanou, M.; Binet, S.; Rouet, J.L.; Coquet, Y.; Bruand, A.; Noel, H. Groundwater Vulnerability and Risk Mapping Based on Residence Time Distributions: Spatial Analysis for the Estimation of Lumped Parameters. Water Resour. Manag. 2015, 29, 5489–5504, doi:10.1007/s11269-015-1130-8.

23. Schwartz, M.O. Numerical modelling of groundwater vulnerability: The example Namibia. Environ. Earth Sci. 2006, 50, 237–249, doi:10.1007/s00254-006-0204-6.

24. Molson, J.; Frind, E. On the use of mean groundwater age, life expectancy and capture probability for defining aquifer vul-nerability and time-of-travel zones for source water protection. J. Contam. Hydrol. 2012, 127, 76–87, doi:10.1016/j.jconhyd.2011.06.001.

25. Živanović, V.; Jemcov, I.; Dragišić, V.; Atanacković, N.; Magazinović, S. Karst groundwater source protection based on the time-dependent vulnerability assessment model: Crnica springs case study, Eastern Serbia. Environ. Earth Sci. 2016, 75, 1224, doi:10.1007/s12665-016-6018-2.

26. Andreo, B.; Goldscheider, N.; Vadillo, I.; Vías, J.M.; Neukum, C.; Sinreich, M.; Jiménez, P.; Brechenmacher, J.; Carrasco, F.; Hötzl, H.; et al. Karst groundwater protection: First application of a Pan-European Approach to vulnerability, hazard and risk mapping in the Sierra de Líbar (Southern Spain). Sci. Total Environ. 2006, 357, 54–73, doi:10.1016/j.scitotenv.2005.05.019.

27. Neukum, C.; Hötzl, H.; Himmelsbach, T. Validation of vulnerability mapping methods by field investigations and numer-ical modelling. Hydrogeol. J. 2007, 16, 641–658, doi:10.1007/s10040-007-0249-y.

28. Sadek, M.; El-Samie, A.S. Pollution vulnerability of the Quaternary aquifer near Cairo, Egypt, as indicated by isotopes and hydrochemistry. Hydrogeol. J. 2001, 9, 273–281, doi:10.1007/s100400100125.

29. Bakalowicz, M. Karst groundwater: A challenge for new resources. Hydrogeol. J. 2005, 13, 148–160, doi:10.1007/s10040-004-0402-9.

30. Neukum, C.; Azzam, R. Quantitative assessment of intrinsic groundwater vulnerability to contamination using numerical simulations. Sci. Total Environ. 2009, 408, 245–254, doi:10.1016/j.scitotenv.2009.09.046.

31. Yu, C.; Yao, Y.; Cao, G.; Zheng, C. A field demonstration of groundwater vulnerability assessment using transport model-ing and groundwater age modeling, Beijing Plain, China. Environ. Earth Sci. 2014, 73, 5245–5253, doi:10.1007/s12665-014-3769-5.

32. Chambers, L.; Gooddy, D.; Binley, A. Use and application of CFC-11, CFC-12, CFC-113 and SF6 as environmental tracers of groundwater residence time: A review. Geosci. Front. 2019, 10, 1643–1652, doi:10.1016/j.gsf.2018.02.017.

33. Perrin, J.; Pochon, A.; Jeannin, P.-Y.; Zwahlen, F. Vulnerability assessment in karstic areas: Validation by field experiments. Environ. Earth Sci. 2004, 46, 237–245, doi:10.1007/s00254-004-0986-3.

34. Green, T.R.; Taniguchi, M.; Kooi, H.; Gurdak, J.J.; Allen, D.M.; Hiscock, K.M.; Treidel, H.; Aureli, A. Beneath the surface of global change: Impacts of climate change on groundwater. J. Hydrol. 2011, 405, 532–560, doi:10.1016/j.jhydrol.2011.05.002.

35. Cao, T.; Han, D.; Song, X.; Trolle, D. Subsurface hydrological processes and groundwater residence time in a coastal allu-vium aquifer: Evidence from environmental tracers (δ18O, δ2H, CFCs, 3H) combined with hydrochemistry. Sci. Total Envi-ron. 2020, 743, 140684, doi:10.1016/j.scitotenv.2020.140684.

36. Fienen, M.N.; Nolan, B.T.; Kauffman, L.J.; Feinstein, D.T. Metamodeling for Groundwater Age Forecasting in the Lake Michigan Basin. Water Resour. Res. 2018, 54, 4750–4766, doi:10.1029/2017wr022387.

37. Martínez-Salvador, C.; Moreno-Gómez, M.; Liedl, R. Estimating Pollutant Residence Time and NO3 Concentrations in the Yucatan Karst Aquifer; Considerations for an Integrated Karst Aquifer Vulnerability Methodology. Water 2019, 11, 1431, doi:10.3390/w11071431.

38. Jurgens, B.C.; Böhlke, J.; Kauffman, L.J.; Belitz, K.; Esser, B.K. A partial exponential lumped parameter model to evaluate groundwater age distributions and nitrate trends in long-screened wells. J. Hydrol. 2016, 543, 109–126, doi:10.1016/j.jhydrol.2016.05.011.

39. Małoszewski, P.; Zuber, A. Determining the turnover time of groundwater systems with the aid of environmental tracers. 1. Models and their applicability. J. Hydrol. 1982, 57, 207–231, doi:10.1016/0022-1694(82)90147-0.

40. Martos-Rosillo, S.; Marín-Lechado, C.; Pedrera, A.; Vadillo, I.; Motyka, J.; Molina, J.L.; Ortiz, P.; Ramírez, J.M.M. Methodol-ogy to evaluate the renewal period of carbonate aquifers: A key tool for their management in arid and semiarid regions, with the example of Becerrero aquifer, Spain. Hydrogeol. J. 2013, 22, 679–689, doi:10.1007/s10040-013-1086-9.

41. Pulido-Velazquez, D.; Renau-Pruñonosa, A.; Llopis-Albert, C.; Morell, I.; Collados-Lara, A.-J.; Senent-Aparicio, J.; Bae-na-Ruiz, L. Integrated assessment of future potential global change scenarios and their hydrological impacts in coastal aq-uifers—A new tool to analyse management alternatives in the Plana Oropesa-Torreblanca aquifer. Hydrol. Earth Syst. Sci. 2018, 22, 3053–3074, doi:10.5194/hess-22-3053-2018.

42. Musálem, K.; McDonald, M.; Jiménez, F.; Laino, R. Groundwater vulnerability mapping in two watersheds affected by Yacyreta Dam in Paraguay. Tecnol. Ciencias Agua 2015, 6, 49–61.

43. Ducci, D. Influence of climate changes on vulnerability maps. In Proceedings of the First Conference and Workshop on "Groundwater and Climate Change", Norwich, UK, 4–6 April 2005.

44. Huang, L.; Zeng, G.; Liang, J.; Hua, S.; Yuan, Y.; Li, X.; Dong, H.; Liu, J.; Nie, S.; Liu, J. Combined Impacts of Land Use and Climate Change in the Modeling of Future Groundwater Vulnerability. J. Hydrol. Eng. 2017, 22, 05017007, doi:10.1061/(asce)he.1943-5584.0001493.

45. Ouedraogo, I.; Girard, A.; Vanclooster, M.; Jonard, F. Modelling the Temporal Dynamics of Groundwater Pollution Risks at the African Scale. Water 2020, 12, 1406, doi:10.3390/w12051406.

46. Nistor, M.-M. Groundwater vulnerability in Europe under climate change. Quat. Int. 2020, 547, 185–196, doi:10.1016/j.quaint.2019.04.012.

47. Collados-Lara, A.-J.; Pulido-Velazquez, D.; Mateos, R.M.; Ezquerro, P. Potential Impacts of Future Climate Change Scenari-os on Ground Subsidence. Water 2020, 12, 219, doi:10.3390/w12010219.

48. Morris, B.L.; Foster, S.D. Cryptosporidium contamination hazard assessment and risk management for British groundwater sources. Water Sci. Technol. 2000, 41, 67–77, doi:10.2166/wst.2000.0117.

49. Causapé, J.; Quílez, D.; Aragüés, R. Assessment of irrigation and environmental quality at the hydrological basin level: II. Salt and nitrate loads in irrigation return flows. Agric. Water Manag. 2004, 70, 211–228, doi:10.1016/j.agwat.2004.06.006.

50. Merchán, D.; Otero, N.; Soler, A.; Causapé, J. Main sources and processes affecting dissolved sulphates and nitrates in a small irrigated basin (Lerma Basin, Zaragoza, Spain): Isotopic characterization. Agric. Ecosyst. Environ. 2014, 195, 127–138, doi:10.1016/j.agee.2014.05.011.

51. Dunn, S.; Brown, I.; Sample, J.; Post, H. Relationships between climate, water resources, land use and diffuse pollution and the significance of uncertainty in climate change. J. Hydrol. 2012, 434-435, 19–35, doi:10.1016/j.jhydrol.2012.02.039.

52. Werz, H.; Hötzl, H. Groundwater risk intensity mapping in semi-arid regions using optical remote sensing data as an addi-tional tool. Hydrogeol. J. 2007, 15, 1031–1049, doi:10.1007/s10040-007-0202-0.

53. Kazakis, N.; Voudouris, K.S. Groundwater vulnerability and pollution risk assessment of porous aquifers to nitrate: Modi-fying the DRASTIC method using quantitative parameters. J. Hydrol. 2015, 525, 13–25, doi:10.1016/j.jhydrol.2015.03.035.

54. Conan, C.; De Marsily, G.; Bouraoui, F.; Bidoglio, G. A long-term hydrological modelling of the Upper Guadiana river basin (Spain). Phys. Chem. Earth Parts A/B/C 2003, 28, 193–200, doi:10.1016/s1474-7065(03)00025-1.

55. Yustres, Á.; Navarro, V.; Asensio, L.; Candel, M.; García, B. Groundwater resources in the Upper Guadiana Basin (Spain): A regional modelling analysis. Hydrogeol. J. 2013, 21, 1129–1146, doi:10.1007/s10040-013-0987-y.

56. Martinezsantos, P.; Llamas, M.; Martinezalfaro, P. Vulnerability assessment of groundwater resources: A modelling-based approach to the Mancha Occidental aquifer, Spain. Environ. Model. Softw. 2008, 23, 1145–1162, doi:10.1016/j.envsoft.2007.12.003.

57. Herrera, S.; Fernández, J.; Gutiérrez, J.M. Update of the Spain02 gridded observational dataset for EURO-CORDEX evalua-tion: Assessing the effect of the interpolation methodology. Int. J. Clim. 2016, 36, 900–908, doi:10.1002/joc.4391.

58. World Climate Research Programme. Coordinated Regional Climate Downscaling Experiment (CORDEX); 2014.

59. Panagopoulos, G.P.; Antonakos, A.K.; Lambrakis, N.J. Optimization of the DRASTIC method for groundwater vulnerability assessment via the use of simple statistical methods and GIS. Hydrogeol. J. 2006, 14, 894–911, doi:10.1007/s10040-005-0008-x.

60. Antonakos, A.; Lambrakis, N. Development and testing of three hybrid methods for the assessment of aquifer vulnerability to nitrates, based on the drastic model, an example from NE Korinthia, Greece. J. Hydrol. 2007, 333, 288–304, doi:10.1016/j.jhydrol.2006.08.014.

61. Lapworth, D.J.; Macdonald, A.M.; Tijani, M.N.; Darling, G.; Gooddy, D.C.; Bonsor, H.C.; Araguás-Araguás, L.J. Residence times of shallow groundwater in West Africa: Implications for hydrogeology and resilience to future changes in climate. Hydrogeol. J. 2013, 21, 673–686, doi:10.1007/s10040-012-0925-4.

62. Wachniew, P. Environmental tracers as a tool in groundwater vulnerability assessment. Acque Sotter. Ital. J. Groundw. 2015, 4, doi:10.7343/as-108-15-0135.

63. Smith, M. CROPWAT: A Computer Program. for Irrigation Planning and Management; Food & Agriculture Organization: Rome, Italy, 1992; ISBN 9251031061.

64. Duda, R.; Kowalczyk, P. Assessment of factors affecting the intrinsic vulnerability of groundwater rated by the mean resi-dence time estimation method. Geol. Q. 2019, 63, 126–138, doi:10.7306/gq.1454.

Capítulo 7: Conclusiones generales, limitaciones e investigación futura

En esta tesis se desarrollan metodologías que permitan analizar de forma agregada el estado global y la vulnerabilidad de las masas de agua subterránea. Se realizan contribuciones orientadas a la armonización de la evaluación de la vulnerabilidad y el riesgo a la contaminación mediante métodos agregados de estimación, validación y síntesis de resultados. Se analizan los impactos de potenciales escenarios de CC en el estado global, vulnerabilidad y riesgo a la contaminación, valorando e identificados potenciales medidas de adaptación. Finalmente, se identifican acuíferos estratégicos para una gestión sostenible de los recursos hídricos. La aplicabilidad de los métodos propuestos se ha demostrado en diversos casos de estudio, a escala de acuífero y de cuenca.

1. Contribuciones y principales conclusiones

En cada uno de los capítulos anteriores (artículos SCI) se exponen de forma detallada las conclusiones alcanzadas en las diferentes contribuciones realizadas, las cuales se recogen a continuación de forma resumida:

- Propuesta de metodología basada en índices para sintetizar el estado global y la vulnerabilidad a la intrusión en acuíferos costeros.

Este método está basado en un enfoque conceptual de la intrusión que permite sintetizar los resultados de una manera visual a escala de acuífero. Los resultados se presentan mediante mapas y secciones transversales representativas de valores instantáneos o medios en un periodo determinado, así como series temporales de índices agregados para todo el acuífero. Las series temporales permiten además analizar la evolución del problema de manera agregada, así como la resiliencia y tendencia de la intrusión en el acuífero. Los índices propuestos se obtienen a partir de información sobre la geometría del acuífero y datos históricos de monitoreo (concentración de cloruros y nivel piezométrico). El método no requiere la implementación de modelos complejos y se puede aplicar incluso en casos de estudio con un reducido número de datos disponibles Este método puede ser útil para identificar acuíferos en riesgo de no alcanzar los objetivos de la DMA y permite comparar el problema de intrusión en diferentes acuíferos y periodos temporales.

- Análisis del impacto de potenciales escenarios futuros de cambio global (CG) en el estado y vulnerabilidad de acuíferos costeros.

En el acuífero costero Plana de Oropesa-Torreblanca, que presenta graves problemas de contaminación por intrusión marina, se analizan los impactos de potenciales escenarios de CG (incluyendo CC y medidas de adaptación) en el estado global y vulnerabilidad a la intrusión. La metodología propuesta sintetiza el impacto de los potenciales escenarios de CG en términos de intrusión y vulnerabilidad a escala de acuífero mediante mapas y secciones transversales representativas de valores instantáneos o medios en un periodo determinado, así como series temporales de índices agregados para todo el acuífero. Los resultados muestran que los escenarios de CG producirán una mayor variabilidad en el estado global y vulnerabilidad a la intrusión. El análisis de impactos de escenarios de CG muestra el efecto de algunas medidas de adaptación basadas en cambios de usos del suelo previstos en el Plan de Ordenación Urbana. Medidas de adaptación complementarias serán necesarias para definir estrategias sostenibles que reduzcan sensiblemente los impactos del CC.

- Desarrollo de una herramienta automática en entorno ArcGIS para facilitar la aplicación de la metodología propuesta de análisis y síntesis del estado global y la vulnerabilidad a la intrusión a escala de acuífero.

Se ha desarrollado una nueva herramienta de ArcGIS, GIS-SWIAS (GIS tool to analyse SeaWater Intrusion status and vulnerability at Aquifer Scale), que implementa la metodología anterior para el análisis del estado global y vulnerabilidad a la intrusión a escala de acuífero. Se trata de una herramienta amigable, de fácil manejo, que puede ser utilizada en cualquier caso de estudio, completamente integrada en el entorno ArcGIS. Es la primera herramienta en la literatura para

realizar un análisis de este tipo en ArcGIS. Se puede utilizar para analizar la intrusión en casos en los que no hay disponible un modelo de flujo, mediante la interpolación de datos de monitoreo, aunque si se dispone de información de concentración de cloruros y nivel piezométrico de un modelo previamente calibrado, la herramienta permite también analizar la sostenibilidad de escenarios de gestión futuros. Dada su versatilidad, GIS-SWIAS es una herramienta útil tanto para investigadores como técnicos para analizar la intrusión a escala de acuífero bajo diferentes escenarios, lo que puede ser de ayuda en el proceso de toma de decisiones para la selección de estrategias de gestión sostenibles.

- Estudio de la vulnerabilidad a la contaminación de masas de agua subterráneas en sistemas a escala de cuenca. Armonización de la evaluación mediante una metodología aplicable a acuíferos detríticos y kársticos.

Se propone una metodología para adaptar el método DRASTIC con el objetivo de obtener mejores estimaciones de la vulnerabilidad en acuíferos carbonatados, sin perder precisión en la evaluación para acuíferos detríticos. Se pretende encontrar una correspondencia razonable entre los mapas de vulnerabilidad DRASTIC y los obtenidos por el método COP, más apropiado para el estudio de masas carbonatadas. Para ello se plantea un problema de optimización que minimiza las diferencias entre ambos y es resuelto combinando técnicas de análisis estadístico espacial y minería de datos. La solución óptima encontrada para los acuíferos carbonatados fue también testeada en los acuíferos detríticos de la cuenca, mostrando una mejora significativa en los resultados de validación de los mapas de vulnerabilidad con respecto al método original. Los resultados muestran que los factores "Medio acuífero", "Tipo de suelo" y "Características de la zona no saturada" tienen una mayor influencia en la vulnerabilidad en acuíferos carbonatados.

- Análisis agregado del riesgo a la contaminación a partir del tiempo de renovación medio del acuífero. Estudio de impactos del CC en la sostenibilidad de la explotación de los sistemas analizados.

Se propone un nuevo método que permite realizar una primera estimación y/o validación agregada del riesgo a la contaminación en un acuífero a partir del tiempo medio de residencia del agua subterráneas en el mismo, estimado preliminarmente con un índice agregado sencillo (T = Almacenamiento/recarga media). Se presenta un nuevo índice agregado (L-RISK) para evaluar el riesgo a la contaminación a escala de acuífero. El modelo de regresión calibrado con estos dos índices permite realizar un análisis agregado del riesgo a la contaminación a partir del índice T. Así, se pueden analizar un gran número de acuíferos utilizando datos que se encuentran disponibles fácilmente. El método es útil para identificar potenciales acuíferos estratégicos con el fin de establecer medidas de gestión sostenibles de los recursos hídricos subterráneos, especialmente durante periodos de sequía. Además, también permite realizar un análisis preliminar del impacto del CC en el índice L-RISK. Los resultados muestran una amplia variabilidad del índice T en los distintos acuíferos (8-76 años). Aquellos que tienen un índice T mayor pueden considerarse como recursos subterráneos estratégicos. El análisis futuro muestra un incremento en el valor medio de T (entre un 8 y 44%) y un descenso del índice L-RISK en todos los acuíferos (1-18%). Estos resultados son útiles para la definición de medidas de gestión sostenibles.

2. Limitaciones y futuras líneas de investigación

Como en todo trabajo de investigación, para el desarrollo de esta tesis ha sido necesario establecer ciertas hipótesis que conllevan algunas limitaciones. A continuación, se exponen las principales limitaciones, las cuales ayudan a identificar futuras líneas de investigación.

- La metodología propuesta para el análisis del estado global y vulnerabilidad a la intrusión no es aplicable en acuíferos en pequeñas islas, en las que la intrusión presenta una distribución particular. Como línea futura se plantea la adaptación de la misma para su estudio de estos casos.

- La identificación de la zona afectada por intrusión, se ha llevado a cabo a partir del umbral de concentración de cloruros establecido para las aguas de consumo humano y los valores de referencia determinados por la Confederación para la evaluación del estado químico de las masas de agua subterráneas. Como futura línea de investigación, teniendo en cuenta las significativas diferencias resultantes de la aplicación de diferentes métodos descritos en la literatura, se propone avanzar en la identificación de una aproximación que permita homogeneizar criterios para la identificación del fondo hidrogeoquímico y los valores umbrales, y que sea aplicable de forma general a cualquier caso de estudio.
- La optimización del método DRASTIC desarrollada con el objetivo de armonizar una metodología para cualquier tipo de acuífero ha sido aplicada en los ocho acuíferos de la cuenca del Alto Guadiana. Como trabajo futuro se plantea verificar la aplicabilidad de la solución óptima obtenida en otros casos de estudio.
- La validez del modelo de regresión propuesto para el análisis del riesgo a la contaminación a partir del tiempo de residencia medio también podría ser estudiada en otros casos de estudio.
- En el análisis del riesgo a la contaminación en la cuenca del Alto Guadiana no se han tenido en cuenta variables como el grado de fertilización aplicada a cada cultivo, tipo de regadío ni los procesos de lixiviación del nitrógeno. En el futuro se plantea considerarlos en algunos acuíferos piloto de la cuenca, analizando y modelando los procesos físico-químicos que afectan al transporte de contaminantes tanto en la zona saturada como no saturada.
- En relación con la estimación del tiempo medio de residencia del agua subterránea, además de testear otros índices agregados sencillos, se propone realizar en algunos casos piloto una evaluación distribuida más precisa mediante la calibración de modelos de flujo y transporte en los que se integre información sobre edades del agua deducida de ensayos previos con trazadores.
- Para propagar los impactos del CC se utilizan modelos previamente calibrados (recarga, requerimiento de cultivos, modelos de flujo), en los que se asume que los parámetros permanecen invariantes en los horizontes futuros, manteniendo la relación entre los inputs y outputs identificada en el periodo histórico.
- Los escenarios futuros de CC simulados corresponden al escenario de emisiones más pesimista (RCP 8.5) publicado en el último informe del IPCC (AR5). Sería interesante evaluar otros escenarios más probables.